

**Chelating Diamide Complexes of Titanium, Zirconium and
Scandium: New Polymerization Catalysts based on Non-Cp
Ligand Environments**

by

John D. Scollard

B.Sc., The University of Western Ontario, 1991
M.Sc., The University of Western Ontario, 1993


A thesis submitted in partial fulfillment
of the requirements for the degree of

Doctor of Philosophy

in

Faculty of Graduate Studies
Department of Chemistry

We accept this thesis as conforming
to the required standard


The University of British Columbia

March, 1998

© John D. Scollard 1998

In presenting this thesis in partial fulfilment of the requirements for an advanced degree at the University of British Columbia, I agree that the Library shall make it freely available for reference and study. I further agree that permission for extensive copying of this thesis for scholarly purposes may be granted by the head of my department or by his or her representatives. It is understood that copying or publication of this thesis for financial gain shall not be allowed without my written permission.

Department of Chemistry

The University of British Columbia
Vancouver, Canada

Date 03/11/98

Abstract

The reaction of $\text{RHN}(\text{CH}_2)_3\text{NHR}$ (**2.3a,b**) (**a**, $\text{R} = 2,6\text{-Me}_2\text{C}_6\text{H}_3$; **b**, $\text{R} = 2,6\text{-}^i\text{Pr}_2\text{C}_6\text{H}_3$) with two equivalents of butyl lithium (BuLi) followed by two equivalents of ClSiMe_3 yields the silylated diamines $\text{R}(\text{Me}_3\text{Si})\text{N}(\text{CH}_2)_3\text{N}(\text{SiMe}_3)\text{R}$ (**2.9a,b**). The reaction of **2.9a,b** with TiCl_4 yields the dichloride complexes $[\text{RN}(\text{CH}_2)_3\text{NR}]\text{TiCl}_2$ (**2.10a,b**) and two equivalents of ClSiMe_3 . An X-ray study of **2.10b** ($\text{P2}_1/\text{n}$, $a = 9.771(1) \text{ \AA}$, $b = 14.189(1) \text{ \AA}$, $c = 21.081(2) \text{ \AA}$, $\beta = 96.27(1)^\circ$, $V = 2905.2(5) \text{ \AA}^3$, $Z = 4$, $T = 25^\circ\text{C}$, $R = 0.0701$, $R_w = 0.1495$) revealed a distorted tetrahedral geometry about titanium with the aryl groups lying perpendicular to the TiN_2 -plane. Complexes **2.10a,b** react with two equivalents of MeMgBr to give the dimethyl derivatives $[\text{RN}(\text{CH}_2)_3\text{NR}]\text{TiMe}_2$ (**2.11a,b**). An X-ray study of **2.11a** ($\text{P2}_12_12_1$, $a = 8.0955(10) \text{ \AA}$, $b = 15.288(4) \text{ \AA}$, $c = 16.909(3) \text{ \AA}$, $V = 2092.8(7) \text{ \AA}^3$, $Z = 4$, $T = 23^\circ\text{C}$, $R = 0.0759$, $R_w = 0.1458$) again revealed a distorted tetrahedral geometry about titanium with titanium-methyl bond lengths of $2.100(9) \text{ \AA}$ and $2.077(9) \text{ \AA}$. These titanium dimethyl complexes are active catalyst precursors for the polymerization of α -olefins, when activated with methylaluminoxane (MAO). Activities up to 350,000 g of poly(1-hexene)/mmol catalyst \cdot h were obtained in neat 1-hexene at 68°C . These systems actively engage in chain transfer to aluminum. Equimolar amounts of **2.11a** or **2.11b** and $\text{B}(\text{C}_6\text{F}_5)_3$ catalyze the living polymerization α -olefins. Polydispersities (M_w/M_n) as low as 1.05 were measured. Highly active living systems are obtained when **2.11a** is activated with $\{\text{Ph}_3\text{C}\}^+[\text{B}(\text{C}_6\text{F}_5)_4]^-$. A primary insertion mode (1,2 insertion) has been assigned based on isotopically labeling the initiator and purposeful termination of the polymer chain with iodine.

The addition of a pentane solution of complexes **2.11a,b** to a pentane solution of $\text{B}(\text{C}_6\text{F}_5)_3$ at 23°C yields an insoluble yellow-orange solid (**2.52a,b**) in nearly quantitative yield. Complexes **2.52a,b** are catalysts for the living polymerization of 1-hexene at 23°C . In the absence of monomer, complex **2.52b** slowly evolves methane over the course of several

hours to give a new pentane soluble derivative $[\text{RN}(\text{CH}_2)_3\text{NR}]\text{Ti}[\text{CH}_2\text{B}(\text{C}_6\text{F}_5)_2](\text{C}_6\text{F}_5)$ (**2.54b**) in quantitative yield as indicated by NMR spectroscopy. The molecular structure of **2.54b** was confirmed by X-ray crystallography ($\text{P}2_1/\text{n}$, $a = 20.292(2) \text{ \AA}$, $b = 11.253(2) \text{ \AA}$, $c = 23.459(2) \text{ \AA}$, $\beta = 114.967(7)^\circ$, $V = 4856(1) \text{ \AA}^3$, $Z = 4$, $T = 21^\circ\text{C}$, $R = 0.041$, $R_w = 0.034$). Complex **2.54b** is *inactive* for the polymerization of α -olefins.

The reaction of diamines **2.3b** with $\text{Zr}(\text{NMe}_2)_4$ yields the complex, $[\text{RN}(\text{CH}_2)_3\text{NR}]\text{Zr}(\text{NMe}_2)_2$ (**4.1b**), and two equivalents of NHMe_2 . Compound **4.1b** reacts with two equivalents of $[\text{Me}_2\text{NH}_2]\text{Cl}$ to yield the complex $[\text{RN}(\text{CH}_2)_3\text{NR}]\text{ZrCl}_2(\text{NHMe}_2)_2$ (**4.5b**) and in the presence of excess pyridine affords the complex $[\text{RN}(\text{CH}_2)_3\text{NR}]\text{ZrCl}_2\text{py}_2$ (**4.6b**). The base-free dichloride complex $[\text{RN}(\text{CH}_2)_3\text{NR}]\text{ZrCl}_2$ (**4.7b**) can be prepared from **4.1b** and excess ClSiMe_3 . The alkylation of compound **4.6b** or **4.7b** with two equivalents of MeMgBr , two equivalents of PhCH_2MgCl , and one equivalent of $\text{NaCp}(\text{DME})$ yields the alkyl derivatives $[\text{RN}(\text{CH}_2)_3\text{NR}]\text{ZrR}_2$ (**4.12a**, $\text{R} = \text{Me}$; **4.13b**, $\text{R} = \text{CH}_2\text{Ph}$) and $[\text{RN}(\text{CH}_2)_3\text{NR}]\text{Zr}(\eta^5\text{-C}_5\text{H}_5)\text{Cl}$ (**4.26b**), respectively. The reaction of two equivalents of $\text{PhMe}_2\text{CCH}_2\text{MgCl}$ with complex **4.6b** yields the η^2 -pyridyl complex $[\text{RN}(\text{CH}_2)_3\text{NR}]\text{Zr}(\eta^2\text{-N,C-NC}_5\text{H}_4)(\text{CH}_2\text{CMe}_2\text{Ph})$ (**4.20b**). An X-ray study of **4.20b** ($\text{P}\bar{1}$, $a = 10.146(2) \text{ \AA}$, $b = 12.336(2) \text{ \AA}$, $c = 16.723(2) \text{ \AA}$, $\alpha = 81.00(2)^\circ$, $\beta = 74.99(2)^\circ$, $\gamma = 76.24(2)^\circ$, $V = 1953.6(6) \text{ \AA}^3$, $Z = 2$, $T = 25^\circ\text{C}$, $R = 0.0951$, $R_w = 0.2287$) revealed an edge-capped tetrahedral geometry with the pyridyl nitrogen occupying the capping position. Complex **4.20b** is likely formed via proton abstraction from coordinated pyridine. The catalyst system **4.12b**/MAO polymerizes 1-hexene to a mixture of high polymer and oligomers. Activation with $\{\text{Ph}_3\text{C}\}[\text{B}(\text{C}_6\text{F}_5)_4]$ yields only oligomers ($n = 2\text{--}7$). Rapid β -hydride elimination precludes polymer formation in these systems.

Table of Contents

Abstract	ii
Table of Contents	iv
List of Tables	viii
List of Figures	x
List of Schemes	xiii
List of Abbreviations	xv
Acknowledgments	xviii
Dedication	xix
Chapter 1: Introduction	1
Historical Background	1
Introduction to Ziegler–Natta Catalysis	2
Heterogenous Catalysis	2
Homogenous Catalysis	4
Comparison between amide ligands and cyclopentadienyl ligands	8
History of Metal Amides	11
Synthesis of Early Transition Metal Amides	11
Transmetallation	11
Ammonium Halide Elimination	11
Transamination	12
Alkane Elimination	12
Other Elimination Reactions	13
Reactions of Metal Amides	13
Insertion reactions	14
Alkyne insertion	14
CX ₂ insertion, X = O, S	15
Protonolysis	15
Disproportionation and Conproportionation	16
Metathesis	17
Characterization of Metal Amides	19
Nuclear Magnetic Resonance Spectroscopy	19
X–Ray Crystallography	19
Research Proposal	21
References	24

Chapter 2: Chelating Diamide Complexes of Titanium.....	30
Introduction	30
Synthesis of New Diamines	31
Ethylene Linked diamines.....	31
Propylene Linked diamines.....	32
Butylene Linked Diamines.....	34
Propylene Linked Chelating Diamide Complexes of Titanium	37
Butylene Linked Chelating Diamide Complexes of Titanium.....	51
Ethylene Linked Chelating Diamide Complexes of Titanium	60
Ene-diamide complexes	65
Alternative ligand Systems	74
Rotameric Isomers of a Chelating Diamido Titanium Complex	77
Reaction of Titanium Complexes with Lewis Acids	81
Boron-Carbon Bond Cleavage	81
Attempted Preparation of an Electron Deficient Analogue to Tebbe's Reagent.....	88
Conclusions	93
Experimental	95
References	117
Chapter 3: Polymerization of α -olefins.....	121
Introduction	121
Metallocene Catalysts	123
Initiation	123
Aluminum activators.....	123
Borane activators.....	127
Propagation	130
Termination	132
β -hydride elimination	132
β -alkyl elimination	134
Chain transfer to cocatalyst.....	134
Living Polymerizations	135
Characterization of Polymers.....	137
Results and Discussion.....	139
Propylene Linked Diamides of Titanium	139

Living Polymerization of α -olefins	149
Ene-Diamide complexes of titanium	159
Other Diamide Catalyst Precursors	161
Conclusions	167
Experimental Details	168
References	173
Chapter 4: Chelating Diamide Complexes of Zirconium	180
Introduction	180
Results and Discussion	182
Polymerization Reactions	208
Conclusions	215
Experimental	217
References	226
Chapter 5: Chelating Diamide Complexes of Scandium	230
Introduction	230
Results and Discussion	231
Oligomerization of 1-hexene	233
Conclusions	234
Experimental	235
References	237
Chapter 6: Future Considerations	238
Cyclotrimerization of Alkynes	238
Dehydropolymerization of Silanes	239
Synthesis of Block Co-polymers	241
Potentially Stereoselective Catalysts	241
Single Component Catalysts	243
References	245
Appendix A: X-ray Crystallography	247

X-ray Crystallography of Complex 2.10b	247
X-ray Crystallography of Complex 2.11a	255
X-ray Crystallography of Complex 2.41a	261
X-ray Crystallography of Complex 2.54b •CH ₂ Cl ₂	268
X-ray Crystallography of Complex 4.20b	277
References:	285
Curriculum Vitae.....	286

List of Tables

Table 1.1:	Selected Metal–Amido bond distances and Angles	20
Table 2.1:	Selected bond lengths and angles for 2.10b	43
Table 2.2:	Selected bond lengths and angles for dimethyl complex 2.11a	46
Table 2.3:	Selected bond angles of diamide complexes of titanium	48
Table 2.4:	Selected bond distances and angles for complex 2.41a	71
Table 2.5:	Selected bond lengths and angles for 2.54b •CH ₂ Cl ₂	86
Table 3.1:	Polymerization of 1-Hexene	140
Table 3.2:	Living polymerization of α -olefins.....	150
Table 3.3:	Polymerization of 1-Hexene	155
Table 3.4:	Polymerization of 1-hexene with ene-diamide titanium complexes	160
Table 3.5:	Polymerization of 1-Hexene	162
Table 4.1:	Selected bond distances (Å) and angles (°)	200
Table A1.	Crystal Data and Experimental Details for complex 2.10b	248
Table A2:	Atomic coordinates (x 10 ⁴) and equivalent isotropic displacement parameters (Å ² x 10 ³) of complex 2.10b . U(eq) is defined as one third of the trace of the orthogonalized U _{ij} tensor.	250
Table A3.	Bond Lengths (Å) of Complex 2.10b	251
Table A4.	Bond Angles (°) of Complex 2.10b	252
Table A5.	Calculated Hydrogen Atom Positional (x 10 ⁴) and Thermal (x 10 ³) Parameters for complex 2.10b	253
Table A6.	Crystal Data and Experimental Details for complex 2.11a	256

Table A7.	Atomic coordinates ($\times 10^4$) and equivalent isotropic displacement parameters ($\text{\AA}^2 \times 10^3$) for complex 2.11a . $U(\text{eq})$ is defined as one third of the trace of the orthogonalized U_{ij} tensor.	258
Table A8.	Bond Distances (\AA) for complex 2.11a	259
Table A9.	Bond Angles($^\circ$) for complex 2.11a	259
Table A10.	Calculated Hydrogen Atom Positional ($\times 10^4$) and Thermal ($\times 10^3$) Parameters for complex 2.11a	260
Table A11.	Crystal Data and Experimental Details for complex 2.41a	262
Table A12.	Atomic coordinates ($\times 10^4$) and equivalent isotropic displacement parameters ($\text{\AA}^2 \times 10^3$) for complex 2.41a . $U(\text{eq})$ is defined as one third of the trace of the orthogonalized U_{ij} tensor.....	264
Table A13.	Bond Distances (\AA) for complex 2.41a	265
Table A14.	Bond Angles ($^\circ$) for complex 2.41a	266
Table A15.	Calculated Hydrogen Atom Positional ($\times 10^4$) and Thermal ($\times 10^3$) Parameters for complex 2.41a	267
Table A16.	Crystallographic data for 2.54b $\cdot\text{CH}_2\text{Cl}_2$	269
Table A17.	Atomic coordinates, B_{eq} and Occupancy Factors for complex 2.54b $\cdot\text{CH}_2\text{Cl}_2$	271
Table A18.	Bond Lengths(\AA) for complex 2.54b $\cdot\text{CH}_2\text{Cl}_2$	273
Table A19.	Bond Angles($^\circ$) for complex 2.54b $\cdot\text{CH}_2\text{Cl}_2$	274
Table A20.	Calculated hydrogen atom coordinates and B_{iso} for complex 2.54b $\cdot\text{CH}_2\text{Cl}_2$	276
Table A21.	Crystal Data and Experimental Details for complex 4.20b	278
Table A22.	Atomic coordinates ($\times 10^4$) and equivalent isotropic displacement parameters ($\text{\AA}^2 \times 10^3$) for complex 4.20b . $U(\text{eq})$ is defined as one third of the trace of the orthogonalized U_{ij} tensor.	280
Table A23.	Bond Distances(\AA) for complex 4.20b	281
Table A24.	Bond Angles($^\circ$) for complex 4.20b	282
Table A25.	Calculated Hydrogen Atom Positions ($\times 10^4$) and Thermal ($\times 10^3$) Parameters for complex 4.20b	283

List of Figures

Figure 1.1:	Structure of HDPE and LDPE	3
Figure 1.2:	Triad structures iso-, syndio- and atactic polypropylene	3
Figure 1.3:	Bonding modes of cyclopentadienyl ligand	9
Figure 1.4:	Bonding modes of amide ligands	10
Figure 1.5:	Electron count for various group 4 complexes used in olefin polymerizations	21
Figure 2.1:	Predicted N–Ti–N bite angle for chelating diamides	31
Figure 2.2:	Separation diagram for isolating diamine 2.3b	34
Figure 2.3:	Newman projections of the intermediate in the synthesis of the diamino ligands	35
Figure 2.4:	¹ H NMR spectrum of complex 2.10b	41
Figure 2.5:	Chem3D Plus representation of the molecular structure of 2.10b	42
Figure 2.6:	¹ H NMR spectrum of complex 2.11a	45
Figure 2.7:	Chem3D Plus representation of the molecular structure of 2.11a ...	46
Figure 2.8:	Possible dimeric structures of complexes 2.25a,b	58
Figure 2.9:	Chem 3D Plus drawing of complex 2.41a	70
Figure 2.10:	Alternative view of ene–diamide 2.41a	70
Figure 2.11:	Possible decomposition pathway for the alkylation of complexes 2.40a,c	73
Figure 2.12:	Possible geometrical isomers for complex 2.50d	79
Figure 2.13:	The two rotamers of complex 2.51d (propyl backbone omitted for clarity)	80
Figure 2.14:	¹ H NMR spectrum of complex 2.54b •CH ₂ Cl ₂	83
Figure 2.15:	Molecular structure of complex 2.54b •CH ₂ Cl ₂	85
Figure 3.1:	Titanium–ethylene bonding interactions	123

Figure 3.2:	Characterized cationic alkyl complexes.....	126
Figure 3.3:	Living homogeneous Ziegler–Natta polymerization catalysts.....	137
Figure 3.4:	Authentic η^6 -aryl complexes of group 4 metals.....	142
Figure 3.5:	^1H NMR spectrum of poly(1-hexene).....	143
Figure 3.6:	$^{13}\text{C}\{^1\text{H}\}$ NMR spectrum of poly(1-hexene).....	144
Figure 3.7:	Syndiotactic and isotactic pentads in poly(1-hexene).....	142
Figure 3.8:	Plot of M_n and M_w/M_n versus equivalents of MAO. Conditions: 6.8 mmol of 2.11b in 1 mL of pentane was added to MAO (400, 800, 1200, and 1600 equiv) in 9.0 g of 1-hexene and 1.0 g of toluene at 68°C and stirred for 10 s.	147
Figure 3.9:	Plot of activity (g poly(1-hexene)/mmol cat.·h) versus equivalents of MAO. Conditions: 6.8 mmol of 2.11b in 1 mL of pentane was added to MAO (400, 800, 1200, and 1600 equiv) in 9.0 g of 1- hexene and 1.0 g of toluene at 68°C and stirred for 10 s.	148
Figure 3.10:	M_n and M_w/M_n vs. time for the living polymerization of 1-hexene	152
Figure 3.11:	M_n vs. time for the living polymerization of 1-hexene.....	153
Figure 3.12:	Possible products from polymerization with $^{13}\text{C}_2$ - 2.11b / $\text{B}(\text{C}_6\text{F}_5)_3$.	157
Figure 3.13:	Possible stereoplacements formed in the first three insertions of 1- hexene	158
Figure 3.14:	Possible products from quenching polymerization of 1-hexene with I_2	158
Figure 3.15:	Proposed coordination of the double bond to the cationic alkyl	159
Figure 3.16:	Comparison of the symmetry elements of a syndiospecific catalyst precursor and <i>meso</i> - 2.50d	165
Figure 4.1:	Zirconocene complexes formed by aminolysis of $\text{Zr}(\text{NMe}_2)_4$	181
Figure 4.2:	^1H NMR spectrum of complex 4.1b	186
Figure 4.3:	Restricted rotation of 2,6-diisopropylphenyl group (propyl backbone omitted for clarity)	185
Figure 4.4:	Possible diastereomers in complex 4.5b	187

Figure 4.5:	Comparison of the kinetic protection afforded the nitrogen atoms in complex 4.1b and 4.2b	191
Figure 4.6	Variable temperature ^1H NMR of complex 4.12b	194
Figure 4.7:	The interconversion between η^2 and η^1 benzyl groups.....	195
Figure 4.8:	Mirror symmetry element associated with η^2 -pyridyl complex 4.20b	197
Figure 4.9:	^1H NMR spectrum of complex 4.20b	198
Figure 4.10:	Chem 3D Plus representations of complex 4.20b and the core of 4.20b	199
Figure 4.11:	Expected coupling constants for geminal and vicinal coupling.....	212
Figure A1:	Molecular Structure of Complex 2.10b	249
Figure A2:	Molecular structure of Complex 2.11a	257
Figure A3:	Molecular Structure of Complex 2.41a	263
Figure A4.	Molecular Structure of complex 2.54b • CH_2Cl_2	270
Figure A5:	Molecular Structure of Complex 4.20b	279

List of Schemes

Scheme 1.1:	Insertion into a metal–amido bond.....	14
Scheme 2.1:	Synthesis of an ethane bridged diamine.....	32
Scheme 2.2:	Transmetallation reaction between $\text{TiCl}_4(\text{THF})_2$ and dilithium diamide 2.7b	38
Scheme 2.3:	Silylation of diamides 2.7a,b followed by reaction with TiCl_4	40
Scheme 2.4:	Alkylation of the titanium dichlorides 2.10a,b	44
Scheme 2.5:	Synthesis of the trimethylsilyl derivatives of diamines 2.6a,b	52
Scheme 2.6:	Reaction of the magnesium salt 2.20a,b with $\text{TiCl}_4(\text{THF})_2$	55
Scheme 2.7:	Transamination of TiCl_4 with distannanes 2.21a,b	57
Scheme 2.8:	Synthesis of disilylamine 2.28b	60
Scheme 2.9:	Attempted alkane elimination reaction via precoordination of the diamine ligand.....	63
Scheme 2.10:	Reduction of Diazadienes 2.39a,c	69
Scheme 2.11:	Attempted synthesis of a xylyl linked diamide complex of titanium.....	75
Scheme 2.12:	Successful synthesis of a xylyl linked diamide complex of titanium.....	76
Scheme 2.13:	Synthesis of an unsymmetrically disubstituted diamine.....	78
Scheme 2.14:	Borane activation of dimethyl complexes 2.11a,b and possible reaction paths.....	82
Scheme 2.15:	Proposed intermediates in the formation of complex 2.54b	87
Scheme 2.16:	Addition of PMe_3 to complex 2.54b	88
Scheme 2.17:	Mechanism for the ROMP of Cycloolefins.....	89
Scheme 2.18:	Reaction of Tebbe's reagent with olefins.....	90
Scheme 2.19:	Polymerization of norbornene with the metallocyclobutane 2.64	91
Scheme 3.1:	Cossee–Arlman Mechanism.....	122

Scheme 3.2:	Activation of titanocene dichloride by diethylaluminum chloride ...	125
Scheme 3.3:	Activation with tetrafluoroborate salts	128
Scheme 3.4:	C–H activation of a tetraphenylborate anion	129
Scheme 3.5:	Possible modes of insertion for propene	131
Scheme 3.6:	Chain termination by β –hydrogen transfer	133
Scheme 3.7:	Chain termination by β –methyl transfer	134
Scheme 3.8:	Chain termination by transfer to co–catalyst	135
Scheme 4.1:	Proposed equilibrium in a sealed system between (BAIP) H_2 and Zr(NMe $_2$) $_4$	183
Scheme 4.2:	Synthesis of dichlorides from complex 4.1b	188
Scheme 4.3:	Alkylation of complex 4.7b	192
Scheme 4.4:	Formation of complex d_4 – 4.20b via an intermediate alkylidene complex	200
Scheme 4.5:	Formation of complex d_4 – 4.20b via alkane elimination	201
Scheme 4.6:	The activation of complex 4.12b with various co–catalysts	209
Scheme 4.7:	Possible modes of insertion of 1–hexene	211
Scheme 4.8:	Proposed products from the reaction of complex 4.12b with B(C $_6$ F $_5$) $_3$	214
Scheme 6.1:	The proposed mechanism of the dehydrocoupling of silanes	239
Scheme 6.2:	Oscillating metallocene catalysts	242
Scheme 6.3:	Potentially oscillating catalysts based on chelating diamido ligands (alkyl backbone removed for clarity).	243

List of Abbreviations

^1H	Proton	
$^1J_{\text{CH}}$	1 bond carbon-hydrogen coupling constant	
$^{11}\text{B}\{^1\text{H}\}$	Boron-proton decoupled	
$^{13}\text{C}\{^1\text{H}\}$	Carbon-proton decoupled	
^{19}F	Fluorine	
$^{31}\text{P}\{^1\text{H}\}$	Phosphorus-proton decoupled	
Å	Angstrom	
acac	Acetylacetonate	$(\text{CH}_3\text{CO})_2\text{CH}_2$
Ar	Substituted or unsubstituted aryl group	
BAED		$[\text{MeC}=\text{N}(2,6\text{-Et}_2\text{C}_6\text{H}_3)]_2$
BAIB		$\{[\text{CH}_2\text{CH}_2\text{N}(2,6\text{-}^i\text{Pr}_2\text{C}_6\text{H}_3)]_2\}^{2-}$
BAID		$[\text{MeC}=\text{N}(2,6\text{-}^i\text{Pr}_2\text{C}_6\text{H}_3)]_2$
BAIE		$\{[\text{CH}_2\text{N}(2,6\text{-}^i\text{Pr}_2\text{C}_6\text{H}_3)]_2\}^{2-}$
BAIP		$\{\text{CH}_2[\text{CH}_2\text{N}(2,6\text{-}^i\text{Pr}_2\text{C}_6\text{H}_3)]_2\}^{2-}$
BAMB		$\{[\text{CH}_2\text{CH}_2\text{N}(2,6\text{-Me}_2\text{C}_6\text{H}_3)]_2\}^{2-}$
BAMD		$[\text{MeC}=\text{N}(2,6\text{-Me}_2\text{C}_6\text{H}_3)]_2$
BAME		$\{[\text{CH}_2\text{N}(2,6\text{-Me}_2\text{C}_6\text{H}_3)]_2\}^{2-}$
BAMP		$\{\text{CH}_2[\text{CH}_2\text{N}(2,6\text{-Me}_2\text{C}_6\text{H}_3)]_2\}^{2-}$
Bu	Butyl	$[\text{CH}_3\text{CH}_2\text{CH}_2\text{CH}_2]^-$
cat.	Catalyst	
Cp	Cyclopentadienyl	$\eta^5\text{-C}_5\text{H}_5$
Cp*	Pentamethylcyclopentadienyl	$\eta^5\text{-C}_5\text{Me}_5$
DAD	Diazadiene	$\text{RN}=\text{CH}-\text{CH}=\text{NR}$
deg	Degrees	
DME	Dimethoxyethane	$\text{CH}_3\text{OCH}_2\text{CH}_2\text{OCH}_3$

EI	Electron Ionization	
η^n	Polyhapticity	
Et	Ethyl	$[\text{CH}_3\text{CH}_2]^-$
Et ₂ O	Diethylether	$\text{CH}_3\text{CH}_2\text{OCH}_2\text{CH}_3$
g	Grams	
GC-MS	Gas Chromatography–Mass Spectroscopy	
GPC	Gel Permeation Chromatography	
HDPE	High Density Polyethylene	
HMQC	Heteronuclear Multi-Quantum Coherence	
Hz	Hertz	
<i>i</i> Pr	Isopropyl	CHMe_2
LDPE	Low Density Polyethylene	
MAO	Methylaluminoxane	$(\text{MeAlO})_n$
Me	Methyl	CH_3^-
Mes	Mesityl	$[\text{2,4,6-Me}_3\text{C}_6\text{H}_2]^-$
MMAO	Modified methylaluminoxane	$(i\text{BuAlO})_m(\text{MeAlO})_n$
M_n	Number Average Molecular Weight	
mol	Mole	
mmol	Millimole	
M_w	Weight Average Molecular Weight	
m/z	Mass to charge ratio	
NMR	Nuclear Magnetic Resonance	
P	Polymer	
Ph	Phenyl	$[\text{C}_6\text{H}_5]^-$
ROMP	Ring-Opening Metathesis Polymerization	
s	Seconds	
SEC	Size exclusion chromatography	

THF	Tetrahydrofuran	$\overline{\text{O}(\text{CH}_2)_3}\text{CH}_2$
tmeda	N,N,N',N'-tetramethylethylenediamine	$(\text{CH}_3)_2\text{NCH}_2\text{CH}_2\text{N}(\text{CH}_3)_2$

Acknowledgments

I would like to express my deepest gratitude to Dave McConville for always having great ideas. His input during the course of this work and especially with the preparation and editing of this thesis was truly appreciated. His assiduous support will not be forgotten.

Many thanks go out to the various members of our research group for the support and wealth of knowledge they bestowed. I am indebted to Mr. Peter Borda for obtaining numerous micro analyses and to Liane Dirage for running countless NMR spectra. I would also like to thank Steve Rak and Brin Powell for all the work they did to help us set up our laboratory.

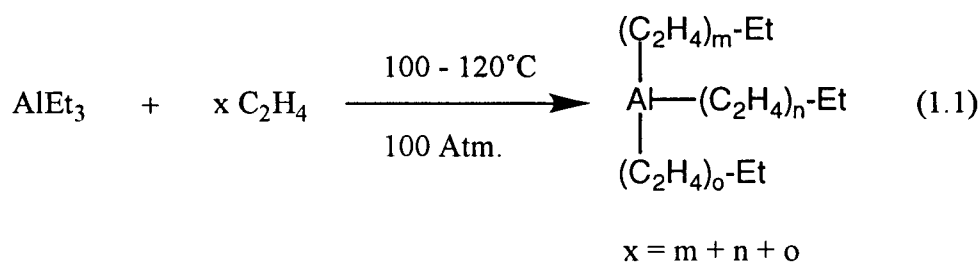
Last, but certainly not least, I am grateful for the inexhaustible support my parents have provided over all these years. None of this would have been possible without them.

For Mom and Dad

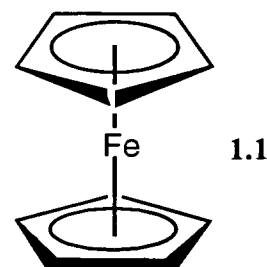
Chapter 1: Introduction

Historical Background

Although some organometallic compounds have been known for well over a hundred years, the development of the subject, especially of the organometallic chemistry of the transition elements is much more recent. The study of organometallic compounds has often contributed significantly to chemical theory and practice. For example, the preparation and investigation of the properties of ethylzinc iodide and of diethylzinc led Frankland to make the first clear statement of a theory of valency, in which he suggested that each element has a definite limiting combining capacity.¹ From a more practical standpoint, the discovery of the organomagnesium halides, or Grignard reagents, in 1900 provided readily handled and versatile intermediates for a variety of organic and organometallic syntheses. More recently, the discovery of aluminum alkyls, by Ziegler in 1950,²⁻⁴ has led to their use as catalysts for the large scale polymerization and oligomerization of olefins (eq. 1.1).

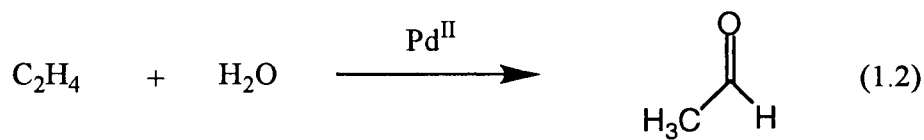


The chance synthesis of ferrocene (1.1), by Paulson in 1951, and the subsequent determination of its structure one year later has opened up a field of research of unforeseen variety. Normally, the cyclopentadienyl ligand coordinates to metals in an η^5 fashion and is formally a uninegative, six-electron donor, occupying three coordination sites. The stabilizing effects of cyclopentadienyl ligands were rapidly realized, and the organometallic chemistry of the transition metals has since been dominated by cyclopentadienyl complexes. The subsequent development of this



area of chemistry owes much to new methods of structure determination, especially nuclear magnetic resonance spectroscopy and X-ray crystallography.

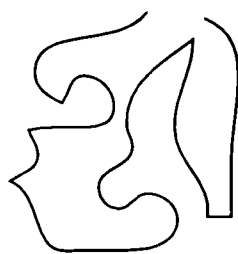
Organotransition metal complexes are now finding wide application as intermediates in many catalytic processes, some of which are used for the large scale conversion of carbon monoxide, hydrogen, alkenes and other small molecules into useful organic chemicals and materials. For example, the Wacker process in which alkenes are converted to aldehydes using a palladium catalyst (eq. 1.2).⁵



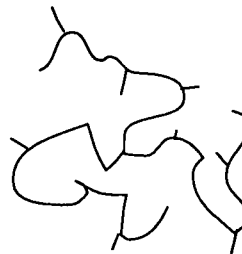
Introduction to Ziegler–Natta Catalysis

Heterogenous Catalysis

In 1953, Karl Ziegler and his group discovered the “Aufbaureaktion”, a process by which ethylene is oligomerized by a combination of aluminum alkyls and certain transition metals.⁶ Specifically, in the presence of aluminum alkyl activators, nickel salts catalyze the dimerization of ethylene, while zirconium and titanium halides catalyze the polymerization of ethylene to form linear high density polyethylene (HDPE) at atmospheric pressure. In contrast, low density polyethylene (LDPE) is prepared by free radical polymerization of ethylene. This process, which was developed by Imperial Chemical Industries (ICI) during the mid-1930s, required very high ethylene pressures > 1000 atm and temperatures around 200°C to produce long-chain branched material. The properties of HDPE are quite different from LDPE. Figure 1.1 shows the structures of HDPE and LDPE. HDPE consists of long linear strands of polyethylene with no branching while LDPE are long linear branched strands of polyethylene.



HDPE



LDPE

Figure 1.1: Structure of HDPE and LDPE

In 1954, Giulio Natta and co-workers found that the catalyst disclosed by Ziegler was able to polymerize propene to a partly crystalline polymer.⁷ This polymer was eventually shown to be a mixture of atactic and isotactic polypropylene (Figure 1.2). This discovery was so revolutionary that the terms 'isotactic' and 'atactic' had to be coined for this occasion. It was soon recognized that under the polymerization conditions, TiCl_4 and aluminum trialkyls react to form a brown modification of TiCl_3 (later found to be $\beta\text{-TiCl}_3$), which is insoluble in the reaction medium. This prompted Natta to explore the catalytic activity of preformed modifications of TiCl_3 (α , γ or δ) in hydrocarbon medium, in a mixture of aluminum trialkyls and aluminum dialkyl halides. These were the first generation Ziegler–Natta catalysts.⁸

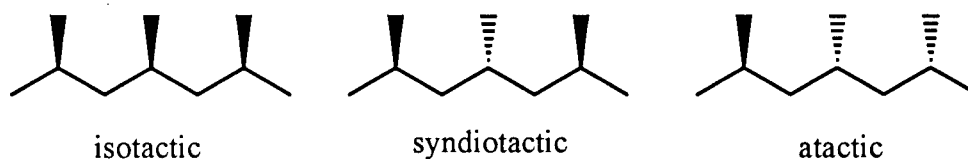


Figure 1.2: Triad structures iso-, syndio- and atactic polypropylene

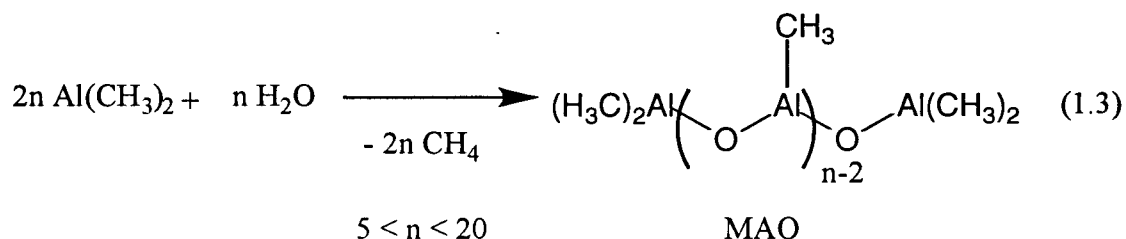
During the 1960's, it was well recognized that only transition metals with vacant coordination sites located at the catalyst surface were catalytically active.⁹ The second generation of Ziegler–Natta catalysts were typically low valent chromium and transition metal alkyls such as tetrabenzyl titanium or zirconium immobilized on silica or alumina surfaces. A major breakthrough in catalyst research occurred during the 1970's. Catalysts, supported on a MgCl_2 lattice, were developed which delivered extremely high yields and

high stereoselectivity. Magnesiumdichloride is isostructural to γ - TiCl_3 , used in the first generation Ziegler–Natta catalysts, and offers the identical coordination sites at the support surface.⁸ Therefore incorporation of the catalyst at the surface of the support is facile.

During the mid–1980's, the major focus of catalyst and process development was on controlled polymer formation. Polymers with controlled molecular weight distribution and comonomer incorporation were sought as modifiers of the mechanical properties of polymers. The discovery of novel high activity metallocene/MAO catalyst systems, or single-site catalysts (*vide infra*), was crucial to the development of new polyolefin materials. For the first time in the history of Ziegler–Natta catalysis, well-defined structures of catalytically active sites could be tailored to control molecular weight, stereo and regioselectivity, and comonomer sequence distribution. Single-site catalyst technology marked the beginning of a new era in polyolefin technology.

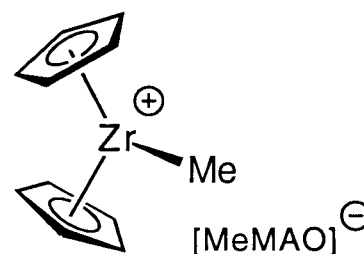
Homogenous Catalysis

Metallocene catalysts, e.g., Cp_2TiCl_2 activated with aluminum alkyls, are well known as traditional catalysts and were investigated during the late 1950's by Natta¹⁰ and Breslow.¹¹ In the early days of Ziegler–Natta catalysis such homogeneous catalysts were widely applied as model systems to elucidate the polyinsertion mechanisms of ethylene polymerization. However, these catalysts were unable to polymerize propylene. In 1973 Reichert and Meyer discovered that traces of water improved the $\text{Cp}_2\text{TiEtCl}/\text{EtAlCl}_2$ catalyst productivity's in ethylene polymerization.¹² Breslow and Long attributed this unusual finding to the formation of alumoxanes resulting from the partial hydrolysis of aluminum alkyls.¹³ At the end of the 1970's, Sinn and Kaminsky introduced high molecular weight methylalumoxanes, or MAO. This new class of aluminum activators are produced by the controlled hydrolysis of trimethylaluminum (eq. 1.3).^{14,15} The reaction of water with

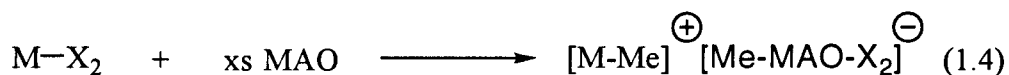


trimethylaluminum yields a rather complex reaction mixture containing linear, branched and cyclic MAO that still contains sizable amounts of trimethylaluminum.¹⁶

Since the discovery by Sinn and Kaminsky¹⁷ of the highly active dimethylzirconocene/methyl–alumoxane (MAO) system (1.2), the catalytic reactivity of homogeneous early transition metal metallocenes with ethylene and α -olefins has attracted considerable attention.¹⁷⁻²² These catalysts, known as single-site



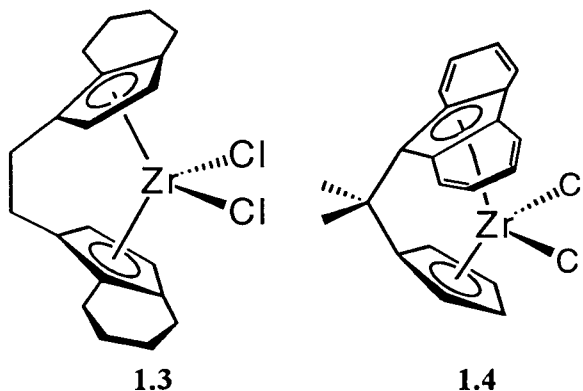
catalysts because there is a single active species in solution, are desirable for their ability to produce polymers with controllable stereoregularity and molecular weight. The role of MAO in activating these polymerizations is threefold. First, MAO can act as an alkylating agent effectively forming metal–alkyl moieties. Second, MAO acts as an alkyl abstractor thus removing an alkyl group and forming the metal cation (eq. 1.4). Third, MAO acts as a scavenger for water thus helping to dry reaction solvents and monomers.



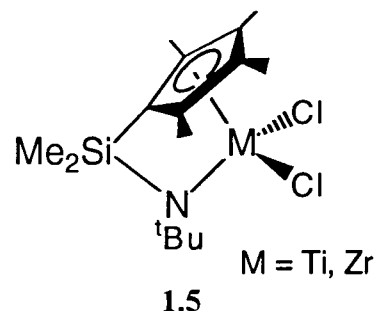
$\text{X} = \text{NR}_2, \text{R}, \text{halide}$

The next major advancement in single site catalysts was the development of bridged metallocenes, sometimes referred to as *ansa*-metallocenes. By application of the appropriate bridged metallocene, the molecular architecture of the resultant polyolefin can be controlled and the factors that influence the propagation and termination kinetics can be studied. For instance, the *ansa*-metallocene complexes developed by Brintzinger²¹ (1.3), and Ewen²²

(1.4), once activated by MAO, catalyze the polymerization of α -olefins in an isospecific and syndiospecific manner, respectively.

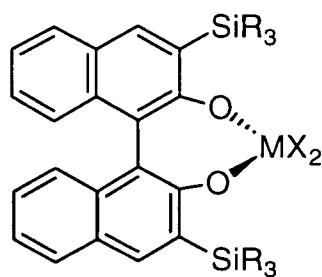


The investigation of complexes bearing alternative ligands for olefin polymerization is being explored extensively. Despite the diversity of new ligand environments recently discovered,²³⁻²⁶ few have proved amenable to α -olefin polymerization. Considerable attention has been given to 'constrained geometry' complexes (1.5), that contain a linked cyclopentadienyl-amide ligand. By replacing one Cp moiety with an amide group, the electron deficiency of the metal is necessarily increased, which results in a more electrophilic metal centre. Patent claims by The Dow Chemical Company²⁷ and Exxon Chemical Patents Inc.²⁸ have shown that titanium and zirconium complexes bearing this ligand type, once activated, are active single-site polymerization catalysts. Ethylene, 1-hexene, 1-octene, and 4-methyl-1-pentene homopolymers as well as ethylene/propene, /1-hexene, /1-octene, /styrene, and /norbornene co-polymers have been formed with these systems.

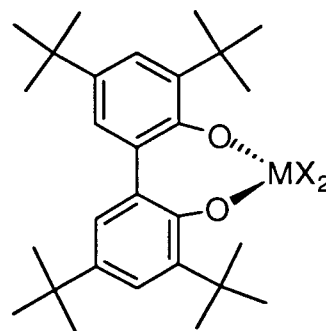


Schaverien has recently shown that chelating binaphtholate (1.6) and biphenolate (1.7) complexes of titanium and zirconium are active catalyst precursors for the polymerization of ethylene and α -olefins.²⁵ Furthermore, by substituting the 3 and 3'

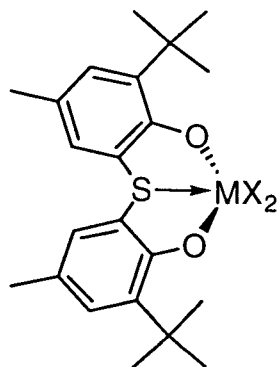
positions of compound **1.6** with sterically demanding auxiliary groups ($\text{SiR}_3 = \text{SiMe}_3$, SiMePh_2 , SiPh_3), the ligand environment can be tuned for regio and stereospecific polymerization of α -olefins. The 'Sumitomo catalyst' (**1.8**) has also been reported to be highly active for the polymerization of ethylene and propene when activated with MAO.^{29,30} Okuda has prepared syndiotactic polystyrene and ethylene/styrene copolymers from complex **1.9** and MAO.³¹



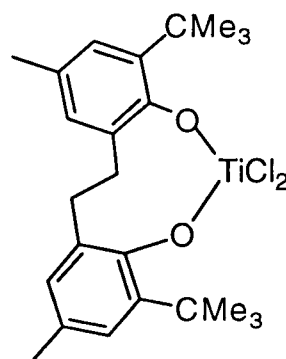
1.6



1.7



1.8

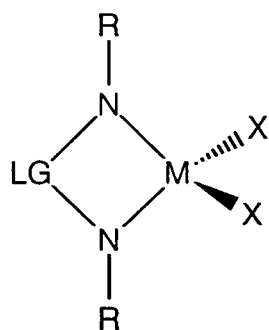


1.9

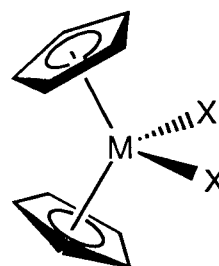


A recent patent by Exxon Chemical Patents Inc. noted that the bis(amide) complex $[(\text{Me}_3\text{Si})_2\text{N}]_2\text{ZrCl}_2$ is an active catalyst for the polymerization of ethylene and α -olefins when activated with MAO.³² The polymers obtained from α -olefins with this system are about 90% isotactic. This is likely a result of chain-end control where the orientation of the incoming monomer is influenced by the propagating chain. One uncertainty with studying

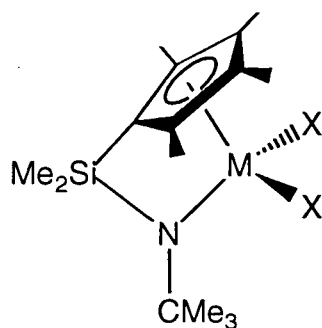
these complexes is that the N–M–N angle can vary considerably during the polymerization. If a chelating diamide ligand was used the N–M–N angle could be controlled. Complexes of the general type (RN–LG–NR)MX₂ (**1.10**; LG = linking group)³³⁻⁵¹ containing bidentate bis(amide) ligands are promising systems for applications in catalysis due to their relationship to the well studied metallocene analogues Cp₂MX₂ (**1.11**),⁵²⁻⁵⁴ constrained geometry (C₅R₄SiR₂NR)MX₂ complexes (**1.12**),^{27,28,55-57} and bis(amide) (R₂N)₂MX₂ complexes (**1.13**).^{32,58-68}



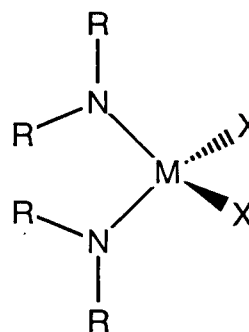
1.10



1.11



1.12



1.13

Comparison between amide ligands and cyclopentadienyl ligands

Cyclopentadienyl (Cp) ligands can formally donate two, four or six electrons to a metal centre (Figure 1.3). Cp ligands are typically considered relatively soft donors. Cp ligands are generally bound to metals in a η^5 fashion thus donating six electrons. However, the Cp ligand can 'slip' to η^3 coordination thereby donating only four electrons.

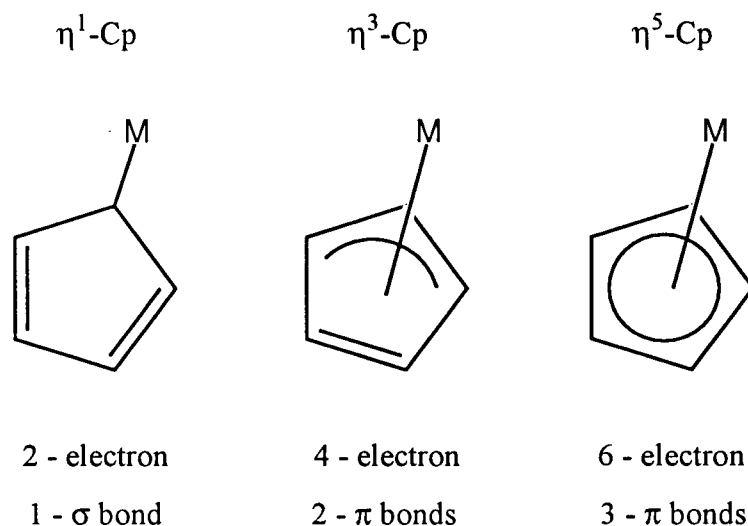


Figure 1.3: Bonding modes of cyclopentadienyl ligand

Amide ligands, like the alkoxide ligands, are relatively hard donors. They usually show multiple bonding character to early transition metals through the donation of four electrons. Two electrons form a σ -bond with the metal and two more electrons are donated into an empty d-orbital on the metal making up the π -bond (figure 1.4). In this case the nitrogen atom is sp^2 hybridized and has trigonal planar geometry. Although the metal-nitrogen bond may be considered a double bond, there is free rotation about the $M\text{-NR}_2$ bond. The amide ligand can also donate four electrons by bridging two different metals. The $\mu\text{-NR}_2$ ligand donates two electrons to each metal for a total of four electrons. In this case the nitrogen will have tetrahedral geometry. A third way in which an amide may bond to a metal is through only one σ -bond. This may give pyramidal geometry at nitrogen. It also results in a non-bonding lone pair of electrons on the nitrogen. More commonly however, the lone pair will be delocalized as a ligand centred non-bonding pair resulting in trigonal geometry about nitrogen.

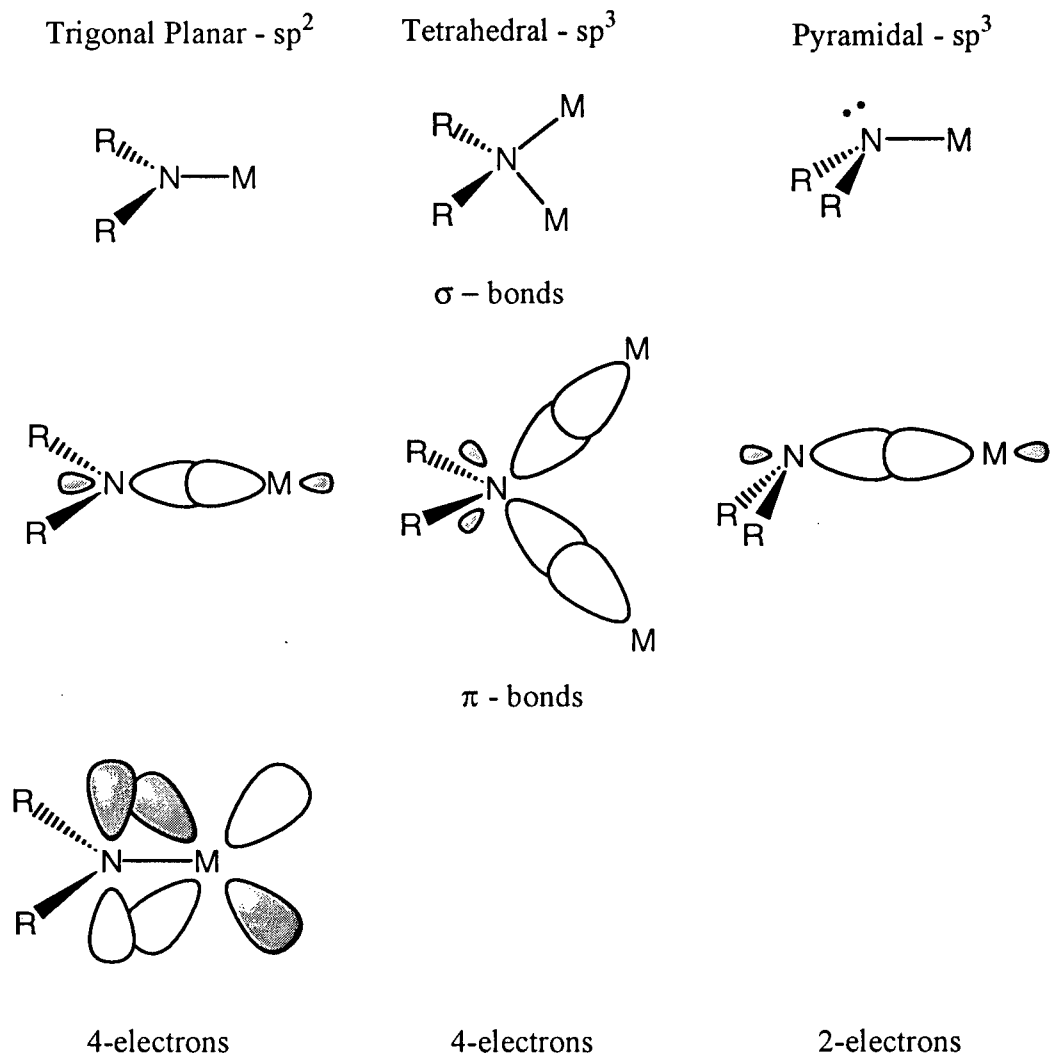
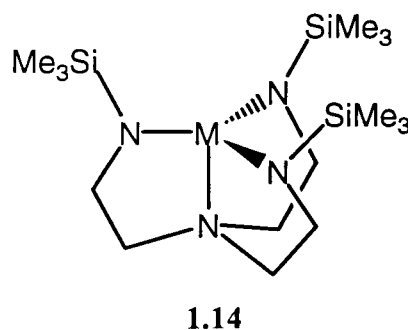


Figure 1.4: Bonding modes of amide ligands

For example, the triamidoamine ligand $[(\text{Me}_3\text{SiNCH}_2\text{CH}_2)_3\text{N}]^{3-}$ bonds to early transition metals in a tetradentate manner (1.14).⁶⁹ The three-fold symmetry exerted by the ligand dictates that only two metal- $\text{N}_{\text{eq}} \pi$ -bonds are possible since one linear combination of the three 'in plane' p-orbitals on the three equatorial nitrogens is a ligand centred nonbonding orbital. Therefore, the $[\text{N}_3\text{N}]^{3-}$ ligand can only contribute a maximum of 12 electrons to the metal in a C_3 -symmetric environment. Dialkylamide ligands will generally bind to early transition metals donating 4 electrons. Therefore,



1.14

the amide ligand, when compared with the Cp ligand, donates two less electrons rendering the metal more electrophilic in nature.

History of Metal Amides

The first metal amide, bis(dimethylamido)zinc, was reported by Frankland in 1856.⁷⁰ It wasn't until 80 years later that the first transition metal amide complex, tetrakis(diphenylamido)titanium, was reported by Derner and Fernelius.⁷¹ In 1959, Bradley and Thomas initiated a study of the reactions of transition metal chlorides with lithium dialkylamides.⁷² Since that time, amido complexes of almost all the elements have been synthesized, with the early transition metal amides being more common than the late transition metal amides. This can be rationalized in terms of the bonding properties of the dialkylamide ligand, which acts as both a two-electron σ -donor and a two-electron π -donor. The amide ligand will form stronger bonds to early transition metals containing empty d-orbitals than with later transition metals which have filled or partially filled d-orbitals. The following discussion relates primarily to early transition metals.

Synthesis of Early Transition Metal Amides

Transmetallation

The most common route to metal-amido complexes is through transmetallation (eq. 1.5). The dialkyl amides of Ti(IV),⁷³ Zr (IV)⁷³, Hf(IV),⁷⁴ V(IV),^{74,75} Nb(IV)^{76,77},

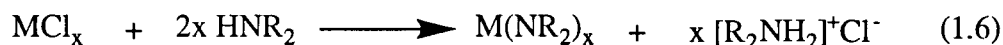


Nb(V),^{74,76} Ta(V),^{74,78} Cr(III),⁷⁹⁻⁸¹ Mo(III),⁸²⁻⁸⁴ Mo(IV),⁸⁵ W(III)⁸⁶⁻⁸⁸ and W(VI)⁸⁹ were isolated in this way.

Ammonium Halide Elimination

The elimination of $[\text{R}_2\text{NH}_2]^+\text{Cl}^-$ has also been used to synthesize metal amides. The dialkylamides of Ti(IV),⁹⁰⁻⁹² Zr(IV),⁹³ V(IV),⁹⁴ Nb(V)⁹⁵, Ta(V),⁹⁶ W(IV)⁹⁷, W(V),⁹⁷ and

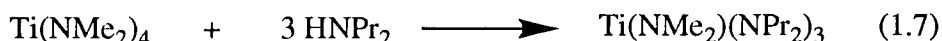
W(VI)⁹⁷⁻⁹⁹ have been synthesized in this fashion (eq. 1.6). The major drawback with this



method is the formation of a donor ligand complex. For example $[\text{MoCl}_3(\text{NHMe}_2)(\text{NMe}_2)_2]$ is formed as a result of coordination of dimethylamine to the metal centre.¹⁰⁰ Therefore the use of sterically demanding alkyl groups is required to prevent the coordination of the amine.

Transamination

Transamination reactions are usually used to generate heteroleptic amide complexes. The steric bulk of the exchanging amine determines the degree of substitution. For smaller dialkylamines, the greater the substitution (eq. 1.7), whereas for larger dialkylamines the



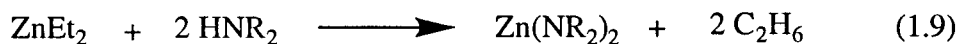
substitution will be limited (eq. 1.8).⁷³ The primary driving force for these reactions is the



elimination of a volatile amine. In general, the more volatile amine is displaced from the metal centre. As noted above, since an amine is being generated the possibility exists for the formation of mixed amide-amine metal complexes.

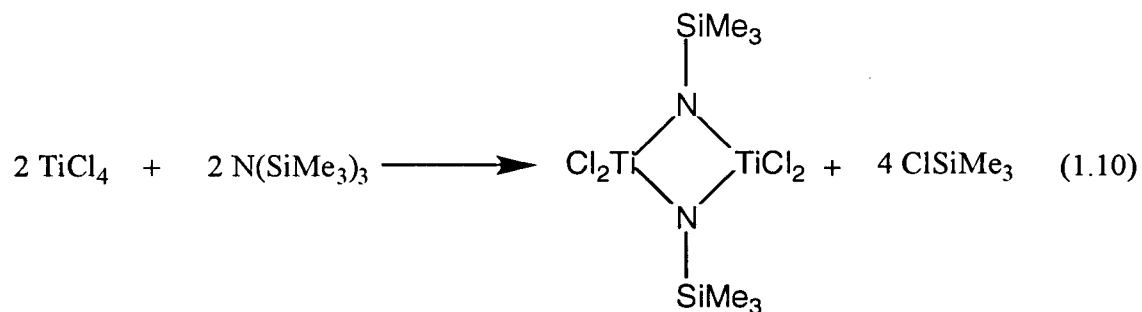
Alkane Elimination

The elimination of alkanes offers some advantages over the transamination reaction or the elimination of ammonium halide salts. The alkane being generated is unreactive towards the products of the reaction and does not have any donor functionality. This route was used by Frankland to synthesize the first metal amide bis(dimethylamido)zinc (eq. 1.9).⁷⁰ The lack of suitable metal alkyls has limited the use of this route and only lately has it found expanded utility.^{46,50}



Other Elimination Reactions

The elimination of chlorotrimethylsilane and chlorotrimethylstannane is also a route to metal–amide formation. The reaction of tris(trimethylsilyl)amine with TiCl_4 results in the initial formation of the imine $[(\text{Me}_3\text{Si})\text{N}=\text{TiCl}_2]$ and two equivalent of chlorotrimethylsilane followed by dimerization (eq. 1.10).¹⁰¹ These reactions usually require heat, however, the



elimination of chlorotrimethylstannane should occur at lower temperatures than the silane analogues since the $\text{Sn}-\text{N}$ bond strength is less than the $\text{Si}-\text{N}$ bond strength.¹⁰²

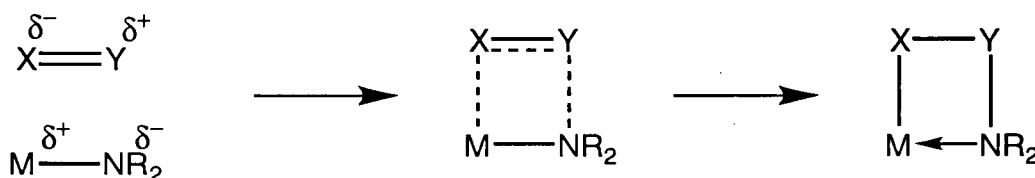
Reactions of Metal Amides

The reactivity of a metal–amide bond is determined by its polarity and bond strength, in other words, it depends on the overlap of the metal–ligand orbitals. The polarization of a metal amide bond is $\text{M}^{\delta+}-\text{N}^{\delta-}$. Many reactions can occur at the metal–amide bond. These include insertion reactions, protonolysis, con- and disproportionation, and elimination reactions.

Insertion reactions

One of the most common organometallic reactions is the insertion reaction. The insertion reaction is concerted and proceeds by way of a four-centred transition state (Scheme 1.1). The compound to be inserted must first align along the direction of polarity of

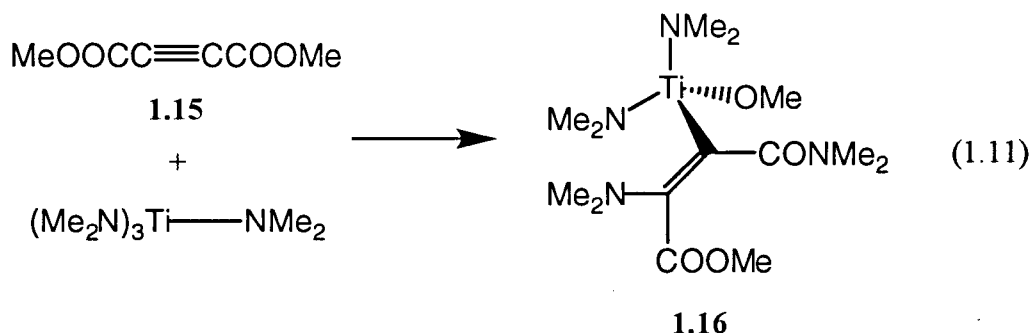
Scheme 1.1: Insertion into a metal–amido bond



the metal–amide bond. This will lead to a four-centred transition state which then proceeds to the insertion product in a concerted fashion. In some cases the resulting amine may remain coordinated to the metal.

Alkyne insertion

Simple aliphatic alkynes do not react with metal–amide bonds. Electron withdrawing substituents on the alkynes are required for these insertion reactions to occur. For example, addition of dimethylacetylenedicarboxylate **1.15** to $\text{Ti}(\text{NMe}_2)_4$ leads to insertion into the triple bond concomitant with amination of the ester group to give complex **1.16** (eq. 1.11).¹⁰²

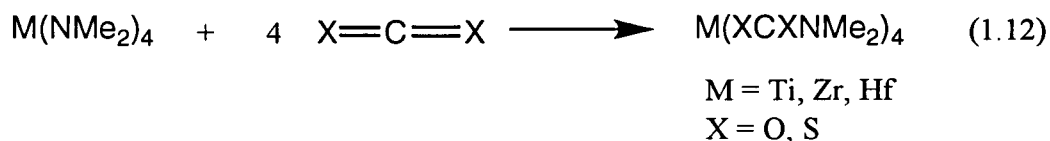


Formation of the titanium alkoxide provides the thermodynamic driving force needed for this

reaction to occur. The low reactivity of alkynes probably reflects the strength of the carbon–carbon triple bond.

CX₂ insertion, X = O, S

Insertion of carbon dioxide and carbon disulfide occurs much more readily than does alkyne insertion. The carbon–oxygen and carbon–sulfur bond is strongly polarized with a δ^+ on the carbon atom and a δ^- on oxygen or sulfur. Furthermore, the formation of a metal–oxygen or metal–sulfur bond, provides a thermodynamic driving force for these reactions. Addition of four equivalents of CX₂ to Ti(NMe₂)₄ results in clean insertion into the four titanium–amide bonds to give either the carbamate (X = O) or sulfamate (X = S) (eq. 1.12).¹⁰³⁻¹⁰⁵

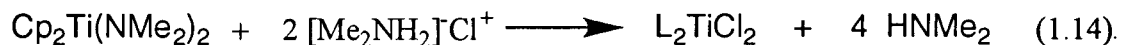


Protonolysis

Metal–amide bonds are highly susceptible to protonolysis. Equation 1.13 shows



the general method of protonolysis. The accessibility of electrons in the π -bond of the metal amide is crucial to this type of reaction. As the steric bulk of the dialkylamide is increased the rate of protonolysis will be reduced. It is possible to selectively protonate one type of amide over another. Usually the proton source is an ammonium salt (e.g. [Me₂NH₂]⁺Cl[−]) or an anilinium salt (e.g. [C₆H₅NMe₂H]⁺Cl[−]). Addition of dimethylammonium chloride to Cp₂Ti(NMe₂)₂ generates the dichloride and four equivalents of dimethylamine (eq. 1.14).⁶⁸



A key driving force for these reactions is the formation of dimethylamine, which is a gas, and can be removed from the reaction. The transamination reaction is also an example of protonolysis of an metal–amido group (eq. 1.7 and 1.8).

The proton source does not have to come from an ammonium salt. Terminal alkynes are sufficiently acidic to protonate the amide groups of $\text{Cp}_2\text{Zr}(\text{NMe}_2)_2$ to give the bis(acetylide) and two equivalents of dimethylamine (eq. 1.15).¹⁰⁶ Cyclopentadiene is



also acidic enough to protonate a dimethylamine on $[\text{Ti}(\text{NMe}_2)_3]_2$ to give the mono(Cp) complex $\text{CpTi}(\text{NMe}_2)_2$ (eq. 1.16).¹⁰⁴



Alcohols are also a common source of protons. The alcoholysis of $\text{Ti}(\text{NMe}_2)_4$ and $\text{Zr}(\text{NMe}_2)_4$ occurs rapidly at room temperature to give the tetraalkoxides and four equivalents of dimethylamine (eq. 1.17).⁷³



$\text{M} = \text{Ti, Zr}$

$\text{R} = \text{Me, Et, } ^i\text{Pr}$

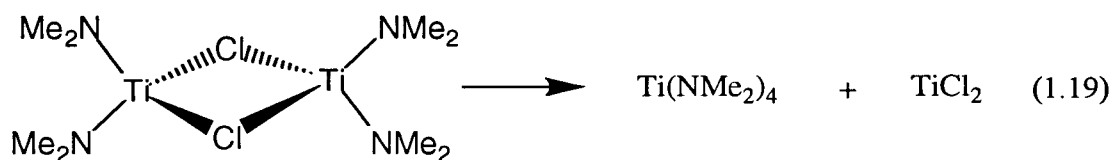
Disproportionation and Conproportionation

A disproportionation reaction occurs when a single reactant reacts to give two different products. One example of such a reaction is the disproportionation of $\text{Zr}(\text{NMe}_2)_2\text{Cl}_2$ to $\text{Zr}(\text{NMe}_2)_4$ and ZrCl_4 (eq. 1.18). This reaction occurs rapidly at room

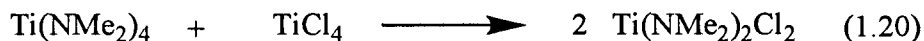


temperature and makes the synthesis of $\text{Zr}(\text{NMe}_2)_2\text{Cl}_2$ possible only at low temperatures.⁷² This disproportionation occurs with no change in the formal oxidation state of the metal. It is possible to have autoredox in a disproportionation reaction where the complex is both

oxidized and reduced to form two new products. This is most common among lower oxidation state metal amides. The Ti(III) dimer $[\text{Ti}(\text{NMe}_2)_2\text{Cl}]_2$ disproportionates to $\text{Ti}^{\text{IV}}(\text{NMe}_2)_4$ and $\text{Ti}^{\text{II}}\text{Cl}_2$ when gentle heating is applied (eq. 1.19).¹⁰⁴ Similar reactions are observed for V(III)¹⁰³ and Cr(III)⁸¹ tris(amides).



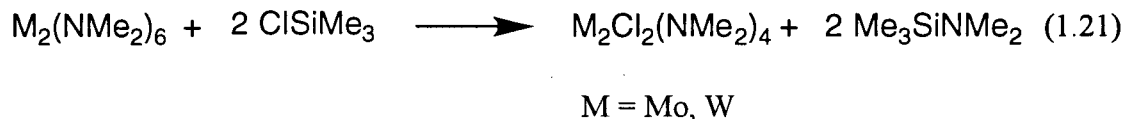
A conproportionation reaction occurs when two reactants are reacted to give a single product. An example of this reaction is shown in eq. 1.20. The reaction between



equal amounts of $\text{Ti}(\text{NMe}_2)_4$ and TiCl_4 causes the conproportionation to occur to give $\text{Ti}(\text{NMe}_2)_2\text{Cl}_2$ in nearly quantitative yield.¹⁰⁷ Conversely, $\text{Ti}(\text{NMe}_2)_2\text{Cl}_2$ cannot be prepared in high yield from TiCl_4 and two equivalents of LiNMe_2 .

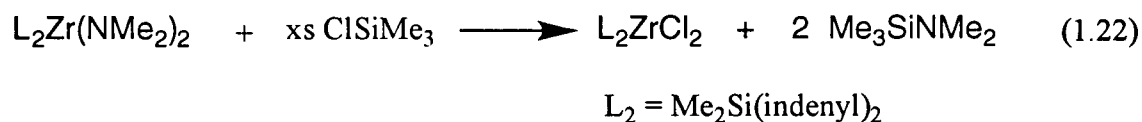
Metathesis

Metathesis reactions of metal amides are very similar to the insertion reactions discussed previously. They typically involve the elimination of smaller relatively stable molecules. The π -bond between the metal and the amido group must be available to the incoming reagent. Very bulky amides are therefore less reactive. The first reported use of this reaction was to obtain the dichlorides $\text{M}_2\text{Cl}_2(\text{NMe}_2)_4$ from $\text{M}_2(\text{NMe}_2)_6$ ($\text{M} = \text{Mo}, \text{W}$) (eq. 1.21) and ClSiMe_3 .¹⁰⁸ The driving force for these reactions is the formation of a

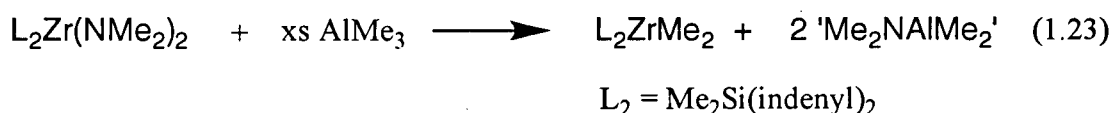


strong bond between silicon and nitrogen. More recently, however, Jordan has used this

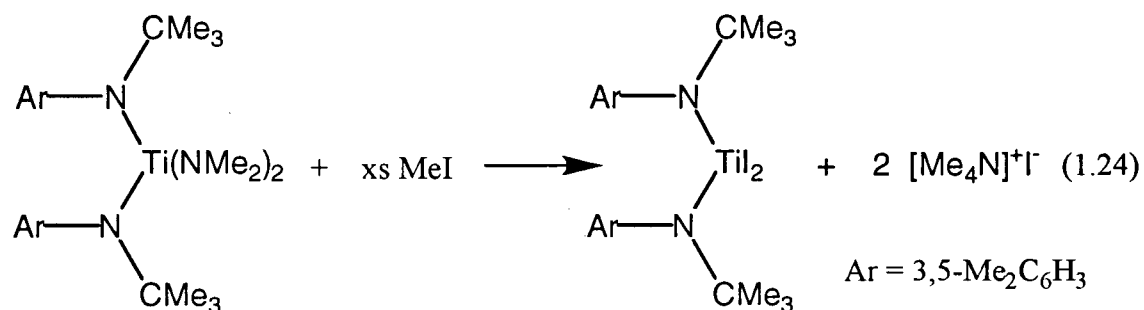
mode of reactivity to obtain *rac*-Me₂Si(indenyl)₂ZrCl₂ from the bis(dimethylamido) derivative (eq. 1.22).¹⁰⁹



Metathesis reactions are not only limited to reaction with chlorotrimethylsilane. The addition of excess trimethylaluminum to *rac*-Me₂Si(indenyl)₂Zr(NMe₂)₂ results in the direct formation of the dimethyl derivative (eq. 1.23).¹⁰⁹



Methyl iodide is also a common reagent used to obtain metal-iodides.¹¹⁰ This type of reaction is a non-protic alternative to the use of amine hydrohalides. Cummins has recently used methyl iodide in the selective cleavage of titanium dimethylamide bonds. The reaction results in the replacement of the dimethylamide groups by iodide and gives tetramethylammonium iodide as a solid byproduct (eq. 1.24).^{111,112} Precipitation of [Me₄N]I



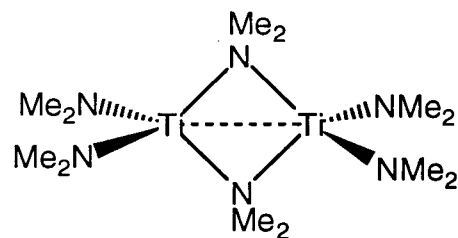
is the driving force for these reactions. Although the starting material is a mixed amide complex, the other amido ligands are protected from methylation due to the large *t*-butyl and 3,5-dimethylphenyl groups.

Characterization of Metal Amides

Nuclear Magnetic Resonance Spectroscopy

The advent of modern instrumentation for nuclear magnetic resonance (NMR) spectroscopy has resulted in an easy and convenient method for the characterization of diamagnetic metal–amides. In general, a downfield shift is observed in the ^1H NMR spectrum of metal amide complexes versus the free amine. For example, the methyl groups of dimethylamine are observed at 2.18 ppm in the ^1H NMR spectrum while the same methyl resonances in $\text{Ti}(\text{NMe}_2)_4$ and $\text{Zr}(\text{NMe}_2)_4$ occur at 3.04 ppm and 2.90 ppm, respectively. Heteroleptic complexes also experience a downfield shift as observed by ^1H NMR spectroscopy. The methyl resonances of $(\text{Me}_2\text{N})_2\text{TiCl}_2$ occur at 3.10 ppm. Similar downfield chemical shifts are observed for the methyl carbon resonances in the $^{13}\text{C}\{^1\text{H}\}$ NMR spectrum.

Proton NMR spectroscopy can also be useful to elucidate fluxional behaviour in metal–amido complexes. For example, the methyl groups of the titanium dimer $[\text{Ti}(\text{NMe}_2)_3]_2$ (1.17) appear as a sharp singlet in the room temperature ^1H NMR spectrum.



1.17

However, in the low temperature (-80°) ^1H NMR spectrum they appear as two singlets in a 2:1 ratio. This is consistent with four terminal dimethylamido and two bridging dimethylamido groups. At warmer temperatures, interconversion between the two sites is occurring rapidly. As a result, the time averaged NMR spectrum is observed at room temperature.

X-Ray Crystallography

Many metal–amide complexes have been characterized through the use of single crystal X-ray diffraction. This technique becomes important when characterizing

paramagnetic complexes in which it is difficult to gain useful structural information from their NMR spectra. Table 1.1 contains a representative example of some metal–nitrogen bond distances and N–M–N angles.

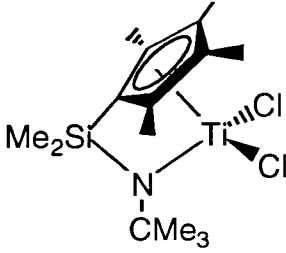
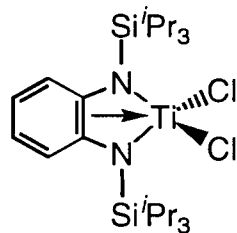
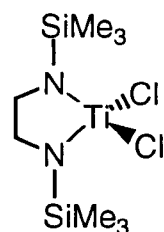
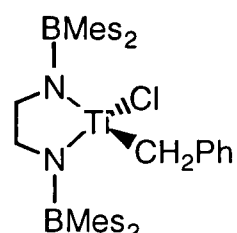
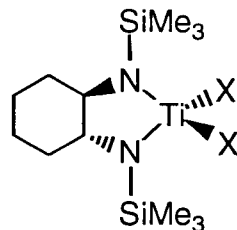
Metal Amide	N–M–N (deg)	M–N (Å)	Ref.
$[(\text{Me}_3\text{Si})_2\text{N}]_2\text{Ti}(\text{CH}_2\text{Ph})_2$	120.6(1)	1.931(3)	65
	107.6 (Cp–M–N)	1.907(4)	57
	92.6(2)	1.878(4)	33
	91.0(1)	1.844(2)	43
	89.2(2)	1.894(6)	35
	X = Cl 91.97(8) X = CH ₂ Ph 93.0(2)	1.879(1) 1.836(2)	46

Table 1.1: Selected Metal–Amido bond distances and Angles

Research Proposal

The design and synthesis of well-defined olefin polymerization catalysts has developed rapidly in the last fifteen years with the group 4 metallocene class of compounds receiving considerable attention.^{53,113,114} Detailed studies in this area have been concerned with the way in which the stereoregularity, catalytic activity, and co-monomer incorporation can be altered with changes to the Cp ligand(s). The active species in these polymerizations is believed to be a cationic alkyl derivative $[\text{Cp}_2\text{MR}]^+$ ($\text{M} = \text{Ti}, \text{Zr}$).¹¹⁵ Although these complexes will polymerize ethylene with high activity, the homopolymerization of α -olefins and co-polymerizations of ethylene/ α -olefin is relatively slow. This is largely due to the fact that two cyclopentadienyl groups render the metal centre relatively inaccessible to α -olefins. In contrast, linked Cp-amide derivatives 'constrained geometry', such as $[(\eta^5\text{-C}_5\text{Me}_4)\text{SiMe}_2(\text{NCMe}_3)]\text{ML}_n$ ($n = 2$; $\text{M} = \text{Ti}, \text{Zr}, \text{Hf}$; $n = 1$; $\text{M} = \text{Sc}$; $\text{L} = \text{halide or alkyl}$), readily incorporate α -olefins.^{27,28} By replacing one of the cyclopentadienyl ligands with an amide group the metal is now rendered more electrophilic. The amide group can formally donate a maximum of four electrons to the metal versus six electrons for the cyclopentadienyl group (Figure 1.5). By linking the cyclopentadienyl ligand to the amide the metal is made more accessible to α -olefins.

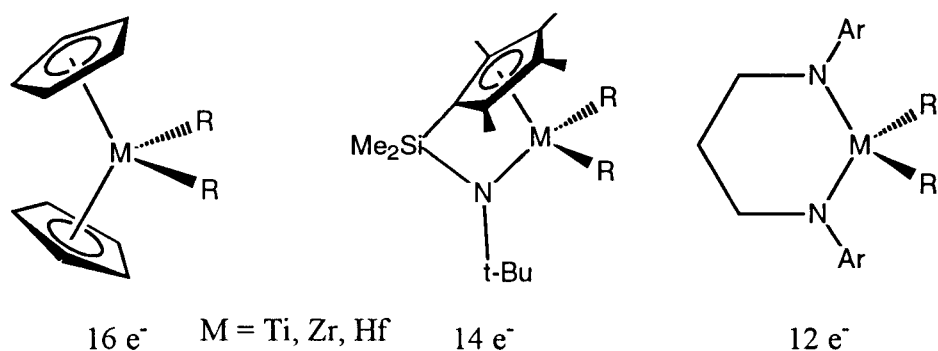


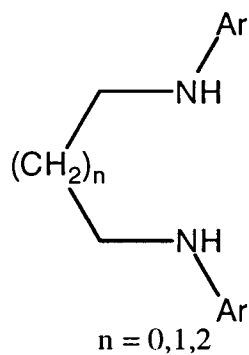
Figure 1.5: Electron count for various group 4 complexes used in olefin polymerizations

Given the success of the 'constrained geometry' ligands, there is considerable interest in the use of chelating diamide ligands in olefin polymerization catalysis.^{33,35,38,43-45,47} By

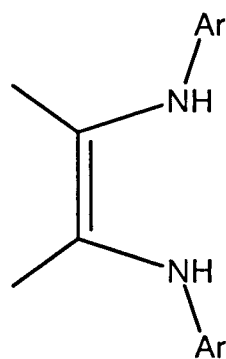
replacing the second Cp moiety with an amide donor, the formal electron count at the metal centre is necessarily reduced (Fig. 1.5). This results in an even more electrophilic catalyst. Although the chemistry of diamide complexes of the group 4 metals have been studied at length, their use as olefin polymerization catalysts has not been examined extensively. The first example of a diamide complex in the role of an α -olefin polymerization catalyst occurred in 1992. It was shown that the diamide complex $[(\text{Me}_3\text{Si})_2\text{N}]_2\text{ZrCl}_2$,⁵⁸ when activated with MAO, was able to polymerize propylene to 90% isotactic poly(propylene).³²

A number of chelating diamide complexes of the group 4 metals have been prepared,^{38-40,58,116-119} however, most contain silyl substituents at nitrogen and many have not been evaluated as α -olefin polymerization catalysts. The drawback to silyl substituents at nitrogen is that some complexes bearing silylated amides are prone to C-H activation.⁴⁴ Judicious choice of substitution at the nitrogen atom is therefore very important. The groups should be large enough to prevent dimer formation but not too large as to prevent access to the metal centre and, they should be unreactive towards metallation.

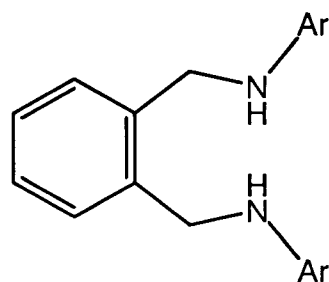
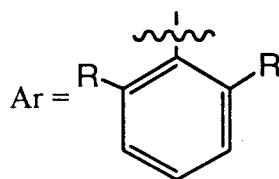
Chelate ring size is also an important consideration when designing bidentate diamide ligands. By controlling the bite angle of the N-M-N bonds, it may be possible to control which orbitals on the metal interact with the ligand and hence tune the chemistry of the bis(amide) complexes. Furthermore, if the N-M-N angle is too small, dimer formation would be unavoidable. With all these factors in mind, a series of bulky chelating diamines that incorporate voluminous 2,6-substituted phenyl groups at nitrogen were designed. The first diamine designed was to have the nitrogens joined through a simple aliphatic chain (1.18). The diamines were designed to have two, three or four methylene groups linking the two nitrogens. A second class of diamines was designed to have an unsaturated link between the two nitrogens (1.19). This raises the possibility that the double bond in the ligand may help stabilize the metal through π -donation into an empty metal d-orbital. A third diamine was designed with an *ortho*-xylyl group linking the two nitrogens (1.20).



1.18



1.19



1.20

The synthesis and characterization of a number of group 4 and group 3 metal complexes bearing these diamines (as dianionic diamide ligands) will be reported in the following chapters. A rich diversity of chemistry has been observed for these complexes including the polymerization of α -olefins,^{41,42,120} C-H activation,^{34,121} and C-B activation.¹²²

References

- (1) Frankland, J. *J. Chem. Soc.* **1857**, 419.
- (2) Ziegler, K.; Gellert, H.-G. *Justus Liebigs Ann. Chem.* **1950**, 567, 185.
- (3) Ziegler, K.; Gellert, H.-G. *Justus Liebigs Ann. Chem.* **1950**, 567, 179.
- (4) Ziegler, K.; Gellert, H.-G. *Angew. Chem.* **1952**, 64, 323.
- (5) Parshall, G. W. *Homogeneous Catalysis*; Wiley: New York, 1980.
- (6) Ziegler, K. In Bulg. Pat. 533 362: 1953.
- (7) Natta, G.; Pino, P.; Corradini, P.; Danusso, F.; Mantica, E.; Moraglio, G. *J. Am. Chem. Soc.* **1955**, 77, 1708.
- (8) Mülhaupt, R. In *Ziegler Catalysts*; G. Fink, R. Mülhaupt and H. H. Brintzinger, Ed.; Springer-Verlag: New York, 1995.
- (9) Rodriguez, L. A. M.; Gabant, J. A. *J. Polym. Sci., Part A-1* **1965**, 4, 1971.
- (10) Natta, G.; Pino, P.; Mazzanti, P.; Giannini, U. *J. Am. Chem. Soc.* **1957**, 79, 2975.
- (11) Breslow, D. S.; Newburg, N. R. *J. Am. Chem. Soc.* **1957**, 79, 5072.
- (12) Reichert, K. H.; Meyer, K. R. *Makromol. Chem.* **1973**, 169, 163.
- (13) Long, W. P.; Breslow, D. S. *Justus Liebigs Ann. Chem.* **1975**, 463.
- (14) Kaminsky, W.; Kopf, J.; Sinn, H.; Vollmer, H.-J. *Angew. Chem., Int. Ed. Engl.* **1976**, 15, 630.
- (15) Anderson, A.; Cordes, H.-G.; Herwig, J.; Kaminsky, W.; Merck, A.; Mottweiler, R.; Pein, J.; Sinn, H.; Vollmer, H.-J. *Angew. Chem., Int. Ed. Engl.* **1976**, 15, 630.
- (16) Sinn, H.; Bliemeister, J.; Clausnitzer, D.; Tikwe, L.; Winter, H.; Zarncke, O. In *Transition Metals and Organometallics as Catalysts for Olefin Polymerization* Springer-Verlag: Berlin, 1988; pp 257.
- (17) Sinn, H.; Kaminsky, W.; Vollmer, H.-J.; Woldt, R. *Angew. Chem., Int. Ed. Engl.* **1980**, 19, 390.
- (18) Jordan, R. F. *Adv. Organomet. Chem.* **1991**, 32, 325.
- (19) Marks, T. J. *Acc. Chem. Res.* **1992**, 25, 57.
- (20) Jordan, R. F.; Bajgur, C. S.; Willett, R.; Scott, B. *J. Am. Chem. Soc.* **1986**, 108, 7410.

- (21) Kaminsky, W.; Kulper, K.; Brintzinger, H. H.; Wild, F. R. W. P. *Angew. Chem., Int. Ed. Engl.* **1985**, *24*, 507.
- (22) Ewen, J. A. *J. Am. Chem. Soc.* **1984**, *106*, 6355.
- (23) Hughes, A. K.; Meetsma, A.; Teuben, J. H. *Organometallics* **1993**, *12*, 1936.
- (24) Mu, Y.; Piers, W. E.; MacGillivray, L. R.; Zaworotko, M. K. *Polyhedron* **1995**, *14*, 1.
- (25) van der Linden, A.; Schaverien, C. J.; Meijboom, N.; Ganter, C.; Orpen, A. G. *J. Am. Chem. Soc.* **1995**, *117*, 3008.
- (26) Black, D. G.; Swenson, D. C.; Jordan, R. F.; Rogers, R. D. *Organometallics* **1995**, *14*, 3539.
- (27) Stevens, J. C.; Timmers, F. J.; Wilson, D. R.; Schmidt, G. F.; Nickias, P. N.; Rosen, R. K.; Knight, G. W.; Lai, S. Y. In (Dow) European Patent Application EP-416-815-A2: March 13, 1991.
- (28) Canich, J. A. In (Exxon) European Patent Application EP-420-436-A1: April 4, 1991.
- (29) Miyatake, T.; Mizunuma, K.; Seki, Y.; Kakugo, M. *Makromol. Chem., Rapid Comm* **1989**, *10*, 349.
- (30) Miyatake, T.; Mizunuma, K.; Kakugo, M. *Makromol. Chem., Macromol. Symp.* **1993**, *66*, 203.
- (31) Fokken, G.; Spaniol, T. P.; Okuda, J.; Sernetz, F. G.; Mülhaupt, R. *Organometallics* **1997**, *16*, 4240.
- (32) Canich, J. A.; Turner, H. W. In (Exxon) PCT Int. Appl. WO 92/12162: July 23, 1992.
- (33) Aoyagi, K.; Gantzel, P. K.; Kalai, K.; Tilley, T. D. *Organometallics* **1996**, *15*, 923.
- (34) Scollard, J. D.; McConville, D. H.; Vittal, J. J. *Organometallics* **1995**, *14*, 5478.
- (35) Warren, T. H.; Schrock, R. R.; Davis, W. M. *Organometallics* **1996**, *15*, 562.
- (36) Bol, J. E.; Hessen, B.; Teuben, J. H.; Smeets, W. J. J.; Spek, A. L. *Organometallics* **1992**, *11*, 1981.
- (37) Herrmann, W. A.; Denk, M.; Scherer, W.; Klingan, F. R. *J. Organomet. Chem.* **1993**, *444*, C21.
- (38) Herrmann, W. A.; Denk, M.; Albach, R. W.; Behm, J.; Herdtweck, E. *Chem. Ber.* **1991**, *124*, 683.
- (39) Bürger, H.; Beiersdorf, D. *Z. Anorg. Allg. Chem.* **1979**, *459*, 111.

- (40) Bürger, H.; Geschwandtner, W.; Liewald, G. R. *J. Organomet. Chem.* **1983**, *259*, 145.
- (41) Scollard, J. D.; McConville, D. H.; Vittal, J. J. *Macromolecules* **1996**, *29*, 5241.
- (42) Scollard, J. D.; McConville, D. H. *J. Am. Chem. Soc.* **1996**, *118*, 10008.
- (43) Tinkler, S.; Deeth, R. J.; Duncalf, D. J.; McCamley, A. *J. Chem. Soc. Chem. Comm.* **1996**, 2623.
- (44) Horton, A. D.; de With, J.; van der Linden, A. J.; van de Weg, H. *Organometallics* **1996**, *15*, 2672.
- (45) Cloke, F. G. N.; Geldbach, T. J.; Hitchcock, P. B.; Love, J. B. *J. Organomet. Chem.* **1996**, *506*, 343.
- (46) Tsuie, B.; Swenson, D. C.; Jordan, R. F. *Organometallics* **1997**, *16*, 1392.
- (47) Clark, H. C. S.; Cloke, F. G. N.; Hitchcock, P. B.; Love, J. B.; Wainwright, A. P. *J. Organomet. Chem.* **1995**, *501*, 333.
- (48) Cloke, F. G. N.; Hitchcock, P. B.; Love, J. B.; Wainwright, A. P. *J. Chem. Soc. Dalton Trans.* **1995**, 25.
- (49) Guérin, F.; McConville, D. H.; Payne, N. C. *Organometallics* **1996**, *15*, 5085.
- (50) Guérin, F.; McConville, D. H.; Vittal, J. J. *15* **1996**, 5586.
- (51) Male, N. A. H.; Thornton-Pett, M.; Bochmann, M. *J. Chem. Soc. Dalton Trans.* **1997**, 2487.
- (52) Guram, A. S.; Jordan, R. F. In *Comprehensive Organometallic Chemistry*; 2nd ed.; M. F. Lappert, Ed.; Pergamon: Oxford, 1995; Vol. 4; pp 589-625.
- (53) Brintzinger, H. H.; Fischer, D.; Mülhaupt, R.; Rieger, B.; Waymouth, R. M. *Angew. Chem., Int. Ed. Engl.* **1995**, *34*, 1143.
- (54) Cardin, D. J.; Lappert, M. F.; Raston, C. L. *Chemistry of Organo-Zirconium and Hafnium Compounds*; Halsted Press: New York, 1986.
- (55) Devore, D. D.; Timmers, F. J.; Hasha, D. L.; Rosen, R. K.; Marks, T. J.; Deck, P. A.; Stern, C. L. *Organometallics* **1995**, *14*, 3132.
- (56) du Plooy, K. E.; Moll, U.; Wocadlo, S.; Massa, W.; Okuda, J. *Organometallics* **1995**, *14*, 3129.
- (57) Carpenetti, D. W.; Kloppenburg, L.; Kupec, J. T.; Peterson, J. L. *Organometallics* **1996**, *15*, 1572.

- (58) Andersen, R. A. *Inorg. Chem.* **1979**, *18*, 2928.
- (59) Andersen, R. A. *J. Organomet. Chem.* **1980**, *192*, 189.
- (60) Planalp, R. P.; Anderson, R. A.; Zalkin, A. *Organometallics* **1983**, *2*, 16.
- (61) Bürger, V. H.; Wiegler, K. Z. *Anorg. Allg. Chem.* **1973**, *398*, 257.
- (62) Bürger, V. H.; Neese, H. J. Z. *Anorg. Allg. Chem.* **1969**, *370*, 275.
- (63) Bürger, V. H.; Klüss, C.; Neese, H. J. Z. *Anorg. Allg. Chem.* **1971**, *381*, 198.
- (64) Scoles, L.; Minhas, R.; Duchateau, R.; Jubb, Y.; Gambarotta, S. *Organometallics* **1994**, *13*, 4978.
- (65) Minhas, R. K.; Scoles, L.; Wong, S.; Gambarotta, S. *Organometallics* **1996**, *15*, 1113.
- (66) Herrmann, W. A.; Huber, N. W.; Behm, J. *Chem. Ber.* **1992**, *125*, 1405.
- (67) Horton, A. D.; de With, J. J. *J. Chem. Soc. Chem. Comm.* **1996**, 1375.
- (68) Bradley, D. C.; Chisholm, M. H. *Acc. Chem. Res.* **1976**, *9*, 273.
- (69) Schrock, R. R. *Acc. Chem. Res.* **1997**, *30*, 9.
- (70) Frankland, E. *Proc. Roy. Soc.* **1856**, *8*, 502.
- (71) Derner, D. C.; Fernelius, W. C. Z. *Anorg. Chem.* **1935**, *221*, 83.
- (72) Bradley, D. C.; Thomas, I. M. *Proc. Chem. Soc., London* **1959**, 225.
- (73) Bradley, D. C.; Thomas, I. M. *J. Chem. Soc. Part A* **1960**, 3857.
- (74) Bradley, D. C.; Gitlitz, M. H. *J. Chem. Soc. Part A* **1969**, 980.
- (75) Thomas, I. M. *Can. J. Chem.* **1971**, *39*, 1386.
- (76) Bradley, D. C.; Thomas, I. M. *Can. J. Chem.* **1962**, *40*, 449.
- (77) Bradley, D. C.; Chisholm, M. H. *J. Chem. Soc. Part A* **1971**, 1511.
- (78) Bradley, D. C.; Thomas, I. M. *Can. J. Chem.* **1962**, *40*, 1355.
- (79) Basi, J. S.; Bradley, D. C.; Chisholm, M. H. *Proc. Chem. Soc., London* **1963**, 305.
- (80) Alyea, E. C.; Basi, J. S.; Bradley, D. C.; Chisholm, M. H. *J. Chem. Soc. Chem. Comm.* **1968**, 495.
- (81) Basi, J. S.; Bradley, D. C.; Chisholm, M. H. *J. Chem. Soc. Part A* **1971**, 1433.

- (82) Chisholm, M. H.; Reichert, W. W. *J. Am. Chem. Soc.* **1974**, *96*, 1249.
- (83) Chisholm, M. H.; Cotton, F. A.; Frenz, B. A.; Reichart, W. W.; Shive, L. *J. Chem. Soc. Chem. Comm.* **1974**, 480.
- (84) Chisholm, M. H.; Cotton, F. A.; Frenz, B. A.; Reichart, W. W.; Shive, L.; Stults, B. R. *J. Am. Chem. Soc.* **1976**, *98*, 4469.
- (85) Bradley, D. C.; Chisholm, M. H. *J. Chem. Soc. Part A* **1971**, 274.
- (86) Chisholm, M. H.; Cotton, F. A.; Extine, M.; Stults, B. R.; Troup, J. M. *J. Am. Chem. Soc.* **1975**, *97*, 1242.
- (87) Chisholm, M. H.; Extine, E. *J. Am. Chem. Soc.* **1975**, *97*, 5625.
- (88) Chisholm, M. H.; Cotton, F. A.; Extine, M.; Stults, B. R. *J. Am. Chem. Soc.* **1976**, *98*, 4477.
- (89) Bradley, D. C.; Chisholm, M. H.; Heath, C. E.; Hursthouse, M. B.
- (90) Antler, M.; Laubengayer, A. W. *J. Am. Chem. Soc.* **1955**, *77*, 5250.
- (91) Cowdell, R. T.; Fowles, G. W. A. *J. Chem. Soc.* **1960**, 2522.
- (92) Trost, B. M. *Can. J. Chem.* **1952**, *30*, 842.
- (93) Drake, J. E.; Fowles, G. W. A. *J. Chem. Soc.* **1960**, 1498.
- (94) Fowles, G. W. A.; Pleass, C. M. *J. Chem. Soc.* **1957**, 1674.
- (95) Fowles, G. W. A.; Pleass, C. M. *J. Chem. Soc.* **1957**, 2078.
- (96) Fuggle, J. C.; Sharp, D. W. A.; Winfield, J. M. *J. Chem. Soc. Dalton Trans.* **1972**, 1766.
- (97) Brisdon, B. J.; Fowles, G. W. A.; Osborne, B. P. *J. Chem. Soc.* **1962**, 1330.
- (98) Majid, A.; McLean, R. R.; Sharp, D. W. A.; Winfield, J. M. *Z. Anorg. Allg. Chem.* **1971**, 385, 65.
- (99) Majid, A.; Sharp, D. W. A.; Winfield, J. M.; Handby, I. *J. Chem. Soc. Dalton Trans.* **1973**, 1876.
- (100) Edwards, D. A.; Fowles, G. W. A. *J. Chem. Soc.* **1961**, 24.
- (101) Alcock, N. W.; Pierce-Butler, M.; Willey, G. R. *J. Chem. Soc. Dalton Trans.* **1976**, 707.

- (102) Chandra, G.; Jenkins, A. D.; Lappert, M. F.; Sricastava, R. C. *J. Chem. Soc. Part A* **1970**, 2550.
- (103) Alyea, E. C.; Bradley, D. C.; Lappert, M. F.; Sanger, A. R. *J. Chem. Soc. Chem. Comm.* **1969**, 1064.
- (104) Lappert, M. F.; Sanger, A. R. *J. Chem. Soc. Part A* **1971**, 874.
- (105) Lappert, M. F.; Sanger, A. R. *J. Chem. Soc. Part A* **1971**, 1314.
- (106) Jenkins, A. D.; Lappert, M. F.; Srivastava, R. C. *J. Organomet. Chem.* **1970**, *23*, 165.
- (107) Benzing, E.; Kornicker, W. *Chem. Ber.* **1961**, *94*, 2263.
- (108) Akiyama, M.; Chisholm, M. H.; Cotton, F. A.; Extine, W. M.; Murillo, C. A. *Inorg. Chem.* **1977**, *16*,
- (109) Christopher, J. N.; Diamond, G. M.; Jordan, R. F. *Organometallics* **1996**, *15*, 4038.
- (110) Schultz, H.; Folting, K.; Huffman, C. J.; Streib, W. E.; Chisholm, M. H. *Inorg. Chem.* **1993**, *32*, 6056.
- (111) Johnson, A. R.; Wanandi, P. W.; Cummins, C. C.; Davis, W. M. *Organometallics* **1994**, *13*, 2907.
- (112) Johnson, A. R.; Davis, W. M.; Cummins, C. C. *Organometallics* **1996**, *15*, 3825.
- (113) Bochmann, M. *J. Chem. Soc. Dalton Trans.* **1996**, 255.
- (114) Mohring, P. C.; Coville, N. J. *J. Organomet. Chem.* **1994**, *479*, 1.
- (115) Jordan, R. F. *J. Chem. Edu.* **1988**, *65*, 285.
- (116) Bürger, H.; Wiegel, K.; Thewalt, U.; Schomburg, D. *J. Organomet. Chem.* **1975**, *87*, 301.
- (117) Bürger, H.; Wiegel, K. *Z. Anorg. Allg. Chem.* **1976**, *419*, 157.
- (118) Brauer, D. J.; Bürger, H.; Wiegel, K. *J. Organomet. Chem.* **1978**, *150*, 215.
- (119) Brauer, D. J.; Bürger, H.; Essig, E.; Geschwandtner, W. *J. Organomet. Chem.* **1980**, *190*, 343.
- (120) Scollard, J. D.; McConville, D. H.; Payne, N. C.; Vittal, J. J. *J. Mol. Cat. Chemical* **1997**, Accepted for publication.
- (121) Scollard, J. D.; McConville, D. H.; Vittal, J. J. *Organometallics* **1997**, *16*, 4415.
- (122) Scollard, J. D.; McConville, D. H.; Rettig, S. J. *Organometallics* **1997**, *16*, 1810.

Chapter 2: Chelating Diamide Complexes of Titanium

Introduction

Enormous advances have been made in the last decade in the design and synthesis of single-site catalysts for the polymerization of α -olefins.¹ The vast majority of these catalysts are metallocene derivatives, although some are known to contain one cyclopentadienyl ring and a pendant amido ligand.²⁻⁷ Recently, however, complexes containing a chelating diamido ligand have received considerable attention as potential Ziegler-Natta catalysts.⁸⁻¹⁶ When studying chelating diamido ligands there are a couple of factors which are important to consider. They are 1) the thermodynamic and kinetic stability of complexes bearing this type of ancillary ligand, and 2) the electronic factors involved in the reactivity of these compounds. The kinetic stability of chelating diamido complexes will be determined from the steric bulk of the ancillary ligand. The bulk of the chelating ligand can be changed by varying the substitution at the nitrogen atom. The electronic factors which govern the reactivity of these complexes can be studied by changing the size of the chelate ring. The N-M-N 'bite angle' will determine the orbital interactions between the metal and the ligand, and hence the energies of frontier molecular orbitals can be varied. With this in mind, a series of ligands were designed to study the thermodynamic, kinetic and electronic aspects of chelating diamide ancillaries. A quick review of the literature^{13,14,17} and molecular modeling studies¹⁸ have shown that, for an ethane bridged diamide, the N-Ti-N bond angle should be approximately 90°. This angle will increase to approximately 100° for a propane bridge and finally to approximately 110° for the butane bridged diamide (Figure 2.1).

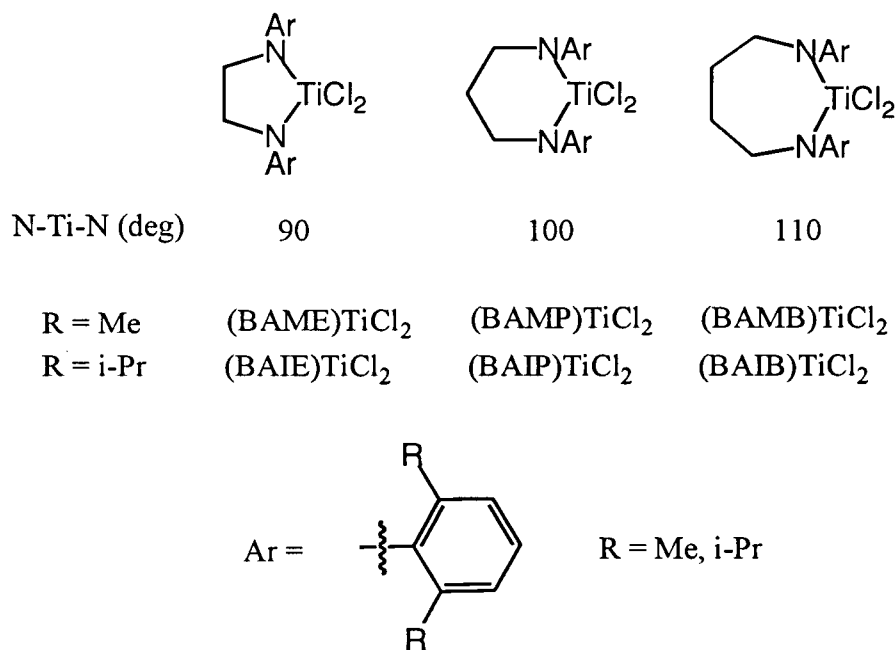


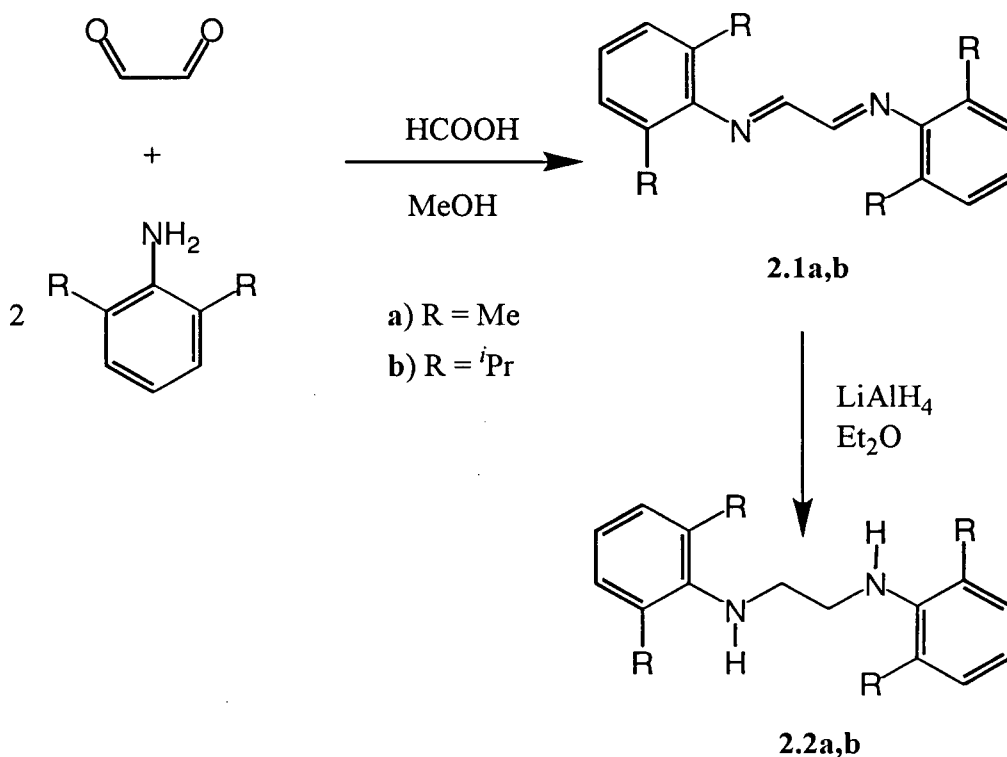
Figure 2.1: Predicted N–Ti–N bite angle for chelating diamides

Synthesis of New Diamines

Ethylene Linked diamines

Synthesis of the ethane bridged diamine was carried out in two steps. A catalytic amount of formic acid was added to a solution of two equivalents of 2,6–dimethylaniline or 2,6–diisopropylaniline and 1,2–ethanedial in methanol to form the yellow bisimines **2.1a,b** in greater than 80% yield (Scheme 2.1).¹⁹ Compounds **2.1a,b** were then reduced with lithium aluminumhydride in diethyl ether to obtain the diamines **2.2a,b** in quantitative yields. Diamines **2.2a,b** are white, highly crystalline solids which can be recrystallized from hexanes. The attempted direct synthesis of diamines **2.2a,b** from 1,2–dibromoethane and two equivalents of lithium anilide resulted in intractable products.

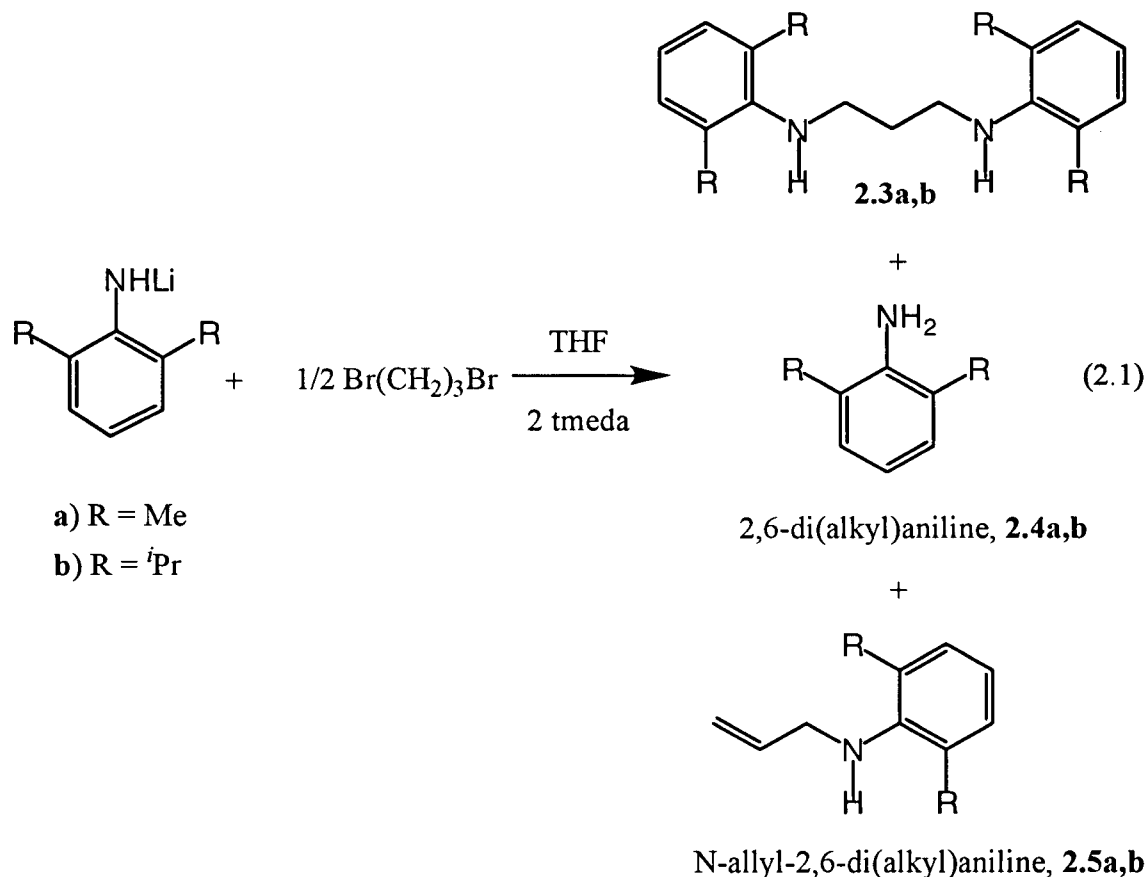
Scheme 2.1: Synthesis of an ethane bridged diamine



Propylene Linked diamines

Synthesis of the propane linked diamine **2.3a,b** was achieved in a single step by quenching two equivalents of 2,6-dimethylolithianilide or 2,6-diisopropylolithianilide, generated *in situ* from the reaction of the appropriate substituted aniline with butyllithium, with one equivalent of 1,3-dibromopropane (eq. 2.1). This reaction does have some drawbacks. Considerable elimination product is formed, presumably after the first equivalent of lithianilide has reacted with the dibromide. Substituting one bromide with the aniline group causes the second equivalent of lithianilide to abstract a proton to form 2,6-di(alkyl)aniline (**2.4a,b**) and N-allyl-2,6-di(alkyl)aniline (**2.5a,b**). The elimination reaction can be minimized by the use of N,N,N',N'-tetramethylethylenediamine (tmeda) which increases the nucleophilicity of the lithianilide, although this side reaction can not be eliminated completely. The products from this reaction are obtained in a 3:1:1 mixture (by ^1H NMR spectroscopy). Similar yields are achieved between the smaller 2,6-

dimethylolithiumanilide and the 1,3-dibromopropane indicating that the elimination reaction does not arise as a result of steric congestion around the nucleophile.



The diamine **2.3a** is a white crystalline solid which can be separated from the oily side products by recrystallization from hexanes. The diamine **2.3b** is an oil and could not be separated from the side products in this same manner. The formation of the insoluble bis(hydrochloride) salt of diamine **2.3b** allows for its facile separation from compounds **2.4b** and **2.5b**. Figure 2.2 shows the separation diagram for the three ammonium chloride salts. By dissolving the three products in diethylether and then adding aqueous HCl, the hydrochloride salts of these three products were formed. The ammonium chloride salt **2.3b**•2 HCl is a white solid completely insoluble in both the organic and aqueous phases, while the other compounds are soluble in either the organic (**2.5b**•HCl) or aqueous (**2.4b**•HCl) phases.

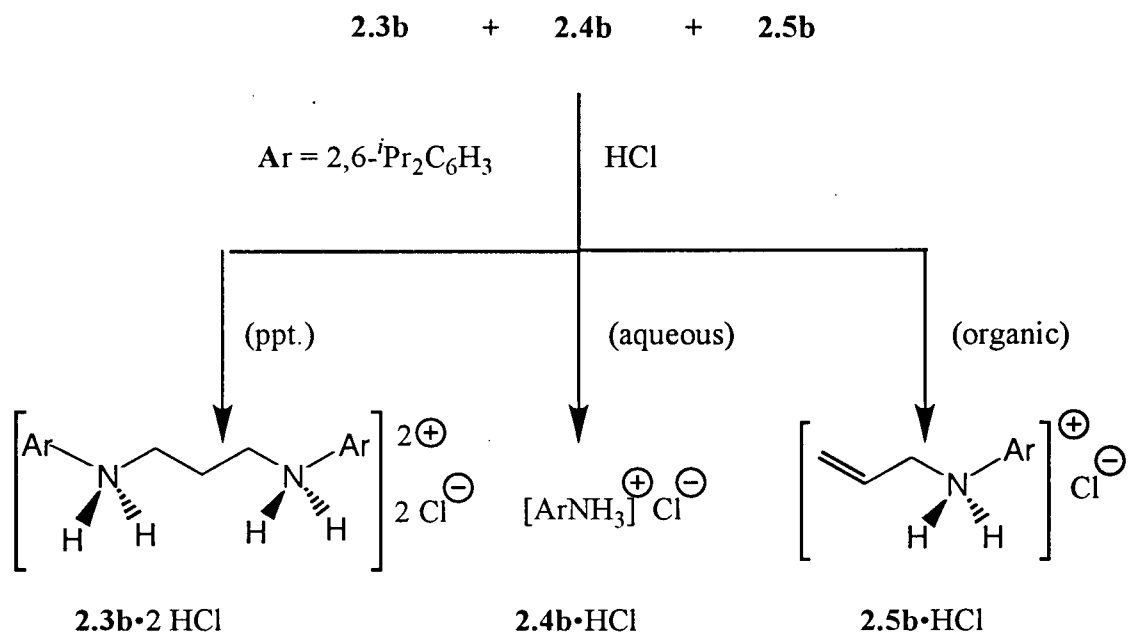
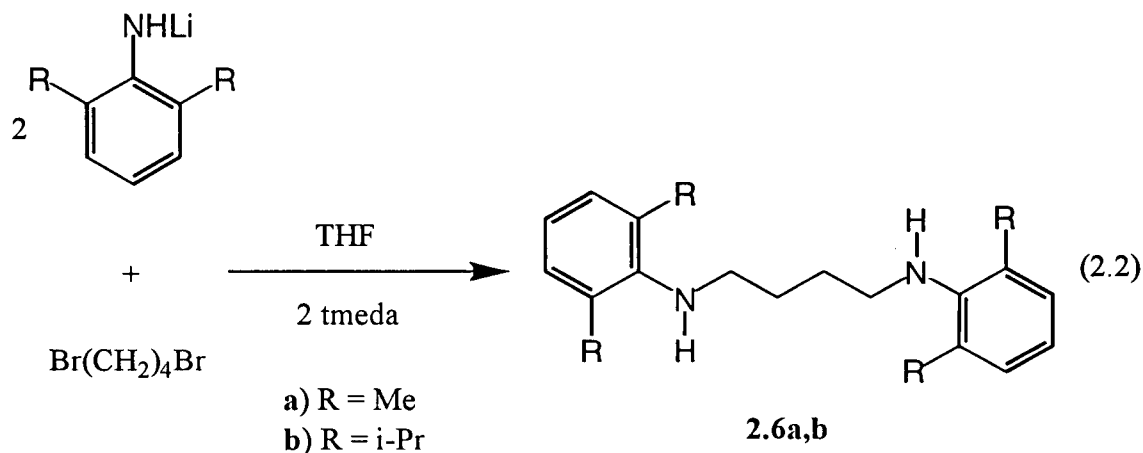


Figure 2.2: Separation diagram for isolating diamine **2.3b**

Simple filtration was suitable to isolate **2.3b·2 HCl** from the other products. The desired diamine **2.3b** was obtained as a yellow oil upon neutralization of compound **2.3b·2 HCl** with NaHCO₃. The overall yields of diamines **2.3a,b** are 50–60% which does not reflect an improvement over the synthesis of diamines **2.2a,b**. However, due to the lack of an appropriate starting dialdehyde, this alternative route was used.

Butyl eneLinked Diamines

The butyl linked diamines were synthesized in an identical manner to the propyl linked diamines **2.3a,b**. Reaction between two equivalents 2,6-dimethylthiolanilide or 2,6-diisopropylthiolanilide and 1,4-dibromobutane gives the desired diamines **2.6a,b** in high yield (eq. 2.2). There is no evidence of any elimination product being formed. Both diamines **2.6a,b** are white crystalline solids which can be recrystallized from hexanes. The overall yields of compounds **2.6a,b** are greater than 80% which reflects the lack of competition with the elimination side reaction observed with the propyl linked diamines.



Why does the elimination reaction occur exclusively with the three carbon backbone? By looking carefully at the intermediate before the second substitution reaction occurs, it may be possible to derive the answer. Figure 2.3 shows the Newman projections of the three intermediates in their anti and gauche conformations. The gauche conformation is necessary

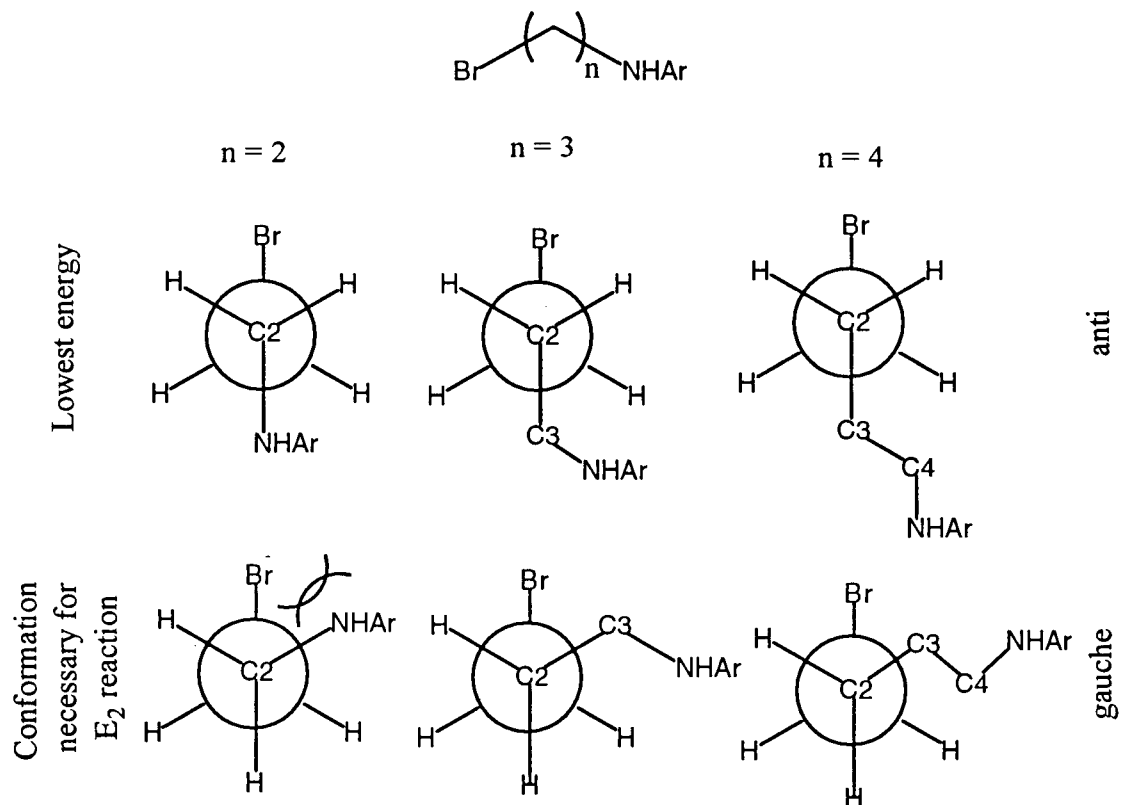


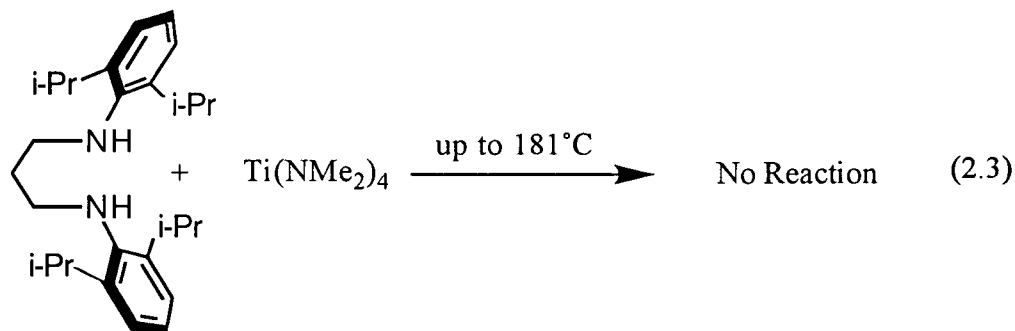
Figure 2.3: Newman projections of the intermediate in the synthesis of the diamino ligands

for the elimination reaction to occur. This conformation is slightly higher in energy than the lowest energy anti conformation. For the case where $n = 2$, the gauche conformation is highly disfavoured because there will be a strong interaction between the aryl group on nitrogen and the bromine atom. Therefore the anti conformation will be highly favoured. Although this places a majority of the steric bulk in the area needed for the backside attack on C1, the aryl group also protects the protons on C2 towards abstraction. These two reasons account for the intractable products arising from the reaction between 1,2-dibromoethane and the lithiuanilide. This problem is overcome by taking the two step route by first forming the bisimines **2.1a,b** and then reducing the products to the diamines **2.2a,b**.

With the three carbon linkage, there is still some difference in energy between the gauche and anti conformations. By moving the amino group one carbon further away the gauche interaction is much smaller than in the $n = 2$ case. However, when the molecule is in the anti conformation there is still a large amount of steric bulk located in the area necessary for backside attack on C1. Couple that with the fact that the incoming nucleophile is also rather large, and the conditions for substitution to occur are disfavoured. On the other hand, when the molecule is in the gauche conformation, the area necessary for backside attack opens up, but the protons on C2 are now in the position necessary for the elimination reaction to occur. Furthermore, the protons on C2 are no longer protected by the phenyl group on nitrogen like they were when $n = 2$. This leads to a situation where both the S_N2 and E2 reactions can compete with each other. For $n = 4$, the gauche and anti conformations will be similar in energy to when $n = 3$. However in the anti conformation, the steric bulk is further removed from the area required for backside attack on C1. The bulk is now far enough removed that the substitution reaction can occur in the anti conformation thus effectively preventing the elimination reaction.

Propylene Linked Chelating Diamide Complexes of Titanium

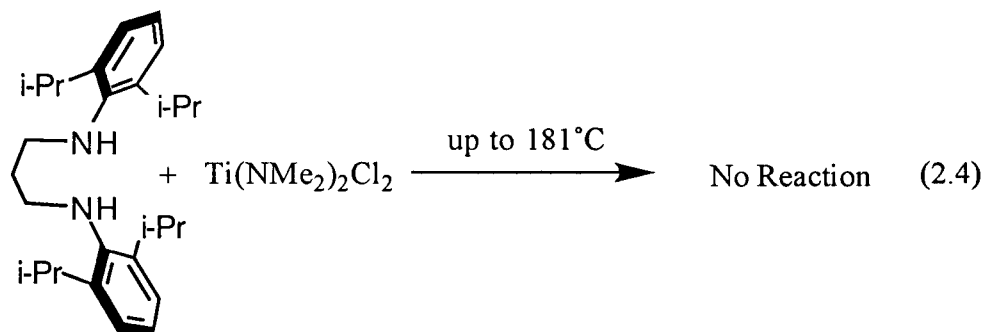
The transamination reaction has been used by Bradley to form heteroleptic amide complexes (Chapter 1).²⁰ The transamination reaction between the diamines **2.3b** and $\text{Zr}(\text{NMe}_2)_4$ proceeds with yields in excess of 90% (chapter 4). The aminolysis of $\text{Ti}(\text{NMe}_2)_4$ with the diamine **2.3b** in refluxing toluene (110°C), xylenes (140°C) or *o*-dichlorobenzene (181°C) does not yield the heteroleptic diamide complex (eq. 2.3). The ^1H NMR spectrum of



the reaction mixture indicated that no reaction had occurred and only starting material remained. Lappert has reported that the reaction of $\text{Ti}(\text{NMe}_2)_4$ with excess cyclopentadiene (CpH) in refluxing benzene yields the mono-Cp compound $\text{CpTi}(\text{NMe}_2)_3$, while the corresponding reaction with $\text{Zr}(\text{NMe}_2)_4$ yields $\text{Cp}_2\text{Zr}(\text{NMe}_2)_2$.²¹ Similarly, the reactions of $\text{M}(\text{NMe}_2)_4$ ($\text{M} = \text{Ti}, \text{Zr}$) with excess NR_2H ($\text{R} = \text{SiMe}_3, ^i\text{Pr}$) yield $\text{M}(\text{NMe}_2)_3(\text{NR}_2)$ for $\text{M} = \text{Ti}$ but $\text{M}(\text{NMe}_2)_2(\text{NR}_2)_2$ for $\text{M} = \text{Zr}$.²⁰⁻²³ Lappert ascribed these reactivity differences to the fact that Ti amides are more crowded than the analogous Zr species due to the smaller metal radius and shorter $\text{M}-\text{NR}_2$ bonds: (effective ionic radii in a tetrahedral environment, $\text{Ti}^{4+} = 0.56 \text{ \AA}$, $\text{Zr}^{4+} = 0.73 \text{ \AA}$;²⁴ $\text{M}-\text{NR}_2$ bond lengths, $\text{Ti} = 1.83 - 1.92 \text{ \AA}$,²⁵⁻²⁷ $\text{Zr} = 2.03 - 2.11 \text{ \AA}$).²⁸⁻³¹ It is likely that the lack of reaction between diamine **2.3b** and $\text{Ti}(\text{NMe}_2)_4$ is a result of steric crowding.

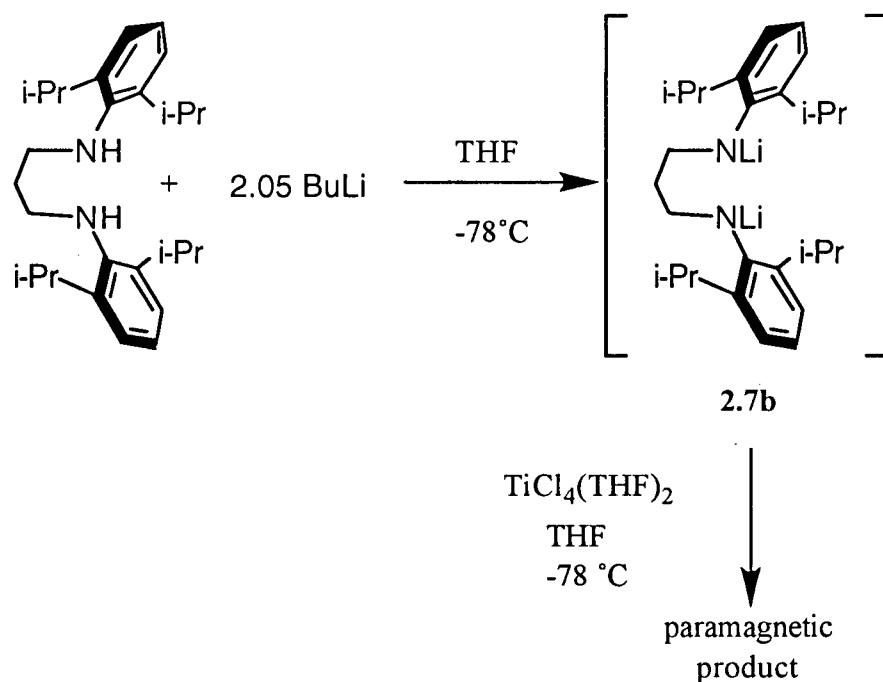
In an effort to circumvent the steric problems associated with amine elimination reactions of $\text{Ti}(\text{NMe}_2)_4$, the complex $\text{Ti}(\text{NMe}_2)_2\text{Cl}_2$ was briefly investigated. The diamine **2.3b** also does not react with $\text{Ti}(\text{NMe}_2)_2\text{Cl}_2$ at temperatures of up to 181°C (eq. 2.4).

Replacing two dimethylamide groups with chlorides did not reduce the steric crowding about the titanium enough to facilitate the reaction.



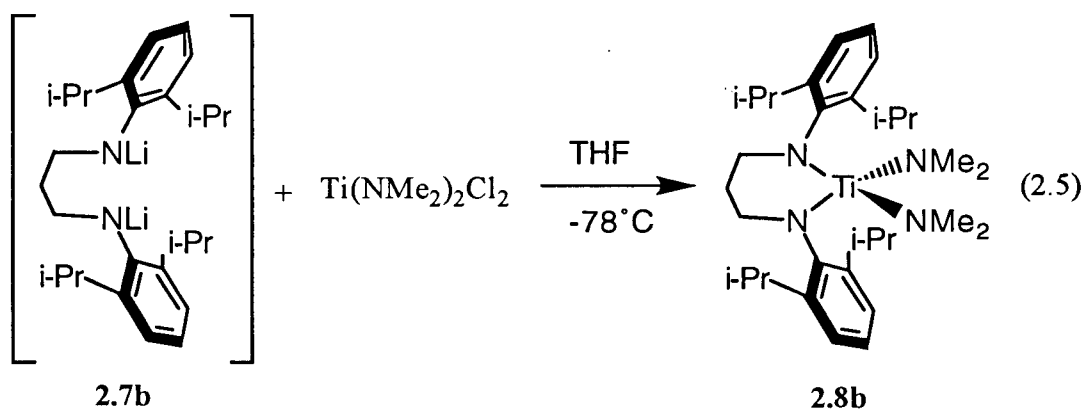
With the failure of the aminolysis reaction, a more direct route to a dichloride precursor was sought. The transmetallation reaction between titanium tetrachloride and the dilithium salt of compound **2.3b** was attempted. The dilithium salt **2.7b** was generated by the double deprotonation of the diamine **2.3b** with 2 equivalents of butyllithium at -78°C . Compound **2.7b** was then added dropwise to a solution of $\text{TiCl}_4(\text{THF})_2$ dissolved in THF at -78°C (Scheme 2.2). Upon warming the solution turned from pale yellow to dark green over

Scheme 2.2: Transmetallation reaction between $\text{TiCl}_4(\text{THF})_2$ and dilithium diamide **2.7b**



a period of a few hours. The only product that could be isolated from the reaction was a paramagnetic dark black solid.

In order to attenuate the reduction at titanium, $\text{Ti}(\text{NMe}_2)_2\text{Cl}_2$ can be substituted for $\text{TiCl}_4(\text{THF})_2$. The softer dimethylamide ligands in $\text{Ti}(\text{NMe}_2)_2\text{Cl}_2$ render the titanium (IV) centre much less susceptible to reduction than is the case for TiCl_4 . This potential side reaction, electron transfer, is important to consider in the context of metathetical salt-elimination reactions involving strongly reducing species such as lithium amides.³² A solution of compound **2.7b** was added dropwise to $\text{Ti}(\text{NMe}_2)_2\text{Cl}_2$ at -78°C (eq. 2.5). Upon

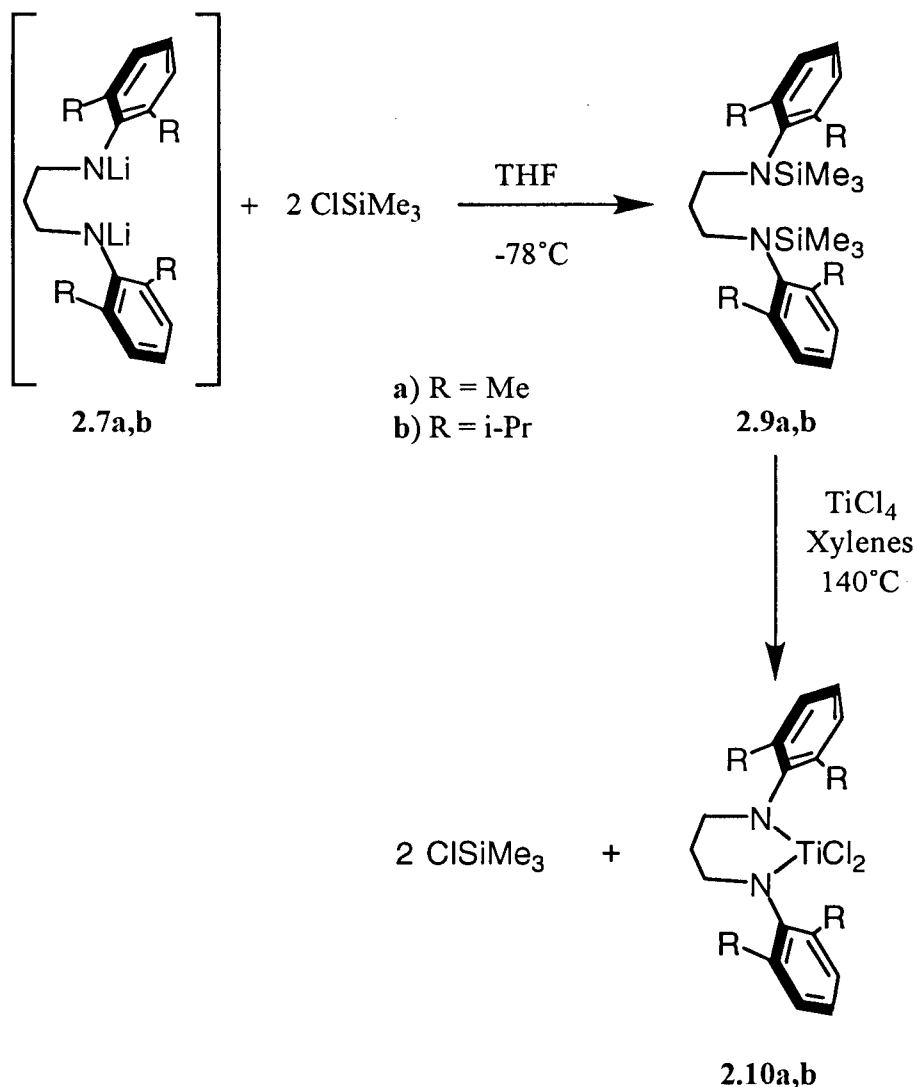


warming, the solution remained orange and eventually turned deep red. Complex **2.8b** was obtained by recrystallization from hexanes in about 20% yield. Although this method was successful, due to the high solubility of the product, the yield was considered too low, and an alternative method was sought.

Another route to obtain the titanium dichlorides directly was attempted. The silylated diamines **2.9a,b** were obtained in quantitative yield by the addition of excess chlorotrimethylsilane to the dilithio salts **2.7a,b** (Scheme 2.3). Compounds **2.9a,b** react cleanly at 140°C with TiCl_4 to afford two equivalents of chlorotrimethylsilane and the highly crystalline orange dichloride complexes **2.10a,b** in greater than 80% yield. The driving force for this reaction is two fold. First, the formation of a strong bond between silicon and

chlorine provides some of the thermodynamic driving force. Although heating to 140°C is required for the reaction to occur. Secondly, the diamide is chelating and therefore entropy is increasing with the formation of two equivalents of chlorotrimethylsilane.

Scheme 2.3: Silylation of diamides **2.7a,b** followed by reaction with TiCl_4



The ^1H NMR spectrum of the dichloride complex **2.10b** is shown in Figure 2.4. Characteristic second-order patterns are observed for the methylene protons (NCH_2 and NCH_2CH_2) of the coordinated ligands in the ^1H NMR spectra of complexes **2.10a,b**. In addition, the isopropyl methyl groups of complex **2.10b** are diastereotopic which is a consequence of restricted rotation about the $\text{N}-\text{C}_{\text{ipso}}$ bond. In particular, the aryl groups lie

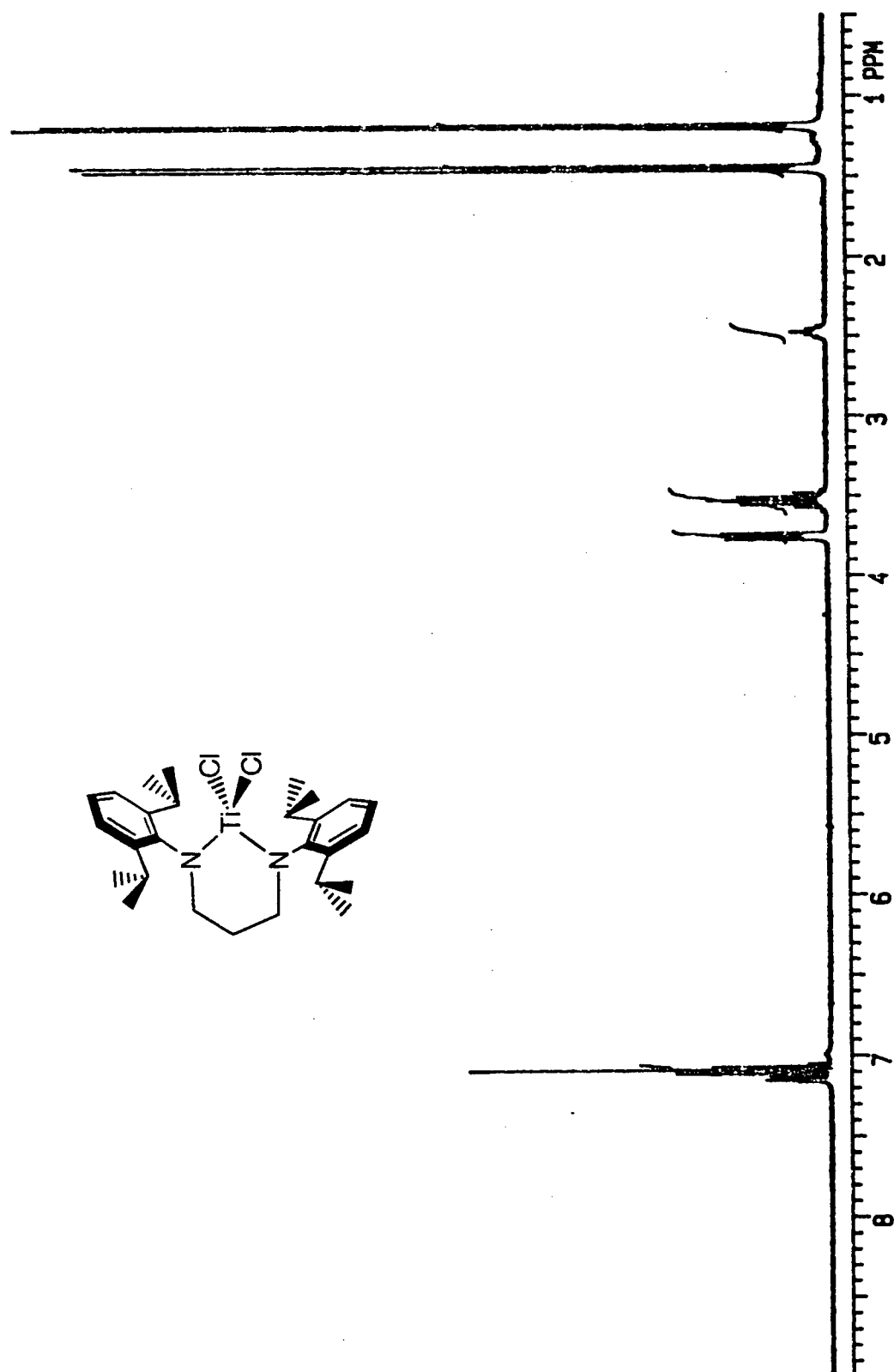


Figure 2.4: 300 MHz ^1H NMR spectrum of dichloride complex 2.10b in C_6D_6 at 23°C

perpendicular to the N_2Ti plane necessarily protecting the metal above and below this plane. A similar observation has been made in late metal complexes bearing the bis(imine) ligand **2.1b**.¹⁹

Orange single crystals of the dichloride complex **2.10b** suitable for X-ray analysis were grown from a toluene/hexane mixture. The molecular structure of complex **2.10b** is shown in Figure 2.5, and selected bond distances and angles in Table 2.1. The structure is best described as a distorted tetrahedron. The N1-Ti-N2 angle of 99.2° is less than the expected 109° for a perfect tetrahedron. This angle is enforced by the propyl bridge between the two nitrogen atoms. In contrast, Cp_2TiCl_2 has a Cp-Ti-Cp angle of 130.9° .³³ Each amide donor N in complex **2.10b** is sp^2 -hybridized as evidenced by the sum of the angles about each nitrogen ($\text{N1} = 360.0^\circ$ and $\text{N2} = 359.9^\circ$). The molecular symmetry is consistent with the spectroscopically observed C_{2v} symmetry.

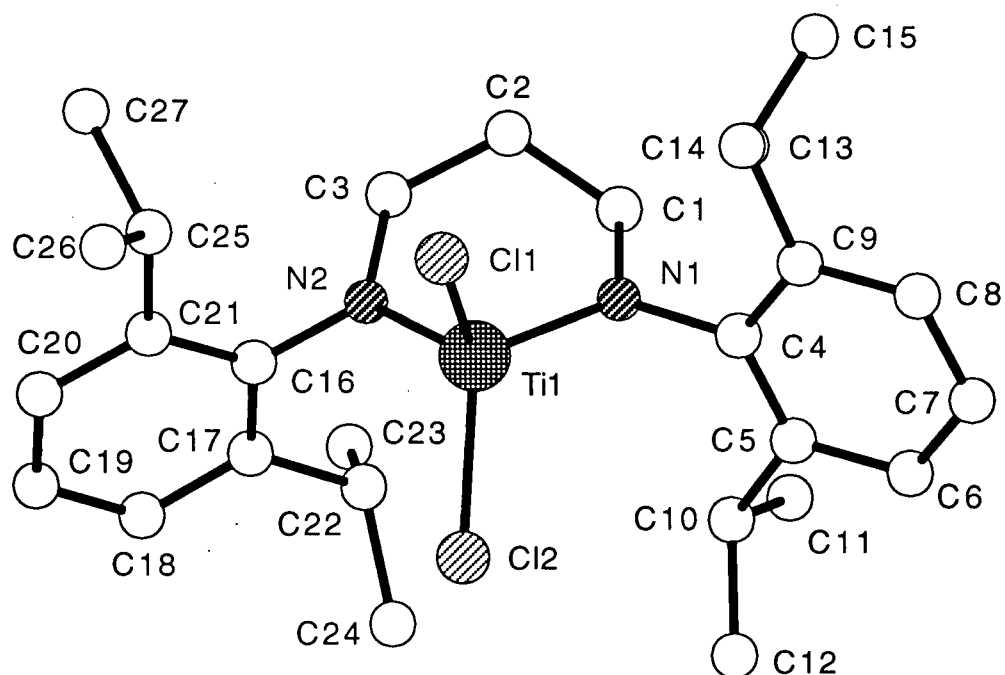
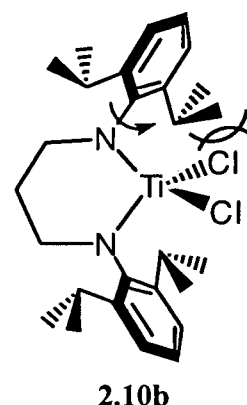


Figure 2.5. Chem3D Plus representation of the molecular structure of **2.10b**

Table 2.1: Selected bond lengths and angles for **2.10b**.

Bond Distances (Å)			
Ti(1)—N(1)	1.839(5)	Ti(1)—N(2)	1.856(5)
Ti(1)—Cl(1)	2.240(2)	Ti(1)—Cl(2)	2.257(2)
N(1)—C(4)	1.439(5)	N(2)—C(16)	1.429(6)
N(1)—C(1)	1.465(8)	N(2)—C(3)	1.469(8)
Bond Angles (°)			
N(1)—Ti(1)—N(2)	99.2(2)	N(1)—Ti(1)—Cl(1)	108.8(2)
N(1)—Ti(1)—Cl(2)	116.8(2)	N(2)—Ti(1)—Cl(1)	110.1(2)
N(2)—Ti(1)—Cl(2)	113.9(2)	Cl(1)—Ti(1)—Cl(2)	107.77(9)
Ti(1)—N(1)—C(4)	123.2(4)	C(4)—N(1)—C(1)	114.8(5)
C(1)—N(1)—Ti(1)	122.0(4)	Ti(1)—N(2)—C(16)	122.5(4)
C(16)—N(2)—C(3)	114.2(5)	C(3)—N(2)—Ti(1)	123.2(4)

Complexes **2.10a,b** react with alkylating reagents to form the corresponding bis(alkyl) complexes (Scheme 2.4). Two equivalents of methyl Grignard react with the dichlorides **2.10a,b** to afford the crystalline, thermally stable, dimethyl derivatives **2.11a,b**.

Scheme 2.4: Alkylation of the titanium dichlorides **2.10a,b**

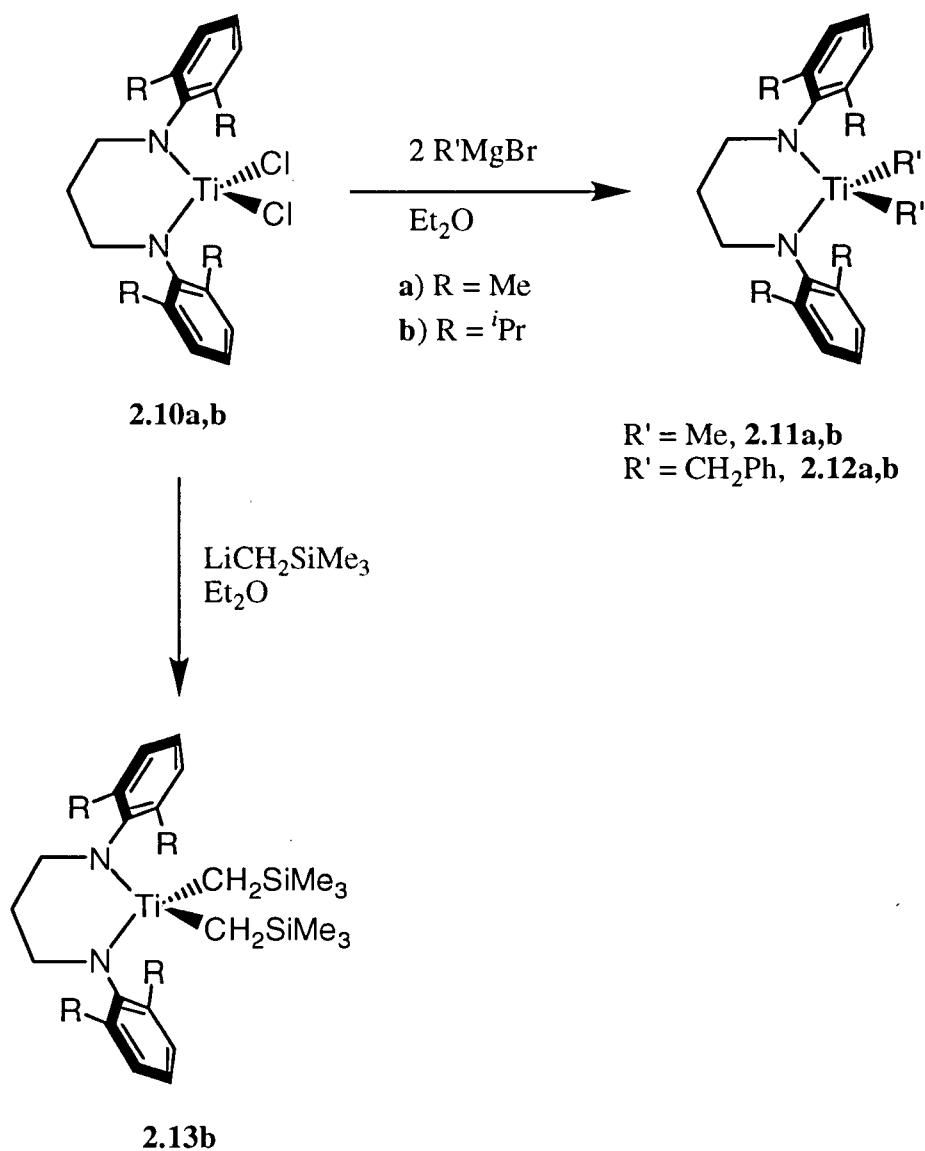


Figure 2.6 shows the ^1H NMR spectrum of **2.11b**. The ^1H NMR spectrum reveals that complex **2.11b** has C_{2v} symmetry. Furthermore, the diisopropylphenyl substituted complex **2.11b** exhibits diastereotopic isopropyl methyl resonances as evidenced by a pair of doublets. The ^1H and $^{13}\text{C}\{^1\text{H}\}$ NMR spectra of **2.11a** display Ti- CH_3 and Ti- CH_3 signals at 0.70 and 51.1 ppm, respectively. Similar shifts are observed for complex **2.11b** at 0.86 and 52.0 ppm. These resonances are comparable to those for other known bis(amide)TiMe₂ species.^{10,14,34-37}

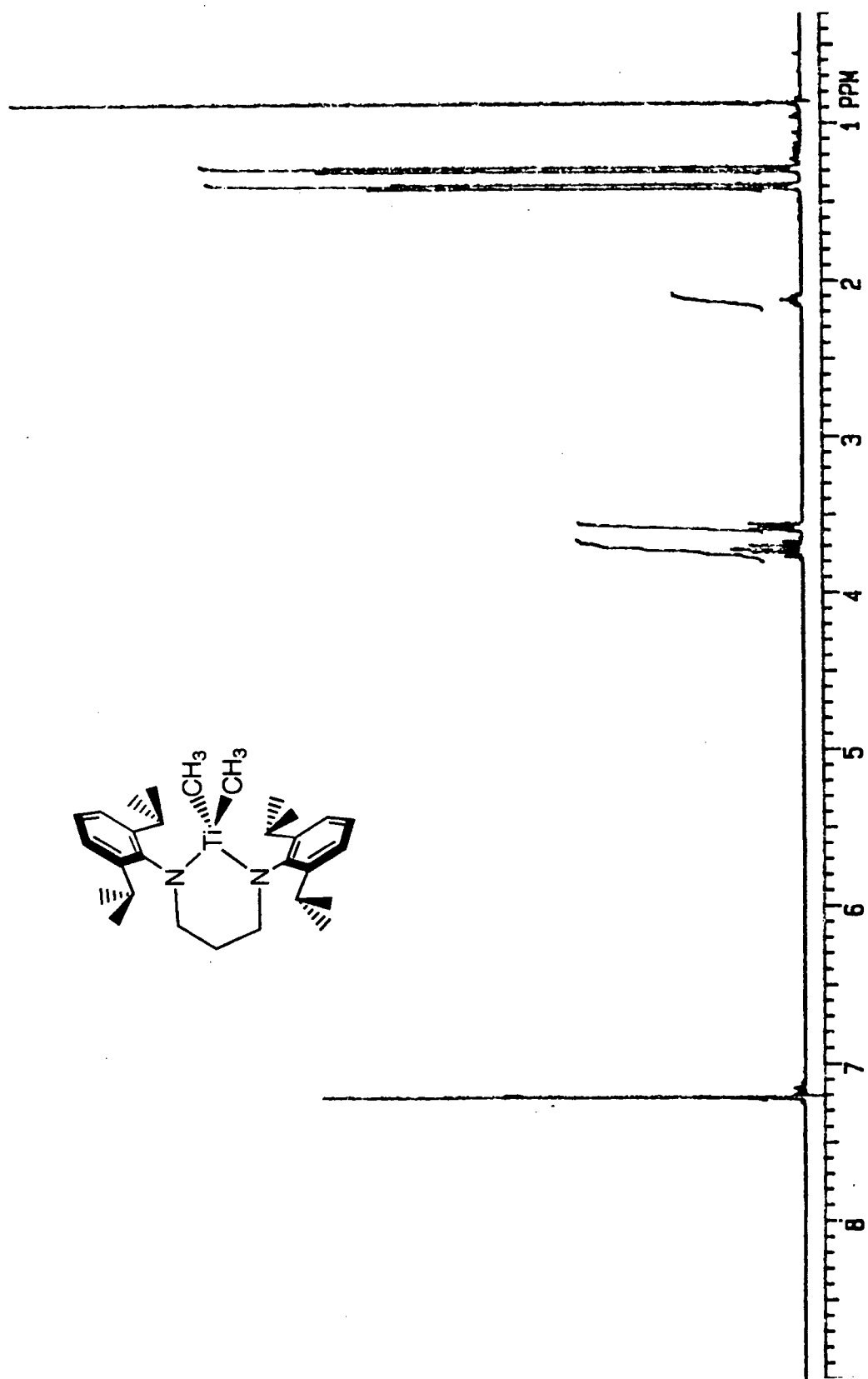


Figure 2.6: 300 MHz ^1H NMR spectrum of dimethyl complex 2.10a in C_6D_6 at 23°C

The molecular structure of complex **2.11a** is shown in Figure 2.7 and selected bond distances and angles are shown in Table 2.2

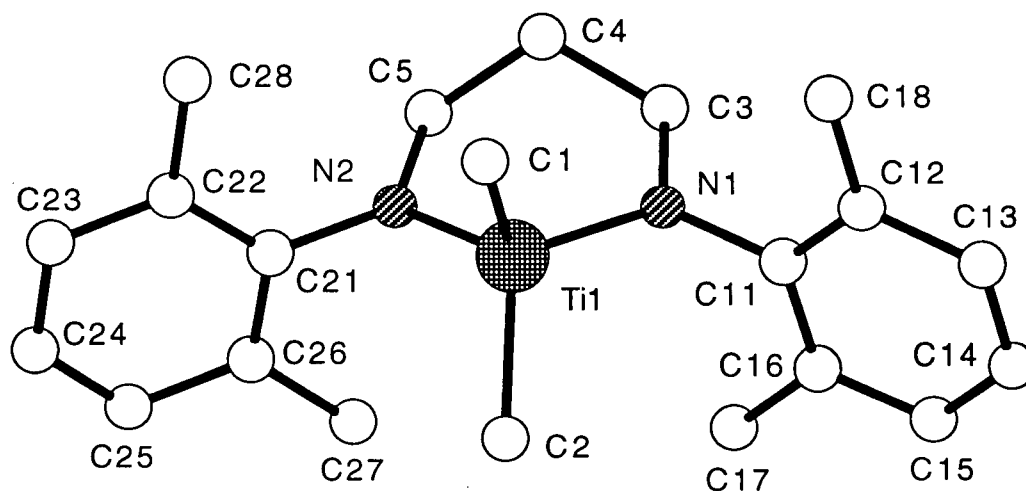


Figure 2.7: Chem3D Plus representation of the molecular structure of **2.11a**.

Table 2.2: Selected bond lengths and angles for dimethyl complex **2.11a**.

Bond Distances (Å)			
Ti(1)—N(1)	1.858(6)	Ti(1)—N(2)	1.867(6)
Ti(1)—C(1)	2.100(9)	Ti(1)—C(2)	2.077(9)
N(1)—C(3)	1.480(9)	N(2)—C(5)	1.470(9)
N(1)—C(11)	1.470(9)	N(2)—C(21)	1.436(9)
Bond Angles (°)			
N(1)—Ti(1)—N(2)	102.6(3)	N(1)—Ti(1)—C(1)	110.3(3)
N(1)—Ti(1)—C(2)	116.7(3)	N(2)—Ti(1)—C(1)	109.2(3)
N(2)—Ti(1)—C(2)	115.4(3)	C(1)—Ti(1)—C(2)	102.7(4)
Ti(1)—N(1)—C(3)	120.6(5)	C(11)—N(1)—C(3)	112.9(6)
C(11)—N(1)—Ti(1)	126.4(5)	Ti(1)—N(2)—C(5)	120.3(5)

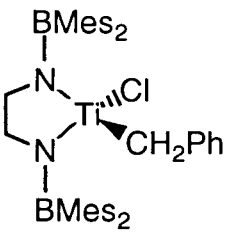
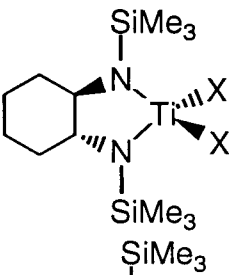
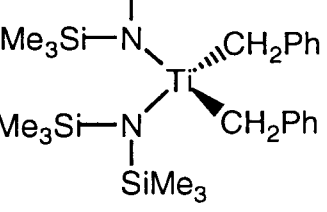
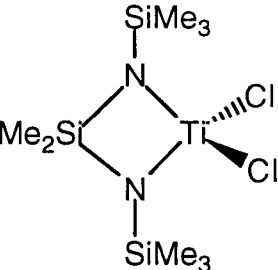
The molecular structure of the dimethyl complex **2.11a** is very similar to that of the dichloro complex **2.10b**. The N—Ti—N bond angle of complex **2.10b** is 99.2° while the same

angle for complex **2.11a** is 102.6° . This difference is probably due to the increased steric bulk of the 2,6-diisopropylphenyl group versus the 2,6-dimethylphenyl group. This added crowding pushes the nitrogens further back constricting the N–Ti–N angle slightly. The Me–Ti–Me angle of complex **2.11a** is smaller than the Cl–Ti–Cl angle in the dichloro complex **2.10b**, 102.7° versus 107.7° respectively. This may reflect the fact that methyl groups are smaller than the chloride atoms but may also be a result of the slightly larger N–Ti–N angle. A comparison of crystallographically characterized diamide complexes shows that, in general, the X–Ti–X angle decreases as the N–Ti–N angle increases (Table 2.3).

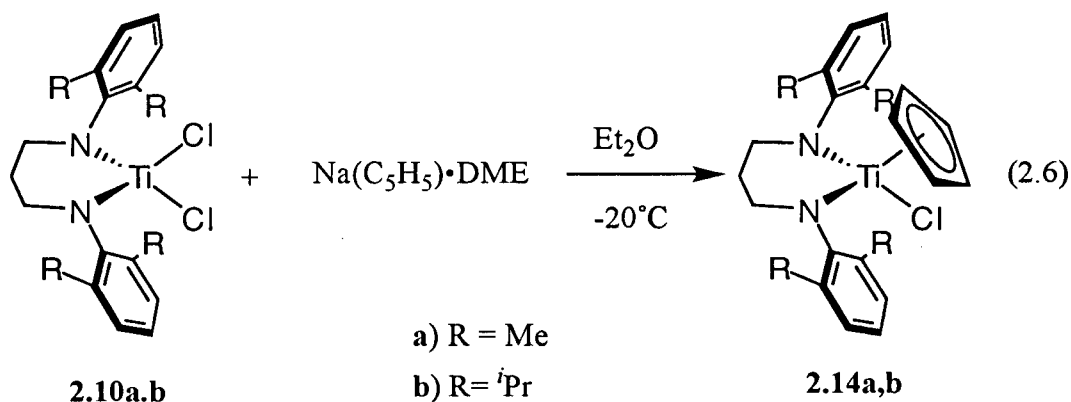
The dibenzyl complexes **2.12a,b** both exhibit local C_{2v} -symmetry in their ^1H NMR spectra. Complex **2.12b** shows two doublets for the isopropyl methyl resonances indicating that there must be restricted rotation about the N–C_{ipso} bond. The ^1H NMR spectra of the dibenzyl complexes **2.12a,b** display benzylic resonances at 2.54 ppm and 2.58 ppm, respectively. The benzylic proton chemical shifts closely resemble those observed for other known bis(amide)Ti(CH₂Ph)₂ complexes.^{17,38} The low temperature ^1H NMR spectra of complexes **2.12a,b** did not indicate any η^2 benzyl interactions. The benzyl groups of complexes **2.12a,b** display η^1 character down to -80°C . However, in the absence of a crystal structure, no definitive type of bonding can be determined.

The ^1H NMR spectra of the bis(trimethylsilylmethyl) complexes **2.13a,b** are similar to the other bis(alkyls). Local C_{2v} -symmetry is indicated in the spectra along with the familiar diastereotopic isopropyl methyl resonances for complex **2.13b**. The Me₃SiCH₂ signals of complexes **2.13a,b** appear as singlets at 1.26 and 1.34 ppm in the ^1H NMR spectrum while the Si(CH₃)₃ signals both appear at 0.04 ppm.

Table 2.3: Selected bond angles of diamide complexes of titanium

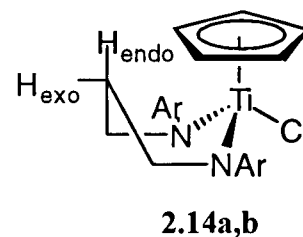
Metal Amide	N-M-N (deg)	X-M-X (deg)	Ref.
	89.2(2)	125.5(2)	13
	X = Cl 91.97(8) X = CH ₂ Ph 93.0(2)	117.8(1) 115.45(3)	17
	120.6(1)	98.4(2)	38
	115.0(2)	96.89(8)	35

The addition of $\text{Na}(\text{C}_5\text{H}_5)\cdot\text{DME}^{39}$ to complexes **2.10a,b** gives the expected mono(Cp) complexes **2.14a,b** in high yield (eq. 2.6). Local C_s -symmetry is indicated by their ^1H NMR spectra. The ^1H NMR spectrum of complex **2.14a** shows two diastereotopic methyl resonances. This is the first example of spectroscopically observed restricted rotation about the N-C_{ipso} bond in the 2,6-dimethylphenyl substituted ligand system. Within C_{2v} symmetry the methyl groups are related via a mirror plane. Therefore restricted rotation could not be confirmed by ^1H NMR spectroscopy. With C_s symmetry the mirror plane which relates the two methyl groups is removed. Therefore only free rotation about the N-



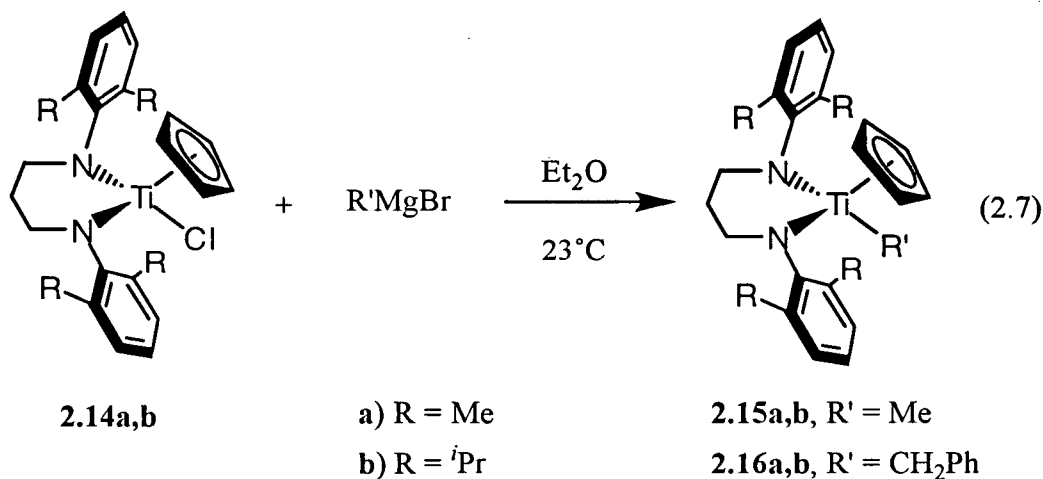
C_{ipso} bond can relate the methyl groups. The same mirror plane which relates the two methyl groups in the 2,6-dimethylphenyl derivative also relates two sets of methyl groups in the 2,6-diisopropylphenyl derivative. Therefore complex **2.14b** now has four doublets in the ¹H NMR spectrum corresponding to the four diastereotopic isopropylmethyl groups.

One proton in the central methylene group shows an unusual chemical shift. The proton endo to the Cp ring is more deshielded than the exo-proton (**2.14a,b**). This extra deshielding results in a downfield shift of the H_{endo} proton resonance for complexes **2.14a,b** to 3.35 ppm and 2.48 ppm, respectively. Complex **2.14b** does not show as pronounced a downfield shift as complex **2.14a** presumably because the added steric bulk of the 2,6-diisopropylphenyl groups reduce the N–Ti–N angle which consequently pushes the proton slightly further from the Cp ring. The H_{exo} proton resonance in complexes **2.14a,b** appear at 1.95 and 1.99 ppm, respectively. This is in agreement with the chemical shifts observed for these protons in other non-Cp complexes.



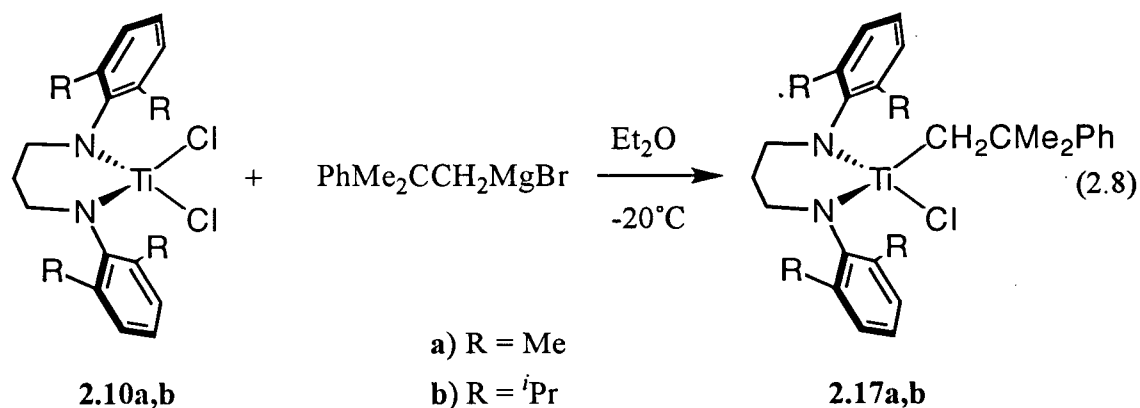
The remaining chloride in complexes **2.14a,b** can be metathesized with various Grignard reagents. Addition of MeMgBr or PhCH₂MgBr to a diethylether suspension of complexes **2.14a,b** leads to the Cp-alkyl complexes **2.15a,b** and **2.16a,b** in high yield (eq.

2.7). The titanium methyl resonance for complexes **2.15a,b** appear at 0.70 ppm and 0.64



ppm in their ^1H NMR spectra, respectively. This is in good agreement with the methyl resonances of the dimethyl complexes **2.11a,b** (0.70 and 0.86 ppm, respectively). Similarly, the benzylic proton resonances of complexes **2.16a,b** are in close agreement with those of the bis(benzyl) derivatives **2.12a,b** (2.70 ppm and 2.58 ppm versus 2.54 and 2.58 ppm respectively). The $^{13}\text{C}\{^1\text{H}\}$ NMR spectra of the Cp-alkyl complexes **2.15a,b** and **2.16a,b** reveal a general upfield shift of the methyl carbon resonances and the benzyl carbon resonances versus the corresponding carbon resonances of the dialkyl complexes **2.11a,b** and **2.12a,b**. This is probably due to the added electron density afforded complexes **2.15a,b** and **2.16a,b** by the cyclopentadienyl group.

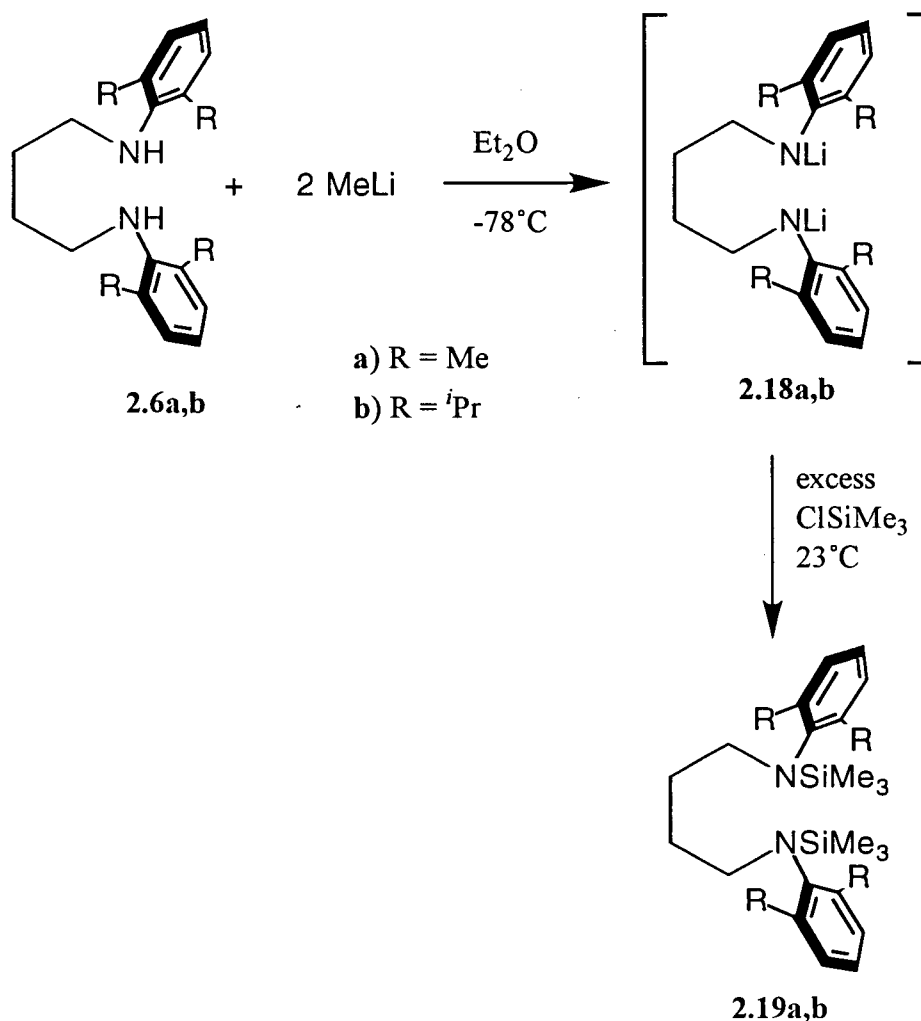
Addition of neophyl Grignard to complexes **2.10a,b** gives exclusively the mono neophyl chloride complexes **2.17a,b** as yellow oils (eq. 2.8). Only the mono neophyl complexes could be synthesized, presumably due to the increased size of the neophyl group over the other alkyl groups studied. Complexes **2.17a,b** both exhibit local C_s-symmetry in their ¹H NMR spectra. Restricted rotation about the N–C_{ipso} bond is also indicated in both spectra. In contrast to complexes **2.14a,b**, the endo- and exo-protons have almost identical shifts. This provides further evidence that the downfield shift of H_{endo} in the ¹H NMR spectrum of the mono-Cp derivatives is a result of deshielding by the cyclopentadienyl ring.



Butylene Linked Chelating Diamide Complexes of Titanium

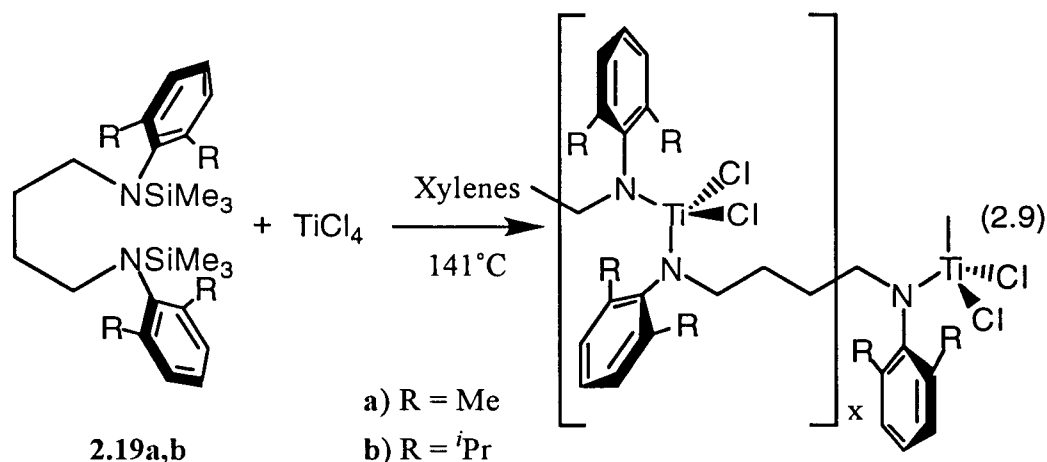
Due to the successful reaction between the silylated amines **2.9a,b** and TiCl_4 , an identical route was attempted with the butyl linked diamines. Addition of two equivalents of methyl lithium to the diamines **2.6a,b** generated the dilithium salts **2.18a,b**. Quenching complexes **2.18a,b** with excess chlorotrimethylsilane gives the corresponding bis(trimethylsilyl)diamines **2.19a,b** as white crystalline solids in quantitative yield (Scheme 2.5).

Scheme 2.5: Synthesis of the trimethylsilyl derivatives of diamines **2.6a,b**

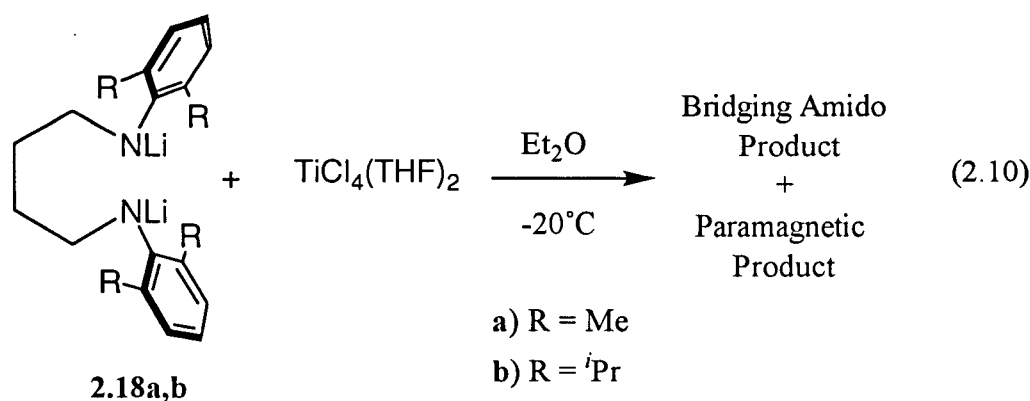


Unlike the propyl linked derivatives **2.9a,b**, the disilylamines **2.19a,b** do not react with TiCl_4 to give the desired chelating bis(amide)titanium dichloride complexes. Instead, an unexpected amide containing titanium species is obtained. The ^1H NMR spectra of the products exhibit resonances for the methylene protons (NCH_2 and NCH_2CH_2) consistent with coordination to titanium, however, the characteristic second-order patterns for magnetically inequivalent protons are absent. The NCH_2 resonance appears as a first-order triplet indicative of magnetically equivalent protons. Furthermore, the lack of any $\text{Si}(\text{CH}_3)_3$ signal in the ^1H NMR spectrum indicates that the metathesis reaction has gone to completion. It would appear that for the butyl linked diamine, the rate of intermolecular reaction is faster

than the rate of intramolecular chelation. Presumably this results in an oligomeric or polymeric species where the titanium atoms are bridged by the ligand (eq. 2.9).

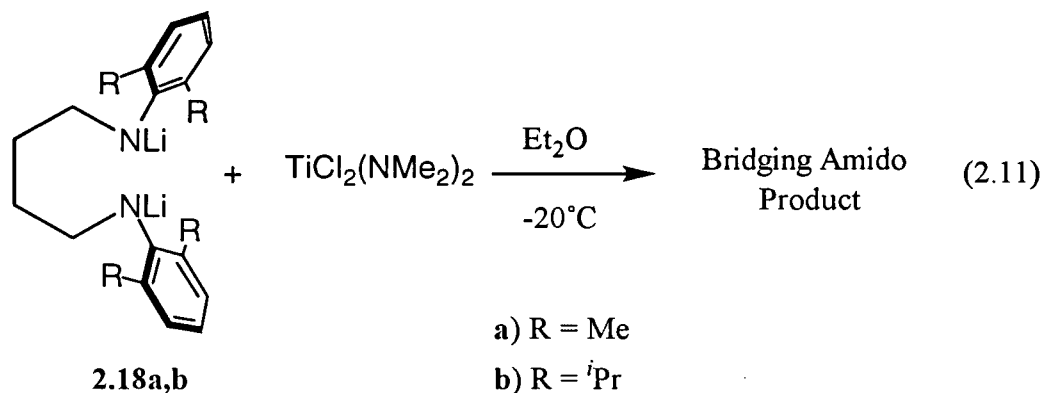


In order to further evaluate the chemistry of the butyl ligand, a transmetallation reaction was attempted between the dilithium complexes **2.18a,b** and $\text{TiCl}_4(\text{THF})_2$. The dilithium salts were added to a slurry of $\text{TiCl}_4(\text{THF})_2$ in diethylether (eq. 2.10). The



reaction slowly turned black over the course of a few hours. With difficulty, two products were separated from the reaction mixture. One product, an orange red oil, had a ^1H NMR spectrum very similar to the product from eq. 2.9. The other product, a dark black solid, was paramagnetic and no attempt was made to determine its composition. The reaction was repeated in a variety of solvents such as THF, toluene, hexanes, benzene and dichloromethane with the same result.

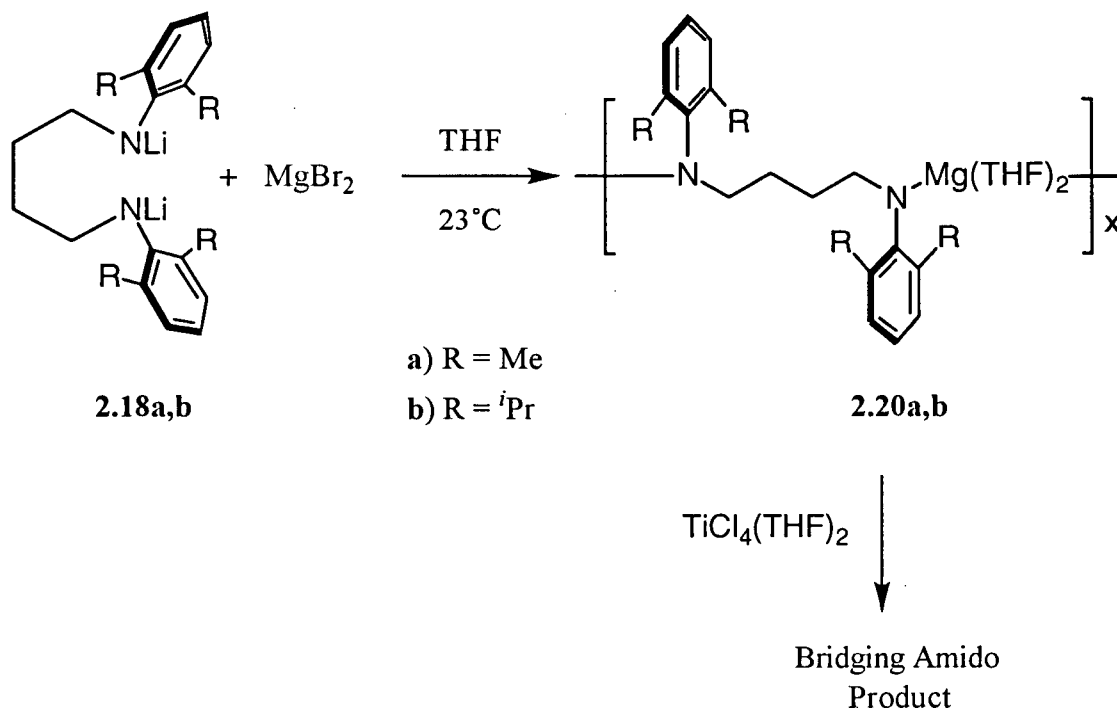
By replacing $\text{TiCl}_4(\text{THF})_2$ with $\text{TiCl}_2(\text{NMe}_2)_2$ the reduction of the titanium starting material should be minimized.⁴⁰ Addition of the dilithium complexes **2.18a,b** to $\text{TiCl}_2(\text{NMe}_2)_2$ results in the formation of a bridging titanium amido product as evidenced by ^1H NMR spectroscopy (eq. 2.11). The product is presumably similar to those in eq.



2.9 except the chlorides are replaced by NMe_2 groups. The reaction was repeated in a variety of solvents. In every case only a bridging titanium product was isolated. Reduction of the titanium starting material was successfully eliminated in this case but the intramolecular chelation still did not take place.

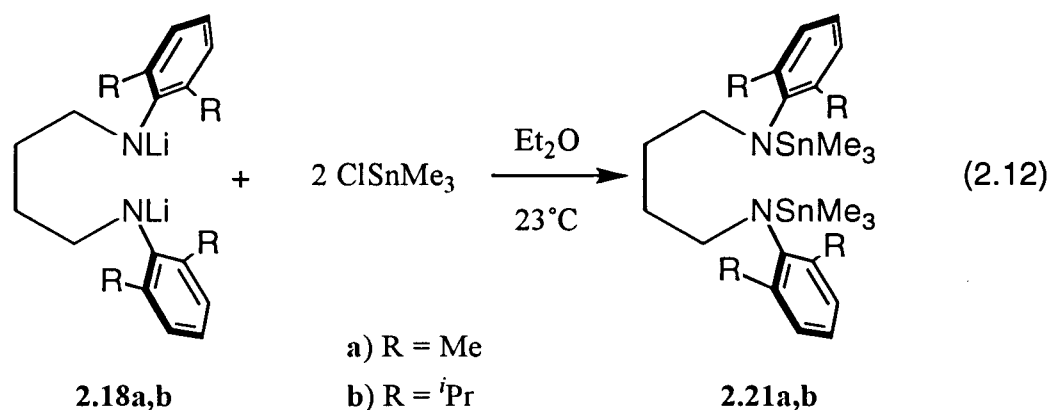
Since the desired product is the chelating diamide, it may be possible to induce the intramolecular chelation by starting with a chelating Grignard reagent. The dilithium complex **2.18a,b** reacts with one equivalent of $\text{MgBr}_2(\text{Et}_2\text{O})_2$ to give the diamide magnesium complexes **2.20a,b** in greater than 90% yields. Complexes **2.20a,b** were insoluble in common deuterated NMR solvents, therefore, the presence of THF was confirmed by ^1H NMR spectroscopy of the hydrolyzed products of **2.20a,b**. Integration of the THF resonances versus the diamine resonances indicated exactly two equivalents of THF. The solubility properties of complexes **2.20a,b** suggest that they are polymeric in nature. Addition of complexes **2.20a,b** to $\text{TiCl}_4(\text{THF})_2$ resulted in the formation of the bridging amido product again (Scheme 2.6). The ^1H NMR spectrum of the product was very similar to the spectra obtained from previous attempts to prepare the chelating bis(amide) titanium

Scheme 2.6: Reaction of the magnesium salt **2.20a,b** with $\text{TiCl}_4(\text{THF})_2$



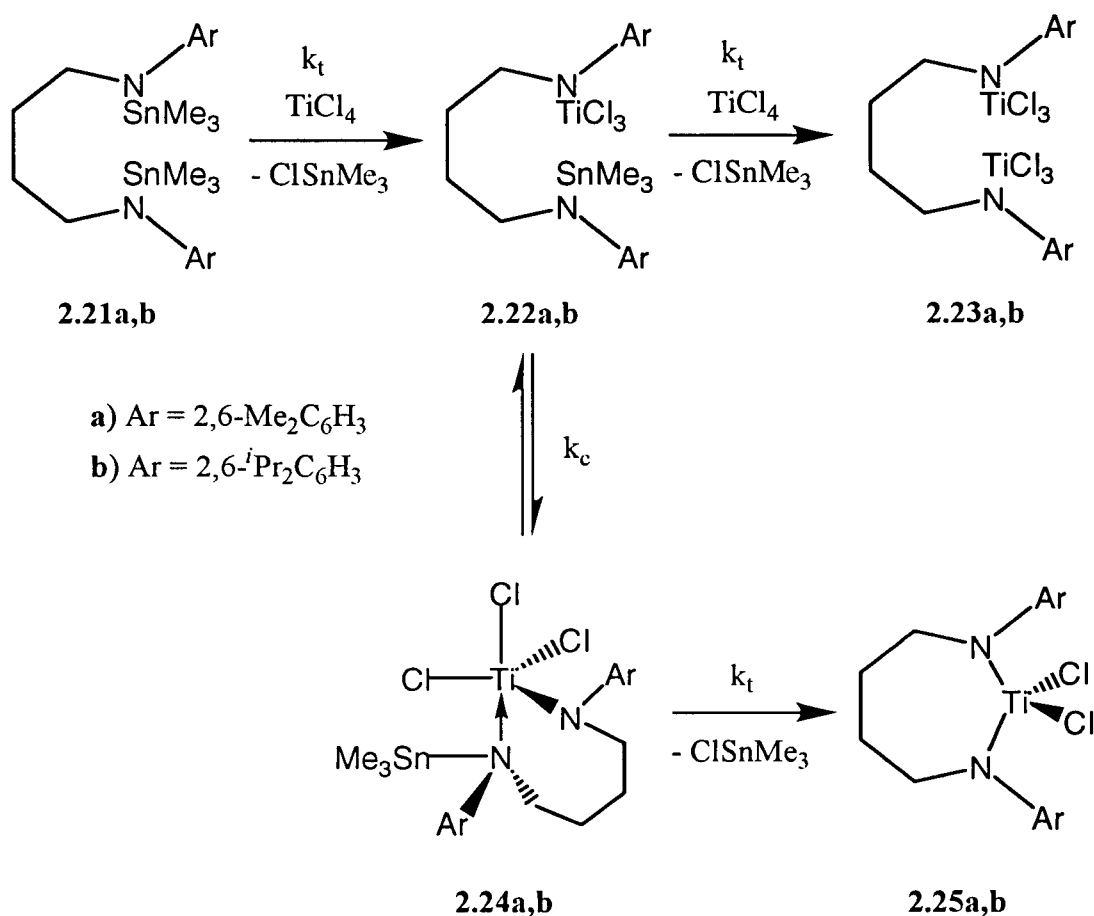
complex. By using the magnesium salt of the diamine rather than the dilithium salt, the reduction of the titanium centre was not observed.

The elimination of chlorotrimethylsilane was successful for the propyl linked diamine and a reaction was observed with the trimethylsilyl derivative of the butyl linked diamine. It seemed reasonable to attempt this reaction again but with a slight modification to the starting material. The elimination of chlorotrimethylstannane should also proceed along the same route as the silane derivative. The trimethylstannyl derivatives **2.21a,b** were synthesized from the dilithium salts **2.18a,b** and two equivalents of chlorotrimethylstannane (eq. 2.12).



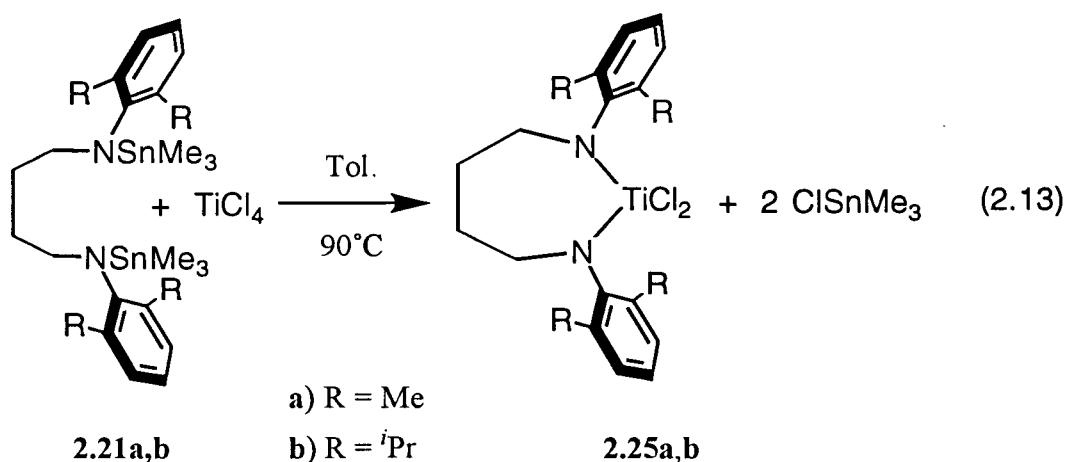
Previous results have indicated that the transmetallation reaction with the trimethylsilyl derivatives of the diamines does not occur at temperatures below 140°C. The group 14 metal–nitrogen bond strengths decrease in the order of Si > C > Ge > Sn > Pb.⁴¹ Therefore the trimethylstannyl derivatives may react at a lower temperature. Hopefully at a lower temperature the rate of transmetallation will be slower than the rate of chelation. Furthermore, the silicon–chlorine bond is stronger than the tin–chlorine bond, 91 kcal/mol versus 77.2 kcal/mol.²⁴ Scheme 2.7 shows the possible pathways for the transmetallation reactions. The first step is the formation of the monodentate amido complexes **2.22a,b** and one equivalent of chlorotrimethylstannane. The transmetallation reaction will occur at a certain rate, say k_t . Complexes **2.22a,b** can follow two different reaction paths. One path is the intramolecular chelation of the ligand to form the chelating amidoamine complexes **2.24a,b**. This chelation will occur at a rate of k_c . However, if the rate of transmetallation is much greater than the rate of intramolecular chelation (e.g. $k_t \gg k_c$), then complexes **2.22a,b** will proceed to the bridging diamido complexes **2.23a,b**. If the rate of chelation is greater than the rate of transmetallation, then complexes **2.24a,b** will be formed. Complexes **2.24a,b** can then undergo the transmetallation reaction to form the chelating diamides **2.25a,b**.

Scheme 2.7: Transamination of TiCl_4 with distannanes **2.21a,b**



Another factor which may aid in the formation of the chelating diamide complex is the relative size of the tin atom versus the silicon atom. Sn(IV) has an ionic radius of 0.69 \AA while Si(IV) has an ionic radius of only 0.40 \AA .²⁴ Since the tin atom has a larger ionic radius, it may be able to react at a greater distance from the chloride atom. A 7-membered ring will be harder to close than a 6-membered ring. Therefore, the larger ionic radius of the tin atom may facilitate the closing of a 7-membered ring.

The reaction between the distannanes **2.21a,b** and TiCl_4 in toluene at 90°C results in the clean formation of the titanium dichlorides **2.25a,b** and two equivalents of chlorotrimethylstannane (eq. 2.13). It appears that exchanging the trimethylsilyl group



with a trimethylstannyl group has altered the rate of transmetallation such that it is now less than the rate of intramolecular chelation. Complexes **2.25a,b** display C_{2v} symmetry in solution as evidenced by ^1H and $^{13}\text{C}\{^1\text{H}\}$ NMR spectroscopy. The NMR spectra of the complexes **2.25a,b** are almost identical to the dichloride complexes **2.10a,b**. Two sets of doublets are observed in the ^1H NMR spectrum for the isopropylmethyl groups of complex **2.25b**. Also the same characteristic second-order patterns for the NCH_2 and NCH_2CH_2 protons are present in the ^1H NMR spectrum.

Another possibility for the structures of complexes **2.25a,b** are that they are dimers with the amido ligands bridging the two titanium centres (Figure 2.8). A similar complex

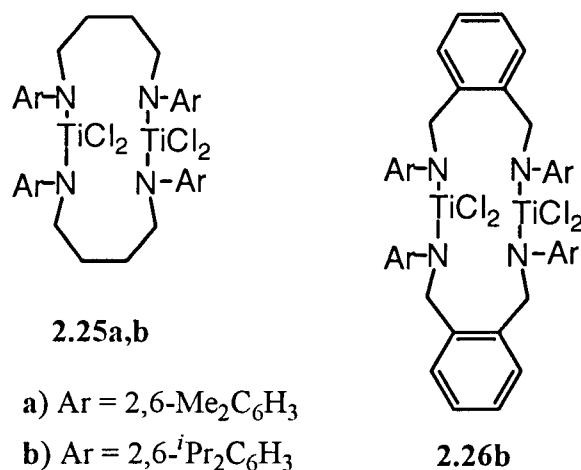
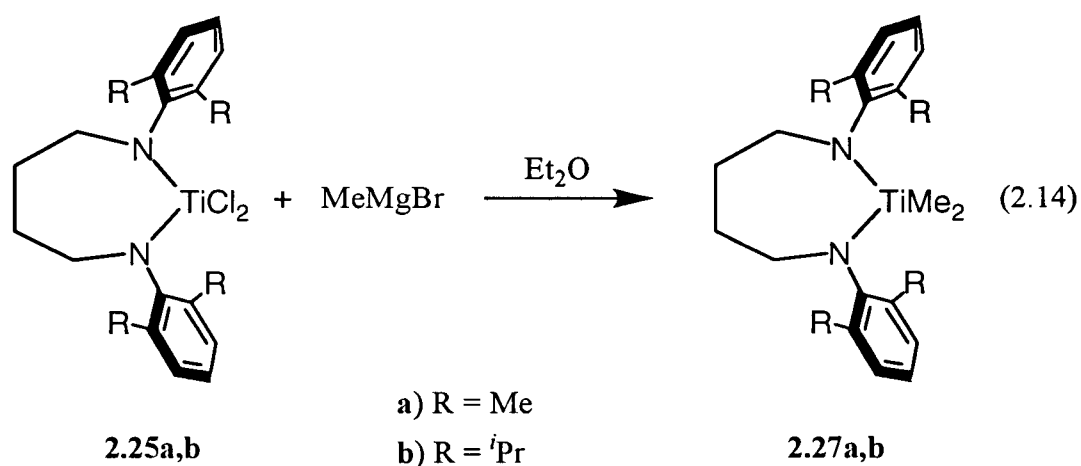


Figure 2.8: Possible dimeric structures of complexes **2.25a,b**

(2.26b) was prepared using a trimethylstannyl substituted bisamine and TiCl_4 . A solution molecular weight determination revealed that complex **2.26b** was dimeric.⁴² Given the rigid nature of the dimer, it is impossible to distinguish which structure accurately describes complex **2.25a,b** by ^1H NMR spectroscopy, and, in the absence of a solution molecular weight for the butyl linked complex, a conclusion one way or the other is impossible.

Dichloride complexes **2.25a,b** react with the two equivalents of MeMgBr to afford the desired dimethyl complexes **2.27a,b** (eq. 2.14). The dimethyl complexes are

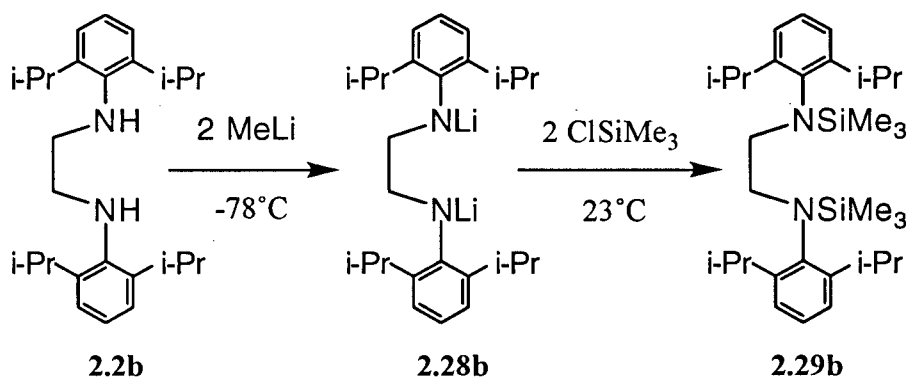


thermally unstable and slowly decompose at room temperature to an unidentifiable dark green paramagnetic complex. Interestingly, similar difficulties were encountered when alkylating complex **2.26**.⁴² Fortunately, complexes **2.27a,b** are stable long enough to characterize by NMR spectroscopy. The ^1H and $^{13}\text{C}\{^1\text{H}\}$ NMR spectra of complexes **2.27a,b** display resonances consistent with C_{2v} -symmetry. The proton resonances of the butyl linkage are similar to the dimethyl complexes **2.11a,b**, however, the titanium methyl resonances appear considerably downfield. A similar downfield shift of the titanium methyl carbon resonance is observed in the $^{13}\text{C}\{^1\text{H}\}$ NMR spectrum of complexes **2.27a,b**. This suggests that complexes **2.25a,b** and **2.27a,b** have a different structure than complexes **2.10a,b** and **2.11a,b**.

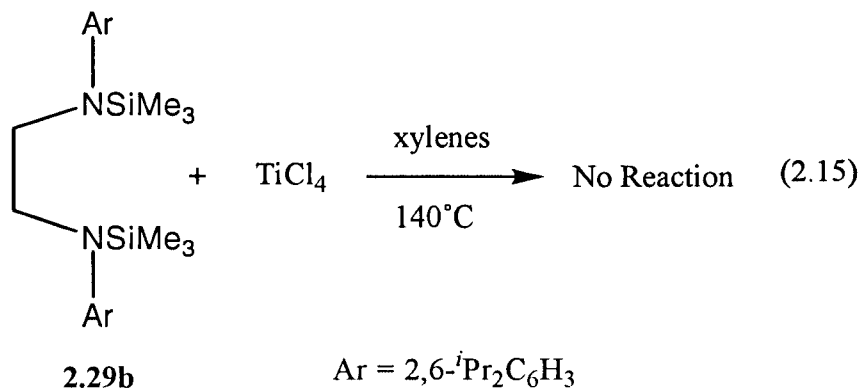
Ethyl Linked Chelating Diamide Complexes of Titanium

The trimethylsilyl derivative **2.29b** was prepared from the diamine **2.2b** (Scheme 2.8). The disilylamine **2.29b** and TiCl_4 were combined in xylenes and heated to 140°C for

Scheme 2.8: Synthesis of disilylamine **2.28b**

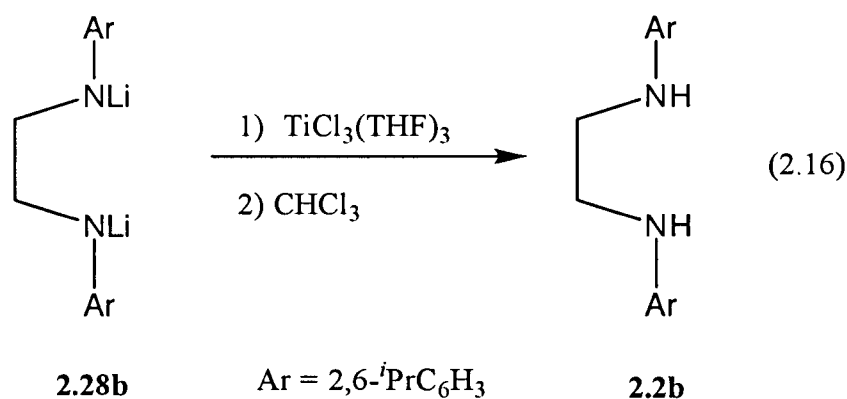


16 hours (eq. 2.15). The lack of reaction was evident in the ^1H NMR spectrum of the reaction mixture which showed only the presence of the disilylamine **2.29b**.



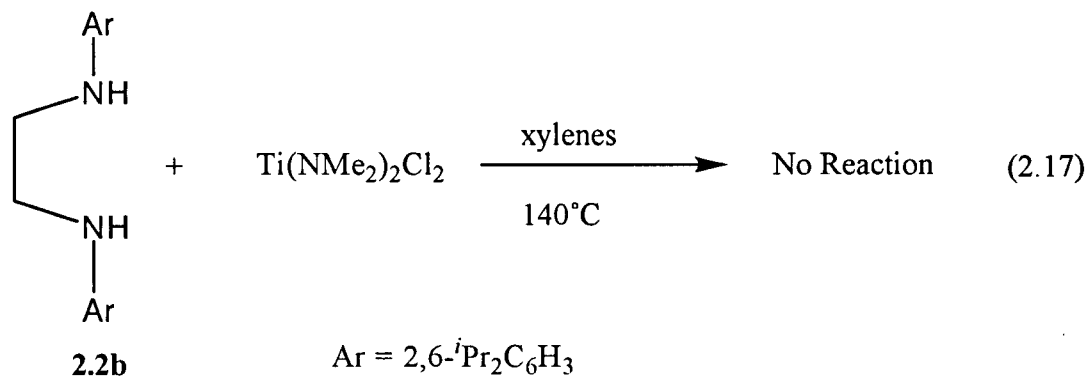
This result is in contrast to the results obtained from the transmetallation of trimethylsilamines **2.9a,b** and **2.19a,b** with TiCl_4 . The amount of steric bulk located around the nitrogen atom of the disilylamine **2.29b** may account for the lack of reaction in this case. Complex **2.29b** must be able to coordinate to the titanium atom in order for the transmetallation reaction to occur. Reducing the carbon linkage from three to two carbon atoms may have created a situation where the complex **2.29b** is too bulky to get within bonding distance of the TiCl_4 .

Previous experience with the reaction between the propyl linked and butyl linked lithium amides **2.7b** and **2.18a,b** with $\text{TiCl}_4(\text{THF})_2$ indicated that reduction of the titanium centre occurs to a great extent. Cummins has recently reported a strategy to overcome the reduction of the titanium atom.³² This involves the addition of a lithium amide to $\text{TiCl}_3(\text{THF})_3$, followed by oxidation with chloroform to give the titanium (IV) dichloride. Addition of the dilithium salt **2.28b** to $\text{TiCl}_3(\text{THF})_3$ followed by the addition of chloroform leads to the isolation of the diamine **2.2b** (eq. 2.16). It may be that the titanium (III) species



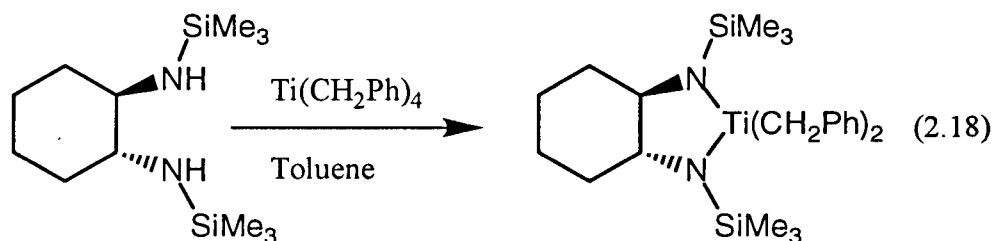
generated is unstable and decomposes. The ligand could then abstract a proton from the solvent to give back the starting diamine. This reaction was not probed further as other methods were explored.

A transamination reaction between the diamine **2.2b** and $\text{Ti}(\text{NMe}_2)_2\text{Cl}_2$ was attempted next. No reaction occurs between these two compounds in refluxing xylenes (eq. 2.17). The ^1H NMR spectrum of the reaction mixture showed the presence of diamine **2.2b**

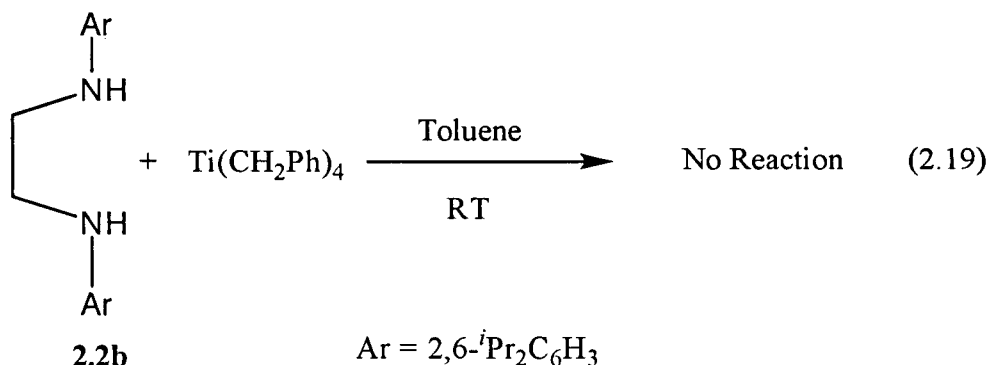


and decomposed $\text{Ti}(\text{NMe}_2)_2\text{Cl}_2$. This result is consistent with previous results obtained from the reaction of diamine **2.3b** with $\text{Ti}(\text{NMe}_2)_2\text{Cl}_2$.

Alkane elimination is another route by which a diamine can be appended to a metal centre. Jordan has successfully prepared a chelating diamide of titanium in this fashion (eq. 2.18).¹⁷ The diamide formed in this reaction is similar to the diamide expected from the



reaction between compound **2.2b** and $\text{Ti}(\text{CH}_2\text{Ph})_4$. In this case, no reaction was observed at room temperature between diamine **2.2b** and $\text{Ti}(\text{CH}_2\text{Ph})_4$ (eq. 2.19). The reaction mixture

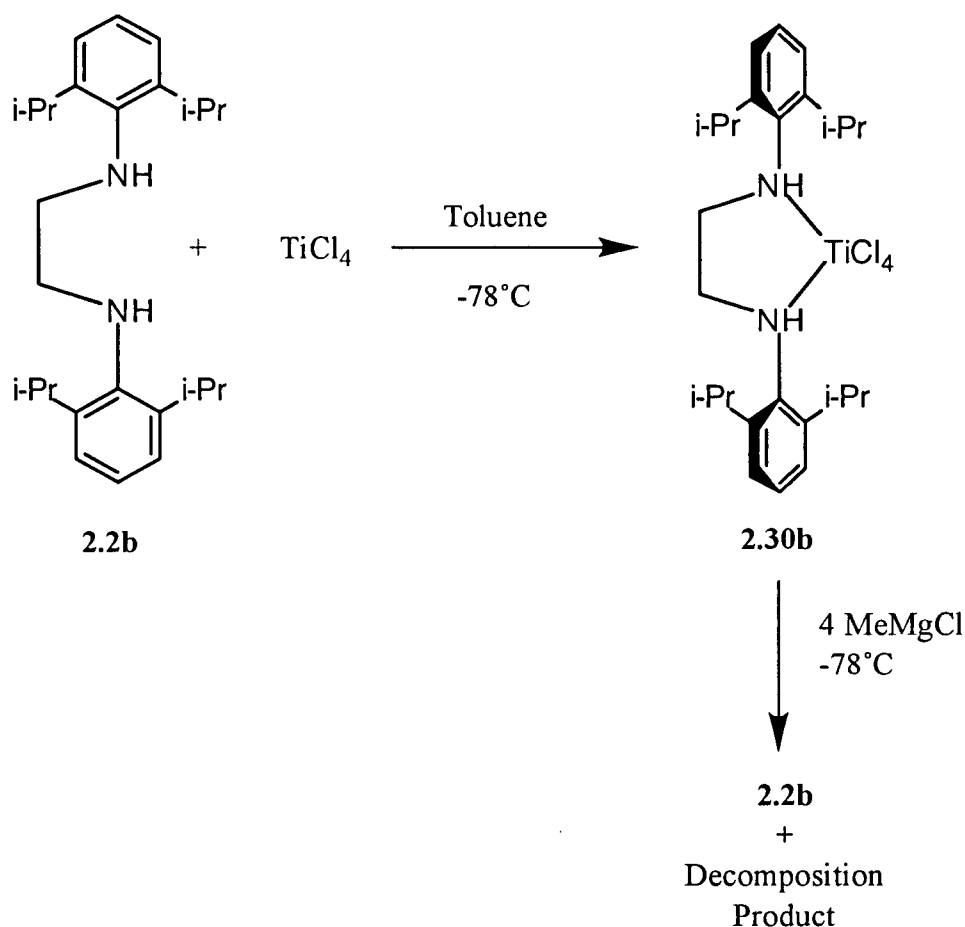


could not be heated since $\text{Ti}(\text{CH}_2\text{Ph})_4$ decomposes at higher temperatures. This result reflects the difference in the steric bulk of the group attached to the nitrogen atom. The 2,6- $^i\text{Pr}_2\text{C}_6\text{H}_3$ group is much larger than the SiMe_3 group and hence prevents coordination to the titanium atom. Furthermore the proton of complex **2.2b** has a higher pK_a than the proton of a silylamine.⁴³ Therefore complex **2.2b** may not be as efficient at protonating the benzyl groups.

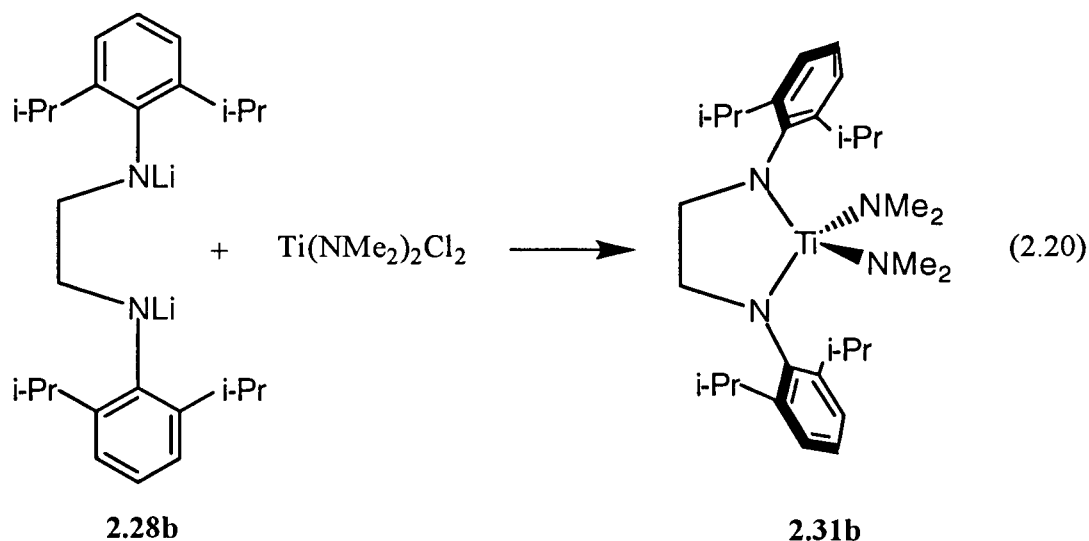
Precoordination of the ligand is necessary for the alkane elimination reaction to occur. It may be possible to precoordinate the diamine to the less sterically encumbered TiCl_4 and

then metathesize the Ti–Cl bonds with methyl Grignard. The diamine **2.2b** was added to TiCl_4 in toluene at -78°C to generate the diamine adduct **2.30b** *in situ*. Addition of four equivalents of MeMgBr did not result in the expected evolution of methane. The only products detected in the ^1H NMR spectrum of the reaction were starting diamine **2.2b** and an unidentifiable black product, presumably decomposed TiMe_4 (Scheme 2.9).

Scheme 2.9: Attempted alkane elimination reaction via precoordination of the diamine ligand.

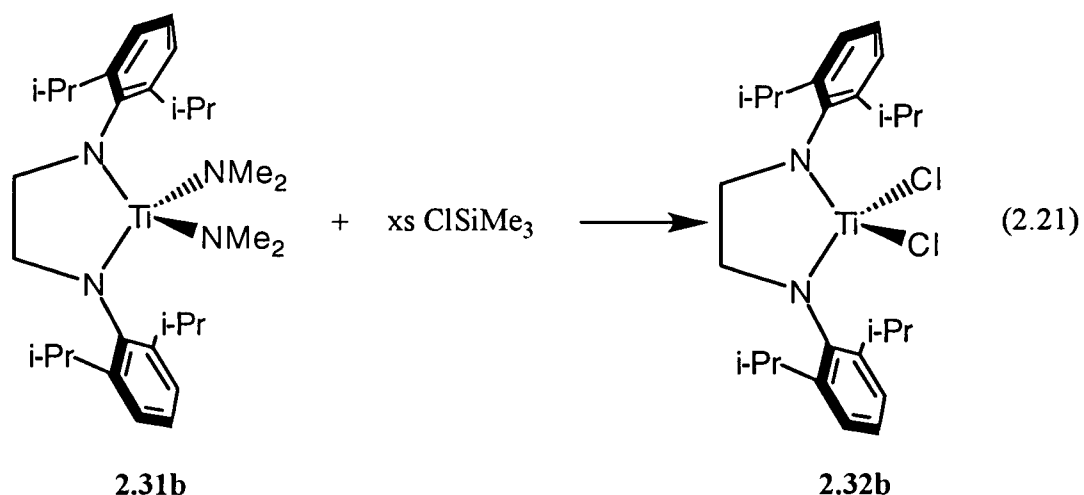


A successful method for appending the propyl linked diamine **2.3b** to titanium was the transmetallation of $\text{Ti}(\text{NMe}_2)_2\text{Cl}_2$ with the dilithium salt **2.7b**. Addition of the dilithium salt **2.28b** to $\text{Ti}(\text{NMe}_2)_2\text{Cl}_2$ affords the mixed amide **2.31b** (eq. 2.20). The yields by ^1H NMR spectroscopy are greater than 90%, however, due to the high solubility of complex **2.31b**, the product could not be isolated. Interestingly, at room temperature, the aryl groups are freely



rotating about the N–C_{ipso} bond as indicated by the presence of only one isopropyl methyl doublet in the ¹H NMR spectrum. This difference is undoubtedly related to the reduced N–Ti–N “bite angle” for complex **2.31b**. The reduced angle effectively pulls the aryl groups further away from the metal thereby allowing them to pass through a molecular plane of symmetry. Another possibility, which may exist, is the resonances for the isopropyl methyl groups are coincident in the ¹H NMR spectrum. However, these resonances are resolved in the other titanium complexes characterized in this chapter. The NCH₂ protons in the ¹H NMR spectrum, appear as a singlet and have shifted downfield from 3.15 ppm (free amine) to 3.90 ppm (chelating).

Excess chlorotrimethylsilane was added to the solution of complex **2.31b** in order to generate the dichloride **2.32b** (eq. 2.21). Complex **2.32b** was formed in nearly quantitative yield as determined by ¹H NMR spectroscopy. Once again, due to the high solubility of complex **2.32b**, pure product could not be isolated from the reaction mixture. As with complex **2.31b**, only one isopropyl methyl doublet is observed in the ¹H NMR spectrum. It is likely, that the added degrees of freedom afforded complexes **2.31b** and **2.32b** is contributing to their high solubility in aliphatic solvents. It may be possible to reestablish the restricted rotation about the N–C_{ipso} bond by introducing bulky substituents on the

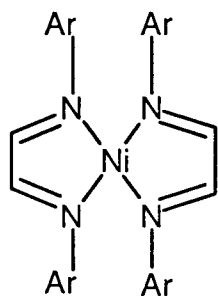


methylene carbons of the ethane linkage. With the synthetic difficulties associated with these complexes, it was decided that a new 2-carbon backbone should be explored.

Ene-diamide complexes

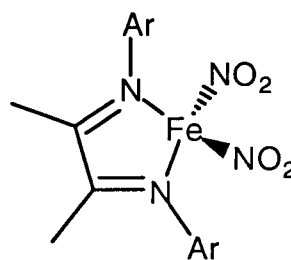
Extensive research into diazadiene (DAD) ligands has been carried out by tom Dieck. His studies have shown that complexes bearing these ligands are easy to prepare and possess considerable reactivity. The majority of the work on DAD ligands has concentrated on the reactions of these ligands with late transition metals. In these cases, tom Dieck found that many new DAD based transition metal complexes could easily be prepared. For example, bis[glyoxal-bis(2,6-dimethylphenylimine)]nickel(0) (**2.33**) was one of the many DAD nickel species synthesized.⁴⁴

tom Dieck also found that the iron species **2.34** was capable of dimerizing both butadiene and isoprene.⁴⁵ These species also show high catalytic activity for the dimerization of conjugated dienes. Most late transition metal catalyst systems generate olefin dimers or oligomers. Studies by Brookhart have shown that the DAD complex **2.35** is able to catalyze the polymerization of ethylene and α -olefins to give highly branched, high molecular weight polymers.⁴⁶ Furthermore, by altering the substitution at the nitrogen and adding MAO to complex **2.36**, polymerization at ambient temperatures could be induced.¹⁹



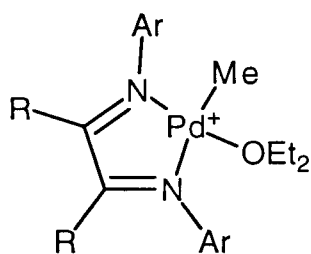
Ar = 2,6-*i*Pr₂C₆H₃

2.33

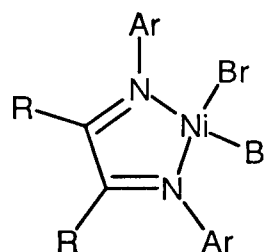


Ar = 2,6-*i*Pr₂C₆H₃, C₆H₅

2.34



2.35

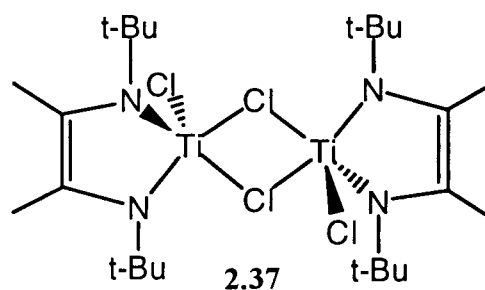


2.36

R = H; Ar = 2,6-(*i*Pr)₂C₆H₃, 2,6-Me₂C₆H₃

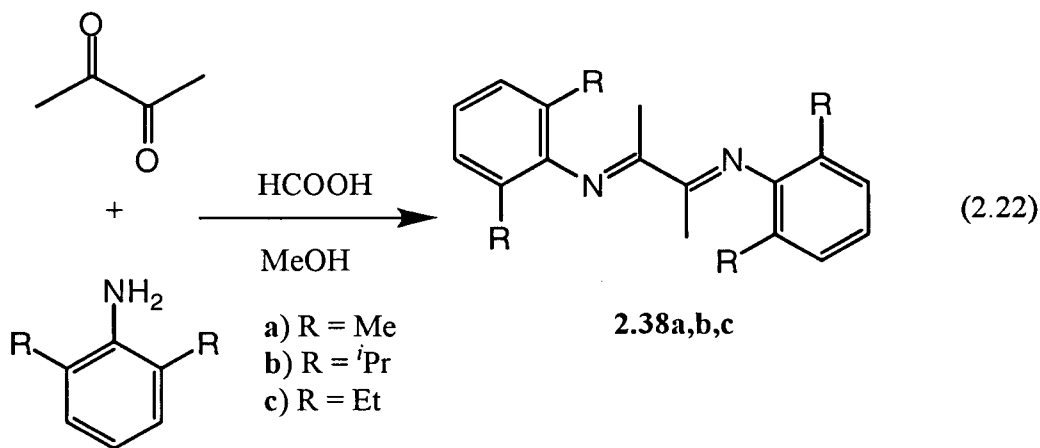
R = Me; Ar = 2,6-(*i*Pr)₂C₆H₃, 2,6-Me₂C₆H₃

tom Dieck's work has also shown that DAD ligands are capable of stabilizing early transition metal complexes. For example, complex **2.37** was synthesized by the reduction of TiCl₄ with lithium in the presence of an aliphatic DAD ligand.⁴⁷ However, DAD type ligands which incorporate bulky aryl groups at nitrogen and methyl groups on the ligand backbone have not been incorporated into Group 4 metal complexes. With the proven ability of other DAD type ligands to coordinate to many transition metal centres there is reason to believe that coordination of this particular form of DAD to Group 4 metals is feasible. Furthermore, the presence of the methyl group on the ligand backbone may provide the steric bulk necessary to prevent the free rotation of the aryl group about the N-C_{ipso} bond.



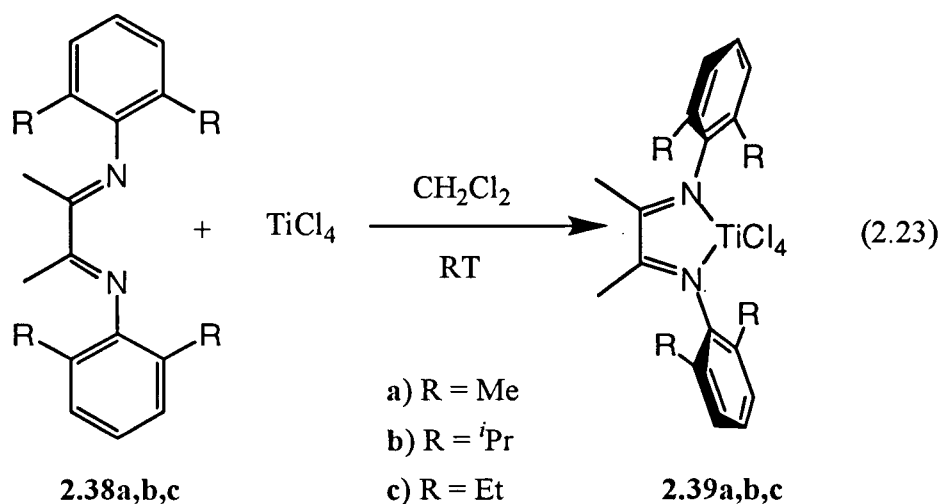
2.37

As reported by tom Dieck, ligands of this type can be easily prepared in high yield from inexpensive starting materials.⁴⁴ Addition of two or three drops of formic acid catalyzes the reaction between 2,3-butanedione and the 2,6-disubstituted anilines to give the bisimines **2.38a,b,c** (eq.2.22).



Bis(imine) **2.38a** exhibits the simplest ¹H NMR spectrum with a single resonance for each of the two methyl groups of the ligand. By replacing the methyl groups of the phenyl ring with ethyl groups (**2.38c**), the spectrum becomes slightly more complicated. Restricted rotation about the N–C_{ipso} bond causes the CH₂CH₃ protons to become diastereotopic. Each hydrogen of the methylene group couples with the methyl group to give a quartet which is further split by the corresponding geminal hydrogen. This leads to an ABM pattern centred at 2.38 ppm. The inequivalent geminal hydrogens also give rise to two overlapping doublets for the corresponding CH₂CH₃ protons. A similar effect is observed for compound **2.38b**. In this case the two isopropyl methyls are diastereotopic and give rise to two doublets in the ¹H NMR spectrum while the isopropyl methine appears as a septet.

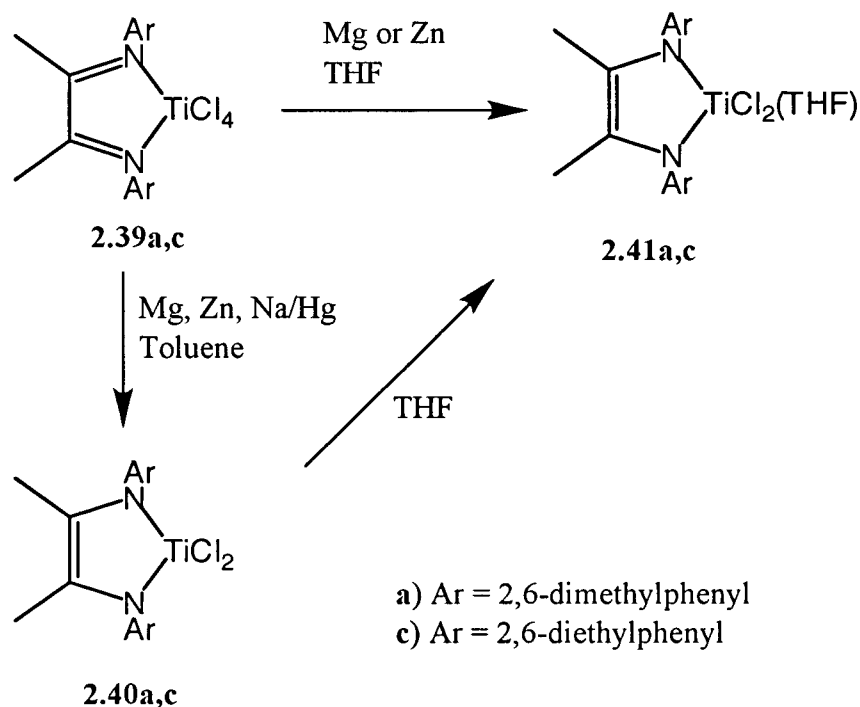
Dropwise addition of TiCl₄ to a dichloromethane solution of bisimines **2.38a,b,c** resulted in the precipitation of analytically pure [bis(imine)]TiCl₄ (**2.39a,b,c**) (eq. 2.23). Due to the highly insoluble nature of complexes **2.39a,b,c**, nearly quantitative yields are obtained for each complex.



Complex **2.39a** was insoluble in all common deuterated solvents and therefore no NMR spectral data were obtained. However, elemental analysis was able to confirm that the 1:1 adduct, **2.39a**, was formed. The ^1H NMR spectrum of complex **2.39c** revealed a downfield shift for the methyl resonance of the carbon linkage and the methylene resonances of the ethyl group. The resonance for the methyl group of the ethyl fragment move downfield from 2.08 ppm (free imine) to 2.30 ppm for complex **2.39c**. Furthermore, the CH_2CH_3 resonances in complex **2.39c** have separated into two distinct multiplets at 3.00 ppm and 2.76 ppm from 2.37 ppm (free imine). A similar downfield shift occurs for complex **2.39b**. The resonance for the isopropyl methine shift downfield from 2.87 ppm to 3.47 ppm. The methyl groups in the carbon linkage also move downfield slightly from 2.15 ppm to 2.39 ppm. The remaining resonances for complexes **2.39b,c** remain relatively unchanged.

The reaction of complexes **2.39a,b,c** with different reducing agents were studied to determine the best method of reduction of the DAD ligand to the ene-diamide form. Concurrent removal of two chloride atoms would give the reduced four-coordinate Ti (II) species. It is expected that the titanium (II) species would in turn reduce the bis(imine) to an ene-diamide **2.40a,b,c** (Scheme 2.10).

Scheme 2.10: Reduction of Diazadienes **2.39a,c**



The products obtained from the reduction of the diazadiene **2.39a,c** with Zn dust and Mg turnings are the same. However, the products are dependent on the solvent utilized in the reaction. Carrying out the reductions in THF gave rise to the ene-diamide THF adducts **2.41a,c** (Scheme 2.10). The THF resonances in the ^1H NMR spectra of complexes **2.41a,c** are broad indicating a slow exchange of coordinated THF. If the THF solvent is replaced with toluene the base-free complexes **2.40a,c** are formed exclusively (Scheme 2.10). The ^1H NMR spectrum of complex **2.40a** displays two broad singlets for the backbone and aryl methyl groups. Complexes **2.40a,c** can be converted to their THF adducts **2.41a,c** by recrystallization from hexanes in the presence of THF. The reduction of complex **2.40c** also results in the formation of significant amounts of bisimine **2.38c**. The ene-diamide **2.40c** can be separated from the bisimine **2.38c** by recrystallization. The reduction of complexes **2.39a,c** can also be carried out with sodium/mercury amalgam in toluene to obtain the base free complexes **2.40a,c** (Scheme 2.10).

The molecular structure of complex **2.41a** was determined by X-ray crystallography (Figure 2.9). The local geometry can best be described as trigonal bipyramidal with the THF and the two nitrogen atoms having a meridional relationship (Figure 2.10).

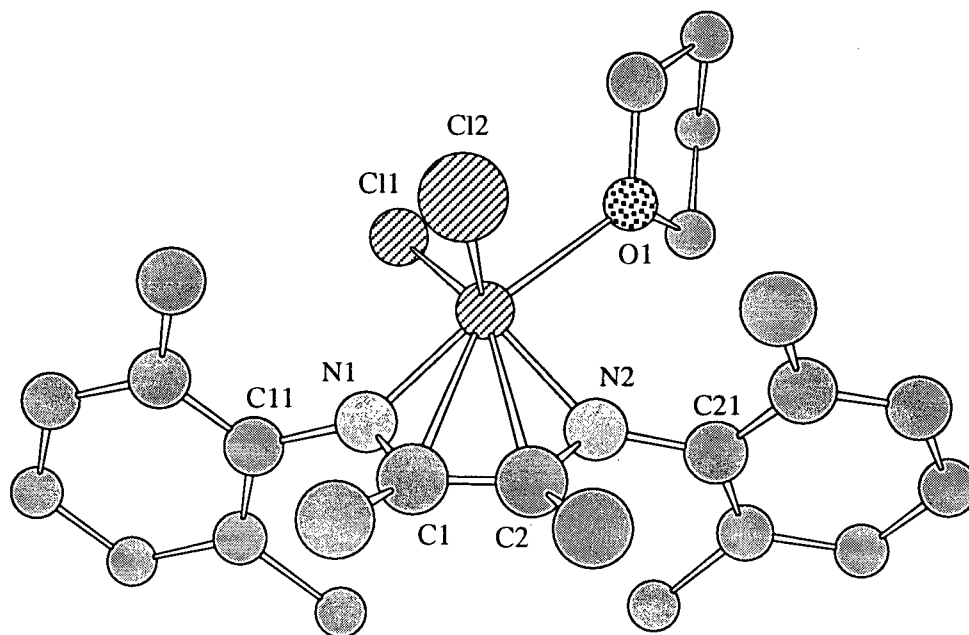


Figure 2.9: Chem 3D Plus drawing of complex **2.41a**

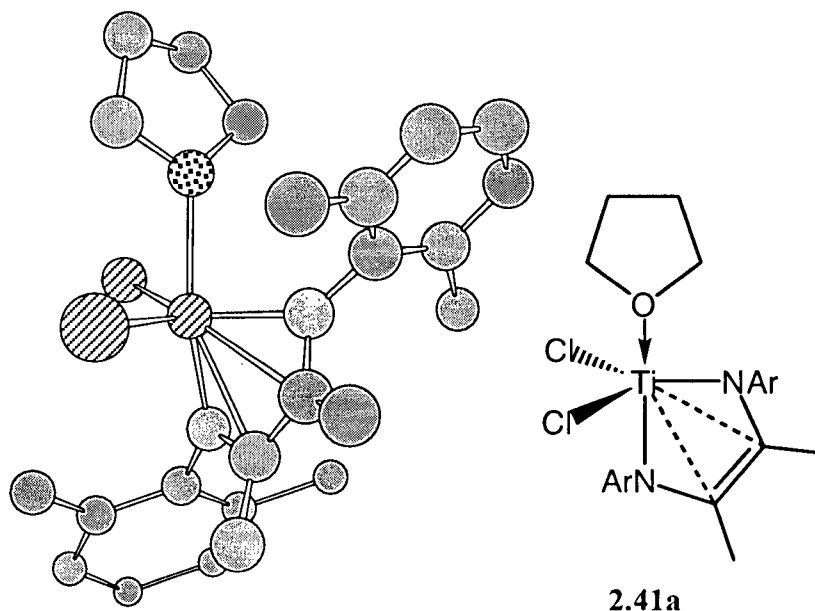


Figure 2.10: Alternative view of ene-diamide **2.41a**

Table 2.4 contains selected bond distances and angles of complex **2.41a**. The sum of the angles around N1 is 355.8° while the sum of the angles around N2 is 358.9°. This indicates that the hybridization about the nitrogen atoms of the ligand is deviating slightly from a planar sp² hybridization. This deviation can be attributed to the existence of π donation from the p-orbitals of the double bond. This causes the carbon linkage of the ligand to be situated closer to the metal centre. In order for this to occur, the Ti–N–C_{aryl} bond angles must increase with a subsequent decrease in the Ti–N–C_{olefin} bond angles. The

Table 2.4: Selected bond distances and angles for complex **2.41a**

Bond Distances (Å)

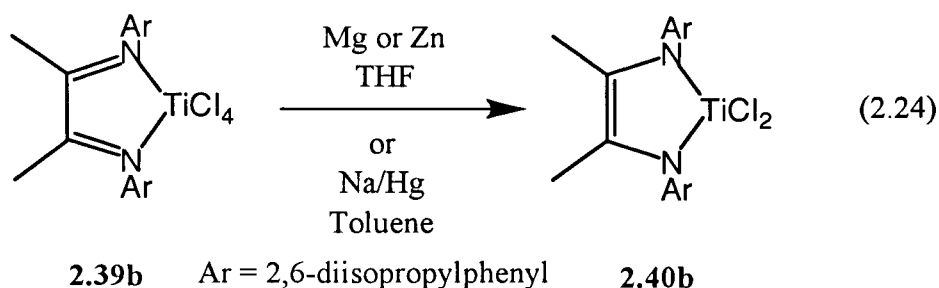
Ti(1)-N(1)	1.906(6)	Ti(1)-N(2)	1.914(5)
Ti(1)-O(1)	2.207(5)	Ti(1)-Cl(1)	2.284(2)
Ti(1)-Cl(2)	2.316(2)	Ti(1)-C(2)	2.417(7)
Ti(1)-C(1)	2.437(7)	N(1)-C(1)	1.382(8)
N(1)-C(11)	1.424(6)	N(2)-C(2)	1.387(8)
N(2)-C(21)	1.424(6)	C(1)-C(2)	1.376(9)

Bond Angles (°)

N(1)-Ti(1)-N(2)	88.1(2)	N(1)-Ti(1)-O(1)	161.6(2)
N(2)-Ti(1)-O(1)	86.9(2)	N(1)-Ti(1)-Cl(1)	107.8(2)
N(2)-Ti(1)-Cl(1)	114.5(2)	O(1)-Ti(1)-Cl(1)	90.35(14)
N(1)-Ti(1)-Cl(2)	88.2(2)	N(2)-Ti(1)-Cl(2)	130.5(2)
O(1)-Ti(1)-Cl(2)	81.66(14)	Cl(1)-Ti(1)-Cl(2)	113.54(10)
N(1)-Ti(1)-C(2)	64.5(2)	N(2)-Ti(1)-C(2)	35.0(2)
O(1)-Ti(1)-C(2)	117.7(2)	Cl(1)-Ti(1)-C(2)	96.2(2)
Cl(2)-Ti(1)-C(2)	145.0(2)	N(1)-Ti(1)-C(1)	34.4(2)
N(2)-Ti(1)-C(1)	64.8(2)	O(1)-Ti(1)-C(1)	150.6(2)
Cl(1)-Ti(1)-C(1)	93.9(2)	Cl(2)-Ti(1)-C(1)	122.5(2)

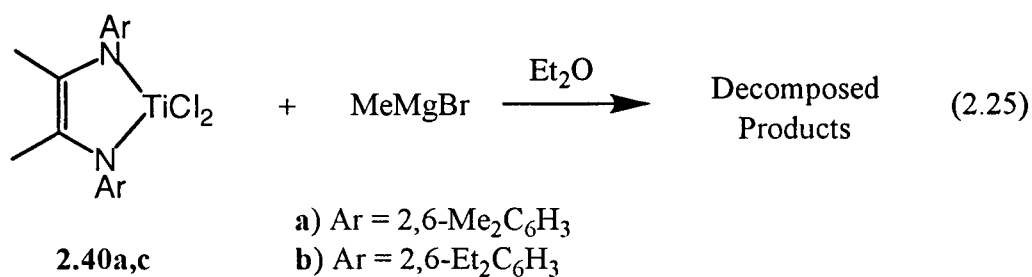
carbon atoms of the backbone are within bonding distance to titanium in the solid state. The bond distance between Ti–C1 is 2.437 Å and Ti–C2 is 2.417 Å. The N–Ti–N bond angle for this complex is 88.1°. The bonding of the DAD ligand is similar to the bonding observed for transition metal butadiene complexes,⁴⁸ however, the bond distance between C1 and C2 (1.376 Å) is significantly shorter than the carbon–carbon single bond distance of butadiene complexes.⁴⁸⁻⁵⁰

The reduction of complex **2.39b** can be achieved using Mg, Zn or Na/Hg amalgam. The presence of THF has no effect on the outcome of these reductions. This is probably a result of the extra steric bulk provided by the isopropyl substituted aryl groups. Regardless of the solvent, the product in each case is the base-free ene-diamide **2.41b** (eq. 2.24).



However, the reactions are not without their drawbacks. Significant amounts of bis(imine) **2.38b** are observed in these reductions. This may be a result of the bulkiness of the DAD ligand, and its inability to remain coordinated to the titanium during reduction. Unfortunately, complex **2.40b** is highly soluble in aliphatic solvents and cannot be separated from **2.38b**. Through repetitive recrystallizations the ratio of **2.40b** to **2.38b** could only be raised to about 2:1.

The alkylation of complexes **2.40a,c** with MeMgBr produced unidentifiable products (eq. 2.25). It is possible that the dimethyl complex is initially formed and then



decomposes through alkylation of the double bond with concomitant reduction of the metal centre from Ti(IV) to Ti(II) (Figure 2.11). Coordination of the olefin portion of the amide linking group to the titanium centre induces a slight positive charge on the carbon atoms of the double bond. Nucleophilic attack by the titanium–methyl on the double bond results in the formal two electron reduction of the titanium centre. The three coordinate Ti(II) species then probably decomposed due to its low coordination number.

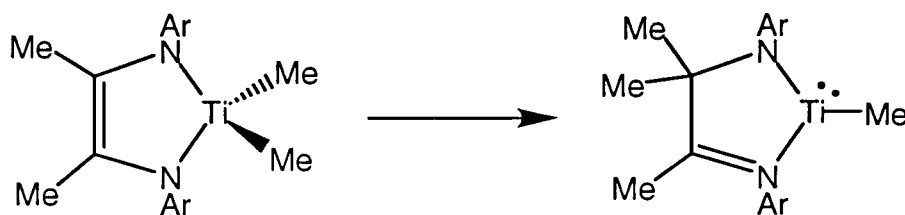
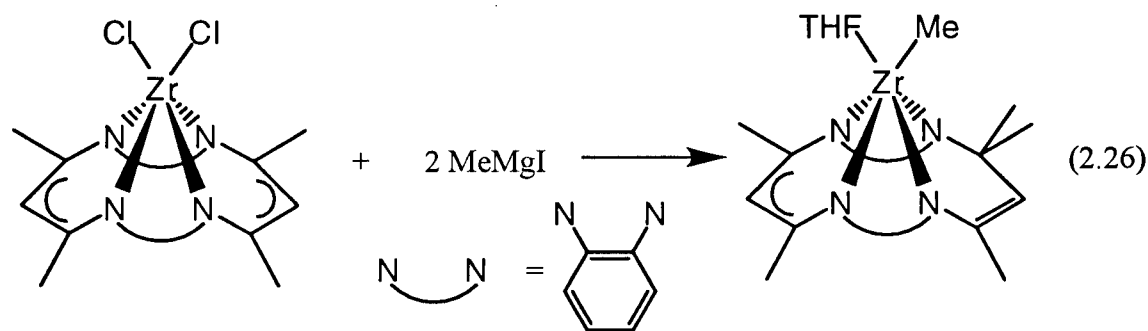
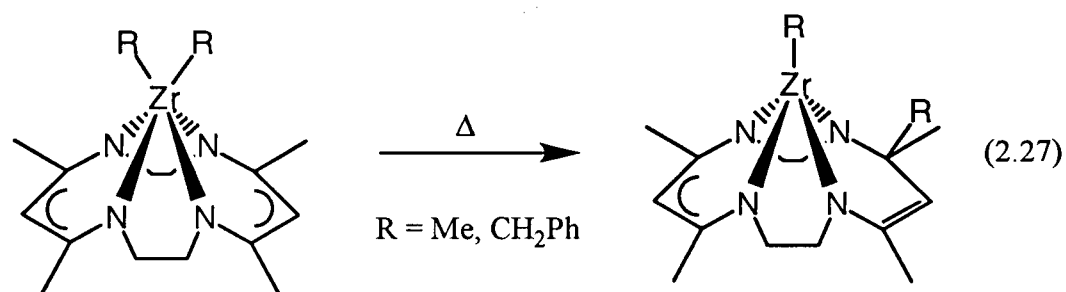


Figure 2.11 Possible decomposition pathway for the alkylation of complexes 2.40a,c

Similar alkyl migrations have been observed by Floriani⁵¹ (eq. 2.26) and Jordan²⁸



(eq. 2.27) with tetraaza macrocyclic zirconium alkyl derivatives. Although alkyl

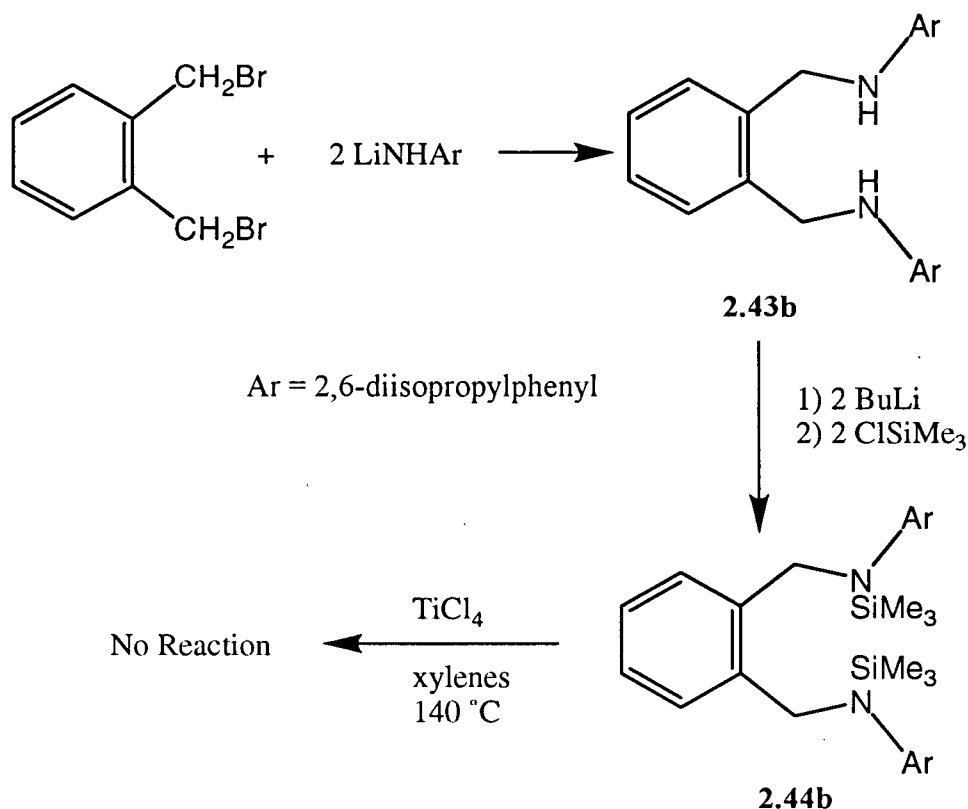


complexes of ene-diamides **2.40a,c** could not be synthesized, the dichlorides still provide the desired complexes to study the polymerization of α -olefins.

Alternative ligand Systems

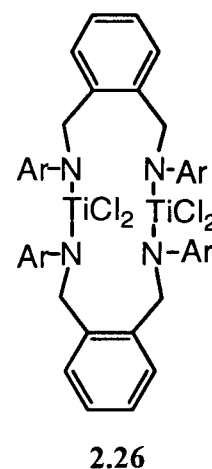
In an effort to study alternative bridging groups for the diamido ligand, an α,α' substituted *ortho*-xylene diamine was synthesized. The xylyl linked diamine **2.43b** can be synthesized in a single step from α,α' -dibromo-*o*-xylene and two equivalents of 2,6-diisopropylolithiumanilide (Scheme 2.11). Diamine **2.43b** is obtained in greater than 80% yields as a white crystalline solid. The *o*-xylyl linked ligand should be similar to the butyl linked ligand although the *o*-xylyl linkage will be slightly more rigid.

Scheme 2.11: Attempted synthesis of a xylyl linked diamide complex of titanium



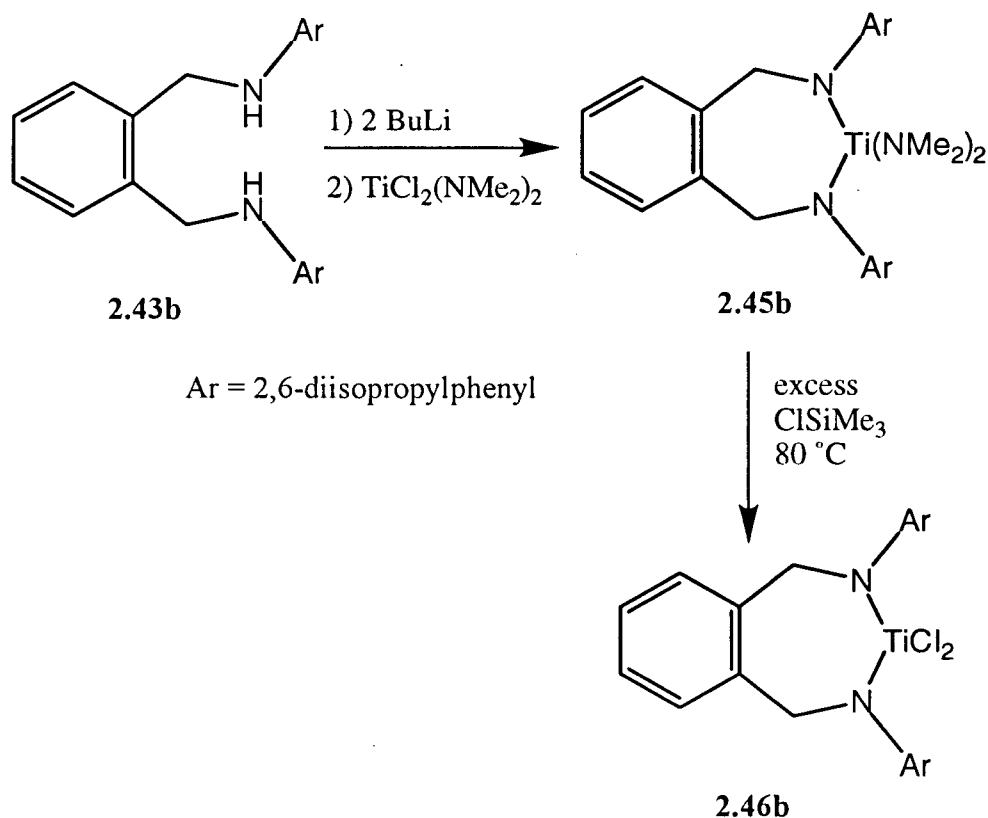
Diamine **2.43b** was derivatized to the bis(trimethylsilyl) complex **2.44b** by generating the dilithium salt *in situ* and quenching with excess chlorotrimethylsilane (Scheme 2.11). A transmetallation reaction between TiCl_4 and complex **2.44b** was attempted in refluxing xylenes. The ^1H NMR spectrum of the mixture revealed that no reaction had occurred. It is very likely that the nitrogens in complex **2.44b** are too crowded to react with TiCl_4 . The steric bulk around the opposing nitrogen atoms protect each other from reaction with TiCl_4 . This is a result of the *ortho*-substitution of the xylyl linkage. This is one way in which the xylyl linkage differs with respect to the butyl linked diamine.

Interestingly, by substituting the trimethylsilyl moiety with a trimethylstannyl moiety for compound **2.44b** in Scheme 2.11, the bridging complex **2.26** is formed.⁴² In an effort to circumvent this



problem, a metathesis reaction between the dilithium salt of **2.43b** and $\text{Ti}(\text{NMe}_2)\text{Cl}_2$ was attempted (Scheme 2.12).

Scheme 2.12: Successful synthesis of a xylyl linked diamide complex of titanium

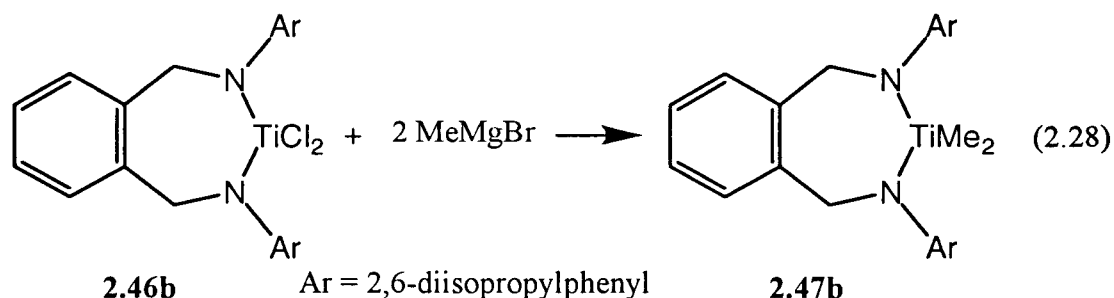


This method was successful in synthesizing the heteroleptic tetraamido complex **2.45b**. Complex **2.45b** was obtained in approximately 50 % yield as orange-red crystals. The dichloride complex **2.46b** can be synthesized from complex **2.45b** by the addition of excess chlorotrimethylsilane and heating to 80°C (Scheme 2.12). Isolated yields of the dichloride **2.46b** were extremely low due to the high solubility of the product in aliphatic solvents.

The room temperature ^1H NMR spectrum of complex **2.45b** exhibits resonances consistent with with local C_{2v} -symmetry. The proton resonance attributable to the methylene protons appear as a broad singlet at 4.85 ppm, while a single isopropylmethine resonance is observed along with two isopropyl methyl doublets. This indicates that there is

restricted rotation about the N-C_{ipso} bond. Since the ¹H NMR spectrum reveals an overall C_{2v}-symmetric structure, it appears that the *o*-xylyl linkage is much more flexible than expected. The low temperature ¹H NMR spectrum reveals that complex **2.45b** maintains the C_{2v}-symmetry down to -80°C. The ¹H NMR spectrum of the dichloride derivative **2.46b** is similar to that of **2.45b**. The low temperature ¹H NMR spectrum of complex **2.46b** maintains the C_{2v}-symmetry down to -80°C.

Complex **2.46b** can be converted into the dimethyl derivative **2.47b** with two equivalents of MeMgBr (eq. 2.28). The titanium methyl resonance in the ¹H NMR



spectrum appears at 0.46 ppm. This is in good agreement with the titanium methyl resonance of the propyl linked bis(amido)titaniumdimethyl complex **2.11b** (*vide supra*). The ¹H NMR spectrum also reveals that complex **2.47b** has C_{2v}-symmetry.

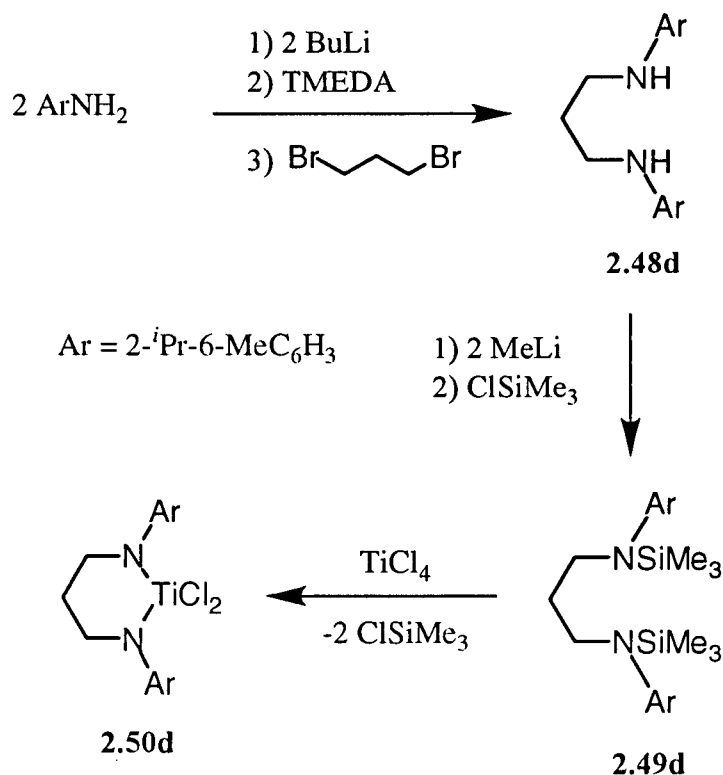
Rotameric Isomers of a Chelating Diamido Titanium Complex

In order to determine if there is any interaction between the two substituted aryl groups of the ligand, an unsymmetrical 2,6-disubstituted aniline was substituted for the 2,6-dialkylanilines used previously. Assuming the addition of the silylated amines to TiCl₄ is stepwise, the aryl group on the first nitrogen may influence the orientation of the second aryl group. The propyl linkage was chosen since complexes bearing this ligand are easy to isolate.

The diamine **2.48d** was synthesized from two equivalents of (2-isopropyl-6-methyl)lithiumanilide and 1,3-dibromopropane (Scheme 2.13). Purification of compound

2.48d was carried out using the same procedure as the diisopropylaryl analogue **2.3b**. The diamine **2.48d** is obtained as a yellow oil in 58% yield after acidification with HCl, isolation of the ammonium hydrochloride salt and neutralization. The trimethylsilyl derivative **2.49d** can be synthesized from dilithium salt of **2.48d** and excess chlorotrimethylsilane (Scheme 2.13). The ^1H NMR spectra of compounds **2.48d** and **2.49d** are nearly identical to the spectra of diamines **2.3a,b** and their trimethylsilyl derivatives **2.9a,b**.

Scheme 2.13: Synthesis of an unsymmetrically disubstituted diamine.



Diamidotitanium dichloride **2.50d** was synthesized by heating complex **2.49d** and one equivalent TiCl_4 to 140°C for 12 hours (Scheme 2.13). The titanium dichloride was obtained in excellent yield as a red highly crystalline solid. Assuming restricted rotation about the N- C_{ipso} bond exists, there are two rotameric isomers possible for complex **2.50d** (Figure 2.12). One of the complexes is *rac*-**2.50d** which will exhibit C_2 -symmetry in its ^1H NMR spectrum. The other complex is *meso*-**2.50d** which will exhibit C_s -symmetry by ^1H NMR spectroscopy.

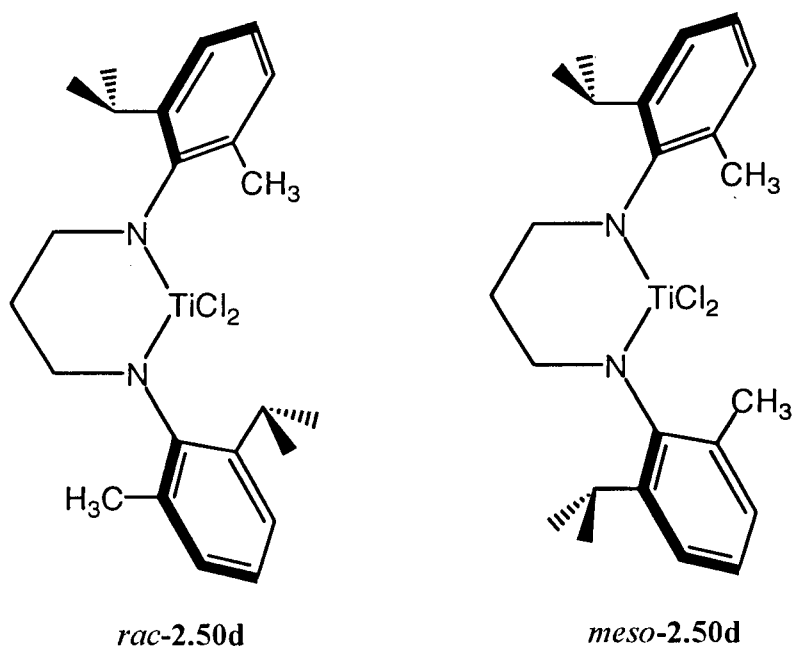
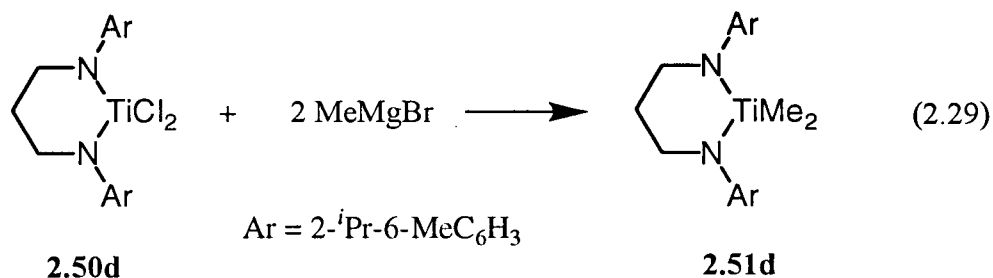


Figure 2.12: Possible geometrical isomers for complex **2.50d**

The ^1H NMR spectrum of complex **2.50d** indicates a product with either local C_2 or C_s -symmetry. Both symmetries give rise to four signals for the NCH_2 and NCH_2CH_2 protons as well as one CH_3 signal and two different CHMe_2 resonances in the ^1H NMR spectrum. Therefore, it is impossible to determine the symmetry by ^1H NMR spectroscopy at this time. It is possible to note, however, that a C_{2v} -symmetric product is not present. If complex **2.50d** was rapidly interconverting between the *rac* and *meso* rotamers it would exhibit a time averaged ^1H NMR spectrum consistent with a C_{2v} -symmetric complex. The only way to isomerize between the *rac* and *meso* isomers would require rotation about the $\text{N}-\text{C}_{\text{ipso}}$ bond. This is highly unlikely due to previous results obtained with the dimethylphenyl derivative **2.9a**. Analysis of the $^{13}\text{C}\{^1\text{H}\}$ NMR spectrum shows exactly twice as many carbon atoms as would be expected if only one rotamer was present. It appears that the two complexes have nearly identical ^1H NMR spectra. However the $^{13}\text{C}\{^1\text{H}\}$ NMR spectrum clearly indicates that *rac*-**2.50d** and *meso*-**2.50d** are present in a 1:1 ratio (identical carbons were integrated assuming that they have similar T_1 relaxation times).

Complex **2.50d** can be alkylated with two equivalents MeMgBr to give the highly crystalline yellow dimethyl derivative **2.51d** (eq. 2.29). The ^1H NMR spectrum of



complex **2.51d** shows three resonances for the titanium methyl groups in a 2:1:1 ratio. This indicates a 1:1 ratio of *meso*-**2.51d** and *rac*-**2.51d** (Figure 2.13). The complex *meso*-**2.51d**

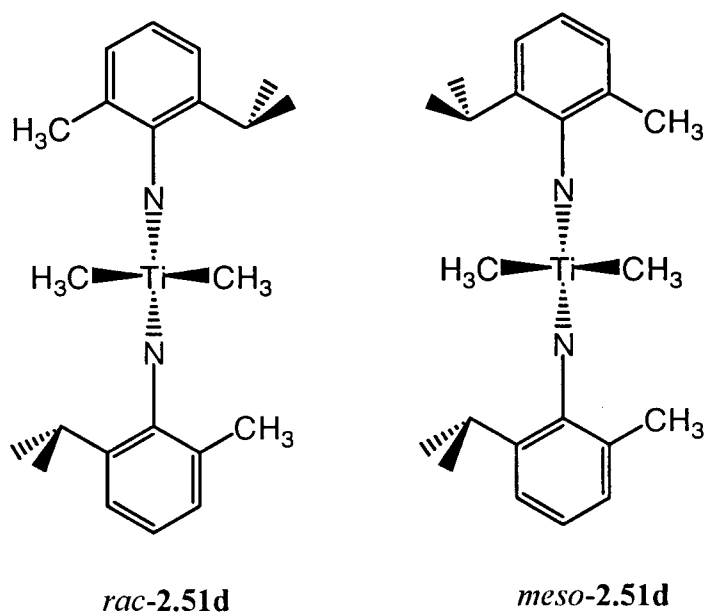


Figure 2.13: The two rotamers of complex **2.51d** (propyl backbone omitted for clarity)

gives rise to two different titanium methyl resonances integrating to three protons each. The complex *rac*-**2.51d** gives rise to a single titanium methyl resonance with an integration corresponding to six protons. There are also four isopropylmethyl resonances and two phenylmethyl resonances consistent with there being two products in a 1:1 ratio. This is in

agreement with the fact that *rac*-2.50d and *meso*-2.50d were present in the starting material in a 1:1 ratio. The remainder of the spectrum is fairly complicated with many overlapping methylene resonances.

Based on the above results, the orientation of the first arylamide does not influence the incoming arylamine. As a result, two rotamers are formed in a 1:1 ratio. Isomerization of these rotomers would not be expected as free rotation about the N-C_{ipso} bond has yet to be observed for the propyl linked diamides.

Reaction of Titanium Complexes with Lewis Acids

Boron–Carbon Bond Cleavage

The addition of pentane solutions of the dimethyl complexes **2.11a,b** to B(C₆F₅)₃⁵² affords the insoluble yellow–orange adducts **2.52a,b** in nearly quantitative yield (Scheme 2.14). Although it has so far proven very difficult to spectroscopically identify complexes **2.52a,b**, their reactivity is consistent with a cationic^{13,53} complex of the type {[ArN(CH₂)₃NAr]TiMe}⁺[MeB(C₆F₅)₃][−] (Ar = 2,6-*i*Pr₂C₆H₃, 2,6-Me₂C₆H₃). For example, complexes **2.52a,b** react rapidly with dichloromethane to give the dichloride derivatives **2.10a,b** (Scheme 2.14).⁵⁴ The deep red insoluble oils **2.53a,b** are formed when complexes **2.52a,b** are ‘dissolved’ in aromatic solvents or when **2.11a,b** and B(C₆F₅)₃ are combined in these solvents. Complexes **2.53a,b**, as well as the isolated adducts **2.52a,b**, are active catalysts for the living polymerization of 1-hexene (Chapter 3). Although pentane suspensions of compound **2.52a** are stable for days, complex **2.52b** slowly evolves methane over the course of several hours to give a new pentane soluble derivative (**2.54b**) in quantitative yield by ¹H NMR spectroscopy (Scheme 2.14).

Scheme 2.14: Borane activation of dimethyl complexes **2.11a,b** and possible reaction paths

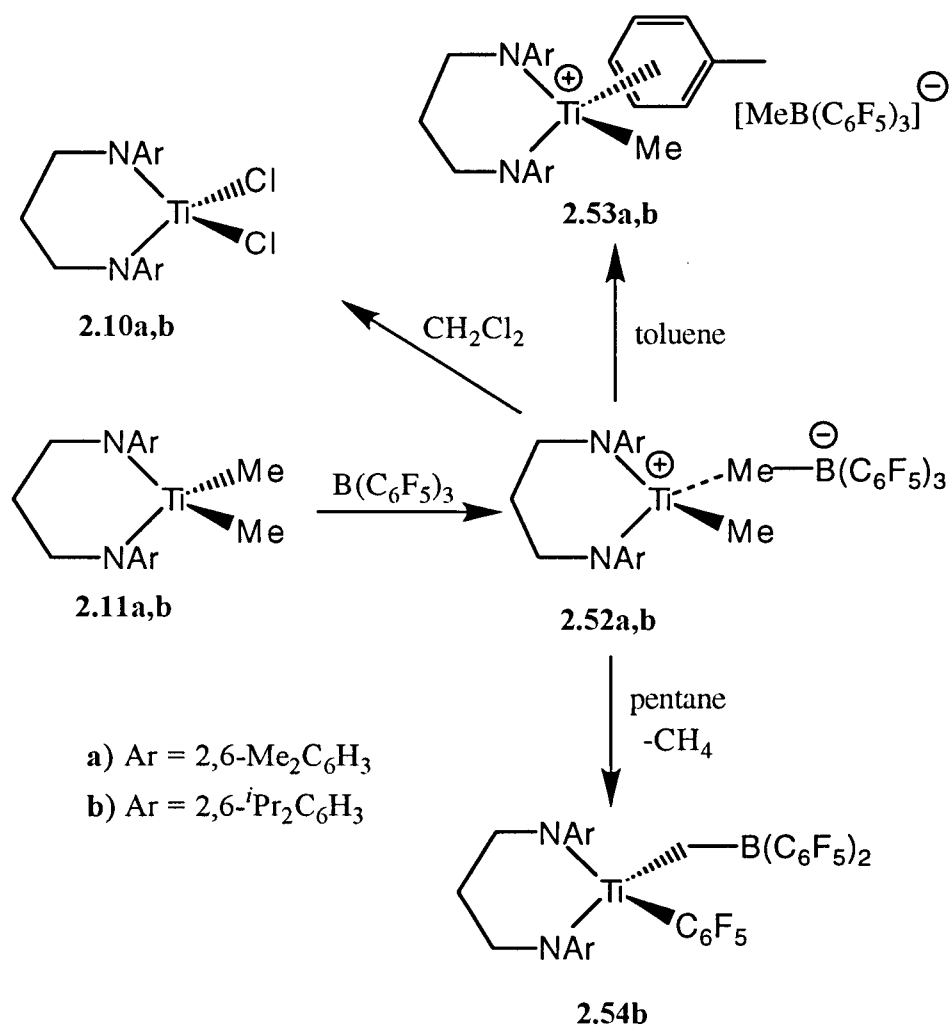


Figure 2.14 shows the ^1H NMR spectrum of **2.54b**. The ^1H NMR spectrum reveals that the complex has C_s symmetry coupled with restricted rotation about the N- C_{ipso} bonds of the ligand. A broad singlet at 3.92 ppm is assigned to the methylene protons based on NMR data from HMQC and DEPT experiments. Furthermore, the methylene protons resonance is split into a doublet ($^1J_{\text{CH}} = 114$ Hz) in the isotopically labeled complex $[\text{ArN}(\text{CH}_2)_3\text{NAr}]\text{Ti}[\text{C}^{13}\text{H}_2\text{B}(\text{C}_6\text{F}_5)_2](\text{C}_6\text{F}_5)$ (^{13}C -**2.54b**, prepared from $[\text{ArN}(\text{CH}_2)_3\text{NAr}]\text{Ti}(\text{C}^{13}\text{H}_3)_2$, ^{13}C -**2.11b**).

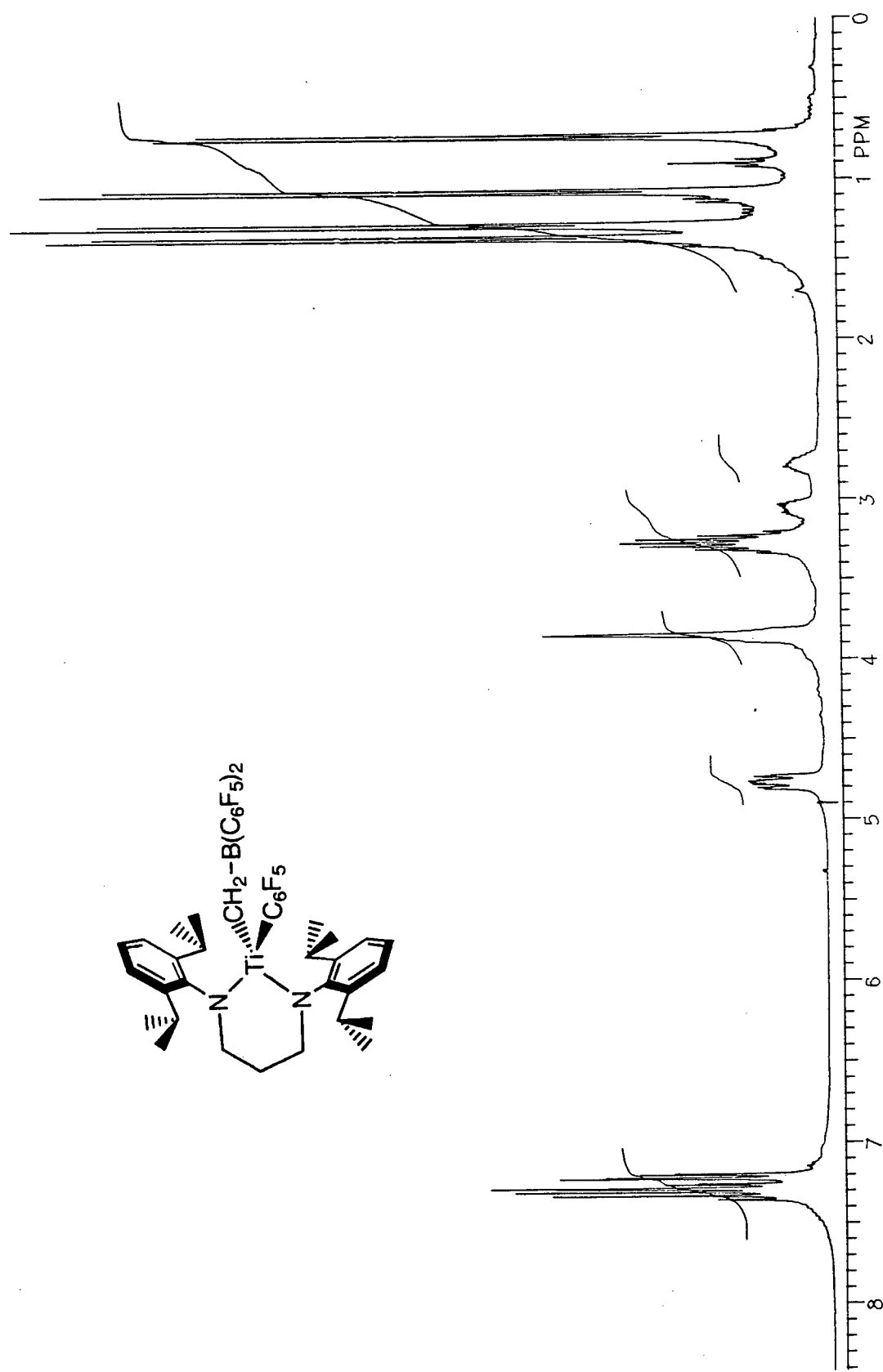
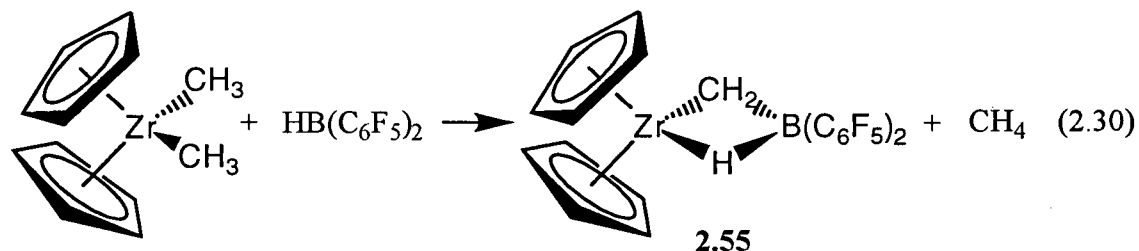
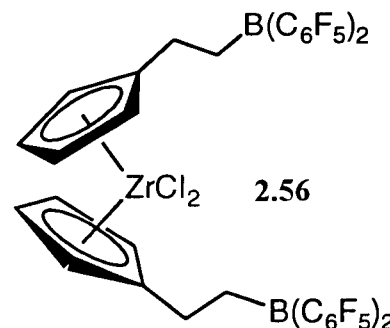


Figure 2.14: 300 MHz ^1H NMR spectrum of complex 2.54b in C_6D_6 at 23°C

Piers has reported a similar complex prepared from Cp_2ZrMe_2 and $\text{HB}(\text{C}_6\text{F}_5)_2$ (eq. 2.30).⁵⁵



For comparison, the methylene protons in complex **2.55** appear at 5.30 ppm (no $^{13}\text{C}\{^1\text{H}\}$ NMR data is reported for this compound).⁵⁵ The $^{13}\text{C}\{^1\text{H}\}$ NMR spectrum of compound **2.54b** shows a broad resonance at 109.5 ppm for the methylene carbon bridging the titanium and boron. The ^{19}F NMR spectrum of **2.54b** shows six different fluorine resonances (2 ortho, 2 meta, and 2 para) consistent with migration^{5,6} of one of the pentafluorophenyl groups to titanium. The $^{11}\text{B}\{^1\text{H}\}$ NMR spectrum of **2.54b** shows a peak at 79.4 ppm which compares well with complex **2.56** (73.9 ppm)⁵⁷ and is typical for three-coordinate boron.⁵⁸



The solid state structure of **2.54b**· CH_2Cl_2 was determined by X-ray crystallography. The molecular structure of complex **2.54b**· CH_2Cl can be found in Figure 2.15 and relevant bond distances and angles in Table 2.5.

The structure is best described as a distorted tetrahedron with the boromethyl group occupying one site. The titanium–amide and titanium–carbon bond lengths are comparable to the distances in the dimethyl complex **2.11a** (*vide supra*).⁵⁴ The $\text{Ti}(1)\text{--C}(34)\text{--B}(1)$ angle is more obtuse than expected for an sp^3 –hybridized carbon, likely due to steric interactions between $\text{B}(\text{C}_6\text{F}_5)_2$ moiety and the pentafluorophenyl group bound to titanium. A close contact exists between the ortho fluorine $\text{F}(1)$ and the boron atom ($\text{B}(1)\text{--F}(1) = 2.94 \text{ \AA}$), however, the boron centre is trigonal planar as evidenced by the sum of the angles about boron (360.0°).

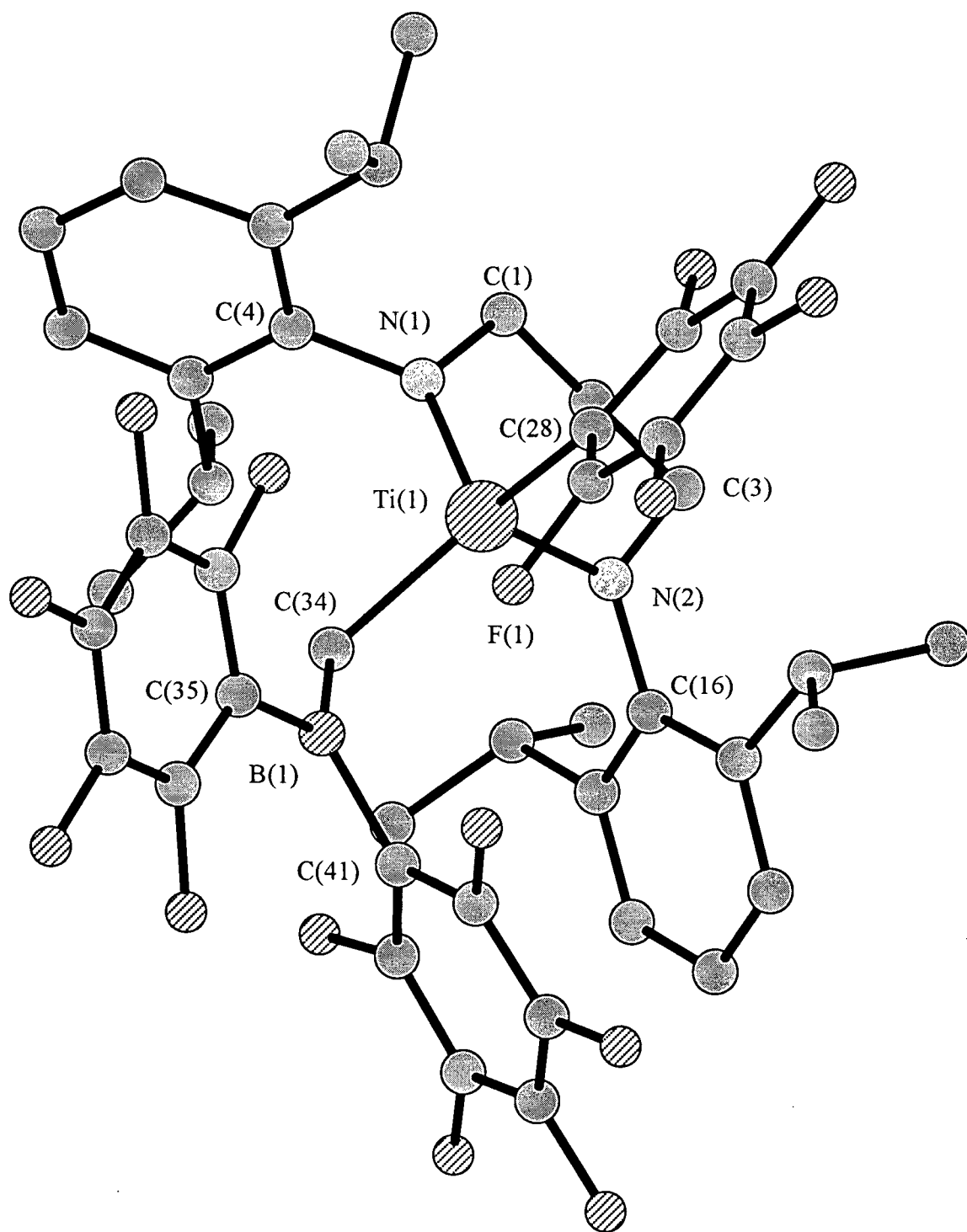


Figure 2.15: Molecular structure of complex **2.54b**·CH₂Cl₂

Table 2.5: Selected bond lengths and angles for **2.54b**•CH₂Cl₂.

Bond Distances (Å)

Ti(1)—N(1)	1.846(4)	Ti(1)—N(2)	1.849(3)
Ti(1)—C(28)	2.191(4)	Ti(1)—C(34)	2.111(4)
C(34)—B(1)	1.503(6)	B(1)—F(1)*	2.94

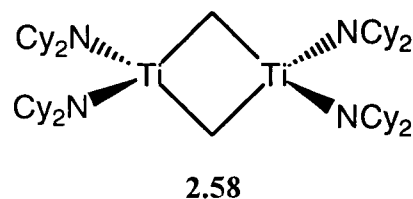
Bond Angles (°)

N(1)—Ti(1)—N(2)	100.8(2)	N(1)—Ti(1)—C(28)	102.8(2)
Ti(1)—N(1)—C(1)	119.1(3)	Ti(1)—N(1)—C(4)	124.5(3)
C(1)—N(1)—C(4)	116.3(4)	Ti(1)—N(2)—C(3)	122.8(3)
Ti(1)—N(2)—C(16)	122.7(3)	C(3)—N(2)—C(16)	114.6(3)
Ti(1)—C(34)—B(1)	125.1(3)	C(34)—B(1)—C(35)	120.9(5)
C(34)—B(1)—C(41)	122.0(5)	C(35)—B(1)—C(41)	117.1(4)

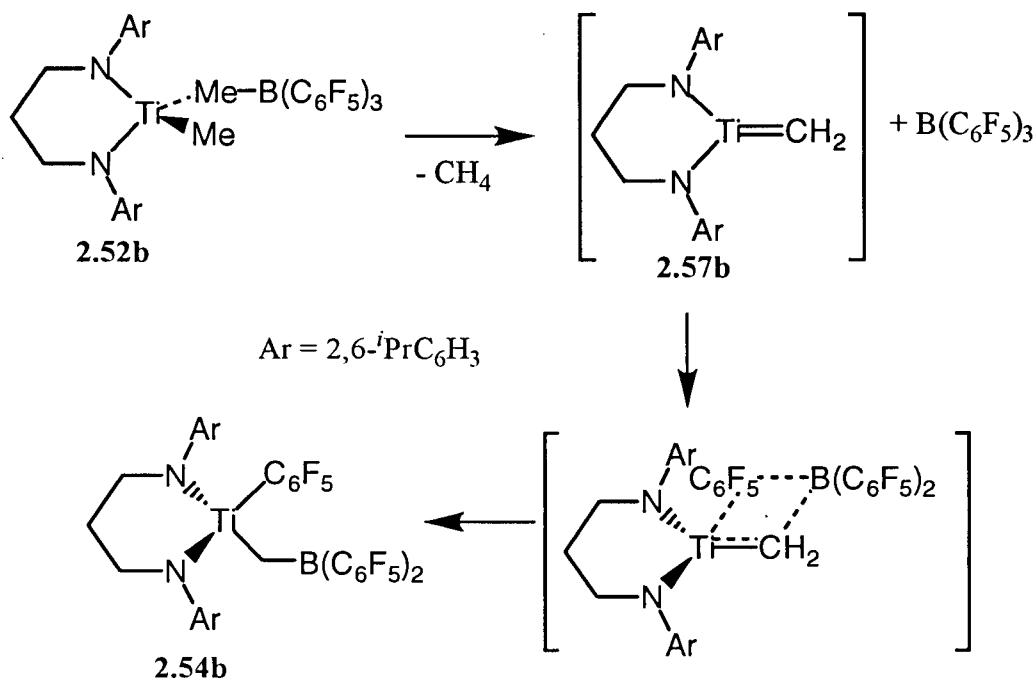
* Close contact.

Complex **2.54b** is significant because of its *inactivity* as an α -olefin polymerization catalyst. In the absence of α -olefin, it is proposed that the methylborate adduct **2.52b** loses methane to give an intermediate 12-electron titanium methyldiene complex **2.57b** which may be stabilized by the released borane (Scheme 2.15).

Notably, Gambarotta has reported that the cyclohexyl amide complex (Cy₂N)₂TiMe₂ slowly evolves methane in the absence of a Lewis acid to give the methylene bridged dimer **2.58**,³⁶ suggesting that this may be a common mode of decomposition for four-coordinate amido complexes bearing methyl groups at titanium. In our system this elimination seems to be assisted by the presence of a Lewis acid.⁵⁹ Addition of the B-C₆F₅ group across the proposed Ti=CH₂ unit yields the final product **2.54b**. Deactivation of metallocene/MAO (MAO = methylaluminoxane) systems concomitant with methane evolution has been

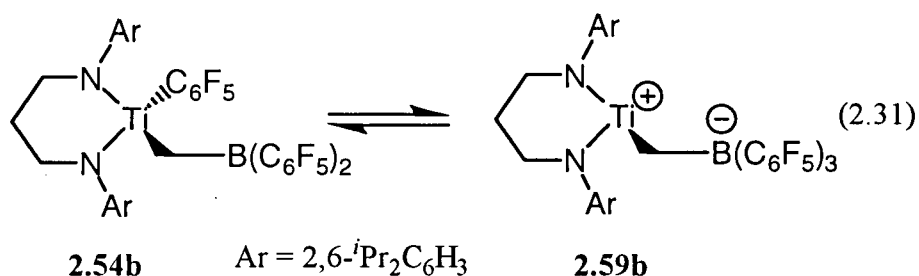


Scheme 2.15: Proposed intermediates in the formation of complex **2.54b**



observed.⁶⁰ Perhaps the formation of complex **2.54b** can be viewed as a model for this process.

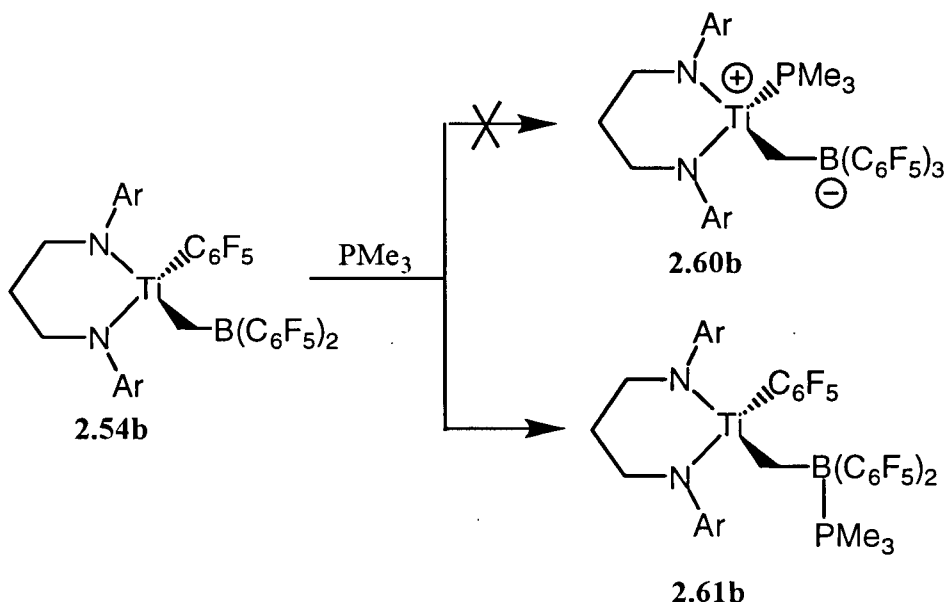
There is also the possibility that an equilibrium exists between the four coordinate neutral complex **2.54b** and a three coordinate titanium cationic alkyl **2.59b** (eq.2.31). If



complexes **2.54b** and **2.59b** are in equilibrium then it may be possible to trap complex **2.59b** with trimethylphosphine.

Addition of trimethylphosphine to complex **2.54b** should lead to either a titanium phosphine complex **2.60b** or the borane-phosphine complex **2.61b** (Scheme 2.16). The only

Scheme 2.16: Addition of PMe_3 to complex **2.54b**

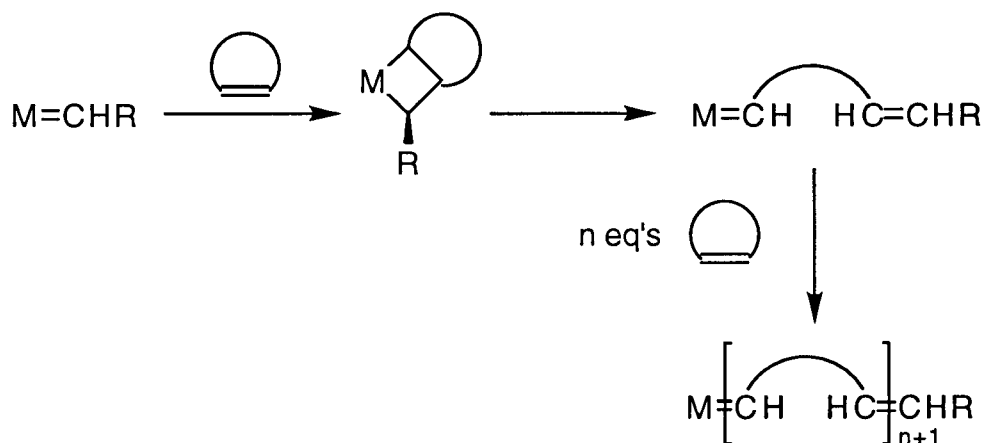


complex observed in the reaction with trimethylphosphine was complex **2.61b**. Although the two complexes look very similar, complex **2.61b** can be easily distinguished from complex **2.60b** through $^{11}\text{B}\{^1\text{H}\}$ and $\{^{19}\text{F}\}$ NMR spectroscopy. The $^{11}\text{B}\{^1\text{H}\}$ NMR spectrum of the product from the reaction with trimethylphosphine clearly shows a doublet at -15.8 ppm ($^1J_{\text{BP}} = 72.4$ Hz) consistent with 4-coordinate boron attached directly to a spin $1/2$ nucleus.⁶¹ Furthermore, the $\{^{19}\text{F}\}$ NMR spectrum exhibits six fluorine resonances consistent with the formulation of complex **2.61b**. Complex **2.60b** would exhibit only three fluorine resonances. This further confirms complex **2.54b**'s lack of reactivity with α -olefins. If the equilibrium did in fact exist, some amount of polymerization activity would have been expected.

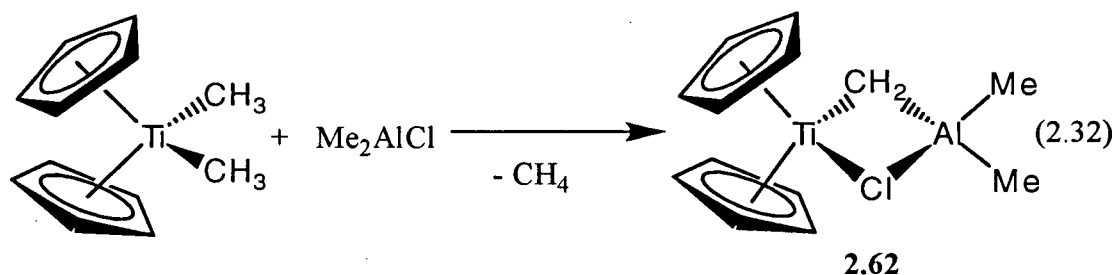
Attempted Preparation of an Electron Deficient Analogue to Tebbe's Reagent

Transition metal-catalyzed ring-opening metathesis polymerization (ROMP) of cyclic olefins is an important application of the olefin metathesis reaction (Scheme 2.17).⁶² Poly(norbornene), poly(octenamer), and poly(dicyclopentadiene) are currently produced on an industrial scale using this process.⁶³

Scheme 2.17: Mechanism for the ROMP of Cycloolefins



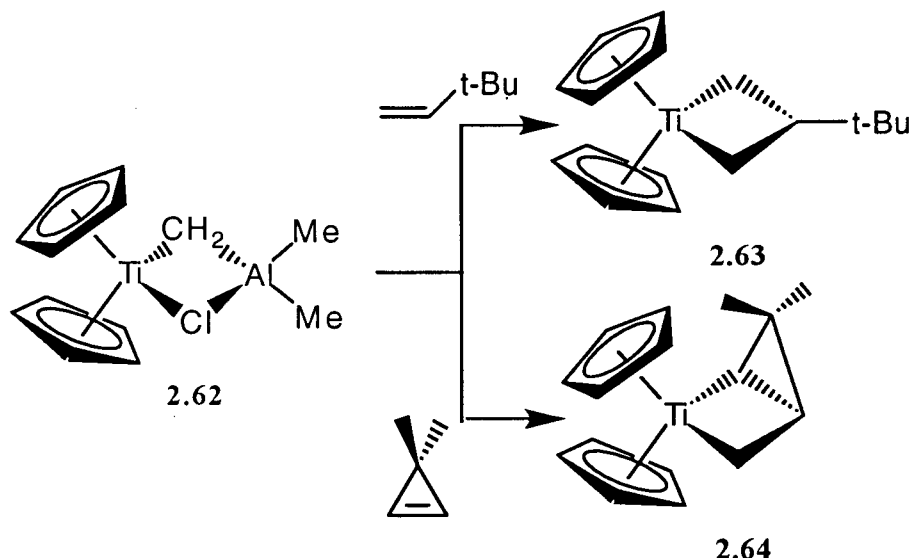
Tebbe's reagent **2.62** can be prepared from Cp_2TiMe_2 and one equivalent of ClAlMe_2 (eq.2.32). Complex **2.62** is of great significance in olefin metathesis.⁶⁴ Complex **2.62** can



be regarded as a titanium carbene $\text{Cp}_2\text{Ti}=\text{CH}_2$ trapped by Me_2AlCl . This was the first example of a well-defined metal carbene that catalyzes olefin metathesis and is re-isolated in high yield at the end of the reaction.⁶²

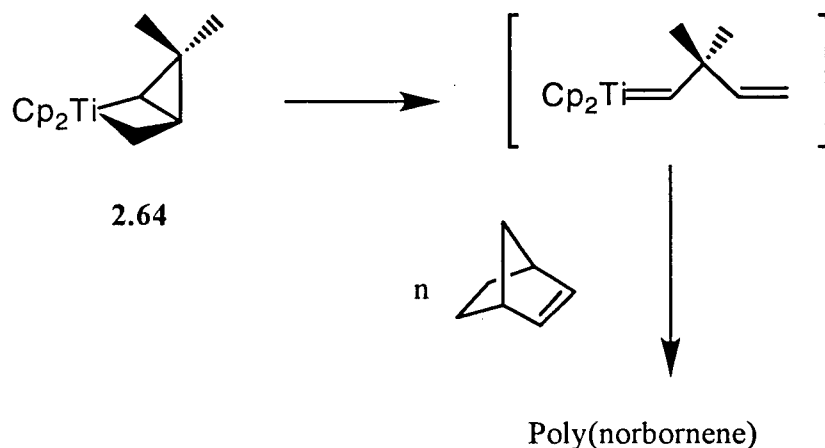
Tebbe's reagent **2.62** will also react with neohexene or 3,3-dimethylcyclopropene to form the titanacyclobutane complexes **2.63** and **2.64**, respectively (Scheme 2.18). These titanacyclobutane complexes were found to provide aluminum-free sources of " $\text{Cp}_2\text{Ti}=\text{CH}_2$ " that catalyze olefin metathesis.⁶⁵

Scheme 2.18: Reaction of Tebbe's reagent with olefins



The first well-documented example of the living ring-opening metathesis polymerization of a cycloolefin was that of norbornene by titanacyclobutane complexes.⁶⁶ The metallacycles **2.63** and **2.64** initiate the polymerization of norbornene at 50°C by the rate-limiting opening of the TiC_3 rings to give alkylidene complexes that are efficiently captured by norbornene to give closely related trisubstituted titanacycles. The new titanacycles react similarly with norbornene to give poly(norbornene) appended to the α -carbon in observable titanacycle intermediates. These intermediates result in the formation of living polymers, that is, materials having controlled molecular weights with narrow molecular weight distributions. The ring-strain in the 3,3-dimethylcyclopropene results in a single alkylidene species at temperatures above 23°C (Scheme 2.19). When complex **2.64** was used to polymerize norbornene, no induction period was observed, there was a linear dependence of molecular weight on monomer consumption and polymers with high molecular weights (M_n of 10^4 – 10^5) and polydispersities lower than 1.1 were prepared.⁶⁶ Studies of Tebbe's reagent are also of interest in connection with Ziegler–Natta polymerization of alkenes.

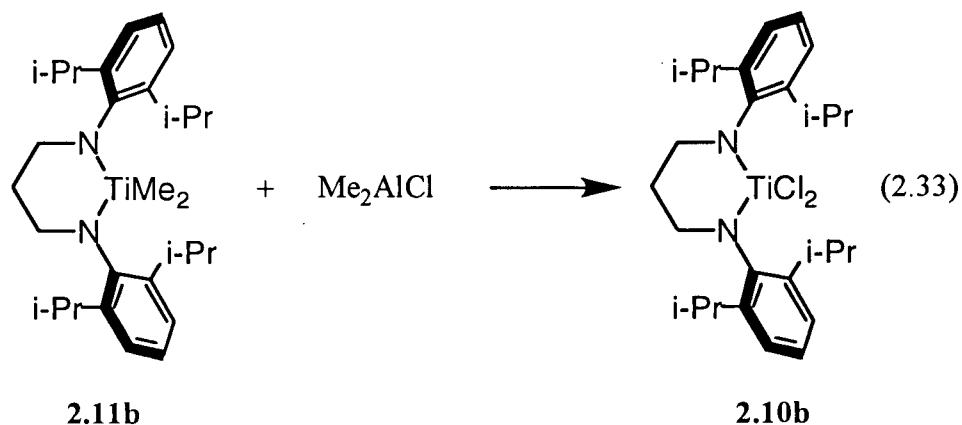
Scheme 2.19: Polymerization of norbornene with the metallocyclobutane **2.64**



Complex **2.11b** is closely related to the metallocene Cp_2TiMe_2 . It seems reasonable that this complex should undergo similar reactions as the titanocene derivative. An attempt was made to synthesize a stabilized titanium alkylidene supported by a chelating diamide ligand. If successful, the complex could be thought of as an electron deficient analogue of Tebbe's reagent.

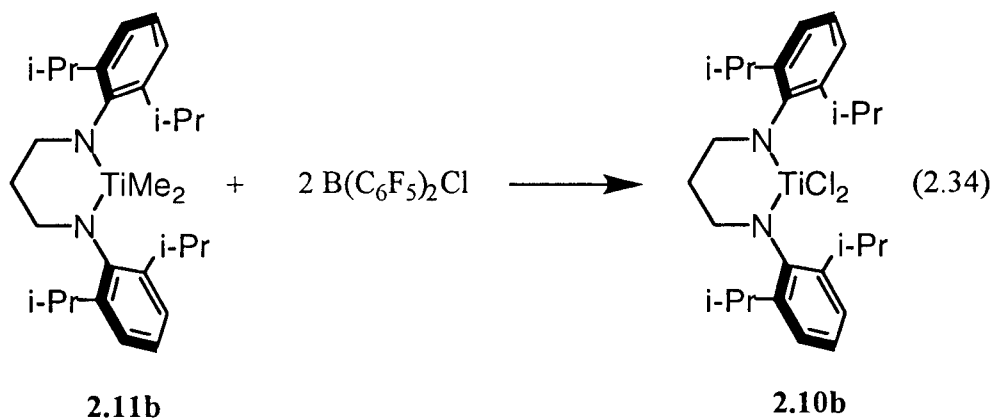
Previous studies have shown that $\text{B}(\text{C}_6\text{F}_5)_3$ can be used to stabilize a putative titanium alkylidene via transfer of a C_6F_5 moiety to titanium (*vide supra*). However, the reaction is irreversible and access to the titanium alkylidene is effectively sequestered. This complex is related to Tebbe's reagent except that the B–C bond has been broken where as Tebbe's reagent retains the Al–Cl bond.

In an effort to synthesize the analogue of Tebbe's reagent directly, complex **2.11b** was reacted with one equivalent of Me_2AlCl . This reaction proceeds very cleanly, but does not give the desired titanium alkylidene (eq. 2.33). Instead, the dimethyltitanium



complex exchanges the methyl groups with the chloride of the aluminum forming the dichloride complex **2.10b**.

Another attempt to generate a titanium alkylidene using the Lewis acid $\text{B}(\text{C}_6\text{F}_5)_2\text{Cl}$ was carried out. Exchanging one C_6F_5 group of $\text{B}(\text{C}_6\text{F}_5)_3$ with a chloride atom will hopefully avoid the transfer of the pentafluorophenyl group to titanium since the chloride atom can bridge the titanium and boron centres. When $\text{B}(\text{C}_6\text{F}_5)_2\text{Cl}$ ⁶⁷ is added to complex **2.11b**, metathesis of the boron–chloride bond occurs and the dichloro complex **2.10b** is once again the only titanium species formed (eq. 2.34).



It appears from these results that the dimethyl complex **2.11b** undergoes a transmetallation reaction with the Lewis acids ClAlMe_2 and $\text{ClB}(\text{C}_6\text{F}_5)_2$. It would appear that the titanium atom in complex **2.11b** is more electropositive than the aluminum or boron atoms in AlClMe_2 and $\text{ClB}(\text{C}_6\text{F}_5)_2$, respectively. As a result the most electronegative ligand,

chloride, is exchanged for the methyl groups on the titanium atom. In other words, the harder metal, titanium, combines with the harder ligand, chloride.

Conclusions

In summary, a high yield route to chelating bis(amido) complexes of titanium has been demonstrated. The propyl linked chelating bis(amido) ligands that were synthesized are capable of stabilizing a number of titanium complexes. For example, the dichloride complex $[\text{RN}(\text{CH}_2)_3\text{NR}]\text{TiCl}_2$ ($\text{R} = 2,6\text{-}^i\text{Pr}_2\text{C}_6\text{H}_3$, **2.10b**) serves as a starting point for the synthesis of a variety of bis(alkyl) derivatives. Activation of the dimethyl complex $[\text{RN}(\text{CH}_2)_3\text{NR}]\text{TiMe}_2$ (**2.11b**) with $\text{B}(\text{C}_6\text{F}_5)_3$ leads to a methyl borate derivative which is unstable at room temperature. The methyl borate adduct slowly decomposes to an inactive bimetallic complex $[\text{RN}(\text{CH}_2)_3\text{NR}]\text{Ti}[\text{CH}_2\text{B}(\text{C}_6\text{F}_5)_2](\text{C}_6\text{F}_5)$ (**2.54b**).

Problems were encountered when varying the number of carbon atoms linking the nitrogen atoms. The ethyl linked bis(amido) complexes proved too soluble to isolate. The high solubility of these complexes may be a result of free rotation about the N-C_{ipso} bond. An alternative ligand was designed in which the linking group could coordinate to the metal to help stabilize the complexes. Furthermore, the linking group was made bulkier hopefully restoring the restricted rotation of the aryl group. Again, due to the high solubility of these complexes, extremely low isolated yields of the dichloride complexes were achieved. A further complication arose when attempts to alkylate these complexes resulted in decomposition.

Complexes bearing the butyl linkage also proved troublesome. Dichloride complexes were isolated and are stable, however, the corresponding dimethyl complexes decomposed rapidly at room temperature. It is possible that these complexes were dimers, however, in the absence of solution molecular weight data, this could not be confirmed.

A more rigid ligand was designed bearing an *o*-xylyl linking group. Syntheses of the dichloride and dimethyl derivatives were successful. These complexes exhibit properties similar to the propyl linked derivatives.

Another ligand was designed to study the interaction between opposing aryl groups on the propyl linked bis(amido) ligands. It was determined that the orientation of one aryl group does not affect the orientation of the other. Therefore, bulkier substitution is required on the aryl groups before an interaction will be observed.

The dichloride and bis(alkyl) complexes bearing these ancillary bis(amido) ligands will be evaluated as potential Ziegler-Natta polymerization catalysts in the next chapter.

Experimental

General Details: All experiments were performed under an atmosphere of dry dinitrogen using standard Schlenk techniques or in an Innovative Technology Inc. glovebox. Solvents were distilled from sodium/benzophenone ketyl (DME, THF, hexanes, pentane (olefin free), diethylether and benzene), molten sodium (toluene), or Na/K alloy (1-hexene) under argon and stored over activated 4Å molecular sieves. Chemicals were obtained from Aldrich. TiCl_4 , 1,3 dibromopropane, 1,4-dibromopropane, 2,3-butanedione, glyoxal, α,α' -dibromo-o-xylene, and chlorotrimethylstannane were used as received. N,N,N',N'-Tetramethylethylenediamine (tmeda), 2,6-diisopropylaniline, 2,6-dimethylaniline, 2,6-diethylaniline and chlorotrimethylsilane were distilled prior to use. Proton (299.9 MHz), carbon (75.46 MHz), boron (96.2 MHz), phosphorus (121.42 MHz) and fluorine (282.2 MHz) NMR spectra were recorded in CD_2Cl_2 , C_6D_6 or d₈-toluene at approximately 23°C on a Varian XL-300 spectrometer. The proton chemical shifts were referenced to internal CDHCl_2 ($\delta = 5.32$ ppm), $\text{C}_6\text{D}_5\text{H}$ ($\delta = 7.15$ ppm) or $\text{C}_6\text{D}_5\text{CD}_2\text{H}$ ($\delta = 2.09$ ppm) and the carbon resonances to CD_2Cl_2 ($\delta = 53.2$ ppm), C_6D_6 ($\delta = 128.0$ ppm) or $C_{\text{ipso}}\text{-C}_6\text{D}_5\text{CD}_3$ ($\delta = 137.5$ ppm). Phosphorus, fluorine and boron chemical shifts were referenced externally to $\text{P}(\text{OMe})_3$ ($\delta = 0.0$ ppm), CFCl_3 ($\delta = 0.0$ ppm) and $\text{BF}_3 \cdot \text{Et}_2\text{O}$ ($\delta = 0.0$ ppm) respectively. Mass spectra were performed on a Finnigan MAT model 8230 spectrometer coupled to a Varian 3400 Gas Chromatograph. Elemental analyses were performed by Oneida Research Services Inc., Whitesboro, NY, Guelph Chemical Laboratories Ltd., Guelph, Ontario, and by Mr. Peter Borda at the University of British Columbia.

(BAME) H_2 , 2.2a. Bis(imine) **2.1a** (2.50 g, 9.46 mmol) was dissolved in Et_2O (50 mL) and added dropwise to a suspension of 5 equivalents of LiAlH_4 (1.80 g, 47.3 mmol) in Et_2O (250 mL). The resulting solution was refluxed overnight. Excess LiAlH_4 was destroyed by the careful addition of water. The resulting suspension was poured into a 20% solution of potassium sodium tartrate (500 mL), extracted with Et_2O (3 x 100 mL). The combined organic fractions were washed with saturated NaCl solution (100 mL), dried over

anhydrous sodium sulphate and filtered. The solvent was reduced *in vacuo*, and cooled to -78 °C. Pure diamine **2.2a** was collected by filtration as a white crystalline solid (2.41 g, 8.99 mmol, 95 %). ^1H NMR δ 6.98 (m, 4H, Ar), 6.85 (m, 2H, Ar), 3.15 (s, 2H, NH), 2.88 (s, 2H, NCH₂), 2.14 (s, 12H, ArMe). $^{13}\text{C}\{^1\text{H}\}$ NMR δ 146.5, 130.0, 129.8, 129.6, 122.2, 49.0, 18.5.

(BAIE)H₂, 2.2b. Bis(imine) **2.1b** (3.77 g, 10.0 mmol) was dissolved in Et₂O (50 mL) and added dropwise to a suspension of 5 equivalents of LiAlH₄ (1.90 g, 50 mmol) in Et₂O (250 mL). The resulting solution was refluxed overnight. Excess LiAlH₄ was destroyed by the careful addition of water. The resulting suspension was poured into a 20% solution of potassium sodium tartrate (500 mL), extracted with Et₂O (3 x 100 mL). The combined organic fractions were washed with saturated NaCl solution (100 mL), dried over anhydrous sodium sulphate and filtered. The volume of the solution was reduced *in vacuo*, and cooled to -78 °C. Pure diamine **2.2b** was collected by filtration as a white crystalline solid (3.31 g, 8.70 mmol, 87 %). ^1H NMR δ 7.11 (m, 6H, Ar), 3.44 (sept, 4H, CHMe₂), 3.34 (s, 2H, NH), 3.07 (s, 4H, NCH₂), 1.23 (m, 24H, CHMe₂). $^{13}\text{C}\{^1\text{H}\}$ NMR δ 143.6, 142.8, 124.5, 123.9, 52.6, 28.1, 24.4.

(BAMP)H₂, 2.3a. BuLi (2.50 M, 73.0 mL, 183 mmol) was added dropwise to a stirred solution of 2,6-dimethylaniline (20.0 g, 165 mmol) in THF (150 mL) at -78 °C. The solution was warmed to 23 °C where it was kept for 30 minutes. The solution was cooled to 0 °C and tmeda (19.2 g, 165 mmol) was added dropwise followed by 1,3-dibromopropane (16.7 g, 82.5 mmol) dropwise. The solution was stirred overnight at 23 °C. The solution was poured into H₂O (100 mL) and extracted with CH₂Cl₂ (3 x 100 mL). The organic layer was dried over anhydrous Na₂SO₄ and the CH₂Cl₂ removed *in vacuo*. The resulting beige solid was recrystallized from hexanes to leave pure **2.3a** as a white crystalline solid (8.4 g, 59.4 mmol; 36%). ^1H NMR δ 6.98 (m, 4H, Ar), 6.86 (m, 2H, Ar), 2.86 (t, 4H, NCH₂), 2.79 (s, 2H, NH), 2.14 (s, 12H, ArMe), 1.51 (pent, 2H, NCH₂CH₂). $^{13}\text{C}\{^1\text{H}\}$ NMR δ 146.7, 129.6,

129.2, 122.3, 46.9, 32.9, 18.6. MS (EI) m/z 282.20894 (M^+). Calcd. for $C_{19}H_{26}N_2$: 282.20959.

(BAIP) H_2 , 2.3b. n -BuLi (2.50 M, 79.2 mL, 198 mmol) was added dropwise to a stirred THF (150 mL) solution of 2,6-diisopropylaniline (35.12 g, 198.1 mmol) at -78°C . The solution was warmed to 23°C where it was kept for 30 minutes. The solution was cooled to 0°C and tmeda (23.0 g, 198 mmol) was added dropwise followed by 1,3-dibromopropane (20.0 g, 99.1 mmol) dropwise. The solution was warmed to 23°C and stirred overnight. The solution was poured into H_2O (100 mL) and extracted with CH_2Cl_2 (3×100 mL). The organic layer was dried over anhydrous Na_2SO_4 and the CH_2Cl_2 removed *in vacuo*. The resulting yellow oil was dissolved in diethyl ether (30 mL) and concentrated HCl (20 mL) was added. The salt ($[ArH_2N(CH_2)_3NH_2Ar]Cl_2$) was removed by filtration, washed with diethyl ether (20 mL), and dissolved in dichloromethane. This solution was poured into aqueous saturated K_2CO_3 (100 mL). The organic layer was separated and dried over anhydrous Na_2SO_4 . Removal of the solvent yielded pure **2.3b** as a viscous oil (18.2 g, 46.1 mmol; 47%). 1H NMR δ 7.10 (m, 6H, Ar), 3.36 (sept, 4H, $CHMe_2$), 3.01 (t, 4H, NCH_2), 2.97 (s, 2H, NH), 1.77 (pent, 2H, NCH_2CH_2), 1.22 (d, 24H, $CHMe_2$). $^{13}C\{^1H\}$ NMR δ 144.0, 143.7, 123.9, 124.4, 50.8, 32.7, 28.1, 24.5. MS (EI) m/z 394.3342 (M^+). Calcd for $C_{27}H_{42}N_2$: 394.3348.

(BAMB) H_2 , 2.6a. BuLi (2.50 M, 73.0 mL, 183 mmol) was added dropwise to a stirring solution of 2,6-dimethylaniline (20.0 g, 165 mmol) in THF (150 mL) at -78°C . The solution was warmed to 23°C where it was kept for 30 minutes. The solution was cooled to 0°C and tmeda (19.2 g, 165 mmol) was added dropwise followed by 1,4-dibromobutane (17.8 g, 82.5 mmol) dropwise. The solution was stirred overnight at 23°C , poured into H_2O (100 mL) and extracted with CH_2Cl_2 (3×100 mL). The organic layer was dried over anhydrous Na_2SO_4 and the CH_2Cl_2 removed *in vacuo*. The resulting beige solid was recrystallized from hexanes to leave pure **2.6a** as a white crystalline solid (20.1 g, 67.6 mmol; 82 %). 1H NMR δ 6.98 (m, 3H, Ar), 6.85 (m, 2H, Ar), 2.77 (t, 4H, NCH_2), 2.69 (s, 2H, NH),

2.16 (s, 12H, ArMe₂), 1.36 (m, 4H, NCH₂CH₂). ¹³C{¹H} NMR δ 146.8, 129.6, 129.2, 122.2, 48.6, 29.0, 18.6. MS (EI) *m/z* 296.22525 (M⁺). Calcd. for C₂₀H₂₈N₂: 296.22524

(BAIB)H₂, 2.6b. BuLi (2.50 M, 73.0 mL, 183 mmol) was added dropwise to a stirring solution of 2,6-diisopropylaniline (29.3 g, 165 mmol) in THF (150 mL) at -78 °C. The solution was warmed to 23 °C where it was kept for 30 minutes. The solution was cooled to 0 °C and tmeda (19.2 g, 165 mmol) was added dropwise followed by 1,4-dibromobutane (17.8 g, 82.5 mmol) dropwise. The solution was stirred overnight at 23 °C, poured into H₂O (100 mL) and extracted with CH₂Cl₂ (3 × 100 mL). The organic layer was dried over anhydrous Na₂SO₄ and the CH₂Cl₂ removed *in vacuo*. The resulting beige solid was recrystallized from hexanes to leave pure **2.6b** as a white crystalline solid (26.8 g, 66.0 mmol; 80 %). ¹H NMR δ 7.11 (m, 6H, Ar), 3.35 (sept, 4H, CHMe₂), 2.88 (m, 4H, NCH₂), 2.78 (s, 2H, NH), 1.63 (m, 4H, NCH₂CH₂), 1.23 (d, 24H, CHMe₂). ¹³C{¹H} NMR δ 143.9, 142.8, 124.4, 123.9, 52.4, 29.2, 28.0, 24.5. MS (EI) *m/z* 408.35046 (M⁺). Calcd. for C₂₈H₄₄N₂: 408.35044.

(BAIP)Ti(NMe₂)₂, 2.8b. Diamine **2.3b** (0.25 g, 0.63 mmol) was dissolved in Et₂O (20 mL) and cooled to -78 °C. BuLi (2.5 M, 1.4 mmol, 0.55 mL) was added via syringe and the solution was allowed to warm to 23 °C. The resulting solution was added dropwise to Ti(NMe₂)Cl₂ (0.13 g, 0.63 mmol) in Et₂O (150 mL) at -78 °C. The mixture was warmed slowly to 23 °C and stirred overnight. The solvent was removed *in vacuo* and the resulting brown-red solid was dissolved in hexanes and filtered through celite. The solution was concentrated and cooled to -30 °C. No product crystallized from the solution, however, ¹H NMR spectroscopy of an aliquot revealed that the product was formed. ¹H NMR δ 7.10 (m, 6H, Ar), 3.75 (sept, 4H, CHMe₂), 3.63 (m, 4H, NCH₂), 2.72 (s, 12H, N(CH₃)₂), 2.34 (m, 2H, NCH₂CH₂), 1.31 (d, 24H, CHMe₂).

BAMP(SiMe₃)₂, 2.9a. MeLi (1.56 M, 11.4 mL, 17.8 mmol) was added dropwise to a stirring solution of compound **2.3a** (2.52 g, 8.90 mmol) in THF (50 mL) at -78 °C. The solution was warmed to 23 °C where it was kept for 30 minutes. The solution was cooled to

0°C and chlorotrimethylsilane (1.94 g, 17.8 mmol) was added dropwise. The solution was stirred overnight at 23 °C. The solvent was removed *in vacuo* and the resulting slurry dissolved in hexanes. The solution was filtered through Celite and the solvent removed *in vacuo* to leave pure **2.9a** as a clear colorless oil (3.54 g, 8.30 mmol; 93%). ¹H NMR δ 6.96 (m, 4H, Ar), 6.89 (m, 2H, Ar), 2.84 (t, 4H, NCH₂), 2.19 (s, 12H, ArMe), 1.55 (m, 2H, NCH₂CH₂), 0.04 (s, 18H, NSiMe₃). ¹³C{¹H} NMR δ 146.5, 137.9, 128.7, 125.0, 48.7, 32.9, 19.6, 0.4. MS (EI) *m/z* 426.28798 (M⁺). Calcd. for C₂₅H₄₂N₂Si₂: 426.28760.

BAIP(SiMe₃)₂, 2.9b. MeLi (1.48 M, 35.3 mL, 52.2 mmol) was added dropwise to a stirring solution of compound **2.3b** (10.0 g, 26.1 mmol) in THF (150 mL) at -78°C. The solution was warmed to 23 °C where it was kept for 30 minutes. The solution was cooled to 0°C and chlorotrimethylsilane (5.67 g, 52.2 mmol) was added dropwise. The solution was stirred overnight at 23 °C. The solvent was removed *in vacuo* and the resulting slurry dissolved in hexanes. The solution was then filtered through Celite and the solvent removed *in vacuo* to leave a yellow solid. Recrystallization from diethylether yields pure **2.9b** as a white crystalline solid (13.9 g, 25.9 mmol; 99%). ¹H NMR δ 7.04 (m, 6H, Ar), 3.46 (sept, 4H, CHMe₂), 3.01 (t, 4H, NCH₂), 1.77 (m, 2H, NCH₂CH₂), 1.20 (d, 12H, CHMe₂), 1.17 (d, 12H, CHMe₂), 0.09 (s, 18H, NSiMe₃). ¹³C{¹H} NMR δ 148.6, 143.8, 126.2, 124.2, 51.0, 32.3, 28.0, 25.3, 24.9, 0.5. MS (EI) *m/z* 538.41368 (M⁺). Calcd. for C₃₃H₅₈N₂Si₂: 538.41385.

(BAMP)TiCl₂, 2.10a. **2.9a** (2.85 g, 6.68 mmol) and TiCl₄ (1.27 g, 6.68 mmol) were refluxed in xylenes for 12h. The resulting deep red solution was filtered through Celite, the volume of the filtrate was reduced until a slurry formed and hexanes is added to complete the precipitation. Recrystallization from a toluene/hexanes mixture yields pure **2.10a** as dark orange-red crystals (2.15 g, 5.41 mmol, 81%). ¹H NMR δ 6.93 (m, 6H, Ar), 3.46 (m, 4H, NCH₂), 2.34 (s, 12H, ArMe), 2.34 (m, 2H, NCH₂CH₂). ¹³C{¹H} NMR δ 144.2, 133.3, 129.4, 128.5, 62.1, 32.4, 19.0. Anal. Calcd. for C₁₉H₂₄Cl₂N₂Ti: C, 57.16; H, 6.06; N, 7.02. Found: C, 57.28; H, 6.19; N, 6.89.

(BAIP)TiCl₂, **2.10b**. **2.9b** (3.09 g, 5.73 mmol) and TiCl₄ (1.09 g, 5.73 mmol) were refluxed in xylenes for 12h. The resulting deep red solution was filtered through Celite, the volume of the filtrate was reduced until a slurry formed and hexanes is added to complete the precipitation. Recrystallization from a toluene/hexanes mixture yields pure **2.10b** as dark orange-red crystals (2.20 g, 4.29 mmol, 75%). ¹H NMR δ 7.09 (m, 6H, Ar), 3.75 (m, 4H, NCH₂), 3.53 (sept, 4H, CHMe₂), 2.48 (m, 2H, NCH₂CH₂), 1.44 (d, 12H, CHMe₂), 1.18 (d, 12H, CHMe₂). ¹³C{¹H} NMR δ 144.5, 143.3, 129.2, 125.0, 64.4, 31.1, 28.9, 26.2, 24.4. Anal. Calcd. for C₂₇H₄₀Cl₂N₂Ti: C, 63.41; H, 7.88; N, 5.48. Found: C, 63.05; H, 8.12; N, 5.27.

(BAMP)TiMe₂, **2.11a**. MeMgBr (2.4 M, 2.1 mL, 5.0 mmol) was added dropwise to a stirring suspension of **2.10a** (1.00 g, 2.50 mmol) in Et₂O (50 mL) at -20°C. The solution was allowed to warm to 23 °C and stirred overnight. The solvent was removed *in vacuo* and the resulting solid extracted with hexanes and filtered through Celite. The solution was concentrated and cooled to -30°C to yield yellow crystalline **2.11a** (0.65 g, 1.80 mmol, 72%). ¹H NMR δ 7.11 (m, 4H, Ar), 7.02 (m, 2H, Ar), 3.40 (m, 2H, NCH₂), 2.39 (s, 12H, ArMe), 2.04 (m, 2H, NCH₂CH₂), 0.70 (s, 6H, TiMe₂). ¹³C{¹H} NMR δ 146.6, 134.4, 129.1, 126.6, 58.5, 51.1, 32.0, 18.7. Anal. Calcd. for C₂₁H₃₀N₂Ti: C, 70.38; H, 8.44; N, 7.82. Found: C, 69.98; H, 8.73; N, 7.56.

(BAIP)TiMe₂, **2.11b**. MeMgBr (2.4 M, 0.82 mL, 2.0 mmol) was added dropwise to a stirring suspension of **2.10b** (0.50 g, 1.0 mmol) in Et₂O (50 mL) at -20°C. The solution was allowed to warm to 23 °C and stirred overnight. The solvent was removed *in vacuo* and the resulting solid extracted with hexanes and filtered through Celite. The solution was concentrated and cooled to -30°C to yield yellow crystalline **2.11b** (0.27 g, 0.58 mmol, 58%). ¹H NMR δ 7.21 (m, 6H, Ar), 3.72 (sept, 4H, CHMe₂), 3.58 (m, 2H, NCH₂), 2.12 (m, 2H, NCH₂CH₂), 1.39 (d, 12H, CHMe₂), 1.28 (d, 12H, CHMe₂), 0.86 (s, 6H, TiMe₂). ¹³C{¹H} NMR δ 145.3, 144.7, 127.4, 124.6, 61.5, 52.0, 31.2, 28.5, 26.4, 24.9. Anal. Calcd. for C₂₉H₄₆N₂Ti: C, 74.02; H, 9.85; N, 5.95. Found: C, 74.32; H, 9.91; N, 5.85.

(BAMP)Ti(CH₂Ph)₂, 2.12a. PhCH₂MgCl (0.90 M, 4.98 mL, 4.50 mmol) was added dropwise to a stirring suspension of **2.10a** (0.90 g, 2.25 mmol) in Et₂O (50 mL) at -20°C. The solution was warmed to 23 °C and stirred overnight. The solvent was removed *in vacuo* and the solid extracted with hexane and filtered through Celite. The solution was concentrated and cooled to -30°C to yield orange crystalline **2.12a** (0.86 g, 1.69 mmol, 75%). ¹H NMR δ 7.04 (m, 6H, Ar), 7.00 (tt, 4H, Ph), 6.82 (tt, 2H, Ph), 6.59 (dd, 4H, Ph), 3.38 (m, 4H, NCH₂), 2.54 (s, 4H, CH₂Ph), 2.25 (s, 12H, ArMe), 2.02 (m, 2H, NCH₂CH₂). ¹³C{¹H} NMR δ 149.4, 146.9, 133.9, 129.2, 128.5, 126.8, 126.6, 122.5, 81.6, 57.8, 30.3, 19.4. Anal. Calcd. for C₃₃H₃₈N₂Ti: C, 77.63; H, 7.50; N, 5.49. Found: C, 77.68; H, 7.42; N, 5.44.

(BAIP)Ti(CH₂Ph)₂, 2.12b. PhCH₂MgCl (0.90 M, 2.16 mL, 1.94 mmol) was added dropwise to a stirring suspension of **2.10b** (0.49 g, 0.97 mmol) in Et₂O (50 mL) at -20°C. The solution was warmed to 23 °C and stirred overnight. The solvent was removed *in vacuo* and the solid extracted with hexane and filtered through Celite. The solution was concentrated and cooled to -30°C to yield orange crystalline **2.12b** (0.38 g, 0.61 mmol, 63%). ¹H NMR δ 7.24 (m, 6H, Ar), 7.02 (tt, 4H, Ph), 6.82 (tt, 2H, Ph), 6.70 (dd, 4H, Ph), 3.77 (sept, 4H, CHMe₂), 3.60 (m, 4H, NCH₂), 2.58 (s, 4H, CH₂Ph), 2.07 (m, 2H, NCH₂CH₂), 1.32 (d, 12H, CHMe₂), 1.23 (d, 12H, CHMe₂). ¹³C{¹H} NMR δ 148.2, 147.3, 144.2, 128.5, 127.4, 126.8, 124.9, 122.6, 82.5, 60.9, 30.2, 28.4, 26.6, 24.7. Anal. Calcd. for C₄₁H₅₄N₂Ti: C, 79.07; H, 8.74; N, 4.50. Found: C, 78.45; H, 8.98; N, 4.27.

(BAMP)Ti(CH₂SiMe₃)₂, 2.13a. **2.10a** (1.00 g, 2.50 mmol) was dissolved in Et₂O (50 mL) and cooled to -20°C. LiCH₂SiMe₃ (0.471 g, 5.00 mmol) dissolved in Et₂O was added dropwise. The resulting solution was allowed to warm to 23 °C and stirred overnight. The solvent was removed *in vacuo* and the resulting solid dissolved in toluene and filtered through Celite. The toluene was removed *in vacuo* to leave a orange-yellow solid. Analytically pure **2.13a** is obtained as a yellow crystalline solid after recrystallization from hexanes (0.942 g, 1.88 mmol, 75%). ¹H NMR δ 7.05 (m, 6H, Ar), 3.41 (m, 4H, NCH₂), 2.46 (s, 12H, ArMe₂), 2.16 (m, 2H, NCH₂CH₂), 1.26 (s, 4H, CH₂SiMe₃), 0.03 (s, 18H, SiMe₃).

$^{13}\text{C}\{^1\text{H}\}$ NMR δ 148.9, 133.7, 129.3, 126.4, 74.1, 58.0, 31.0, 19.6, 2.7. Anal. Calcd. for $\text{C}_{35}\text{H}_{62}\text{N}_2\text{Si}_2\text{Ti}$: C, 64.51 H, 9.22; N, 5.57. Found: C, 64.78; H, 9.00; N, 5.67.

(BAIP)Ti(CH_2SiMe_3)₂, **2.13b**. **2.10b** (1.00 g, 1.96 mmol) was dissolved in Et_2O (50 mL) and cooled to -20°C . $\text{LiCH}_2\text{SiMe}_3$ (0.376 g 4.00 mmol) dissolved in Et_2O was added dropwise. The resulting solution was allowed to warm to 23°C and stirred overnight. The solvent was removed *in vacuo* and the resulting solid dissolved in toluene and filtered through Celite. The toluene was removed *in vacuo* to leave a orange–yellow solid. Analytically pure **2.13b**, as yellow crystals, is obtained by recrystallization from toluene at -30°C (0.52 g, 0.84 mmol, 43%). ^1H NMR δ 7.19 (m, 6H, Ar), 3.86 (sept, 4H, CHMe_2), 3.61 (m, 4H, NCH_2), 2.31 (m, 2H, NCH_2CH_2), 1.45 (d, 12H, CHMe_2), 1.34 (s, 4H, CH_2SiMe_3), 1.31 (d, 12H, CHMe_2), 0.04 (s, 18H, SiMe_3). $^{13}\text{C}\{^1\text{H}\}$ NMR δ 147.8, 143.9, 127.1, 125.0, 60.0, 30.3, 28.0, 26.6, 25.3, 2.3. Anal. Calcd. for $\text{C}_{35}\text{H}_{62}\text{N}_2\text{Si}_2\text{Ti}$: C, 64.51 H, 9.22; N, 5.57. Found: C, 64.78; H, 9.00; N, 5.67.

(BAMP)Ti($\eta^5\text{-C}_5\text{H}_5$)Cl, **2.14a**. **2.10a** (1.00 g, 2.50 mmol) was dissolved in THF (50 mL). $\text{NaCp}\cdot\text{DME}$ (0.446 g, 2.50 mmol) was then added as a solid. The solution was stirred overnight at 23°C . The solvent was removed *in vacuo* and the resulting solid taken up in hexane and filtered through Celite. The hexane was reduced to ca. 2 mL and the solution cooled in a freezer. Analytically pure **2.14a** formed as orange crystals (0.913 g, 2.13 mmol, 85 %). ^1H NMR: δ 6.95 (m, 6H, Ar), 5.73 (s, 5H, C_5H_5), 3.81 (m, 2H, NCH_2), 3.35 (m, 1H, NCH_2CH_2), 3.20 (m, 2H, NCH_2), 2.37 (s, 6H, ArMe_2), 2.10 (s, 6H, ArMe_2), 1.95 (m, 1H, NCH_2CH_2). $^{13}\text{C}\{^1\text{H}\}$ NMR δ 157.9, 134.4, 129.3, 129.2, 128.7, 125.5, 116.6, 59.5, 31.5, 20.1, 18.9. Anal. calcd. for $\text{C}_{24}\text{H}_{29}\text{ClN}_2\text{Ti}$: C, 67.22; H, 6.82; N, 6.53. Found: C, 67.46; H, 7.01; N, 6.31.

(BAIP)Ti($\eta^5\text{-C}_5\text{H}_5$)Cl, **2.14b**. **2.10b** (1.00 g, 1.96 mmol) was dissolved in THF (50 mL). $\text{NaCp}\cdot\text{DME}$ (0.356 g, 2.00 mmol) was then added as a solid. The solution was stirred overnight at 23°C . The solvent was removed *in vacuo* and the resulting solid taken up in hexane and filtered through Celite. The hexane was reduced to ca. 2 mL and the solution

cooled in a freezer. Analytically pure **2.14b** formed as orange crystals (0.952 g, 1.76 mmol, 90%). ^1H NMR: δ 7.12 (m, 6H, Ar), 5.92 (s, 5H, C_5H_5), 4.34 (m, 2H, NCH_2), 3.77 (sept, 2H, CHMe_2), 3.36 (sept, 2H, CHMe_2), 3.22 (m, 2H, NCH_2), 2.48 (m, 1H, NCH_2CH_2), 1.99 (m, 1H, NCH_2CH_2), 1.34 (d, 6H, CHMe_2), 1.33 (d, 6H, CHMe_2), 1.22 (d, 6H, CHMe_2), 1.05 (d, 6H, CHMe_2). $^{13}\text{C}\{^1\text{H}\}$ NMR δ 156.6, 144.6, 140.1, 126.4, 124.8, 123.8, 116.2, 63.1, 32.7, 28.0, 27.6, 26.5, 26.2, 24.0. Anal. calcd. for $\text{C}_{32}\text{H}_{45}\text{ClN}_2\text{Ti}$: C, 71.04; H, 8.38; N, 5.18. Found: C, 71.12; H, 8.51; N, 5.14.

(BAMP)Ti($\eta^5\text{-C}_5\text{H}_5$)Me, **2.15a**. **2.14a** (1.0 g, 2.3 mmol) was suspended in Et_2O (50 mL). MeMgBr (3.0 M, 0.83 mL, 2.5 mmol) was then added dropwise. The solution was stirred overnight at 23 °C. The solvent was removed *in vacuo* and the resulting solid taken up in hexane and filtered through celite. The hexane was reduced to ca. 2 mL and the solution cooled in a freezer. Analytically pure **2.15a** formed as yellow crystals (0.76 g, 1.9 mmol, 81 %). ^1H NMR: δ 7.01 (m, 6H, Ar), 5.53 (s, 5H, C_5H_5), 3.55 (m, 2H, NCH_2), 3.31 (m, 2H, NCH_2), 3.08 (m, 1H, NCH_2CH_2), 2.20 (s, 6H, ArMe_2), 2.18 (s, 6H, ArMe_2), 1.98 (m, 1H, NCH_2CH_2), 0.70 (s, 3H, TiMe). $^{13}\text{C}\{^1\text{H}\}$ NMR δ 156.5, 133.9, 130.6, 128.9, 128.8, 124.8, 114.2, 58.4, 36.4, 31.6, 19.7, 18.9. Anal. calcd. for $\text{C}_{25}\text{H}_{32}\text{N}_2\text{Ti}$: C, 73.52; H, 7.90; N, 6.86. Found: C, 73.67; H, 8.01; N, 6.69.

(BAIP)Ti($\eta^5\text{-C}_5\text{H}_5$)Me, **2.15b**. **2.14b** (1.0 g, 1.9 mmol) was suspended in Et_2O (50 mL). MeMgBr (3.0 M, 0.67 mL, 2.0 mmol) was then added dropwise. The solution was stirred overnight at 23 °C. The solvent was removed *in vacuo* and the resulting solid taken up in hexane and filtered through celite. The hexane was reduced to ca. 2 mL and the solution cooled in a freezer. Analytically pure **2.15b** formed as yellow crystals (0.80 g, 1.5 mmol, 81 %). ^1H NMR: δ 7.12 (m, 6H, Ar), 5.70 (s, 5H, C_5H_5), 4.06 (m, 2H, NCH_2), 3.57 (sept, 2H, CHMe_2), 3.43 (sept, 2H, CHMe_2), 3.26 (m, 2H, NCH_2), 2.39 (m, 1H, NCH_2CH_2), 2.07 (m, 1H, NCH_2CH_2), 1.38 (d, 6H, CHMe_2), 1.27 (d, 6H, CHMe_2), 1.21 (d, 6H, CHMe_2), 1.13 (d, 6H, CHMe_2), 0.64 (s, 3H, TiMe). $^{13}\text{C}\{^1\text{H}\}$ NMR δ 155.2, 144.0, 141.3, 125.7, 124.3, 123.8, 113.7, 61.8, 40.1, 33.1, 28.0, 27.4, 26.8, 26.0, 24.2, 24.0.

(BAMP)Ti(η^5 -C₅H₅)Bz, **2.16a**. **2.14a** (1.0 g, 2.3 mmol) was suspended in Et₂O (50 mL). BzMgCl (0.67 M, 3.7 mL, 2.5 mmol) was then added dropwise. The solution was stirred 3 days at 23 °C. The solvent was removed *in vacuo* and the resulting solid taken up in hexane and filtered through celite. The hexane was reduced to ca. 2 mL and the solution cooled in a freezer. Analytically pure **2.16a** formed as orange crystals (0.98 g, 2.0 mmol, 88 %). ¹H NMR: δ 7.28 (t, 2H, Bz), 7.18 (d, 2H, Bz), 7.00 (m, 7H, Ar,Bz), 5.47 (s, 5H, C₅H₅), 3.48 (m, 2H, NCH₂), 3.35 (m, 2H, NCH₂), 3.18 (m, 1H, NCH₂CH₂), 2.70 (s, 2H, CH₂Ph), 2.18 (s, 6H, ArMe₂), 2.15 (s, 6H, ArMe₂), 1.98 (m, 1H, NCH₂CH₂). ¹³C{¹H} NMR δ 157.3, 154.6, 133.8, 130.4, 129.0, 129.0, 128.4, 126.0, 125.0, 121.4, 116.0, 58.1, 57.8, 30.3, 20.6, 19.1.

(BAIP)Ti(η^5 -C₅H₅)Bz, **2.16b**. **2.14b** (1.0 g, 1.8 mmol) was suspended in Et₂O (50 mL). BzMgCl (0.67 M, 3.0 mL, 2.0 mmol) was then added dropwise. The solution was stirred 3 days at 23 °C. The solvent was removed *in vacuo* and the resulting solid taken up in hexane and filtered through celite. The hexane was reduced to ca. 2 mL and the solution cooled in a freezer. Analytically pure **2.16b** formed as orange crystals (0.90 g, 1.5 mmol, 84 %). ¹H NMR: δ 7.12 (m, 6H, Ar), 5.71 (s, 5H, C₅H₅), 4.02 (m, 2H, NCH₂), 3.43 (sept, 2H, CHMe₂), 3.35 (sept, 2H, CHMe₂), 3.38 (m, 2H, NCH₂), 2.58 (s, 2H, PhCH₂), 2.51 (m, 1H, NCH₂CH₂), 2.06 (m, 1H, NCH₂CH₂), 1.34 (d, 6H, CHMe₂), 1.21 (d, 6H, CHMe₂), 1.14 (d, 6H, CHMe₂), 1.14 (d, 6H, CHMe₂). ¹³C{¹H} NMR δ 156.2, 153.5, 144.1, 141.3, 128.7, 126.2, 125.9, 124.7, 124.2, 121.6, 115.4, 66.0, 61.4, 32.5, 27.9, 27.8, 26.7, 26.1, 24.6, 24.0. Anal. calcd. for C₃₉H₅₂N₂Ti: C, 78.50; H, 8.78; N, 4.69. Found: C, 78.35; H, 8.78; N, 4.66.

(BAMP)Ti(CH₂CMe₂Ph)Cl, **2.17a**. PhCMe₂CH₂MgCl (0.69 M, 1.88 mL, 1.30 mmol) was added dropwise to a stirring suspension of **2.10a** (0.50 g, 1.25 mmol) in Et₂O (50 mL) at 23 °C. The solution was stirred overnight. The solvent was removed *in vacuo* and the resulting solid extracted with hexanes and filtered through Celite. The solution was concentrated and cooled to -30 °C to yield complex **2.17a** as a yellow oil (0.45 g, 0.91 mmol, 72 %). ¹H NMR δ 7.00 (m, 11H, Ar, Ph), 3.62 (m, 2H, NCH₂), 3.16 (m, 2H, NCH₂), 2.54 (s,

6H, ArMe₂), 2.30 (s, 6H, ArMe₂), 2.11 (s, 2H, CH₂CMe₂Ph), 1.90 (m, 1H, NCH₂CH₂), 1.60 (m, 1H, NCH₂CH₂), 1.15 (s, 6H, CH₂CMe₂Ph). ¹³C{¹H} NMR δ 152.5, 147.7, 134.5, 132.5, 129.6, 129.2, 128.2, 127.4, 125.2, 125.1, 58.6, 43.3, 31.3, 30.7, 19.2, 18.7.

(BAIP)Ti(CH₂CMe₂Ph)Cl, 2.17b. PhCMe₂CH₂MgCl (0.69 M, 4.3 mL, 3.0 mmol) was added dropwise to a stirring suspension of **2.10b** (1.0 g, 2.5 mmol) in Et₂O (50 mL) at room temp. The solution was stirred overnight. The solvent was removed *in vacuo* and the resulting solid extracted with hexanes and filtered through Celite. The solution was concentrated and cooled to -30 °C to yield complex **2.17b** as a yellow oil (0.86 g, 1.4 mmol, 56 %). ¹H NMR δ 7.10 (m, 11H, Ar, Ph), 3.70 (m, 2H, NCH₂), 3.22 (m, 2H, NCH₂), 2.15 (s, 2H, CH₂CMe₂Ph), 1.87 (m, 1H, NCH₂CH₂), 1.48 (m, 1H, NCH₂CH₂), 1.38 (d, 6H, CHMe₂), 1.24 (d, 6H, CHMe₂), 1.11 (d, 6H, CHMe₂), 1.05 (d, 6H, CHMe₂), 1.10 (s, 6H, CH₂CMe₂Ph).

BAMB(SiMe₃)₂, 2.19a. MeLi (1.48 M, 35.3 mL, 52.2 mmol) was added dropwise to a stirring solution of compound **2.6a** (7.74 g, 26.1 mmol) in THF (150 mL) at -78 °C. The solution was warmed to 23 °C where it was kept for 30 minutes. The solution was cooled to 0 °C and chlorotrimethylsilane (5.67 g, 52.2 mmol) was added dropwise. The solution was stirred overnight at 23 °C, removed *in vacuo* and the resulting slurry dissolved in hexanes. The solution was then filtered through Celite and the solvent removed *in vacuo* to leave a yellow solid. Recrystallization from hexanes yields pure **2.19a** (16.1 g, 25.9 mmol; 99%). ¹H NMR δ 7.10 (m, 3H, Ar), 6.95 (m, 2H, Ar), 3.01 (t, 4H, NCH₂), 2.20 (s, 12H, ArMe₂), 1.35 (m, 4H, NCH₂CH₂), 0.10 (s, 18H, SiMe₃).

BAIB(SiMe₃)₂, 2.19b. MeLi (1.48 M, 35.3 mL, 52.2 mmol) was added dropwise to a stirring solution of compound **2.6b** (10.0 g, 26.1 mmol) in THF (150 mL) at -78 °C. The solution was warmed to 23 °C where it was kept for 30 minutes. The solution was cooled to 0 °C and chlorotrimethylsilane (5.67 g, 52.2 mmol) was added dropwise. The solution was stirred overnight at 23 °C, removed *in vacuo* and the resulting slurry dissolved in hexanes. The solution was then filtered through Celite and the solvent removed *in vacuo* to leave a

yellow solid. Recrystallization from diethylether yields pure **2.19b** (19.0 g, 25.9 mmol; 99%). ^1H NMR δ 7.08 (m, 6H, Ar), 3.49 (sept, 4H, CHMe_2), 3.05 (t, 4H, NCH_2), 1.45 (m, 4H, NCH_2CH_2), 1.24 (d, 12H, CHMe_2), 1.20 (d, 12H, CHMe_2), 0.10 (s, 18H, SiMe_3). $^{13}\text{C}\{^1\text{H}\}$ NMR δ 148.7, 143.5, 126.2, 124.3, 52.6, 29.3, 27.9, 25.3, 25.0, 0.5.

BAMB(SnMe₃)₂, 2.21a. MeLi (1.48 M, 35.3 mL, 52.2 mmol) was added dropwise to a stirring solution of compound **2.6a** (7.74 g, 26.1 mmol) in THF (150 mL) at -78°C . The solution was warmed to 23°C where it was kept for 30 minutes. The solution was cooled to 0°C and chlorotrimethylstannane (10.4 g, 52.2 mmol) was added dropwise. The solution was stirred overnight at 23°C , removed *in vacuo* and the resulting slurry dissolved in hexanes. The solution was then filtered through Celite and the solvent removed *in vacuo* to leave a yellow solid. Recrystallization from diethylether yields pure **2.21a** (16.1 g, 25.9 mmol; 99%). ^1H NMR δ 7.05 (m, 3H, Ar), 6.90 (m, 2H, Ar), 3.12 (t, 4H, NCH_2), 2.26 (s, 12H, ArMe_2), 1.45 (m, 4H, NCH_2CH_2), 0.06 (s, 18H, SnMe_3). $^{13}\text{C}\{^1\text{H}\}$ NMR δ 151.6, 137.1, 128.7, 123.4, 54.7, 31.6, 20.0, 6.0. MS (EI) m/z 619.14655 ($[\text{M}-1]^+$). Calcd. for $[\text{C}_{26}\text{H}_{43}\text{N}_2\text{Sn}_2]^-$: 619.14621

BAIB(SnMe₃)₂, 2.21b. MeLi (1.48 M, 35.3 mL, 52.2 mmol) was added dropwise to a stirring solution of compound **2.6b** (10.0 g, 26.1 mmol) in THF (150 mL) at -78°C . The solution was warmed to 23°C where it was kept for 30 minutes. The solution was cooled to 0°C and chlorotrimethylstannane (10.4 g, 52.2 mmol) was added dropwise. The solution was stirred overnight at 23°C , removed *in vacuo* and the resulting slurry dissolved in hexanes. The solution was then filtered through Celite and the solvent removed *in vacuo* to leave a yellow solid. Recrystallization from diethylether yields pure **2.21b** (19.0 g, 25.9 mmol; 99%). ^1H NMR δ 7.10 (m, 6H, Ar), 3.66 (sept, 4H, CHMe_2), 3.26 (t, 4H, NCH_2), 1.60 (m, 4H, NCH_2CH_2), 1.28 (d, 12H, CHMe_2), 1.18 (d, 12H, CHMe_2), 0.12 (s, 18H, SnMe_3). $^{13}\text{C}\{^1\text{H}\}$ NMR δ 148.5, 148.5, 125.0, 123.8, 57.2, 31.4, 27.8, 25.3, 24.8, 5.7. MS (EI) m/z 732.27960 (M^+). Calcd. for $\text{C}_{34}\text{H}_{60}\text{N}_2\text{Sn}_2$ 732.27924

(BAMB)TiCl₂, 2.25a. **2.21a** (3.56 g, 5.73 mmol) and TiCl₄ (1.09 g, 5.73 mmol) were refluxed in toluene for 12h. The resulting deep red solution was filtered through Celite, the volume of the filtrate was reduced until a slurry formed and hexanes is added to complete the precipitation. Recrystallization from a toluene/hexanes mixture yields pure **2.25a** as dark orange-red crystals (1.77 g, 4.29 mmol, 75%). ¹H NMR δ 6.80 (m, 6H, Ar), 3.90 (t, 4H, NCH₂), 2.06 (s, 12H, ArMe₂), 1.33 (m, 4H, NCH₂CH₂). ¹³C {¹H} NMR δ 146.6, 132.4, 130.1, 129.7, 59.6, 26.5, 19.2.

(BAIB)TiCl₂, 2.25b. **2.21b** (4.21 g, 5.73 mmol) and TiCl₄ (1.09 g, 5.73 mmol) were refluxed in toluene for 12h. The resulting deep red solution was filtered through Celite, the volume of the filtrate was reduced until a slurry formed and hexanes is added to complete the precipitation. Recrystallization from a toluene/hexanes mixture yields pure **2.25b** as dark orange-red crystals (2.05 g, 3.89 mmol, 68%). ¹H NMR δ 7.10 (m, 6H, Ar), 4.13 (t, 4H, NCH₂), 3.15 (sept, 4H, CHMe₂), 1.77 (m, 4H, NCH₂CH₂), 1.30 (d, 12H, CHMe₂), 1.04 (d, 12H, CHMe₂). ¹³C {¹H} NMR δ 143.6, 142.5, 131.5, 125.4, 62.7, 28.9, 26.9, 24.8, 24.7.

(BAMB)TiMe₂, 2.27a. MeMgBr (2.4 M, 1.0 mL, 2.5 mmol) was added dropwise to a stirring suspension of **2.25a** (0.50 g, 1.2 mmol) in Et₂O (50 mL) at -20°C. The solvent was immediately removed *in vacuo* and the resulting solid extracted with pentane, filtered through Celite and removed. The resulting yellow solid was dissolved in C₆D₆ and proton and carbon NMR spectra were obtained. The resulting complex decomposed slowly giving an unidentifiable paramagnetic black complex. ¹H NMR δ 6.90 (m, 6H, Ar), 3.85 (t, 4H, NCH₂), 2.12 (s, 12H, ArMe₂), 1.70 (m, 4H, NCH₂CH₂), 1.30 (s, 6H, TiMe₂). ¹³C {¹H} NMR δ 135.3, 134.0, 129.3, 126.9, 63.6, 54.3, 29.6, 19.3.

(BAIB)TiMe₂, 2.27b. MeMgBr (2.4 M, 0.83 mL, 2.0 mmol) was added dropwise to a stirring suspension of **2.25b** (0.50 g, 0.95 mmol) in Et₂O (50 mL) at -20°C. The solvent was immediately removed *in vacuo* and the resulting solid extracted with pentane, filtered through Celite and removed. The resulting yellow solid was dissolved in C₆D₆ and proton and carbon NMR spectra were obtained. The resulting complex decomposed slowly giving

an unidentifiable paramagnetic black complex. ^1H NMR δ 7.10 (m, 6H, Ar), 3.98 (t, 4H, NCH_2), 3.53 (sept, 4H, CHMe_2), 2.06 (m, 4H, NCH_2CH_2), 1.36 (s, 6H, TiMe_2), 1.20 (d, 12H, CHMe_2), 1.15 (d, 12H, CHMe_2). $^{13}\text{C}\{^1\text{H}\}$ NMR δ 146.7, 139.1, 124.7, 64.0, 58.4, 29.6, 28.1, 25.2, 25.0.

BAIE(SiMe₃)₂, 2.29b. Diamine **2.2b** (2.50 g, 6.56 mmol) was dissolved in Et₂O (200 mL) and cooled to -78 °C. MeLi (1.6 M, 13.8 mmol, 8.61 mL) was added dropwise and the resulting solution warmed to 23 °C. ClSiMe₃ (1.63 g, 15.0 mmol) dissolved in Et₂O (25 mL) was then added dropwise to the solution. The reaction was stirred overnight at 23 °C. The solvent was removed *in vacuo*, the resulting solid dissolved in hexanes and filtered through celite. The solution was concentrated and cooled to -30 °C. Complex **2.29b** was collected as a white crystalline solid (3.27 g, 6.23 mmol, 95 %). ^1H NMR δ 7.00 (m, 6H, Ar), 3.44 (sept, 4H, CHMe_2), 3.15 (s, 4H, NCH_2), 1.16 (d, 12H, CHMe_2), 1.15 (d, 12H, CHMe_2). $^{13}\text{C}\{^1\text{H}\}$ NMR δ 148.5, 142.3, 126.1, 124.2, 51.5, 27.9, 25.1, 24.7.

(BAIE)Ti(NMe₂)₂, 2.31b. Diamine **2.2b** (0.50 g, 1.3 mmol) was dissolved in Et₂O (50 mL) and cooled to -78 °C. BuLi (2.5 M, 2.7 mmol, 1.08 mL) was added via syringe and the solution was allowed to warm to 23 °C. The resulting solution was added dropwise to Ti(NMe₂)Cl₂ (0.35 g, 1.3 mmol) in Et₂O (150 mL) at -78 °C. The mixture was warmed slowly to 23 °C and stirred overnight. The solvent was removed *in vacuo* and the resulting brown-red solid was dissolved in hexanes and filtered through celite. The solution was concentrated and cooled to -30 °C. No product crystallized from the solution, however, ^1H NMR spectroscopy of an aliquot revealed that the product was indeed formed. ^1H NMR δ 7.10 (m, 6H, Ar), 3.90 (s, 4H, NCH_2), 3.70 (sept, 4H, CHMe_2), 2.70 (s, 12H, NMe_2), 1.20 (m, 24H, CHMe_2).

(BAIE)TiCl₂, 2.32b. Complex **2.31b** (0.67 g, 1.3 mmol) was dissolved in hexanes (50 mL) and excess chlorotrimethylsilane (1.50 mL, 11.8 mmol) was added dropwise. The reaction was stirred for 36 hours, upon which the solution was evaporated to dryness to remove all volatiles. The resulting oil was redissolved in hexanes, filtered through celite and

reduced in volume. Cooling the solution to $-30\text{ }^{\circ}\text{C}$ did not result in the crystallization of complex **2.32b**. ^1H NMR spectroscopy of an aliquot revealed that the dichloride **2.32b** was formed. ^1H NMR δ 7.20 (m, 6H, Ar), 4.55 (s, 4H, NCH_2), 4.00 (sept, 4H, CHMe_2), 1.30 (m, 24H, CHMe_2).

BAMD, 2.38a. To a stirred solution of 2,6-dimethylaniline (22.5 g, 186 mmol) in methanol was added dropwise 2,3-butanedione (8.00 g, 93.0 mmol) and three drops of HCOOH as catalyst. The yellow solution was stirred 20 hours after such time a yellow solid formed. The solid was collected by filtration and washed with cold methanol ($2 \times 20\text{ mL}$). A hexanes solution of the yellow product was stirred over Na_2SO_4 for 30 minutes to remove any water. The Na_2SO_4 was removed by filtration and the solvent removed *in vacuo* to give compound **2.38a** (16.8 g, 57.7 mmol, 62 %). ^1H NMR δ 7.00 (m, 6H, Ar), 2.00 (s, 6H, *Me*), 1.97 (s, 12H, *ArMe*). $^{13}\text{C}\{^1\text{H}\}$ NMR δ 168.0, 149.1, 128.4, 124.7, 123.6, 17.9, 15.7. MS (EI) m/z 292.19367 (M^+). Calcd. for $\text{C}_{20}\text{H}_{24}\text{N}_2$ 292.19394

BAID, 2.38b. 2,3-Butanedione (3.99 g, 46.6 mmol) was added to a methanol solution of 2,6-diisopropylaniline (16.5 g, 93.2 mmol) with 2 drops of HCOOH . The solution was stirred 12 hours and then cooled to -78°C to complete precipitation. The yellow solid was collected by filtration, dissolved up in hexanes and dried over Na_2SO_4 . The solution was filtered and the solvent removed *in vacuo* to give pure **2.38b** (12.8 g, 63.4 mmol, 68 %). ^1H NMR δ 7.17 (m, 6H, Ar), 2.87 (sept, 4H, CHMe_2), 2.15 (s, 6H, *Me*), 1.19 (d, 12H, CHMe_2), 1.16 (d, 12H, CHMe_2). $^{13}\text{C}\{^1\text{H}\}$ NMR δ 168.4, 146.7, 135.2, 124.4, 123.5, 29.0, 23.2, 22.7, 16.5. MS (EI) m/z 404.31834 (M^+). Calcd. for $\text{C}_{28}\text{H}_{40}\text{N}_2$ 404.31915

BAED, 2.38c. 2,3-Butanedione (5.02 g, 58.1 mmol) was added dropwise to a stirred solution of 2,6-diethylaniline (17.3 g, 116 mmol) in methanol with 2 drops of HCOOH present. After 24 hours of mixing no product had precipitated from the clear yellow solution. The solution was cooled to -78°C upon which a yellow precipitate formed. The precipitate was collected by filtration and dissolved in hexanes. Na_2SO_4 was then added to remove the last traces of water, the solution was filtered, and the solvent removed *in vacuo* to give

compound **2.38c** (7.05 g, 37.1 mmol, 32 %). ^1H NMR δ 7.10 (m, 6H, Ar), 2.07 (m, 8H, CH_2CH_3), 2.07 (s, 6H, *Me*), 1.11 (t, 12H, CH_2CH_3). $^{13}\text{C}\{^1\text{H}\}$ NMR δ 168.0, 148.0, 130.7, 128.5, 126.7, 124.0, 25.3, 16.1, 13.9, 13.85. MS (EI) m/z 347.24755 (M^+). Calcd. for $\text{C}_{24}\text{H}_{31}\text{N}_2$ 347.24872

(BAMD) TiCl_4 , **2.39a**. **2.38a** (1.0 g, 3.4 mmol) was dissolved in dichloromethane (50 mL). TiCl_4 (0.65 g, 3.4 mmol) was added dropwise causing an immediate orange precipitate. Solution was stirred for 12 hours and the bright orange solid (1.6 g, 3.4 mmol, 99 %) was collected on a sintered glass funnel. Due to the insoluble nature of this compound no spectral data could be obtained. Anal. Calcd. for $\text{C}_{20}\text{H}_{24}\text{Cl}_4\text{N}_2\text{Ti}$: C, 49.82; H, 5.02; N, 5.81. Found: C, 49.88; H, 5.01; N, 5.80.

(BAID) TiCl_4 , **2.39b**. **2.38b** (1.0 g, 2.5 mmol) was dissolved in dichloromethane (50 mL). TiCl_4 (0.47 g, 2.5 mmol) was added dropwise causing an immediate orange precipitate. Solution was stirred for 12 hours and the bright orange solid (1.5 g, 2.5 mmol, 99 %) was collected on a sintered glass funnel. ^1H NMR (CD_2Cl_2) δ 7.34 (m, 6H, Ar), 3.46 (sept, 4H, CHMe_2), 2.39 (s, 6H, *Me*), 1.41 (d, 12H, CHMe_2), 1.13 (d, 12H, CHMe_2). $^{13}\text{C}\{^1\text{H}\}$ NMR δ 175.9, 146.4, 140.0, 128.9, 125.6, 29.4, 25.5, 25.0, 23.4. Anal. Calcd. for $\text{C}_{28}\text{H}_{40}\text{Cl}_4\text{N}_2\text{Ti}$: C, 56.58; H, 6.78; N, 4.71. Found: C, 56.86; H, 6.84; N, 4.60.

(BAED) TiCl_4 , **2.39c**. **2.38c** (1.0 g, 2.9 mmol) was dissolved in dichloromethane (50 mL). TiCl_4 (0.54 g, 2.9 mmol) was added dropwise causing an immediate orange precipitate. Solution was stirred for 12 hours and the bright orange solid (1.5 g, 2.8 mmol, 99 %) was collected on a sintered glass funnel. ^1H NMR (CD_2Cl_2) δ 7.32 (m, 6H, Ar), 3.00 (m, 4H, CH_2CH_3), 2.76 (m, 4H, CH_2CH_3), 2.30 (s, 6H, *Me*), 1.28 (t, 12H, CH_2CH_3). $^{13}\text{C}\{^1\text{H}\}$ NMR δ 175.5, 147.7, 135.3, 128.5, 127.3, 25.7, 22.1, 14.8. Anal. Calcd. for $\text{C}_{24}\text{H}_{32}\text{Cl}_4\text{N}_2\text{Ti}$: C, 53.56; H, 5.99; N, 5.20. Found: C, 53.79; H, 6.10; N, 5.18.

(BAMD) TiCl_2 , **2.40a**. **2.39a** (1.0 g, 2.1 mmol) was suspended in toluene. Sodium (95 mg, 4.1 mmol) dissolved in mercury (9.50 g) was added and the solution stirred overnight to leave a black/green solution. The solution was filtered through celite and the

toluene removed to yield a dark purple solid (0.20 g, 0.48 mmol, 23 %). Analytically pure **2.40a** was obtained from recrystallization from a combination of toluene and hexanes. ^1H NMR (C_6D_6) δ 6.89 (m, 6H, Ar), 2.20 (s, 12H, ArMe_2), 1.62 (s, 6H, *Me*). $^{13}\text{C}\{^1\text{H}\}$ NMR δ 148.4, 131.0, 129.2, 126.8, 109.2, 19.9, 14.0. Anal. Calcd. for $\text{C}_{20}\text{H}_{24}\text{Cl}_2\text{N}_2\text{Ti}$: C, 58.42; H, 5.88; N, 6.81. Found: C, 58.78; H, 5.99; N, 7.00.

(BAMD) $\text{TiCl}_2(\text{THF})$, **2.41a**. Preparation of **2.41a** is identical to the preparation of complex **2.40a** except THF is used as solvent. ^1H NMR (C_6D_6) δ 6.93 (m, 6H, Ar), 3.70 (br m, 4H, CH_2), 2.18 (s, 12H, ArMe_2), 1.94 (s, 6H, *Me*), 1.23 (br m, 4H, CH_2). $^{13}\text{C}\{^1\text{H}\}$ NMR δ 149.1, 133.0, 128.7, 126.6, 108.6, 70.2, 25.5, 19.9, 14.1.

(BAID) TiCl_2 , **2.40b**. **2.39b** (1.0 g, 1.7 mmol) was suspended in toluene. Sodium (77 mg, 3.4 mmol) dissolved in mercury (7.7 g) was added and the solution stirred overnight to leave a black/green solution. The solution was filtered through celite and the toluene removed to yield a dark purple solid (0.31 g, 0.59 mmol, 35%). Complex **2.40b** and **2.38b** co-crystallize from solutions of pentane and an analytically pure sample of **2.40b** could not be isolated. ^1H NMR (CD_2Cl_2) δ 7.10 (m, 6H, Ar), 3.65 (sept, 4H, CHMe_2), 1.73 (s, 6H, *Me*), 1.55 (d, 12H, CHMe_2), 0.94 (d, 12H, CHMe_2).

(BAED) TiCl_2 , **2.40c**. **2.39c** (1.0 g, 1.9 mmol) was suspended in toluene. Sodium (85 mg, 3.7 mmol) dissolved in mercury (8.5 g) was added and the solution stirred overnight to leave a black/green solution. The solution was filtered through celite and the toluene removed to yield a dark purple solid (0.22 g, 0.47 mmol, 25%). Analytically pure **2.40c** was obtained from recrystallization from a combination of toluene and hexanes. ^1H NMR (C_6D_6) δ 7.00 (m, 6H, Ar), 2.58 (br, 8H, CH_2CH_3), 1.69 (s, 6H, *Me*), 1.15 (br, 12H, CH_2CH_3). $^{13}\text{C}\{^1\text{H}\}$ NMR δ 147.2, 137.2, 127.5, 126.7, 109.0, 25.3, 15.1, 14.2. Anal. Calcd. for $\text{C}_{24}\text{H}_{32}\text{Cl}_2\text{N}_2\text{Ti}$: C, 61.68; H, 6.90; N, 5.99. Found: C, 61.83; H, 6.76; N, 5.87.

(BAIX) H_2 , **2.43b**. 2,6-Diisopropylaniline (5.00 g, 28.2 mmol) was dissolved in 50 mL of THF and cooled to -78°C . Butyllithium (1.94 M, 28.2 mmol, 14.6 mL) was added dropwise via a syringe. The reaction was stirred for 10 minutes, allowed to warm to 23°C

and stirred for an additional 30 min. Tmeda (3.28 g, 28.2 mmol) was added to the mixture. A solution of α,α' -dibromo-o-xylene (3.72 g, 14.1 mmol) in THF was prepared and the yellow lithium anilide solution was added dropwise via cannula to the dibromide. The resulting mixture was stirred overnight at 23 °C. The solvent was then removed *in vacuo* giving a dark brown solid which was taken up in hexanes, filtered through celite and reduced in volume before being cooled to -25°C. After 12 hours a white solid was collected by filtration, washed with cold hexanes and dried *in vacuo*. The solid recrystallized once more from hexanes to give analytically pure **2.43b** (3.53 g, 7.75 mmol 55 %). ^1H NMR δ 7.55 (m, 4H, C_6H_4), 7.15 (m, 6H, Ar), 4.20 (d, 4H, NCH_2), 3.30 (m, 6H, CHMe_2 superimposed on NH), 1.20 (d, 24H, CHMe_2).

BAIX(SiMe₃)₂, 2.44b. MeLi (1.48 M, 3.25 mL, 4.82 mmol) was added dropwise to a stirring solution of diamine **2.43b** (1.00 g, 2.19 mmol) in THF (150 mL) at -78°C. The solution was warmed to 23 °C where it was kept for 30 minutes. The solution was cooled to 0°C and chlorotrimethylsilane (0.543 g, 5.00 mmol) was added dropwise. The solution was stirred overnight at 23 °C. The solvent was removed *in vacuo* and the resulting slurry dissolved in hexanes. The solution was then filtered through Celite and the solvent removed *in vacuo* to leave a yellow solid. Recrystallization from diethylether yields pure **2.44b** as a white crystalline solid (1.17 g, 1.94 mmol; 89%). ^1H NMR δ 7.10 (m, 2H, Ar), 7.02 (m, 2H, Ar), 6.99 (m, 2H, Ar), 6.94 (m, 2H, C_6H_4), 6.76 (m, 2H, C_6H_4), 4.45 (s, 4H, N-CH_2), 3.36 (sept, 4H, CHMe_2), 1.17 (d, 12H, CHMe_2), 0.98 (d, 12H, CHMe_2), 0.23 (s, 18H, $\text{Si}(\text{CH}_3)_3$).

(BAIX)Ti(NMe₂)₂, 2.45b. Compound **2.43b** (1.1 g, 2.0 mmol) was dissolved in diethylether and cooled to -78°C. Butyllithium (2.5 M, 4.25 mmol, 1.7 mL) was added dropwise and the solution stirred 2 hours at -78°C. The resulting lithium salt was then added dropwise to $\text{Ti}(\text{NMe}_2)_2\text{Cl}_2$ (0.41 g, 2.0 mmol) dissolved in diethylether at -78°C. The solution was then allowed to warm to 23 °C slowly and stirred 12 hours. The solvent was removed *in vacuo* and the resulting orange-brown solid dissolved in hexanes, filtered through celite and concentrated and stored at -25°C. Compound **2.45b** was then collected by

filtration as a red–orange crystalline solid (0.57 g, 0.97 mmol, 44 %). ^1H NMR δ 7.24 (m, 10H, Ar), 4.73 (s, 4H, NCH_2), 3.73 (sept, 4H, CHMe_2), 2.38 (s, 12H, NMe_2), 1.37 (d, 12H, CHMe_2), 1.27 (d, 12H, CHMe_2). $^{13}\text{C}\{^1\text{H}\}$ NMR δ 150.5, 145.4, 140.4, 131.2, 125.9, 124.2, 63.9, 44.5, 28.2, 26.2, 24.8.

(BAIX)TiCl₂, 2.46b. In a glass pressure vessel, an excess of chlorotrimethylsilane (1.71 g, 15.8 mmol) was added to complex **2.45b** (0.59 g, 1.0 mmol) dissolved in toluene. The solution was heated at 80°C for three days. The solvent was removed *in vacuo*, and the resulting orange–red solid taken up in pentane and filtered through celite. The pentane solution was concentrated and cooled to –25°C. Solid orange–red crystals of **2.46b** was collected by filtration (98.0 mg, 0.18 mmol, 18%). ^1H NMR δ 7.15 (m, 6H, Ar), 6.98 (m, 2H, Ar), 6.80 (m, 2H, Ar), 4.85 (s, 4H, NCH_2), 3.73 (sept, 4H, CHMe_2), 1.40 (d, 12H, CHMe_2), 1.10 (d, 12H, CHMe_2). $^{13}\text{C}\{^1\text{H}\}$ NMR δ 146.2, 144.0, 136.4, 130.7, 129.3, 129.2, 125.1, 62.9, 29.2, 25.6, 24.8. Anal. Calcd. for $\text{C}_{32}\text{H}_{42}\text{Cl}_2\text{N}_2\text{Ti}$: C, 67.02; H, 7.38; N, 4.88. Found: C, 67.22; H, 7.37; N, 4.70.

(BAIX)TiMe₂, 2.47b. The titanium dichloride **2.46b** 0.25 g, 0.44 mmol) was dissolved in diethylether and cooled to –20°C. MeMgBr (3.0 M, 0.90 mmol, 0.30 mL) was added dropwise via syringe. The solution went from orange to deep yellow with a whit precipitate. The reaction was allowed to stir for 5 hr's, then the solvent was removed *in vacuo*. The solid was then dissolved in pentane and filtered through celite to give a bright yellow solution. The pentane was concentrated and cooled to –25°C. Yellow crystals of **2.47b** formed and were collected by filtration (0.15 g, 0.29 mmol, 65%). ^1H NMR δ 7.24 (m, 6H, Ar), 7.02 (m, 4H, Ar), 4.64 (s, 4H, NCH_2), 3.73 (sept, 4H, CHMe_2), 1.35 (d, 12H, CHMe_2), 1.30 (d, 12H, CHMe_2), 0.64 (s, 6H, TiMe_2). $^{13}\text{C}\{^1\text{H}\}$ NMR δ 146.8, 145.1, 138.8, 131.0, 128.4, 127.4, 124.8, 61.9, 55.6, 28.9, 26.2, 25.2. Anal. Calcd. for $\text{C}_{34}\text{H}_{48}\text{N}_2\text{Ti}$: C, 76.67; H, 9.08; N, 5.26. Found: C, 77.00; H, 9.00; N, 5.26.

(BAIMP)H₂, 2.48d. BuLi (2.50 M, 13.4 mL, 33.5 mmol) was added dropwise to 2–isopropyl–6–methylaniline (5.00 g, 33.5 mmol) at –78°C in THF (100 mL). The solution

was allowed to warm to 23 °C and then stirred for 30 min. The solution was cooled to 0 °C and tmeda (3.89 g, 33.5 mmol) was added dropwise followed by 1,3-dibromopropane (3.38g, 16.7 mmol) dropwise. The solution was warmed to 23 °C and stirred overnight. The solution was poured into H₂O (100 mL) and extracted with CH₂Cl₂ (3 × 100 mL). The organic layer was dried over anhydrous Na₂SO₄ and the CH₂Cl₂ removed *in vacuo*. The resulting yellow oil was dissolved in diethyl ether (30 mL) and concentrated HCl (20 mL) was added. The salt ([ArH₂N(CH₂)₃NH₂Ar]Cl₂) was removed by filtration, washed with diethyl ether (20 mL), and dissolved in dichloromethane. This solution was poured into aqueous saturated K₂CO₃ (100 mL). The organic layer was separated and dried over anhydrous Na₂SO₄. Removal of the solvent yielded pure **2.48d** as a viscous oil (3.28 g, 9.69 mmol; 58 %). ¹H NMR δ 7.09 (m, 2H, Ar), 6.98 (m, 4H, Ar), 3.28 (sept, 4H, CHMe₂), 2.92 (t, 4H, NCH₂), 2.87 (s, 2H, NH), 2.20 (s, 6H, ArMe), 1.66 (m, 2H, NCH₂CH₂), 1.20 (d, 12H, CHMe₂). ¹³C{¹H} NMR δ 145.4, 141.5, 128.8, 131.0, 124.2, 123.4, 48.7, 32.7, 27.8, 24.3, 18.8.

BAIMP(TMS)₂, 2.49d. **2.48d** (2.0 g, 5.91 mmol) was dissolved in Et₂O and cooled to -30 °C. MeLi (1.5 M, 12.4 mmol, 8.27 ml) was added dropwise to the cool solution. The solution was allowed to warm to 23 °C and ClSiMe₃ (1.35 g, 12.4 mmol) was added dropwise. The solution was stirred overnight. The solvent was removed *in vacuo* and the resulting oil dissolved in hexanes and filtered through celite. The solvent was reduced in volume and cooled to -30 °C to give complex **2.49d** as a white crystalline solid (2.71 g, 5.61 mmol, 95 %). ¹H NMR δ 6.95 (m, 5H, Ar), 3.15 (sept, 4H, CHMe₂), 2.80 (t, 4H, NCH₂), 2.10 (s, 6H, ArMe), 1.48 (m, 2H, NCH₂CH₂), 1.15 (d, 6H, CHMe₂), 1.11 (d, 6H, CHMe₂), 0.10 (s, 18H, SiMe₃).

(BAIMP)TiCl₂, 2.50d. **2.49d** (4.54 g, 9.40 mmol) and TiCl₄ (1.78 g, 9.40 mmol) were dissolved in xylenes and heated to 120 °C for 12 hours. The solvent was removed *in vacuo* and replaced with toluene and filtered through celite. The solvent was reduced until a slurry appeared then hexanes was added to complete precipitation. Pure complex **2.50d** was obtained as a red crystalline solid (2.50 g, 5.49 mmol, 58 %). ¹H NMR δ 7.05 (m, 6H, Ar),

3.60 (m, 4H, CHMe_2), 3.50 (m, 4H, NCH_2), 2.38 (s, 6H, ArMe), 2.42 (m, 2H, NCH_2CH_2), 1.44 (d, 6H, CHMe_2), 1.60 (d, 3H, CHMe_2), 1.14 (d, 3H, CHMe_2). $^{13}\text{C}\{^1\text{H}\}$ NMR δ 144.4, 143.8, 143.7, 132.8, 132.6, 129.1, 128.9, 125.2, 63.1, 62.8, 31.7, 31.5, 28.6, 28.4, 26.4, 26.3, 23.9, 23.9, 19.4, 19.2.

(BAIMP)TiMe₂, 2.51d. **2.50d** (0.285 g, 0.688 mmol) was suspended in Et_2O (50 mL). MeMgBr (3.0 M, 0.50 mL, 1.50 mmol) was added dropwise to give a deep yellow solution. The reaction was stirred overnight at 23 °C. The solvent was removed and the resulting product dissolved in pentane, filtered through celite, reduced in volume and cooled to -30 °C. Pure dimethyl complex **2.51d** was obtained as a yellow crystalline solid (0.145 g, 0.351 mmol, 51 %). ^1H NMR δ 7.21 (m, 4H, Ar), 7.10 (m, 8H, Ar), 3.70 (m, 8H, CHMe_2), 3.43 (t, 8H, NCH_2), 2.43 (s, 6H, ArMe), 2.42 (s, 6H, ArMe), 2.10 (m, 4H, NCH_2CH_2), 1.37 (d, 12H, CHMe_2), 1.27 (d, 6H, CHMe_2), 1.24 (d, 6H, CHMe_2), 0.81 (s, 6H, TiMe), 0.79 (s, 3H, TiMe), 0.79 (s, 3H, TiMe). $^{13}\text{C}\{^1\text{H}\}$ NMR δ 144.4, 143.8, 143.7, 132.8, 132.6, 129.1, 128.9, 125.2, 63.1, 62.8, 31.7, 31.5, 28.6, 28.4, 26.4, 26.3, 23.9, 23.9, 19.4, 19.2, 14.5, 14.3, 14.0.

(BAIP)Ti[CH₂B(C₆F₅)₂](C₆F₅), 2.54b. $\text{B}(\text{C}_6\text{F}_5)_3$ (76 mg, 0.15 mmol) in pentane (5 mL) was added dropwise at 23 °C to complex **2.11b** (70 mg, 0.15 mmol) dissolved in pentane (5 mL) to give a yellow–orange precipitate. After ca. 2 h the solution turned homogeneous. Stirring was continued for 16 h. The clear solution was passed through a plug of celite and concentrated to ~ 2 mL and cooled to -30 °C. **2.54b** (0.12 g, 0.12 mmol, 83 %) was obtained as an orange crystalline solid. ^1H NMR: δ 7.12 (m, 3H, Ar), 7.01 (m, 3H, Ar), 4.58 (m, 2H, NCH_2), 3.92 (br s, 2H, TiCH_2), 3.31 (sept, 2H, CHMe_2), 3.28 (sept, 2H, CHMe_2), 3.20 (m, 2H, NCH_2), 2.29 (m, 1H, NCH_2CH_2), 1.42 (m, 1H, NCH_2CH_2), 1.30 (d, 6H, CHMe_2), 1.04 (d, 6H, CHMe_2), 0.95 (d, 6H, CHMe_2), 0.78 (d, 6H, CHMe_2). $^{13}\text{C}\{^1\text{H}\}$ NMR δ 145.4, 144.0, 141.4, 129.4, 125.0, 109.5 (TiCH_2), 65.0, 33.4, 29.5, 28.2, 27.0, 26.2, 22.6, 22.4 (the carbon resonances for the perfluorophenyl groups appear as multiplets from 150–135 ppm). ^{19}F NMR δ -119.4 (d, 2F, F_o), -132.3 (d, 4F, F_o), -154.0 (t, 2F, F_p), -155.1

(t, 1F, F_p), -163.2 (m, 2F, F_m), -164.2 (m, 4F, F_m). ¹¹B{¹H} NMR δ 79.4. Anal. Calcd for C₃₈H₆₅ClN₂Ti: C, 58.20; H, 5.70; N, 2.51. Found: C, 58.11; H, 5.56; N, 2.51.

(BAIP)Ti[CH₂B(PMe₃)(C₆F₅)₂](C₆F₅), **2.61b** Complex **2.54b** (50 mg, 0.05 mmol) was dissolved in pentane (5 mL) in a heavy walled Schlenk. Excess PMe₃ was vacuum transferred onto the solution. The reaction was warmed to 23 °C and stirred overnight. The clear solution was passed through a plug of celite and evaporated to dryness. The resulting solid was recrystallized from pentane at -30°C (56 mg, 0.5 mmol, 100%). ¹H NMR: δ 7.12 (m, 3H, Ar), 7.01 (m, 3H, Ar), 4.10 (m, 2H, NCH₂), 3.90 (m, 2H, NCH₂), 3.35 (sept, 2H, CHMe₂), 3.35 (sept, 2H, CHMe₂), 2.75 (m, 1H, NCH₂CH₂), 2.50 (m, 1H, NCH₂CH₂), 2.05 (br s, 2H, TiCH₂), 1.28 (d, 6H, CHMe₂), 1.25 (d, 6H, CHMe₂), 1.05 (d, 6H, CHMe₂), 1.02 (d, 6H, CHMe₂), 0.90 (d, ³J_{PH} = 9 Hz, 9H, PMe₃). ¹³C{¹H} NMR δ 150.5, 144.5, 141.7, 127.4, 124.6, 124.3, 118.4, 62.4, 31.3, 28.9, 27.8, 27.5, 27.2, 23.9, 22.7, 10.5, 10.1 (the carbon resonances for the perfluorophenyl groups appear as multiplets from 150–135 ppm). ¹⁹F NMR δ -119.5 (d, 2F, F_o), -127.3 (d, 4F, F_o), -154.5 (t, 2F, F_p), -158.0 (t, 1F, F_p), -161.5 (m, 2F, F_m), -162.2 (m, 4F, F_m). ¹¹B{¹H} NMR δ -15.7 (d, ¹J_{PB} = 72.4 Hz). ³¹P{¹H} NMR δ 14.6 (s). Anal. Calcd for C₃₃H₅₃ClN₂Ti: C, 57.16; H, 4.38; N, 2.90. Found: C, 57.49; H, 4.81; N, 2.69.

References

- (1) Brintzinger, H. H.; Fischer, D.; Mülhaupt, R.; Rieger, B.; Waymouth, R. M. *Angew. Chem., Int. Ed. Engl.* **1995**, *34*, 1143.
- (2) Mu, Y.; Piers, W. E.; MacGillivray, L. R.; Zaworotko, M. K. *Polyhedron* **1995**, *14*, 1.
- (3) Hughes, A. K.; Meetsma, A.; Teuben, J. H. *Organometallics* **1993**, *12*, 1936.
- (4) Devore, D. D.; Timmers, F. J.; Hasha, D. L.; Rosen, R. K.; Marks, T. J.; Deck, P. A.; Stern, C. L. *Organometallics* **1995**, *14*, 3132.
- (5) Canich, J. A. In (Exxon) European Patent Application EP-420-436-A1: April 4, 1991.
- (6) Stevens, J. C.; Timmers, F. J.; Wilson, D. R.; Schmidt, G. F.; Nickias, P. N.; Rosen, R. K.; Knight, G. W.; Lai, S. Y. In (Dow) European Patent Application EP-416-815-A2: March 13, 1991.
- (7) Shapiro, P. J.; Bunel, E.; Schaefer, W. P.; Bercaw, J. E. *Organometallics* **1990**, *9*, 867.
- (8) Guérin, F.; McConville, D. H.; Vittal, J. J. *15* **1996**, 5586.
- (9) Guérin, F.; McConville, D. H.; Payne, N. C. *Organometallics* **1996**, *15*, 5085.
- (10) Clark, H. C. S.; Cloke, F. G. N.; Hitchcock, P. B.; Love, J. B.; Wainwright, A. P. *J. Organomet. Chem.* **1995**, *501*, 333.
- (11) Cloke, F. G. N.; Hitchcock, P. B.; Love, J. B.; Wainwright, A. P. *J. Chem. Soc. Dalton Trans.* **1995**, 25.
- (12) Cloke, F. G. N.; Geldbach, T. J.; Hitchcock, P. B.; Love, J. B. *J. Organomet. Chem.* **1996**, *506*, 343.
- (13) Warren, T. H.; Schrock, R. R.; Davis, W. M. *Organometallics* **1996**, *15*, 562.
- (14) Aoyagi, K.; Gantzel, P. K.; Kalai, K.; Tilley, T. D. *Organometallics* **1996**, *15*, 923.
- (15) Horton, A. D.; de With, J. *J. Chem. Soc. Chem. Comm.* **1996**, 1375.
- (16) Horton, A. D.; de With, J.; van der Linden, A. J.; van de Weg, H. *Organometallics* **1996**, *15*, 2672.
- (17) Tsuie, B.; Swenson, D. C.; Jordan, R. F. *Organometallics* **1997**, *16*, 1392.
- (18) (1992). "Cache™ system calculations", 1.0, CAChe™ Scientific Inc., Beaverton, Oregon.

- (19) Johnson, L. K.; Killian, C. M.; Brookhart, M. S. *J. Am. Chem. Soc.* **1995**, *117*, 6414.
- (20) Bradley, D. C.; Thomas, I. M. *J. Chem. Soc. Part A* **1960**, 3857.
- (21) Chandra, G.; Lappert, M. F. *J. Chem. Soc. Part A* **1968**, 1940.
- (22) Bradley, D. C.; Thomas, I. M. *Proc. Chem. Soc., London* **1959**, 225.
- (23) Bradley, D. C. *Adv. Inorg. Chem. Radiochem.* **1972**, *15*, 259.
- (24) Huheey, J. E. *Inorganic Chemistry: Principles of Structure and Reactivity*; Third ed.; Harper & Row Inc.: New York, 1983.
- (25) Haaland, A.; Rypdal, K.; Volden, H. V.; A, A. R. *J. Chem. Soc. Dalton Trans.* **1992**, 891.
- (26) Martin, A.; Mena, M.; Yelamos, C.; Serrano, R.; Raithby, P. R. *J. Organomet. Chem.* **1994**, *467*, 79.
- (27) Duan, Z.; Verkade, J. G. *Inorg. Chem.* **1995**, *34*, 4311.
- (28) Black, D. G.; Swenson, D. C.; Jordan, R. F.; Rogers, R. D. *Organometallics* **1995**, *14*, 3539.
- (29) Sartan, W. J.; Huffman, J. C.; Lundquist, E. G.; Streib, W. G.; Caulton, K. G. *J. Mol. Catal.* **1989**, *56*, 20.
- (30) Chisholm, M. H.; Hammond, C. E.; Huffman, J. C. *Polyhedron* **1988**, *7*, 2515.
- (31) Hagan, K.; Holwill, C. J.; Rice, D. A.; Runnacles, J. D. *Inorg. Chem.* **1988**, *27*, 2032.
- (32) Johnson, A. R.; Davis, W. M.; Cummins, C. C. *Organometallics* **1996**, *15*, 3825.
- (33) Clearfield, A.; Warner, D. K.; Saldarriaga-Molina, C. H.; Ropal, R.; Bernal, I. *Can. J. Chem.* **1975**, *53*, 1622.
- (34) Bürger, H.; Klüss, C. *J. Organomet. Chem.* **1976**, *108*, 69.
- (35) Jones, R. A.; Seeberger, M. H.; Atwood, J. L.; Hunter, W. E. *J. Organomet. Chem.* **1983**, *247*, 1.
- (36) Scoles, L.; Minhas, R.; Duchateau, R.; Jubb, Y.; Gambarotta, S. *Organometallics* **1994**, *13*, 4978.
- (37) Planalp, R. P.; Anderson, R. A.; Zalkin, A. *Organometallics* **1983**, *2*, 16.
- (38) Minhas, R. K.; Scoles, L.; Wong, S.; Gambarotta, S. *Organometallics* **1996**, *15*, 1113.
- (39) Smart, J. C.; Curtis, C. J. *Inorg. Chem.* **1977**, *16*, 1788.

- (40) Johnson, A. R.; Wanandi, P. W.; Cummins, C. C.; Davis, W. M. *Organometallics* **1994**, *13*, 2907.
- (41) Lappert, M. F.; Power, P. P.; Sanger, A. R.; Srivastava, R. C. *Metal and Metalloid Amides*; Ellis Horwood: Chichester, West Sussex, U.K., 1980.
- (42) Kah, D.; McConville, D. H. Unpublished Results.
- (43) March, J. *Comprehensive Organic Chemistry*; Springer Verlag: New York, 1991; Vol. 12.
- (44) tom Dieck, H.; Svoboda, M.; Greiser, T. Z. *Naturforsch. TeilB, Anorg., Org. Chem.* **1981**, *36*, 823.
- (45) tom Dieck, H.; Bruder, H.; Hellfeldt, K.; Liebfritz, D.; Feigel, M. *Angew. Chem., Int. Ed. Engl.* **1980**, *19*, 396.
- (46) Brookhart, M.; Johnson, L. K.; Killian, C. M. *J. Am. Chem. Soc.* **1995**, *117*, 6414.
- (47) tom Dieck, H.; Reiger, H. J.; Fendesak, G. *Inorganica Chimica Acta* **1990**, *177*, 191.
- (48) Brisson, B. J.; Walton, R. A. *Polyhedron* **1995**, *14*, 1259.
- (49) Latesky, S. L.; McMullen, A. K.; Niccolai, G. P.; Rothwell, I. P. *Organometallics* **1985**, *4*, 1896.
- (50) Chamberlain, L. R.; Durfee, L. D.; Fanwick, P. E.; Kobringer, L. M.; Latesky, S. L.; K, M. A.; Steffey, B. D.; Rothwell, I. P.; Folting, K.; Huffman, J. C. *J. Am. Chem. Soc.* **1987**, *109*, 6068.
- (51) Floriani, C.; Ciurli, S.; Chesi-Villa, A.; Guastini, C. *acii* **1987**, *26*, 70.
- (52) Massey, A. G.; Park, A. J. *J. Organomet. Chem.* **1964**, *2*, 245.
- (53) Yang, X.; Stern, C. L.; Marks, T. J. *J. Am. Chem. Soc.* **1994**, *116*, 10015.
- (54) Scollard, J. D.; McConville, D. H.; Vittal, J. J. *Macromolecules* **1996**, *29*, 5241.
- (55) Spence, R. E. v. H.; Parks, D. J.; Piers, W. E.; MacDonald, M.; Zaworotko, M. J.; Rettig, S. J. *Angew. Chem., Int. Ed. Engl.* **1995**, *34*, 1230.
- (56) Gómez, R.; Green, M. L. H.; Haggitt, J. L. *cc* **1994**, 2607.
- (57) Spence, R. E. v. H.; Piers, W. E. *Organometallics* **1995**, *14*, 4617.
- (58) Kidd, R. G. In *NMR of Newly Accessible Nuclei*; P. Laszlo, Ed.; Academic Press: New York, 1983; Vol. 2.
- (59) Schrock, R. R.; Sharp, P. R. *J. Am. Chem. Soc.* **1978**, *100*, 2389.

- (60) Kaminsky, W. In *Education in Advanced Chemistry*; B. Marciniec, Ed.; Poznan-Wroclaw: Poland, 1996; Vol. 2.
- (61) Groshens, T. J.; Higa, K. T.; Nisson, R.; Butcher, R. J.; Freyer, A. J. *Organometallics* **1993**, *12*, 2904.
- (62) Dragutan, V.; Balaban, A. T.; Dimonie, M. *Olefin Metathesis and Ring Opening Polymerization of Cyclo-Olefins*; 2nd ed.; Wiley-Interscience: New York, 1985.
- (63) Streck, R. J. *J. Mol. Cat. Chemical* **1988**, *4*, 305.
- (64) Tebbe, F. N.; Parshall, G. W.; Reddy, G. S. *J. Am. Chem. Soc.* **1978**, *100*, 3611.
- (65) Lee, J. B.; Ott, K. C.; Grubbs, R. H. *J. Am. Chem. Soc.* **1982**, *104*, 7491.
- (66) Gilliom, L. R.; Grubbs, R. H. *J. Am. Chem. Soc.* **1986**, *108*, 733.
- (67) Parks, D. J.; Spence, R. E. v. H.; Piers, W. E. *Angew. Chem., Int. Ed. Engl.* **1995**, *34*, 809.

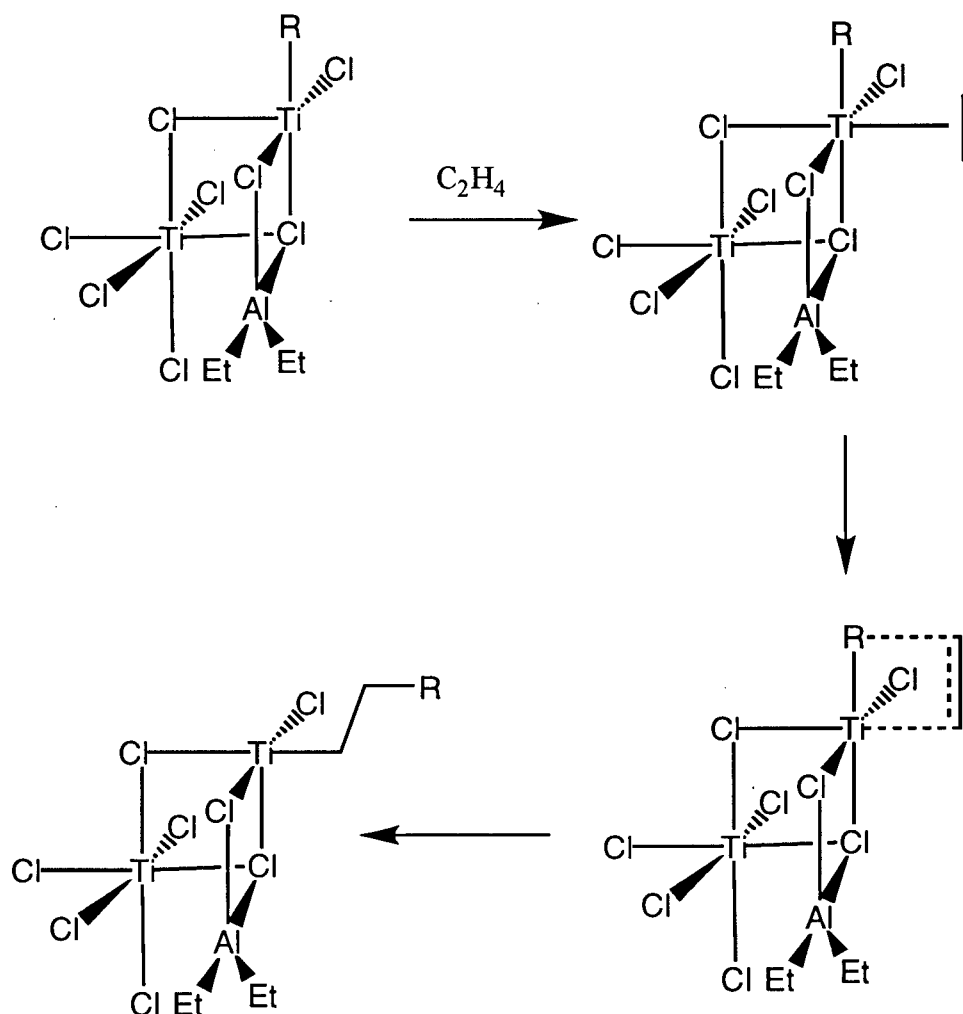
Chapter 3: Polymerization of α -olefins

Introduction

Forty years after Ziegler's discovery of transition metal catalyzed polyinsertion of ethylene and Natta's discovery of the stereoselective polymerization of α -olefins,¹⁻⁴ we are witnessing the evolution of new generations of catalysts. These polyolefin materials originate from studies on homogeneous, metallocene-based polymerization catalysts. Research on metallocene-catalyzed olefin polymerization has derived much of its impetus from the desire to model the reaction mechanisms of heterogeneous polymerization catalysts. Plausible hypotheses concerning these mechanisms have been proposed. Most notable is the Cossee-Arlman model of polymer chain growth by *cis*-insertion of α -olefins into a Ti-C bond on the surface of crystalline TiCl_3 .⁵⁻⁸ The relationship between the properties of a particular catalyst and the coordination geometry of its reaction centres leaves many questions unanswered. This is due to the non uniformity of active sites in these heterogeneous catalysts and the limited access to their structural details.

Cossee first proposed that the essential reaction occurs at a single titanium ion.⁵ The active centre is defined as a titanium ion in the surface layer of a TiCl_3 lattice of which one surface Cl-atom is replaced by an alkyl group R while an adjacent Cl-atom has been completely removed in order to accommodate the monomer molecule. This is a result of the reaction of solid TiCl_3 with aluminum alkyls. Scheme 3.1 shows an active site on the surface of $\alpha\text{-TiCl}_3$. The monomer first coordinates in the vacant site of the Ti-ion and proceeds to a four-centred transition state. The alkyl group then migrates to the olefin. The active site retains a Ti-alkyl bond and a vacancy which have changed places. The process may now repeat itself by insertion of the next monomer into the new Cl-vacancy. During the reaction the aluminum-alkyl may be important as a chain-transfer agent and further in termination reactions. It may also reestablish deactivated centres and act as a scavenger, but it is not essential for the propagation.

Scheme 3.1: Cossee–Arlman Mechanism



Chatt and Duncanson in 1953 proposed the π -type of bonding between transition metals and olefins.⁹ This hypothesis was later confirmed by X-ray crystal analysis for one of the more stable Pt-olefin complexes.¹⁰ It was plausible to suggest that a σ -bond between the titanium-ion and ethylene was formed prior to insertion. Such a bond is shown in Figure 3.1. The ethylene molecule must position itself perpendicular to the free valency of the titanium atom. This allows the π -electrons of the olefin to be used in the σ -bond formation with the $d_{x^2-y^2}$ orbital of the metal. This latter kind of interaction lowers the energy levels of the t_{2g} orbitals. This reduction in energy facilitates breaking of the σ -bonds of the system as a result of easy promotion of electrons from the bonding levels to the suppressed t_{2g} -orbital.¹¹

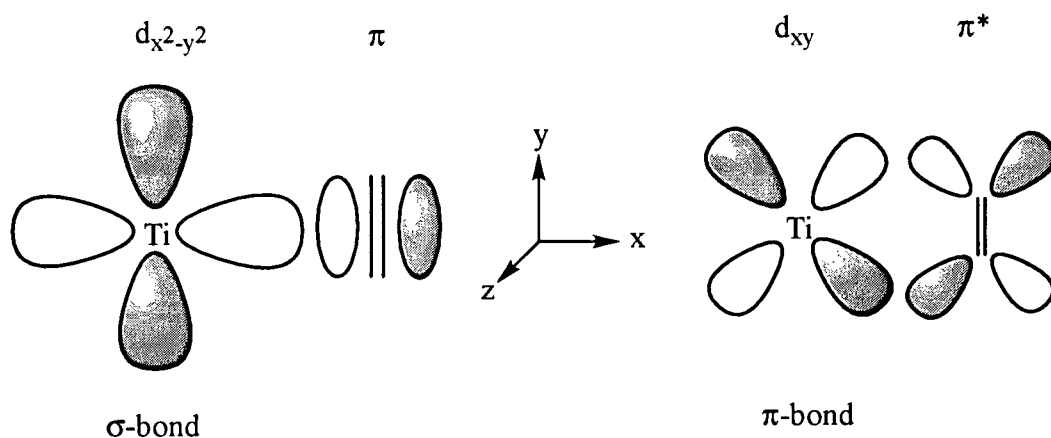


Figure 3.1: Titanium–ethylene bonding interactions

Therefore, the formation of the σ -bond between titanium and ethylene is accompanied by a weakening of the already very labile titanium–alkyl bond, thus facilitating the migration of the alkyl group. A π -bond between ethylene and titanium is possible for Ti(III) complexes. This bond is made up by donation of a d-electron from the d_{xy} orbital of the titanium atom into the π^* orbital of the ethylene (Figure 3.1).

Metallocene Catalysts

Initiation

Ziegler–Natta catalysts encompass a broad class of complexes resulting from the combination of a Group 3–8 transition metal compound with a metal–alkyl activator from Groups 1, 2 or 13. Modern day activators are usually based on either trialkylaluminum and chlorodialkylaluminum complexes, methylaluminoxane (MAO), borate complexes or (aryl)boranes. These co-catalysts are critical to the utility of the transition metal complex as a Ziegler–Natta polymerization catalyst.

Aluminum activators

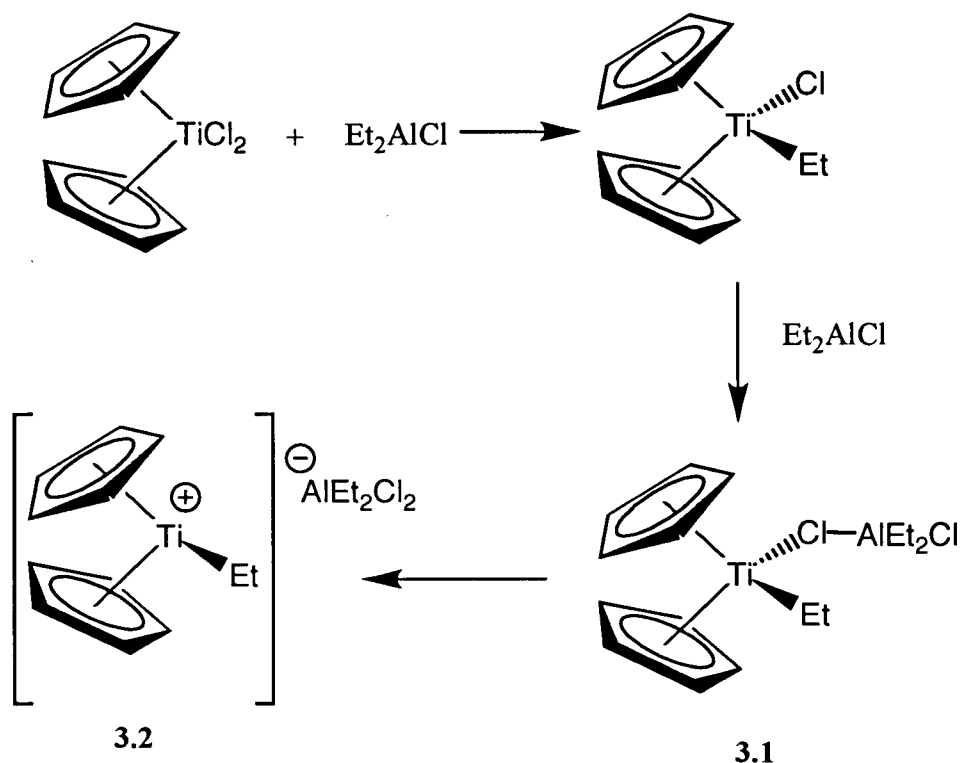
Aluminum–alkyl activated metallocene complexes of the Group 4 transition metals appeared particularly attractive as model systems for studying the Ziegler–Natta

polymerization catalysts. The simple coordination geometry of two mutually *cis*-positioned ligand sites showed great promise for identifying and characterizing essential intermediates of homogeneous polymerization catalysts. Studying these complexes should provide more direct experimental evidence for some of the hypotheses in the field of Ziegler–Natta catalysis.

By the late 1950s, Breslow¹² and Natta¹³ had reported that homogeneous reaction mixtures of Cp_2TiCl_2 and Et_2AlCl catalyze the formation of polyethylene under conditions similar to those used with Ziegler–Natta heterogeneous catalysts. The formation of the alkyl titanocene complex $\text{Cp}_2\text{Ti(R)Cl}$, by ligand exchange with the alkylaluminum cocatalyst, followed by polarization of the Ti–Cl bond by the Lewis acidic aluminum results in the formation of an adduct of the type $\text{Cp}_2\text{Ti(R)–Cl–AlEt}_2\text{Cl}$ (3.1) (Scheme 3.2). Insertion of the olefin into the $\text{Cp}_2\text{Ti–R}$ bond of this (or some closely related) electron deficient species then occurs.¹⁴⁻¹⁷ These early metallocene studies contributed to the ideas put forth by Cossee⁵⁻⁸ with regard to the mechanism of heterogeneous Ziegler–Natta catalysis.

An interesting question remained unresolved by this early research. Does olefin insertion occur via a bimetallic species (3.1), in which an alkyl group or halogen bridges the titanium and aluminum centres?¹⁸⁻²⁵ Or does it require the formation of a truly ionic species $[\text{Cp}_2\text{TiEt}]^+$ (3.2) by abstraction of a halide atom and its incorporation into an anion $[\text{R}_x\text{Cl}_4-x\text{Al}]^-$, as proposed by Shilov.²⁶

Scheme 3.2: Activation of titanocene dichloride by diethylaluminum chloride



This question remained unanswered until Jordan, in 1986, isolated and characterized the tetraphenylborate salts of cations such as $[\text{Cp}_2\text{Zr}(\text{CH}_3)(\text{THF})]^+$ and $[\text{Cp}_2\text{Zr}(\text{CH}_2\text{Ph})(\text{THF})]^+$. These compounds polymerize ethylene without the addition of any activator.²⁷⁻³⁷ These and later findings (Figure 3.2) in the groups of Bochmann³⁸⁻⁴³, Teuben^{44,45}, Taube,⁴⁶ Turner⁴⁷ and Marks⁴⁸⁻⁵¹ led to the general belief that (alkyl)metallocene cations are crucial intermediates in homogeneous polymerization catalysis. This may explain the inability of metallocenes activated by alkylaluminum halides to catalyze the polymerization of propene and higher olefins. The more weakly coordinating substituted α -olefins may be incapable of forming the olefin adduct by displacement of a more tightly coordinating aluminum anion. This limitation was a crucial obstacle to overcome. By the early 1980s, Sinn and Kaminsky discovered that metallocenes, when activated by methyl aluminoxane, were active polymerization catalysts for ethylene, propene and higher α -olefins.^{52,53}

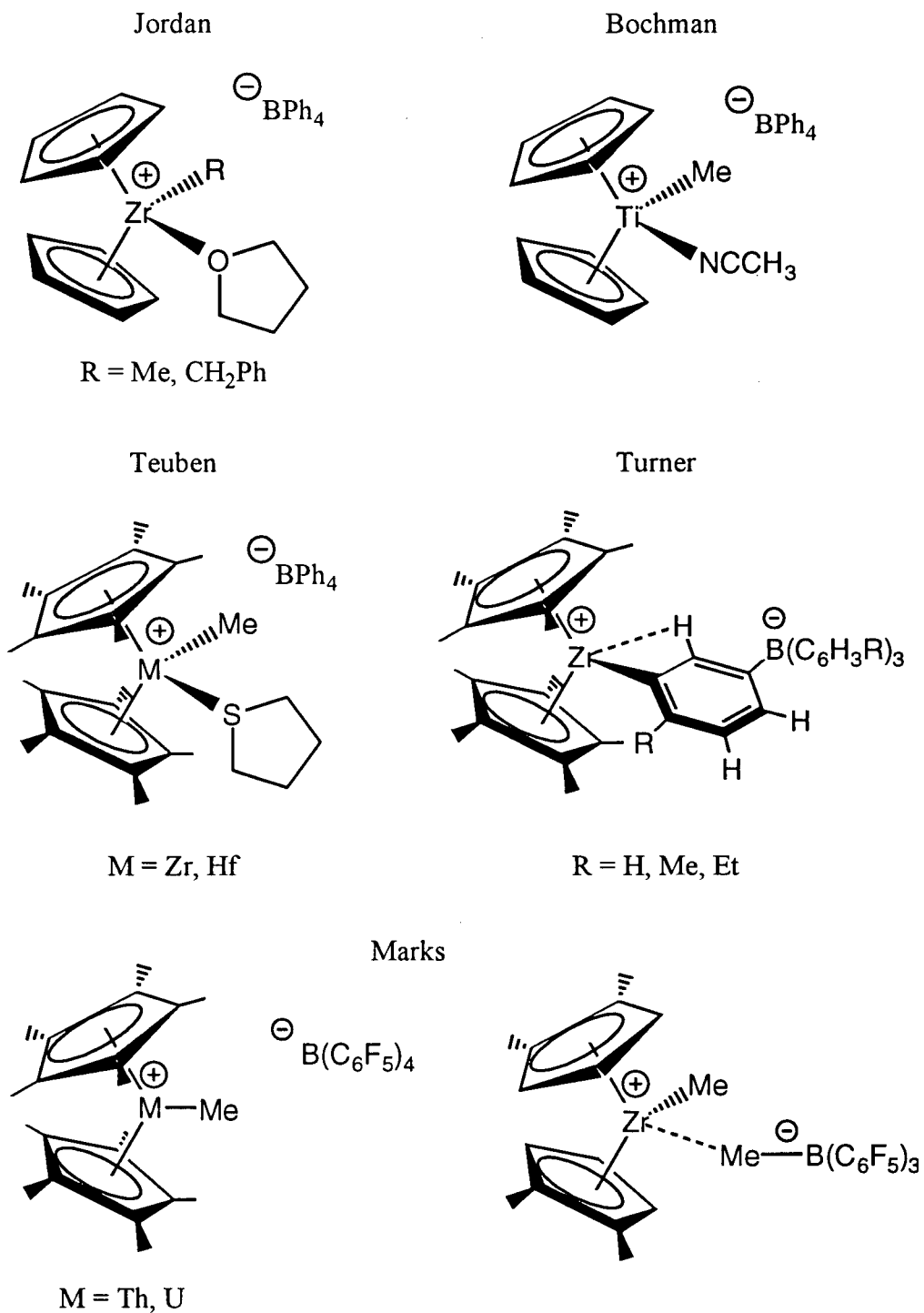


Figure 3.2: Characterized cationic alkyl complexes

Water, long considered to be detrimental to Ziegler–Natta catalysts, was first reported by Reichart to cause a surprising increase in the rate of ethylene polymerization by the catalyst system $\text{Cp}_2\text{TiEtCl}/\text{AlEtCl}_2$.⁵⁴ Subsequent studies by Breslow on the

effects of water in the otherwise inactive system $\text{Cp}_2\text{TiCl}_2/\text{Me}_2\text{AlCl}$ led to the notion that formation of an aluminoxane, by the partial hydrolysis of Me_2AlCl , might generate an exceptionally strong Lewis acid.⁵⁵ At about the same time as Breslow, Sinn and Kaminsky reported that the addition of water to the previously inactive $\text{Cp}_2\text{ZrMe}_2/\text{AlMe}_3$ system resulted in a surprisingly high activity for ethylene polymerization.^{52,53} They observed that an interaction between Cp_2ZrMe_2 and AlMe_3 occurred only when water was added. The suspected formation of methyl aluminoxane (MAO) by partial hydrolysis of AlMe_3 was subsequently supported by its direct synthesis and characterization as a mixture of oligomers of approximate composition $(\text{MeAlO})_n$. Activation of Cp_2ZrMe_2 and Cp_2ZrCl_2 with pre-formed MAO did indeed yield exceedingly active catalysts for the polymerization of ethylene. Furthermore, these MAO activated systems were capable of polymerizing propene and other higher order α -olefins, albeit to low molecular weight.⁵⁶

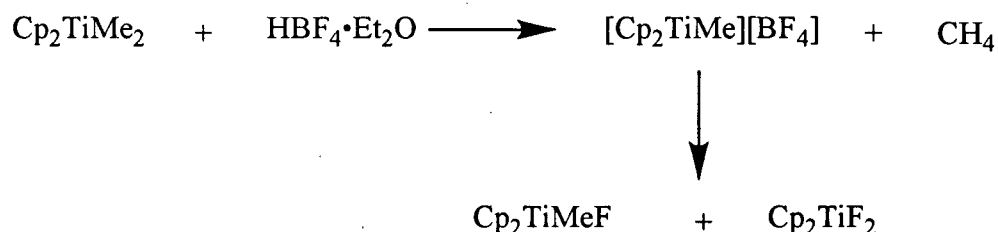
Carbon NMR spectroscopy studies by Marks of the $\text{Cp}_2\text{ZrMe}_2/\text{MAO}$ system indicate the formation of a cation $[\text{Cp}_2\text{ZrMe}]^+$, which is most likely stabilized by a weakly coordinating $[\text{CH}_3\text{-MAO}]^-$ counterion.⁵⁷ The ability of MAO to effectively abstract a CH_3^- ion from Cp_2ZrMe_2 and to sequester it in a very weakly coordinating ion is still not clearly understood. The weakly coordinating anion is easily displaced by olefins, to give the ion pair $[\text{Cp}_2\text{ZrMe}(\text{olefin})]^+[\text{CH}_3\text{-MAO}]^-$, the presumed prerequisite for olefin insertion into the Zr-R bond. This is a proven advantage over the dialkylaluminum halide cocatalysts used earlier which could not be displaced by the weaker coordinating substituted olefins. The idea that the unusually low coordinating capability of the anion A^- in the ion pair $[\text{Cp}_2\text{ZrR}]^+\text{A}^-$ is crucial for catalytic activity led to the discovery of a series of highly active cationic metallocene catalysts for the polymerization of propene and higher α -olefins.⁵⁷

Borane activators

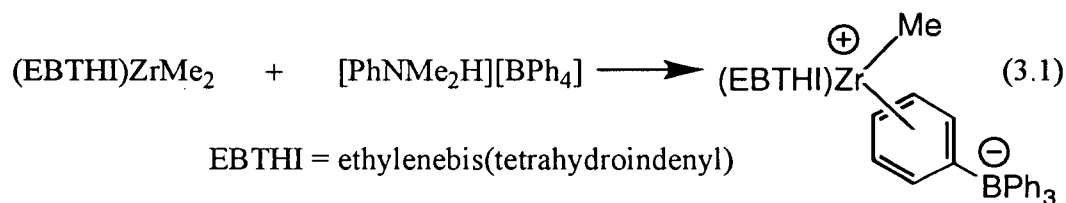
Even for large, weakly coordinating anions such as tetrafluoroborate, tetraphenylborate and the carborane, $\text{C}_2\text{B}_9\text{H}_{12}^-$, fairly strong interactions have been observed

with cationic (alkyl)zirconocene species. For example tetrafluoroborate salts of Cp_2TiMe^+ decompose upon standing to Cp_2TiMeF and Cp_2TiF_2 (Scheme 3.3).³⁸

Scheme 3.3: Activation with tetrafluoroborate salts

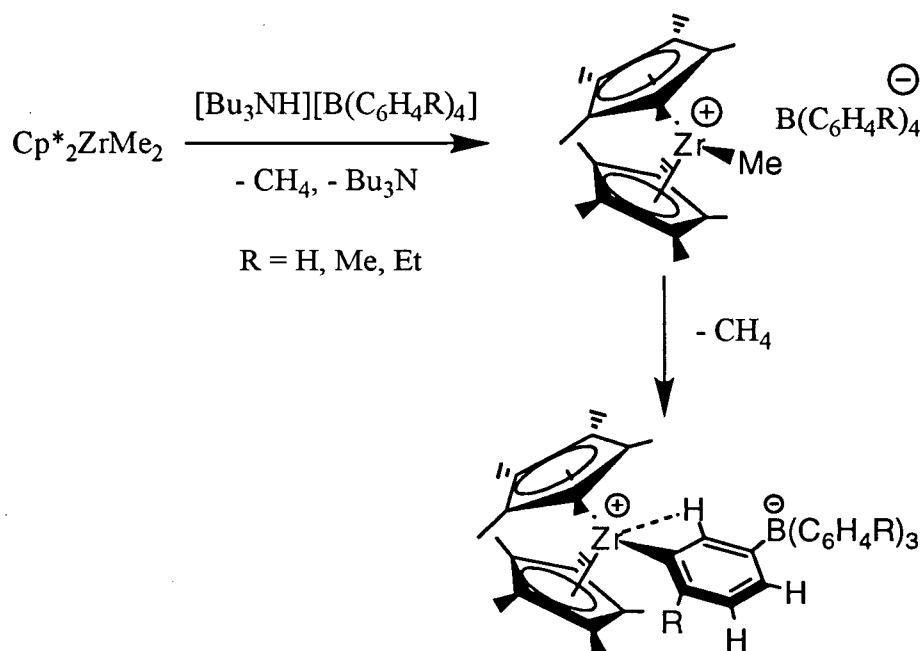


Horton has reported that tetraphenyl borate salts of ethylenebis(tetrahydroindenyl)zirconium cations will coordinate a phenyl group from the counterion to give an η^6 -phenylborate zirconium complex (eq. 3.1).⁵⁸ Hlatky has reported

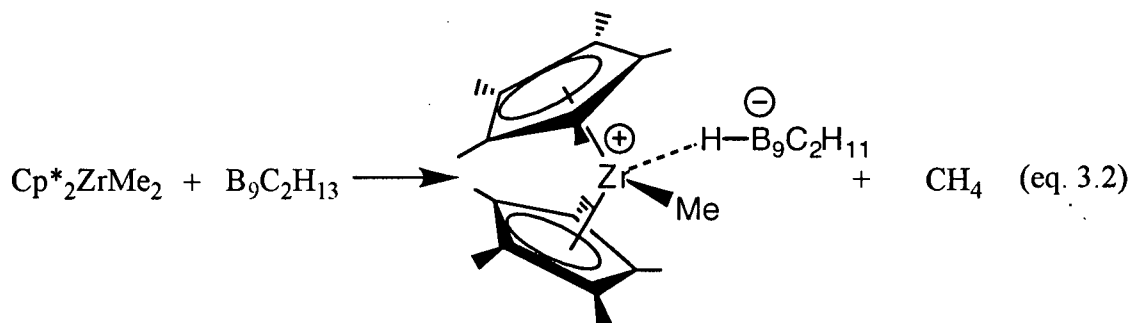


the C–H activation of a tetraphenyl–borate anion by $[\text{Cp}^*_2\text{ZrMe}]^+$ (Scheme 3.4).⁴⁷

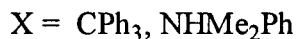
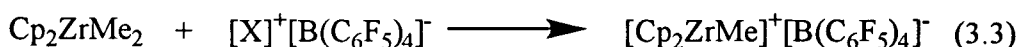
Scheme 3.4: C–H activation of a tetraphenylborate anion



A relatively short Zr–H bond, 2.12(4) Å, has been observed in the carborane activated $\text{Cp}^*_2\text{ZrMe}_2$ (eq. 3.2).⁵⁹ As a result, these systems polymerize propene only at very low rates.^{32,34,38-43,45-47}



The major breakthrough in this regard was the introduction of perfluorinated tetraphenylborate as a counterion by Turner⁶⁰ and independently by Marks.⁴⁸ An ion pair $[\text{Cp}_2\text{ZrMe}]^+ [\text{B}(\text{C}_6\text{F}_5)_4]^-$ is formed by the protonation or abstraction of CH_3^- from Cp_2ZrMe_2 with dimethylanilinium tetrakis(pentafluorophenyl)borate or trityl tetrakis(pentafluorophenyl)borate, respectively (eq. 3.3).⁶¹ The $\text{B}(\text{C}_6\text{F}_5)_4^-$ anion offers

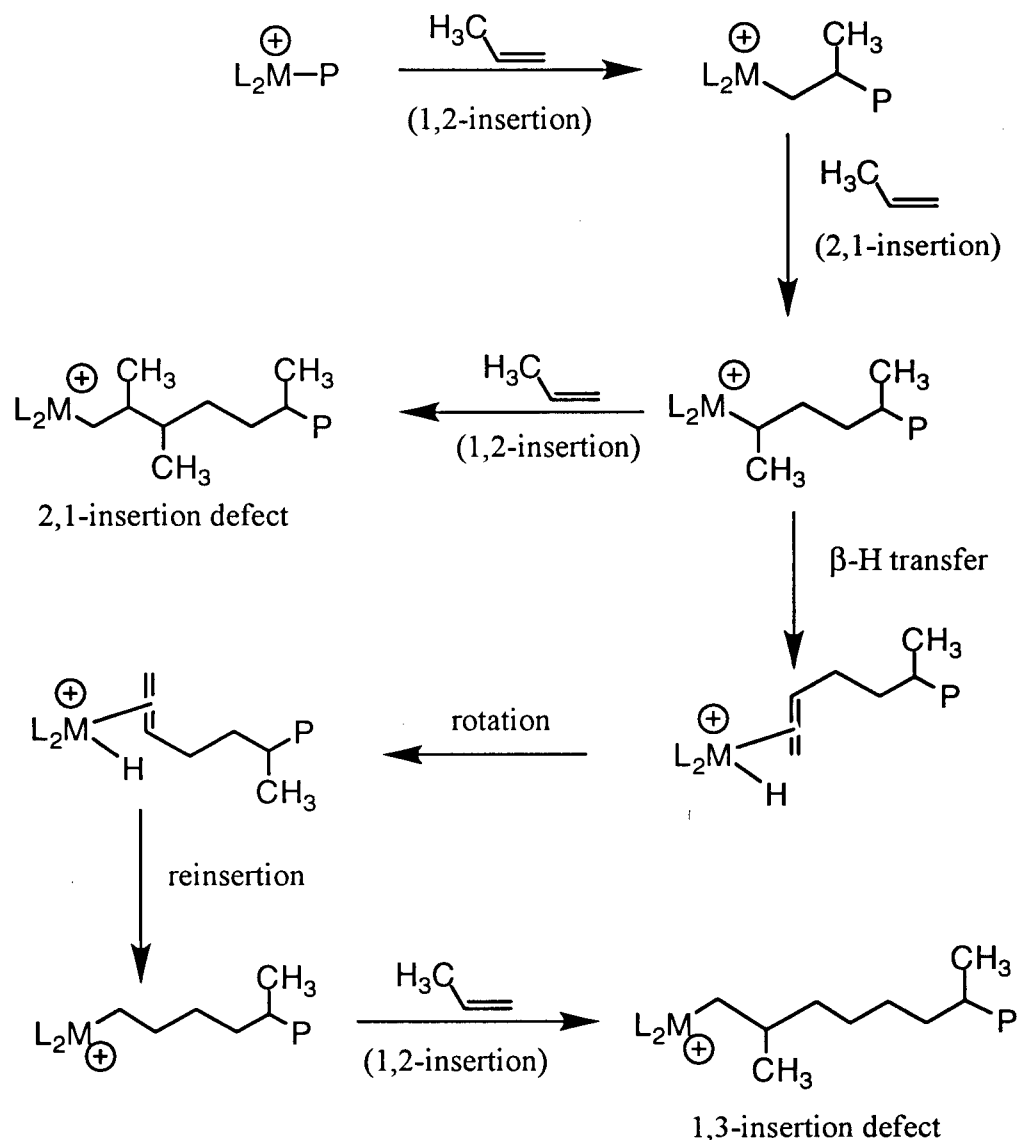


an advantage over the BF_4^- and BPh_4^- anions. The phenyl rings in the perfluorinated complex are less nucleophilic thus preventing the zirconium cation from coordinating the π -electrons of the pentafluorophenyl group. The perfluoro aryl group is also less susceptible to aryl migration than the C_6H_5^- moiety due to its added bulk. Furthermore, C–F activation of the perfluoro aryl group is not possible as the C–F bonds are much stronger than the corresponding C–H bonds. These complexes represent the first well-defined zirconocene catalysts capable of polymerizing ethylene, propene and higher α -olefins at high rates without the addition of a further activator. An equally powerful Lewis acid, $\text{B}(\text{C}_6\text{F}_5)_3$ was likewise found to be an effective alkyl abstraction agent. Cationic (alkyl)metallocenes obtained by abstraction of CH_3^- from a dimethylzirconocene complex by $\text{B}(\text{C}_6\text{F}_5)_3$ were also found to be highly active olefin polymerization catalysts.^{49,51,62}

Propagation

α -Olefin insertion in metallocene-based homogeneous catalysts, as in heterogeneous Ziegler–Natta systems,^{63–67} generally occurs with a 1,2-regioselectivity so as to generate primary M-alkyl units. However, poly(α -olefins) produced with metallocene-based catalysts often contain varying fractions of regioinverted units.^{68–73} Depending on the polymerization temperature and the catalyst used, one finds either head to head concatenations resulting from primary insertion (1,2-insertion) into regioinverted secondary M-alkyl unit (2,1-insertion defect), or tetramethylene units (1,3-insertion defect, Scheme 3.5). The latter arise from an isomerization of a secondary M-alkyl unit to one with a primary M-alkyl bond prior to primary insertion of the next olefin.^{68,69,71–73} This isomerization is a result of β -hydrogen elimination, rotation of the olefin, and reinsertion into the M–H bond.

Scheme 3.5: Possible modes of insertion for propene



Different catalysts produce the regioirregularities in different ratios. In general, catalysts with large propagation rates, k_p , undergo misinsertion in a 2,1 fashion while catalysts with lower k_p 's produce mainly 1,3-misinsertions.^{74,75} This trend arises because a secondary M-alkyl unit typically inserts an α -olefin faster than it rearranges to a primary terminal M-alkyl unit. The irregularities introduced into a polypropylene chain by 2,1- or 1,3-misinsertions decrease its melting point considerably and therefore these defects are of practical concern.

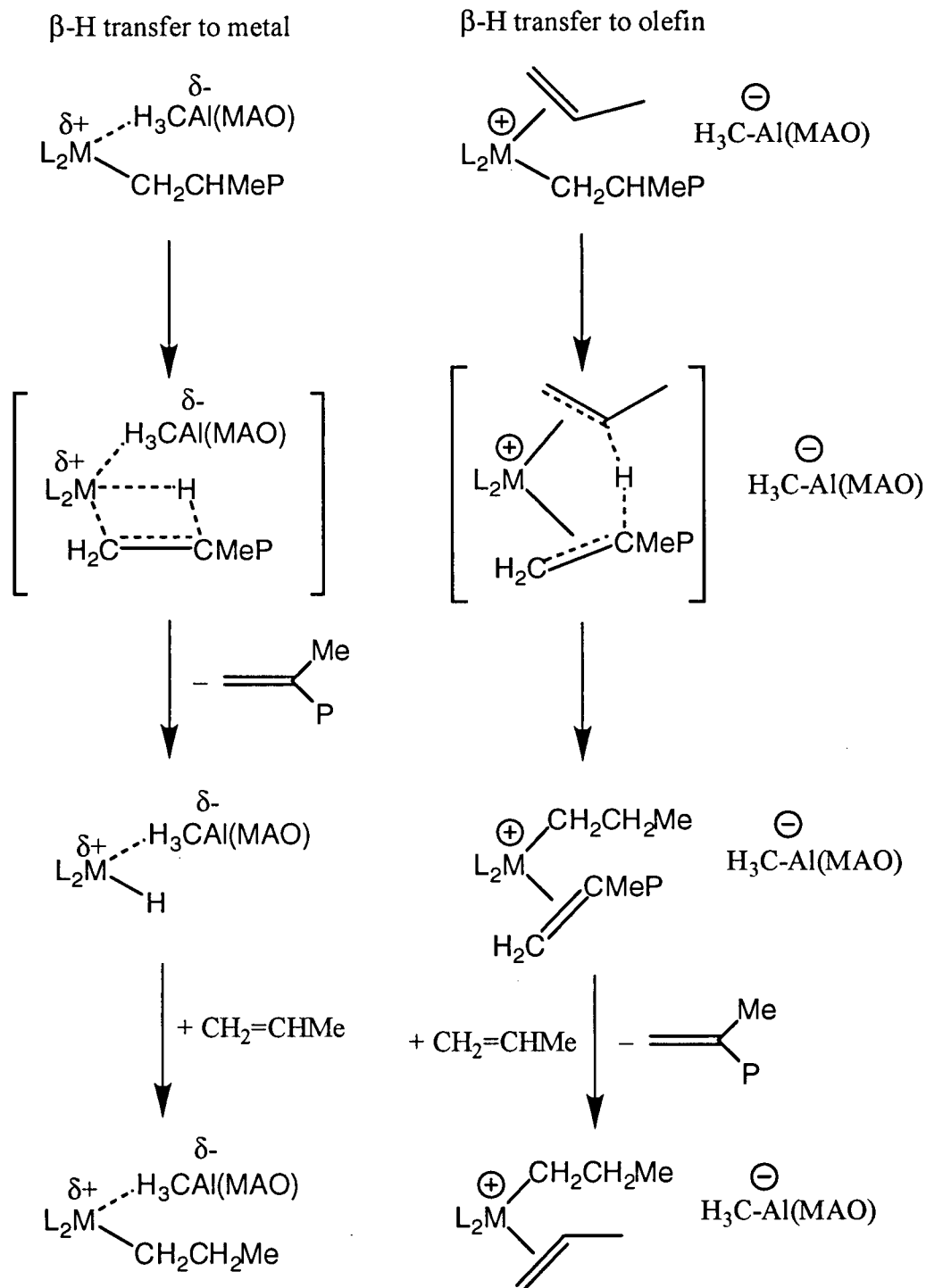
Termination

An important aspect in which homogeneous olefin polymerization by metallocene catalysts differs from heterogeneous Ziegler–Natta catalysis is the narrow molecular weight distribution of the polymers. While polyolefins produced with heterogeneous catalysts have broad molecular weight distributions or polydispersities of $M_w/M_n \approx 5-10$,^{76,77} homogeneous catalysts produce polymers with polydispersities of close to 2.⁷⁸ A polydispersity of 2 is predicted by Schulz–Flory statistics for polymers arising from identical catalyst centres with fixed rates of chain propagation and chain termination, k_p and k_t .⁷⁹ A polydispersity of 2 is therefore regarded as evidence that only a single catalyst species contributes to polymer growth in a homogeneous catalyst system.

β -hydride elimination

Polymerization of ethylene by MAO-activated Cp_2Zr -based catalysts gives rise to polymers with high molecular weights in the range of 100,000 to 1,000,000.^{53,78,80} However, propene polymers obtained under the same conditions with these catalysts have a rather low degree of polymerization, with molecular weights in the range of 200 – 1000.^{81,82} The relative low molecular weights of the polymer products must be either due to an increased rate of chain termination or to a decreased rate of olefin insertion (or both), since the average degree of polymerization P_N is determined by the ratio of the rates of chain propagation and chain termination, $P_N \approx k_p/k_t$.⁷⁹ End-group analysis of low molecular weight poly(α -olefins) from metallocene catalysts has shown that chain termination occurs mostly via β -hydrogen transfer.⁸³⁻⁸⁵ This termination route can be both unimolecular (β -hydrogen transfer to metal) and bimolecular (β -hydrogen transfer to the monomer).⁸³ The vinylidene end groups likely arise from transfer of a β -hydrogen atom from the polymer chain to the metal centre (Scheme 3.6). The M–H unit generated

Scheme 3.6: Chain termination by β -hydrogen transfer



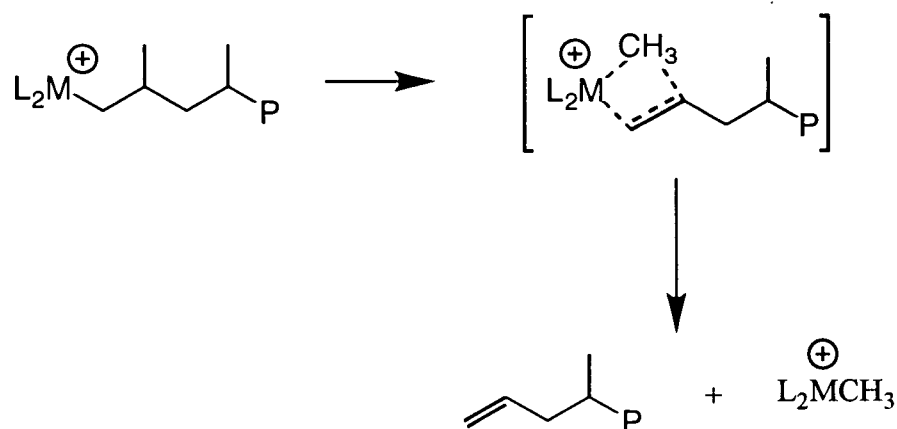
by this process can then react with propene to form an M-*n*-propyl unit, from which a new polymer chain can start to grow. Another conceivable chain termination mechanism is the

transfer of a β -hydrogen atom from the M-bound polymer chain to the β -carbon atom of a coordinated α -olefin molecule.⁸³ In this case the vinylidene terminated polymer chain and a new M-*n*-propyl unit are generated without the intermediacy of a M-H species (Scheme 3.6). The relative rates of the two transfer reactions are a function of monomer concentration.⁸⁶⁻⁸⁸

β -alkyl elimination

Although chain termination normally occurs via facile β -hydrogen elimination, β -methyl transfer has also been observed with metallocene catalysts.^{44,45,50,51,85,89-93} Transfer of the β -methyl group after a primary insertion results in the formation of an allyl end-group (Scheme 3.7). Although β -methyl elimination is uncommon for less sterically encumbered metallocenes (e.g. $[\text{Cp}_2\text{ZrR}]^+$), it is the most important mechanism in propene polymerizations when larger substituted metallocenes (e.g. Cp^*_2M , M = Zr, Hf) are used as catalyst precursors.^{85,89,94,95}

Scheme 3.7: Chain termination by β -methyl transfer

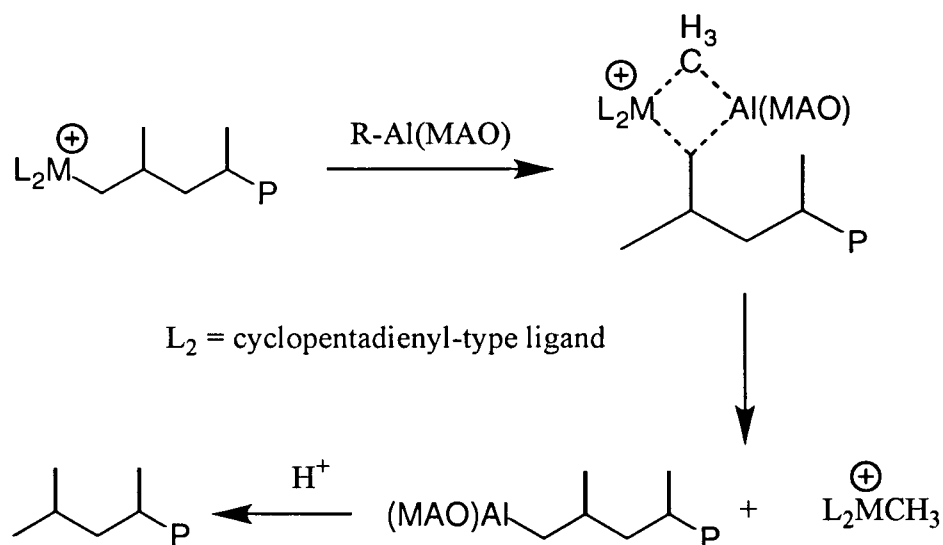


Chain transfer to cocatalyst

Chain transfer to aluminum has also been detected as a chain termination mechanism.⁹⁶⁻⁹⁹ The termination reaction likely proceeds via a four-centred transition state whereby an alkyl group from aluminum is exchanged with the polymer chain (Scheme 3.8).

Protonolysis of the aluminum–polymer chain bond occurs in the subsequent workup of the polymerization to yield a saturated end–group.⁹⁹ The absence of olefinic resonances in the ^1H and $^{13}\text{C}\{^1\text{H}\}$ NMR spectra of poly(α -olefins) are a general indication that chain transfer to cocatalyst is the primary mode of termination. It is important to remember that the presence of olefinic resonances in the ^1H and $^{13}\text{C}\{^1\text{H}\}$ NMR spectra does not exclude chain transfer to aluminum. In fact, several termination reactions may be occurring simultaneously.

Scheme 3.8: Chain termination by transfer to co-catalyst

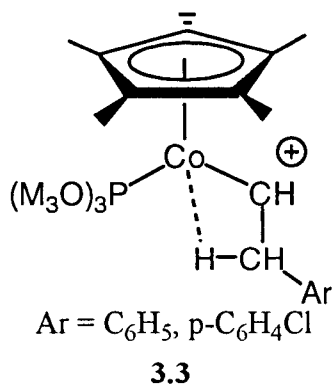


Living Polymerizations

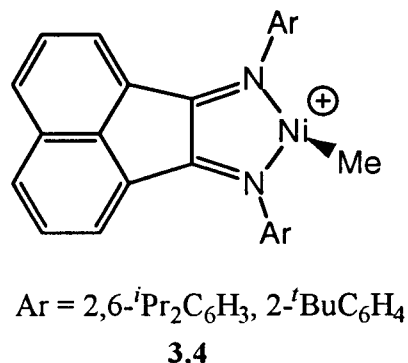
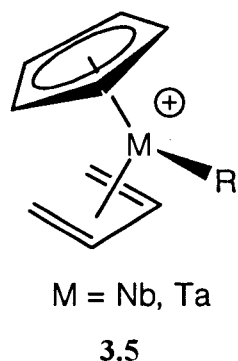
Living polymerizations are polyinsertions in which the propagating centres do not undergo either termination or transfer. An ideal living polymerization may take place only if three unusual restrictions can be achieved in the polymerization system. These three criteria are: (1) the initiation of the catalyst precursor must occur at a rate greater than or equal to the rate of propagation (i.e. $k_i \geq k_p$); (2) there can be no route to a termination step (i.e. $k_t = 0$); and (3) deactivation of the propagating centre does not take place in the absence of monomer.¹⁰⁰ A narrow polydispersity is sometimes indicative of a living polymerization system. A polydispersity of $M_w/M_n \approx 1$ is achieved if the first two criteria are met. The

anionic polymerization of styrene by amide ion in liquid ammonia was the first reported living polymerization.¹⁰¹ Living polymerizations are also observed for ring-opening metathesis polymerizations,¹⁰²⁻¹⁰⁵ cationic polymerizations¹⁰⁶⁻¹⁰⁸ and group-transfer polymerizations.¹⁰⁹⁻¹¹¹ The third criterion is often more difficult to meet with Ziegler-Natta type catalysts.

The term "living polymers" was first applied to the polymerization of α -olefins with Ziegler-Natta catalysts by Bier in 1964.¹¹² Bier found that the polymerization of propene by the $\text{TiCl}_3/\text{Et}_2\text{AlCl}$ system can be interrupted for several hours after removal or consumption of monomer without diminishing the activity of the catalyst on renewed addition of monomer. The first example of a living homogeneous polymerization of an α -olefin was reported by Doi. He found that a soluble catalyst consisting of $\text{V}(\text{acac})_3$ (acac = acetylacetonate) and Et_2AlCl initiates the living coordination polymerization of propene at low temperatures.^{113,114} Doi, however, has been unable to characterize his catalyst and therefore the exact nature of the propagating species is speculative. Brookhart has reported the living polymerization of ethylene with a Co(III) -based catalyst (3.3).^{115,116} Brookhart has also reported the living polymerization of α -olefins with Ni(II) α -diimine catalysts (3.4).¹¹⁷ Mashima has polymerized ethylene in a living manner using Nb(III) - and Ta(III) -based catalysts (3.5).¹¹⁸ Schrock has also reported the living polymerization of 1-hexene with a chelating diamide of zirconium (3.6), albeit at low temperature.¹¹⁹ Clearly there are very few systems which are amenable to a living coordination polymerization of α -olefins. The intermediates in coordination polymerization reactions tend to decompose over time due to their highly reactive nature. Living systems are known (Figure 3.3), however, they all operate at temperatures below 0°C.



Mashima



Schrock

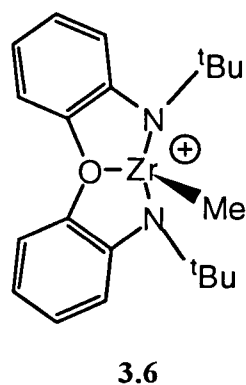


Figure 3.3: Living homogeneous Ziegler–Natta polymerization catalysts

*Characterization of Polymers*¹²⁰

One of the most important properties of a polymer is its molecular weight. The interesting and useful mechanical properties that are uniquely associated with polymeric materials are a consequence of their high molecular weight. Therefore, when analyzing polymers, one of the primary concerns is to determine the molecular weight. The molecular weight of a polymer is something quite different from that which applies to small molecules. Polymers differ from small molecules in that they are polydisperse or heterogeneous in molecular weight. Polymers are actually mixtures of molecules of different molecular weights. The reason for the polydispersity of polymers lies in the statistical variations present in the polymerization process. When the molecular weight of a polymer is discussed,

it is actually referring to the polymers average molecular weight. The control of molecular weight and polydispersity are often used to obtain and improve certain desired physical properties within a polymer product.

Various methods have been used to determine the average molecular weight of polymers. These include methods based on colligative properties, light scattering, and viscosity.¹⁰⁰ These methods tend to be laborious and hence determinations of molecular weights were not routinely performed. However, the development of size exclusion chromatography (SEC), also referred to as gel permeation chromatography (GPC) and the availability of automated commercial instruments have changed the situation. Molecular weight determinations are now routinely performed in most laboratories using GPC.

Gel permeation chromatography¹²¹ involves the permeation of a polymer solution through a column typically packed with microporous beads of crosslinked polystyrene. The packing contains beads of different sized pore diameters. Molecules pass through the column by a combination of transport into and through the beads and through the interstitial volume (the volume between the beads). Smaller molecules which pass through the beads will be slowed down more in moving through the column than larger molecules that move through the interstitial volume. Therefore, the time for passage of polymer molecules through the column decreases with increasing molecular weight. A detector measures the amount of polymer passing through the column as a function of time. This information and a calibration of the column with standard polymer samples of known molecular weight allows the user to obtain the molecular weight distribution and hence calculate the average molecular weight.

The number-average molecular weight M_n is defined as the sum of the mole-fraction of molecules with a particular molecular weight. The weight-average molecular weight M_w is the sum of the weight-fraction of molecules with a particular molecular weight. M_n is biased towards the lower-molecular-weight fractions while M_w is biased towards the higher-molecular-weight fractions. Therefore M_w is greater than M_n in a polydisperse

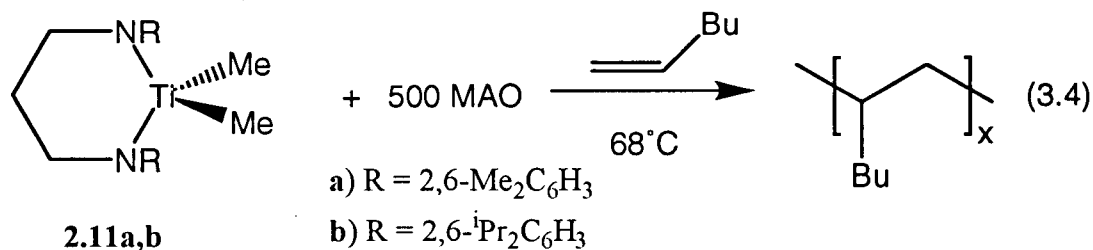
polymer. The ratio of the two average molecular weights M_w/M_n is known as the polydispersity. All the polymers produced in this chapter have their average molecular weights and polydispersities determined by GPC versus polystyrene standards.

Another useful tool for characterizing polymer samples is NMR spectroscopy. Proton and $^{13}\text{C}\{^1\text{H}\}$ NMR spectroscopy can be used to determine a number of useful properties of polymers. The tacticity of poly(α -olefins) can be determined by ^1H and $^{13}\text{C}\{^1\text{H}\}$ NMR spectroscopy.¹²² Proton NMR spectroscopy has also been useful for determining the modes of addition of monomer.¹²³ Proton and $^{13}\text{C}\{^1\text{H}\}$ NMR spectroscopy are used throughout this chapter to characterize the polymer samples and determine tacticity, modes of addition, and modes of termination.

Results and Discussion

Propylene Linked Diamides of Titanium

The titanium diamide complexes (2.10a,b, 2.11a,b) described in chapter 2 are active catalyst precursors for the polymerization of 1-hexene (eq. 3.4). A summary of the



polymerization results is shown in Table 3.1. These catalyst systems generate high molecular weight polymers with narrow molecular weight distributions. The absence of olefinic resonances in the ^1H and $^{13}\text{C}\{^1\text{H}\}$ NMR spectra of the polymers prepared with these catalyst systems indicates that the rate of β -hydrogen elimination is very slow compared to the rate of chain transfer to aluminum. Therefore chain transfer to aluminum appears to be the main source of termination for these catalysts.

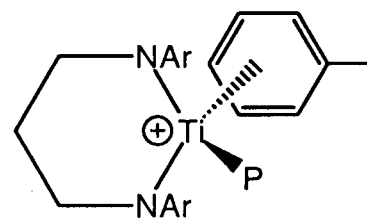
Table 3.1: Polymerization of 1-Hexene^a

entry	catalyst system	yield (g)	time (s)	M_w^b	M_n^b	M_w/M_n	activity ^c
1	2.11b/MAO, 68°C	2.96	30	81500	47000	1.73	350000
2	2.11a/MAO, 68°C	2.42	30	54000	30400	1.78	290000
3	2.11b/MMAO, 68°C	0.25	60	28200	17800	1.58	15000
4	2.11a/MMAO, 68°C	0.73	60	23500	13400	1.75	44000
5	2.11b/B(C ₆ F ₅) ₃ , 22°C ^d	0.18	300	29600	16100	1.84	2000
6	2.11a/B(C ₆ F ₅) ₃ , 22°C ^d	0.22	300	26200	14500	1.81	2000
7	2.11b/MAO, 68°C ^e	0.76	30	32700	18600	1.76	91000
8	2.11a/MAO, 68°C ^e	0.56	30	29900	16500	1.81	67000
9	2.10b/MAO, 68°C ^e	0.96	30	55600	31000	1.79	115000
10	2.10a/MAO, 68°C ^e	0.73	30	33800	19200	1.76	88000
11	2.11/MAO, 68°C ^{f,g}	1.50	10	9100	5100	1.78	51000
12	2.11b/MAO, 68°C ^{f,h}	3.68	10	27600	15700	1.76	125000

^a 1 μ mol of catalyst in 0.5 mL of pentane was mixed with 250 equiv of solid cocatalyst and added to 5.0 g of 1-hexene (250 equiv of cocatalyst as scavenger), unless otherwise stated. ^b By GPC vs. polystyrene standards. ^c g poly(1-hexene)/mmol catalyst \cdot h. ^d 1 equiv of B(C₆F₅)₃ (preactivated) and 500 equiv of MAO as scavenger in the reactor. ^e 1 μ mol of catalyst in 0.5 mL of toluene. ^f 10.6 μ mol of catalyst was mixed with 500 equiv of MAO in 5.0 mL of solvent and added to 5.0 mL of 1-hexene. ^g solvent = toluene. ^h solvent = hexane.

Activities as high as 350,000 g poly(1-hexene)/mmol catalyst•h were obtained for catalyst **2.11b**/MAO in neat 1-hexene at 68 °C. For comparison, the bis(amide) system $[(\text{Me}_3\text{Si})_2\text{N}]_2\text{ZrCl}_2/\text{MAO}$ polymerizes propene with an activity of 62 g polypropylene/mmol catalyst•h under similar conditions.¹²⁴ The chelating bis(amide) system $[(\text{Me}_3\text{SiNCH}_2)_2]\text{TiCl}_2/\text{MAO}$ polymerizes ethylene with an activity of 9.8 g polyethylene/mmol catalyst•h under much lower monomer concentrations.¹²⁵

Lower initial activities are observed for **2.11b**/MAO at room temperature until sufficient heat is released at the onset of polymerization. This apparent activation barrier may reflect the relative difficulty in generating a putative 10-electron cationic alkyl complex in a nonpolar medium.²⁸ An increase in the rate of polymerization would be expected upon addition of toluene.¹²⁶⁻¹²⁸ Toluene is more polar than 1-hexene and its use as a solvent should result in an increase in charge separation between the cation and anion. A direct relationship has been determined between the charge separation of the cation and anion and rate of polymerization.¹²⁶⁻¹²⁸ Interestingly, the activity of **2.11b**/MAO decreases by a factor of nearly 4 when the polymerizations are performed in the presence of small amounts of toluene (350000 vs 91000 g poly(1-hexene)/mmol cat•hr). A similar decrease in activity is observed for **2.11a**/MAO when toluene is present (290000 vs. 67000 g poly(1-hexene)/mmol cat•hr). It was not clear, however, whether this decrease was a result of lower monomer concentrations, since rates typically decrease with decreasing monomer concentration. Hence, the polymerization of 1-hexene with **2.11b**/MAO in toluene:1-hexene (1:1) and hexanes:1-hexene (1:1) was attempted (entries 11 and 12). The polymerization activity decreases by a factor of 2.5 (125000 vs. 51000 g poly(1-hexene)/mmol cat•hr) and the molecular weight of the polymer decreases by a factor of 3 (15700 vs. 5100) when toluene is present. However, the change in solvent has very little affect on the rate of chain transfer to aluminum (M_w/M_n , 1.78 versus 1.76). Assuming a cationic alkyl as the active species in these



3.7

systems,²⁸ these results can be interpreted as competitive binding of toluene to titanium (3.7) which decreases the rate of insertion of 1-hexene.

The preparation of the η^5 -cyclopentadienyl derivatives, $[\text{ArN}(\text{CH}_2)_3\text{NAr}]\text{Ti}(\eta^5\text{-C}_5\text{H}_5)\text{Cl}$ (2.14a,b), suggests that the metal can accommodate η^n -coordinated ligands of this size. Given the low coordination number of these diamide complexes and recent reports of authentic η^6 -aryl complexes of group 4 metals (Figure 3.4),¹²⁹⁻¹³² the binding of toluene is plausible.

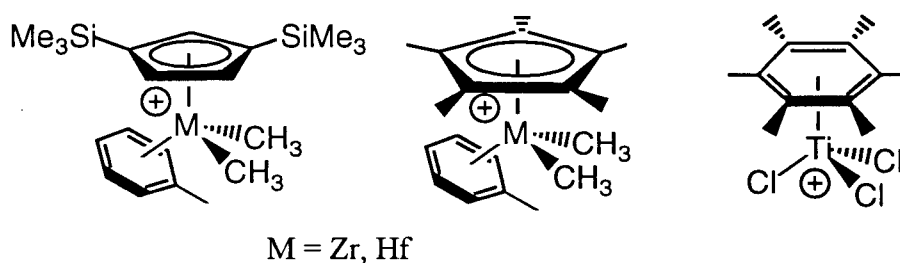


Figure 3.4: Authentic η^6 -aryl complexes of group 4 metals

Figures 3.5 and 3.6 show the ^1H and $^{13}\text{C}\{^1\text{H}\}$ NMR spectra of poly(1-hexene) from entry 1 of Table 3.1, respectively. The region in the $^{13}\text{C}\{^1\text{H}\}$ NMR spectrum of poly(1-hexene), from which the tacticity of the polymer can be derived, occurs in the range of 34 – 35 ppm. Samples of poly(1-hexene) can be analyzed at the pentad level. Isotactic poly(1-hexene) exhibits a signal for the tertiary carbon at 34.70 ppm,¹³³⁻¹³⁶ corresponding to a mmmm-pentad (Figure 3.7).¹³³⁻¹³⁶ The secondary carbon resonance in the $^{13}\text{C}\{^1\text{H}\}$ NMR

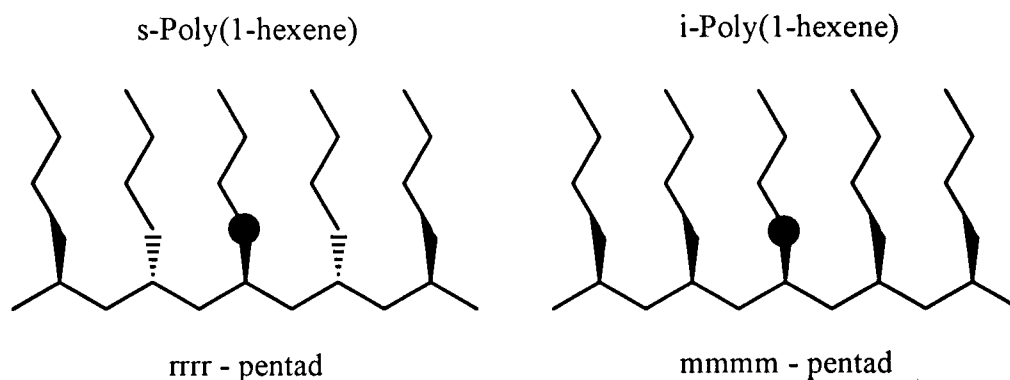


Figure 3.7: Syndiotactic and isotactic pentads in poly(1-hexene)

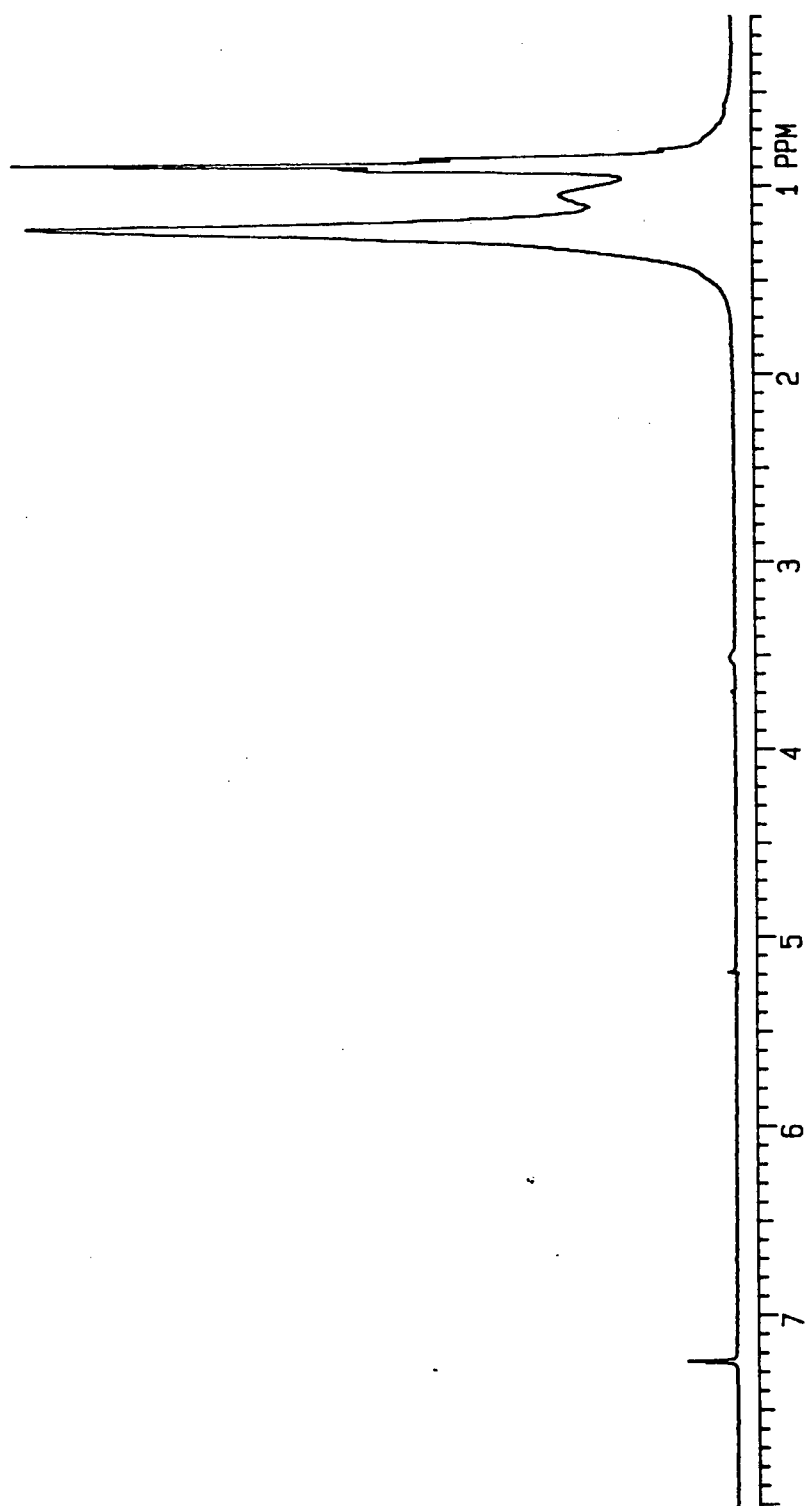


Figure 3.5: 300 MHz ^1H NMR spectrum of poly(1-hexene) in CDCl_3 at 25°C

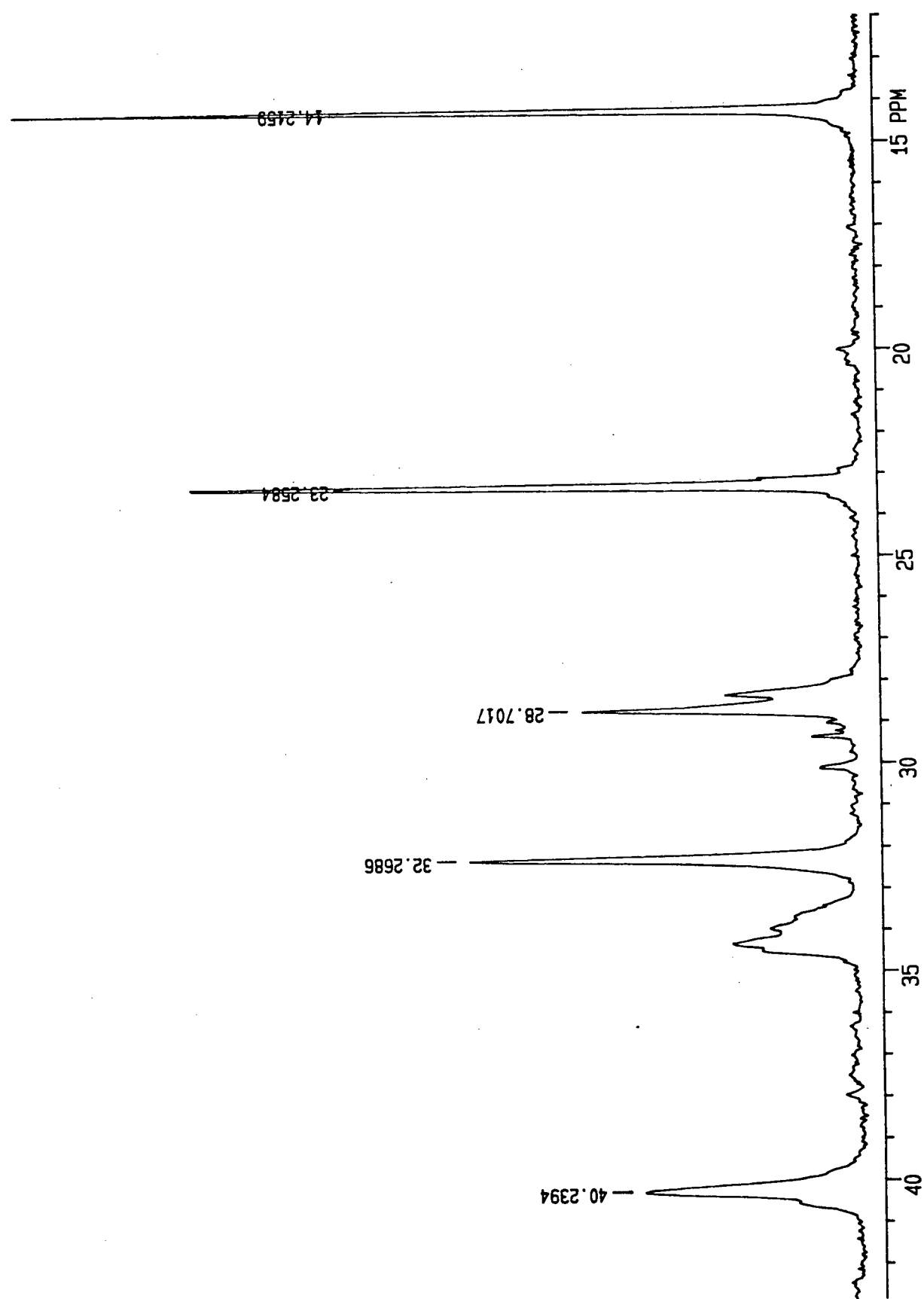
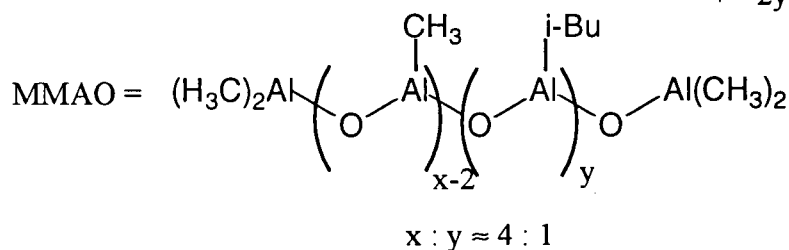
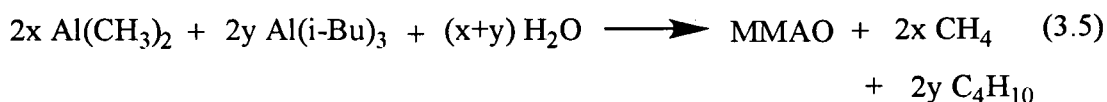


Figure 3.6: 75.45 MHz $^{13}\text{C}\{^1\text{H}\}$ NMR spectrum of poly(1-hexene) in CDCl_3 at 25°C

spectrum of syndiotactic poly(1-hexene) occurs at 34.03 ppm, corresponding to a rrrr-pentad (Figure 3.7).^{136,137} In all samples of poly(1-hexene) produced with catalyst precursors **2.10a,b** and **2.11a,b**, several resonances are observed at approximately 34 ppm corresponding to atactic poly(1-hexene).

The catalysts bearing the 2,6-*i*Pr₂C₆H₃ group at nitrogen (**2.10b**, **2.11b**) show higher activities than the dimethylphenyl substituted complexes (**2.10a**, **2.11a**), possibly a reflection of the increased steric protection afforded by the former ligand. Furthermore, greater charge separation would be expected in the 2,6-diisopropyl substituted catalyst leading to a more active catalyst. In contrast, the catalyst system **2.11b**/MMAO (MMAO = isobutyl modified methyl alumoxane) is less active than **2.11a**/MMAO. This may reflect structural differences between MMAO and MAO.^{138,139} MMAO is prepared in an identical manner to MAO. The only difference being that 20% *i*-Bu₃Al is added to the Me₃Al before hydrolysis to the aluminoxane (eq. 3.5). MMAO has the advantage of being soluble in aliphatic solvents while

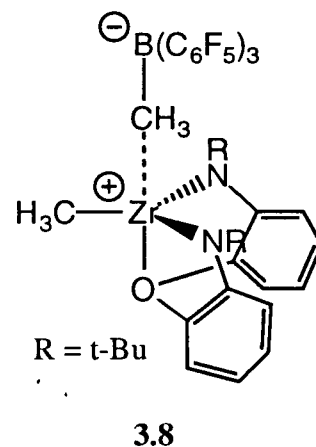


MAO is only soluble in aromatic solvents like toluene. Substitution of a portion of the methyl groups on MAO by isobutyl groups accounts for this increased solubility. However, one drawback of this increased solubility, is the increased steric bulk of the aluminoxane. MMAO may not be as efficient at activating catalyst precursors as MAO. This could account for the lower activity of complex **2.11b**.

Under identical conditions of MAO activation, the dichloride precursors **2.10a,b** are about 30% more active than the dimethyl derivatives **2.11a,b** (Table 3.1 – entries 7–10).

This difference in activity may be due to the difference in the counterion. Although this suggestion is purely speculative since the composition of the MAO anion and its relationship to the cation is not fully understood. It should be noted that complexes **2.10a,b** and **2.11a,b**, when activated with trialkylaluminums (eg. Me_3Al , Et_3Al and $i\text{Bu}_3\text{Al}$), are inactive for the polymerization of α -olefins.

The dimethyl derivatives **2.11a,b** can also be activated with the Lewis acid $\text{B}(\text{C}_6\text{F}_5)_3$ (Table 3.1 – entries 5,6). Complexes **2.11a,b** were combined with $\text{B}(\text{C}_6\text{F}_5)_3$ prior to injection into the monomer. Although MAO is present in the reactor to act as a scavenger for water, the significantly lower activities, and lower average molecular weights suggest that this system is indeed different from the MAO activated system. This probably reflects the structural difference of the anions. It is believed that MAO has the capability to fully sequester the methyl group in a very weakly coordinating anion. This will lead to greater charge separation with the MAO activated systems resulting in a more active catalyst. The methyl borate anion, however, is much more open to interact with the cation. Schrock has recently characterized a zwitterionic chelating diamide of zirconium which displays a partially abstracted methyl group (**3.8**).¹¹⁹ A complex similar to **3.8** may account for the lower activities observed with borane activation.



As previously mentioned, it would appear that the only chain termination process operative in the **2.11a,b**/MAO systems is transfer to aluminum,⁹⁶ as we have been unable to detect olefinic resonances in the ^1H and $^{13}\text{C}\{^1\text{H}\}$ NMR spectra of poly(1-hexene) samples. In fact, the MAO cocatalyst, which is normally insoluble in 1-hexene, slowly 'dissolves' over the course of the polymerization. Replacing the methyl groups in MAO with poly(1-hexene) units would certainly lead to a more soluble aluminoxane (note: the solubility of MMAO). The polymerization of 1-hexene in the presence of increasing amounts of MAO leads to a

decrease in number average molecular weight (M_n) with the polydispersity (M_w/M_n) remaining relatively constant (Figure 3.8).

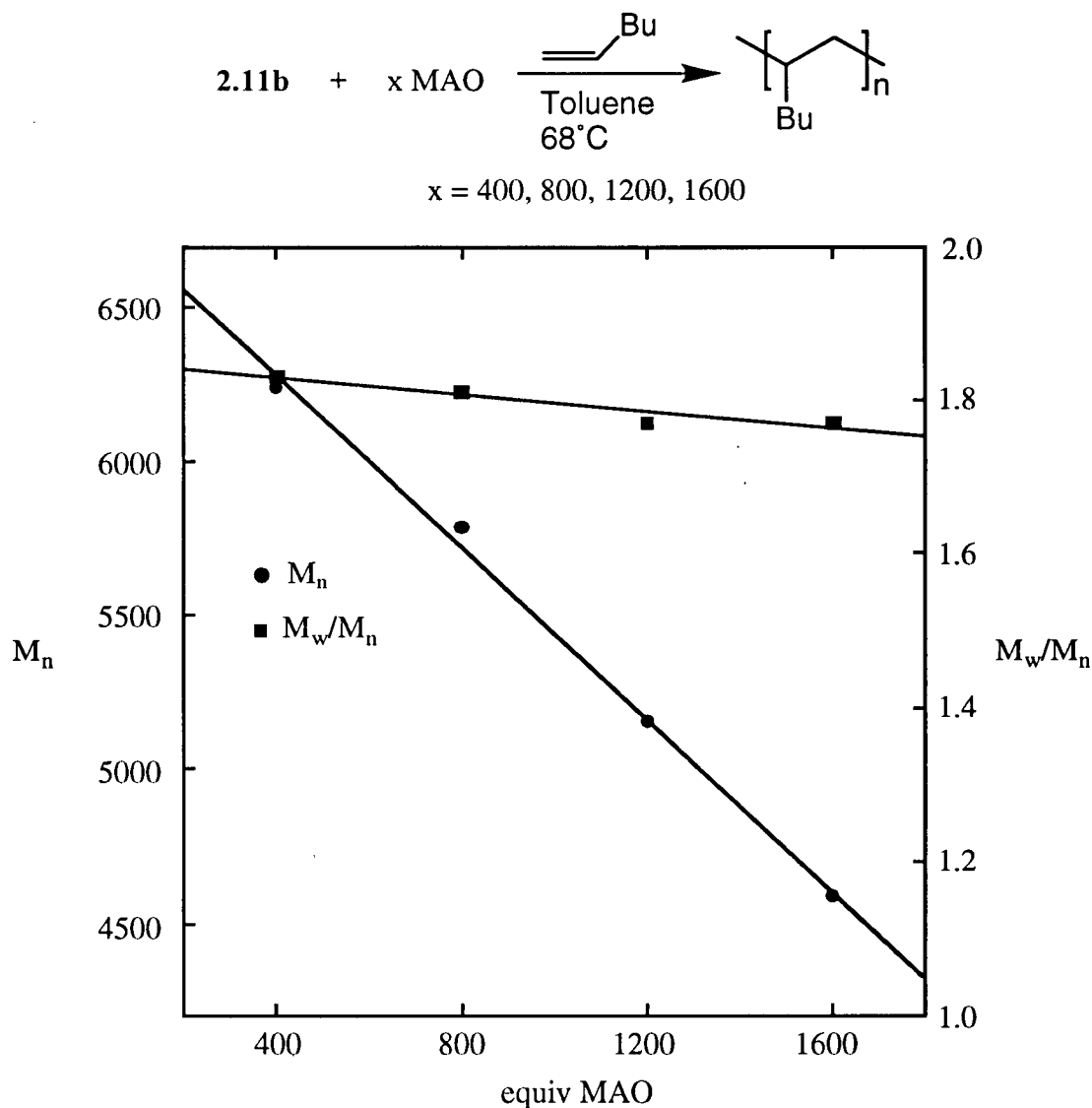


Figure 3.8: Plot of M_n and M_w/M_n versus equivalents of MAO. Conditions: 6.8 μmol of **2.11b** in 1 mL of pentane was added to MAO (400, 800, 1200, and 1600 equiv) in 9.0 g of 1-hexene and 1.0 g of toluene at 68°C and stirred for 10 s.

By increasing the number of aluminum centres available for chain transfer, the rate of termination is increased, causing a corresponding decrease in the molecular weight of the polymer. Furthermore, an increase in activity is observed with increasing equivalents of MAO (Figure 3.9).¹⁴⁰ The increase in activity, however, does not balance the increase in the

rate of termination. It appears that increasing the concentration of MAO increases k_t more than it increases k_p . It is important to note that eventually, the increase in activity will plateau and further addition of MAO will no longer increase the activity.¹¹⁸

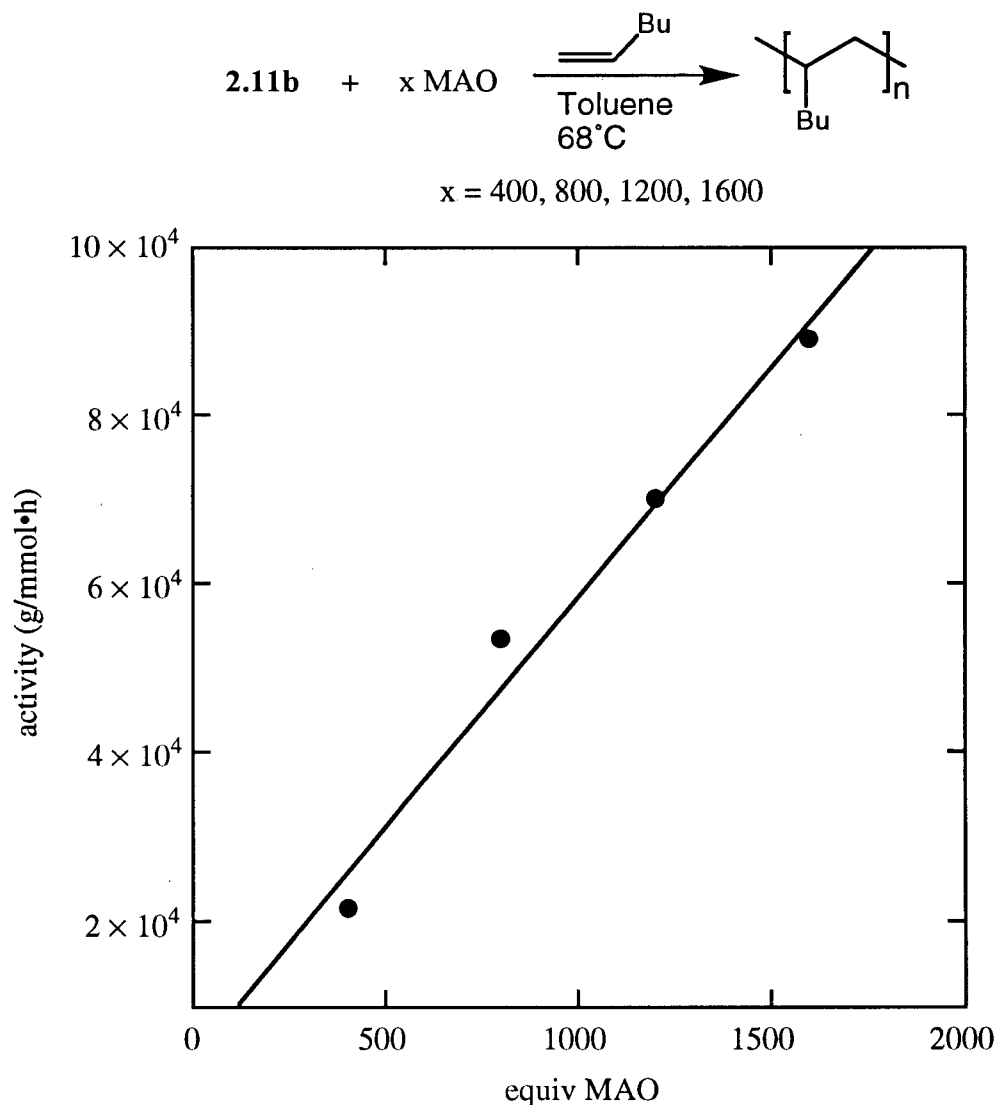
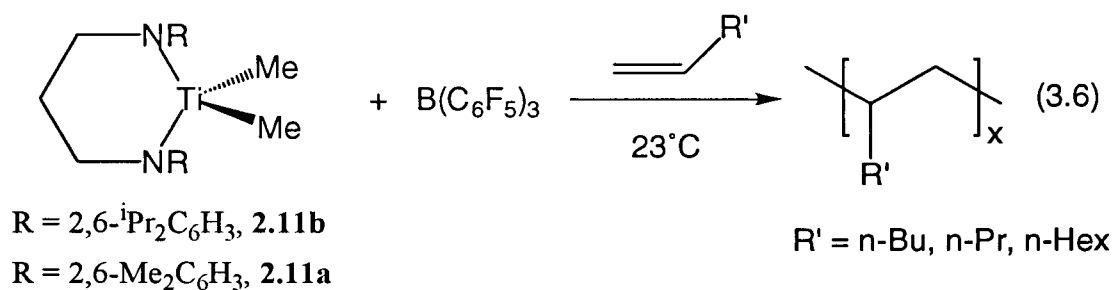


Figure 3.9: Plot of activity (g poly(1-hexene)/mmol cat.·h) versus equivalents of MAO. Conditions: 6.8 μmol of **2.11b** in 1 mL of pentane was added to MAO (400, 800, 1200, and 1600 equiv) in 9.0 g of 1-hexene and 1.0 g of toluene at 68°C and stirred for 10 s.

Living Polymerization of α -olefins

Due to the lack of olefinic resonances in poly(1-hexene) samples prepared from catalyst precursors **2.11a,b** and MAO, it appears that the primary termination step is chain transfer to aluminum cocatalyst. If the rate of termination could be reduced to zero, a living α -olefin coordination polymerization system may result. Removal of MAO from the polymerization system and activating the catalyst precursor with a cocatalyst which cannot undergo chain transfer resulted in the formation of a living Ziegler–Natta polymerization catalyst. Equimolar amounts of the titanium dimethyl complexes **2.11a,b** and $\text{B}(\text{C}_6\text{F}_5)_3$ ¹⁴¹ catalyze the living polymerization α -olefins at room temperature (eq 3.6). In the absence of



excess monomer, attempts to spectroscopically identify the catalytically active species have been thwarted by the extreme reactivity of the catalyst system with chlorinated solvents and its insolubility in aromatic solvents (Chapter 2). A summary of the polymerization results is shown in Table 3.2. The catalyst systems generate very high molecular weight polymers with remarkably narrow molecular weight distributions for a number of α -olefins. The polymer samples are soluble in aliphatic solvents and THF. In the absence of cocatalyst the titanium dimethyl complexes **2.11a,b** do not polymerize these monomers under the conditions studied.

Table 3.2: Living polymerization of α -olefins^a

entry	catalyst precursor	monomer and conditions	yield (mg)	time (min)	M_w^b	M_n^b	M_w/M_n	activity ^c
1	2.11b	1-hexene	50	10	4300	4100	1.05	40
2	2.11b	1-octene	50	10	5100	4900	1.05	40
3	2.11b	1-decene	50	10	5800	5500	1.06	40
4	2.11b	1-hexene/toluene, ^d	100	30	20000	19100	1.05	30
5	2.11b	1-octene/toluene, ^d	110	30	16900	15500	1.09	30
6	2.11b	1-decene/toluene, ^d	110	30	16600	15800	1.05	30
7	2.11b	1-hexene/CH ₂ Cl ₂ , ^e	570	10	176100	164200	1.07	490
8	2.11b	1-octene/CH ₂ Cl ₂ , ^e	870	10	148100	138200	1.07	750
9	2.11b	1-decene/CH ₂ Cl ₂ , ^e	890	10	131000	121500	1.07	760
10	2.11a	1-hexene	90	30	12800	12100	1.06	30
11	2.11a	1-octene	160	30	21900	20900	1.05	50
12	2.11a	1-decene	150	30	19200	17300	1.11	40

^aGeneral conditions: 6.7 μ mol of 2.11a or 2.11b in 0.67 mL of pentane and 6.7 μ mol of B(C₆F₅)₃ in 0.35 mL pentane was added to 6 mL of monomer or monomer/solvent at 23°C. ^bBy GPC in THF vs. polystyrene standards. ^cg polymer/mmol catalyst•h. ^d2 mL of toluene in 4 mL monomer. ^e2 mL of CH₂Cl₂ in 4 mL monomer.

A noticeable increase in activity and hence molecular weight is observed for polymerizations performed in the presence of CH_2Cl_2 (compare Table 3.2 – entries 1–3 to 7–9). The polarity of CH_2Cl_2 may result in greater charge separation between the putative cationic titanium alkyl and the methylborate anion leading to a more active catalyst.¹²⁶⁻¹²⁸ Although the measured activities and polymer yields increase by a factor of about 10, the molecular weights of the polymers increase by a factor of about 30. This suggests that some of the catalyst may not be active in this solvent or is deactivated very early in the polymerization. Complexes **2.11a,b**, when activated by $\text{B}(\text{C}_6\text{F}_5)_3$ in CH_2Cl_2 , in the absence of monomer formed the dichloride complexes **2.10a,b** (Chapter 2). It is reasonable that some of the catalyst is decomposing by abstracting a chloride atom from the solvent. Activities are suppressed when the polymerizations are performed in the presence of toluene (compare Table 3.2 – entries 1–3 to 4–6). Undoubtedly this can be attributed to the same interaction noted with the MAO activated catalyst systems.

The time dependence of the polymerization of 1-hexene with the catalyst system **2.11a**/ $\text{B}(\text{C}_6\text{F}_5)_3$ in a 50:50 mixture of toluene:1-hexene has been measured (Figure 3.10). The ratio of toluene:1-hexene tempers the rate of propagation and permits convenient measurement of molecular weights at regular time intervals with a minimal increase in viscosity. Aliquots were removed from the solution at five minute intervals and the number average molecular weight (M_n) plotted versus time. The gel permeation chromatograph of each sample shows a single, narrow molecular weight peak with polydispersities ranging from 1.06 to 1.07. A linear relationship between M_n and time indicates that the system is living.

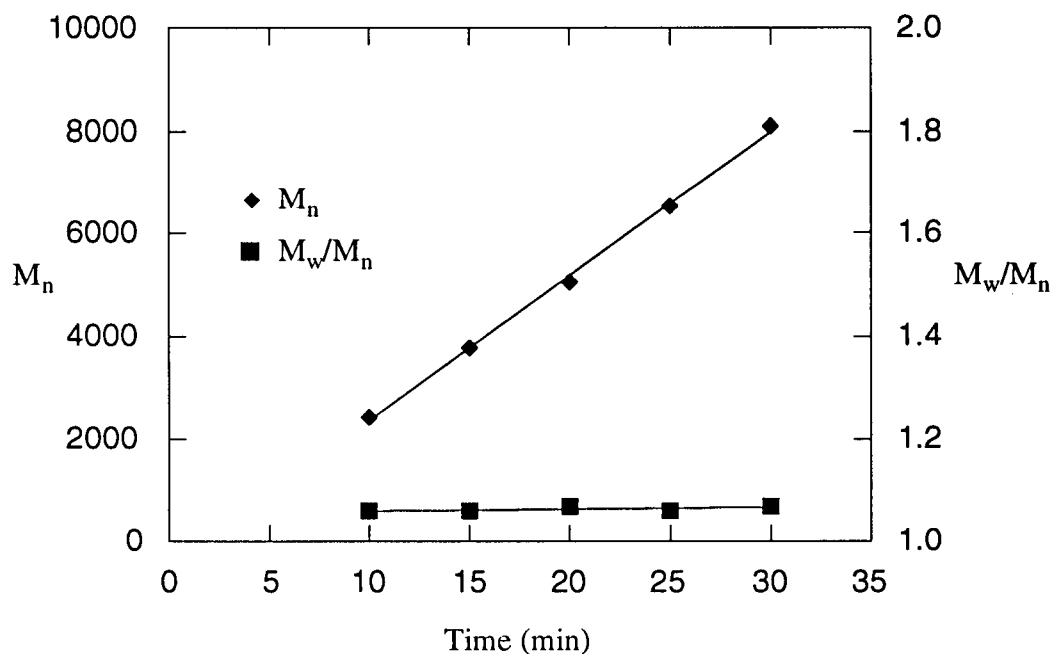


Figure 3.10: M_n and M_w/M_n vs. time for the living polymerization of 1-hexene

In a separate experiment, the time dependence of the polymerization of 1-hexene with the catalyst system **2.11a**/ $B(C_6F_5)_3$ in a 33:67 mixture of toluene:1-hexene was measured (Figure 3.11). The plot of M_n versus time deviates from linearity after 30 minutes, however, the polydispersities remain narrow ($M_w/M_n = 1.05$ – 1.08). A significant increase in viscosity and the declining monomer to catalyst ratio are likely responsible for this observation. If additional monomer and solvent are added periodically, the molecular weights continue to increase with no change in the polydispersities ($M_w/M_n = 1.05$ – 1.08).

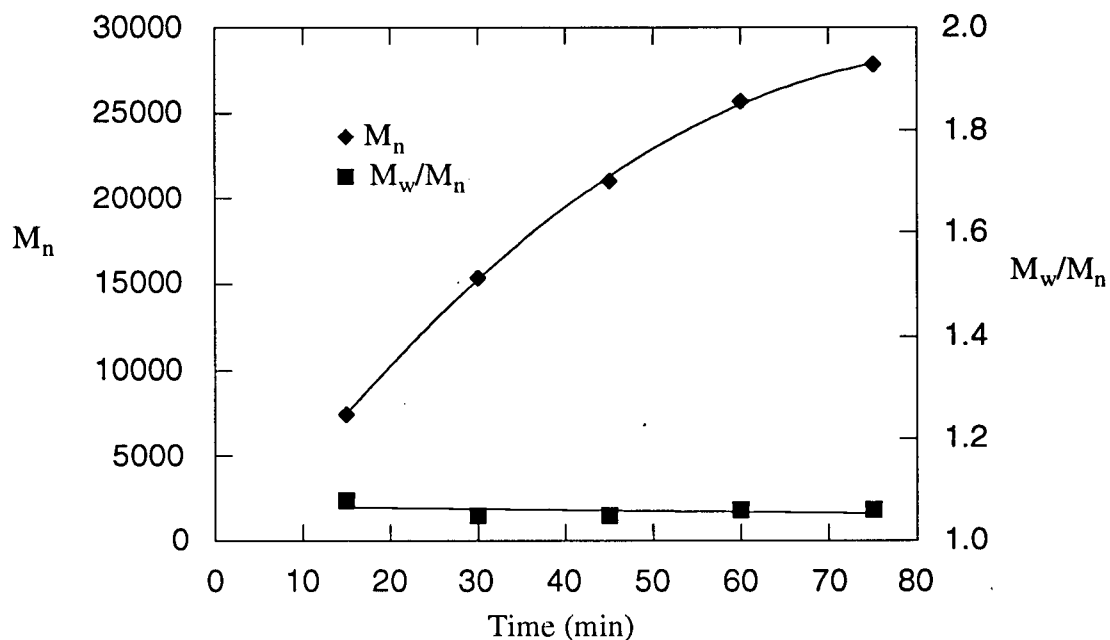


Figure 3.11: M_n vs. time for the living polymerization of 1-hexene

Although the measured activities at 23°C are low, higher activities are attainable at higher temperatures (68°C) at the expense of a slight increase in the molecular weight distribution (M_w/M_n) of the polymer (from 1.05 to 1.15). Under identical conditions, the borane-activated systems are considerably less active than the MAO-activated systems (350000 vs. 1800 g poly(1-hexene)/mmol cat.·h), possibly due to increased charge separation¹²⁶⁻¹²⁸ in the MAO-activated system relative to the borane-activated system. The methyl borate anion is probably more strongly coordinated to the cation than $[\text{MAO-CH}_3]^-$.

In addition to the above mentioned activators, it is also possible to generate highly active living polymerization systems with $\{\text{Ph}_3\text{C}\}^+[\text{B}(\text{C}_6\text{F}_5)_4]^-$ (TB)⁶¹ (eq. 3.7).

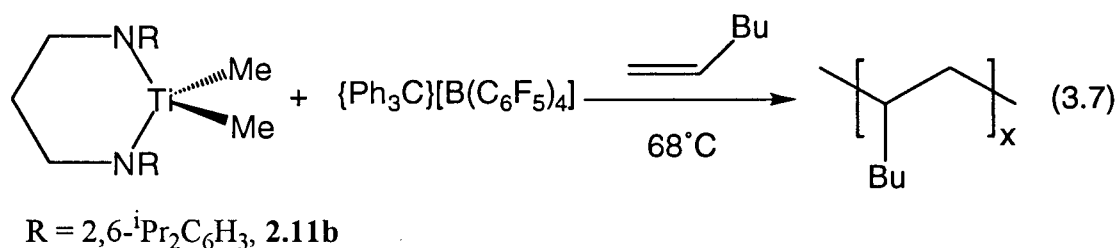


Table 3.3 contains polymerization results of the highly active polymerization systems. Under identical conditions, the TB-activated systems are about 1/3 less active than the MAO-activated systems (153000 vs. 104000 g poly(1-hexene)/mmol cat.·h) and at least two orders of magnitude more active than the borane-activated compounds (1800 g poly(1-hexene)/mmol cat.·h, note that the measured activity in entry 2 is suppressed by toluene relative to entry 1). Less pronounced anion effects of this type have been noted in metallocene systems.^{142,143} The molecular weight distribution measured for the polymers in the TB-activated system is higher than that observed in the less active borane-activated complexes. This increase in the polydispersity may be a result of a change in the relative rates of initiation (k_i) and propagation (k_p), as compared to the borane-activated system, since there is no evidence of β -hydride elimination in low molecular weight polymers (by NMR spectroscopy). In addition, the GPC traces of **2.11b**/TB generated poly(1-hexene) samples are unimodal confirming that no chain termination is operative in these systems.

The **2.11b**/TB catalyst system offers an opportunity to confirm the notion that cationic diamide titanium complexes readily engage in chain transfer to aluminum.¹⁴⁴ Addition of trialkylaluminum to induce chain transfer to aluminum should result in an increase in the polydispersity of the polymer. When 1-hexene is polymerized with **2.11b**/TB in the presence of 100 equivalents of $\text{Al}(i\text{Bu})_3$ an increase in the molecular weight distribution (1.35 vs. 1.45) is observed along with a corresponding decrease in the molecular weight of the polymer (177500 vs. 130900 g poly(1-hexene)/mmol cat.·h). Chain transfer to aluminum is even greater when MAO is present. The molecular weight

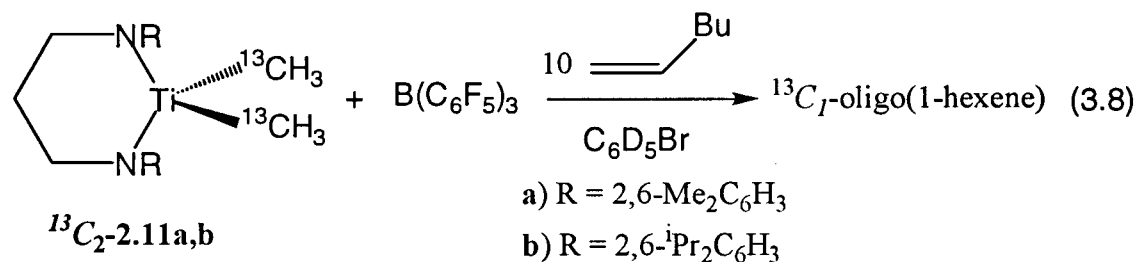
Table 3.3: Polymerization of 1-Hexene

entry	catalyst system and conditions	yield (g)	time	M_w^a	M_n^a	M_w/M_n	activity ^b
1	2.11b/B(C ₆ F ₅) ₃ , 68°C ^c	0.32	30 s	19300	16700	1.15	1800
2	2.11b/TB, 68°C ^{d,e}	3.05	10 s	239100	177500	1.35	104000
3	2.11b/MAO, 68°C ^{d,f}	4.53	10 s	23900	11900	2.01	153000
4	2.11b/TB, 68°C ^{d,e,g}	2.89	10 s	190100	130900	1.45	98000
5	2.11b/TB, 68°C ^{d,e,h}	3.58	10 s	60200	29000	2.08	122000

MAO = methylaluminoxane and TB = {Ph₃C}⁺[B(C₆F₅)₄]⁻. ^aBy GPC vs. polystyrene standards. ^bg poly(1-hexene)/mmol catalyst·h. ^c10.6 μmol of catalyst and 1 equiv of B(C₆F₅)₃ were added to 10.0 mL of 1-hexene. ^d10.6 μmol of catalyst was mixed with cocatalyst in 1.0 mL toluene and added to 9.0 mL of 1-hexene. ^ecocatalyst = 1 equiv of TB. ^fcocatalyst = 500 equiv of MAO. ^g100 equiv Al(ⁱBu)₃ added. ^h100 equiv MAO added.

distribution increases to 2.08 while the number average molecular weight of poly(1-hexene) drops from 177,500 to 29,000. It is reasonable to suggest that MAO would be a better chain transfer agent than $\text{Al}(\text{iBu})_3$ for steric reasons. The isobutyl groups in $\text{Al}(\text{iBu})_3$ provide more kinetic protection than the methyl group on MAO. This phenomenon also manifests itself in the MMAO activated systems. The **2.11b**/MAO system gives rise to polymer with a polydispersity of 1.73 while the MMAO activated system gives polymer with a polydispersity of 1.58. This indicates that the rate of chain transfer to MAO is greater than the rate of chain transfer to MMAO. Furthermore, the activity is 20 times greater for the MAO activated system versus the MMAO activated system. However, the molecular weights of the polymers are only 2.5 times larger. Therefore, although the activity of the MMAO activated system is less, the polymer chains are considerably longer than would be expected. This results from less efficient chain transfer to co-catalyst.

The mode of α -olefin insertion (1,2 versus 2,1 insertion) in the above catalytic systems, **2.11a**/ $\text{B}(\text{C}_6\text{F}_5)_3$ and **2.11b**/ $\text{B}(\text{C}_6\text{F}_5)_3$, can not be determined by end-group analysis of the polymer samples. In order to show this, the isotopically labeled complexes $[\text{RN}(\text{CH}_2)_3\text{NR}]\text{Ti}(\text{}^{13}\text{CH}_3)_2$ ($^{13}\text{C}_2$ -**2.11a,b**) were prepared from **2.10a,b** and 2 equivalents of $^{13}\text{CH}_3\text{MgI}$ in ether at -20°C . In separate experiments, compounds $^{13}\text{C}_2$ -**2.11a** and $^{13}\text{C}_2$ -**2.11b** were mixed with 1 equivalent $\text{B}(\text{C}_6\text{F}_5)_3$ and 10 equivalents of 1-hexene in d_5 -bromobenzene to yield $^{13}\text{C}_1$ -oligo(1-hexene) (eq. 3.8).



Bromobenzene is sufficiently polar to solubilize catalytic amounts of the $^{13}\text{C}_2$ -**2.11a,b**/ $\text{B}(\text{C}_6\text{F}_5)_3$ catalyst system and is unreactive. In contrast, CD_2Cl_2 reacts with the $^{13}\text{C}_2$ -**2.11a,b**/ $\text{B}(\text{C}_6\text{F}_5)_3$ complex to give the dichlorides **2.10a,b** while relatively non-polar

aromatic solvents such as toluene and benzene yield insoluble red oils (Chapter 2). These red oils are, however, active catalysts when exposed to neat 1-hexene. The $^{13}\text{C}\{^1\text{H}\}$ NMR spectra of the $^{13}\text{C}_1$ -oligo(1-hexene) samples are dominated by resonances attributable to the borate anion $[\text{}^{13}\text{CH}_3\text{B}(\text{C}_6\text{F}_5)_3]^-$ (14.0 ppm) and the isotopically labeled methyl group (average 20.4 ppm) which initiated the polymer chain. In addition, weak resonances are observed for atactic oligo(1-hexene) and in the case of the polymer derived from $^{13}\text{C}_2$ -**2.11b**, a small resonance at 109 ppm is assigned to the methylene derivative **2.54b** (Chapter 2). Using 3-methylhexane as a model complex, the pattern at 20.4 ppm can be ascribed to a methyl group bound to a tertiary carbon, in other words, to 1,2-inserted 1-hexene (Figure 3.12).

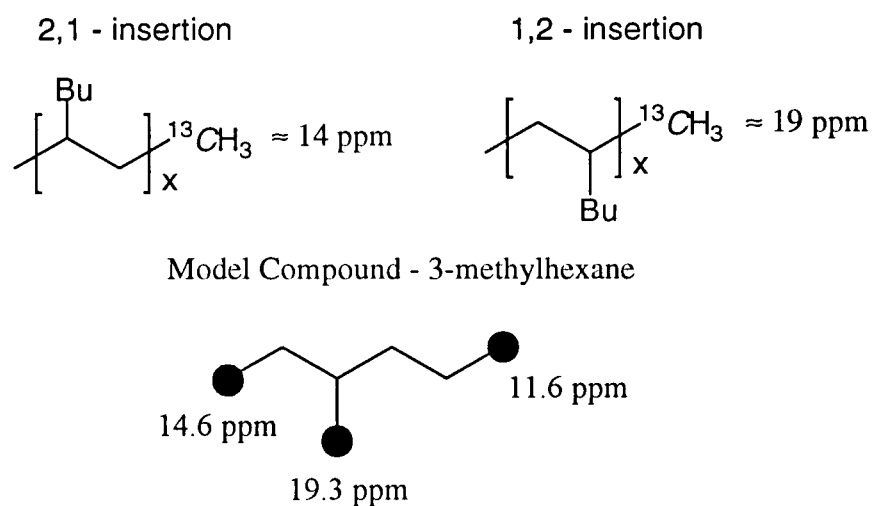


Figure 3.12 Possible products from polymerization with $^{13}\text{C}_2$ -**2.11b**/ $\text{B}(\text{C}_6\text{F}_5)_3$

The pattern at 20.4 ppm is actually a series of four closely spaced resonances which are attributed to the stereoplacements of the first three inserted monomers. Figure 3.13 shows the four possible stereoisomers for the first three insertion products. Each stereoisomer will give rise to one signal for the carbon-13 labeled end group in the $^{13}\text{C}\{^1\text{H}\}$ NMR spectrum of the oligomer. The above chemical shift assignment is consistent with chain end studies reported for polypropylene.⁸⁵

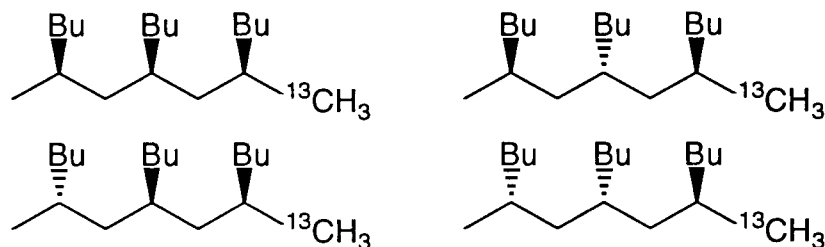


Figure 3.13: Possible stereoplacements formed in the first three insertions of 1-hexene

Additional evidence for the 1,2-insertion of 1-hexene is obtained from iodine quenching reactions.¹²³ For example, 10 equivalents of 1-hexene was polymerized with **2.11a**/ $\text{B}(\text{C}_6\text{F}_5)_3$ in d_5 -bromobenzene followed by quenching with excess I_2 . The ^1H NMR spectrum of this solution shows resonances similar to the dichloride complex **2.10a** (although this complex is actually the diiodo derivative), the typical broad resonances associated with atactic poly(1-hexene), and a broad multiplet at 3.10 ppm which integrates 1:1 with the resonances of the diamido ligand. Using 2-iodobutane and 1-iodo-2-methylpropane as model compounds,¹²³ we assign the multiplet at 3.10 ppm to methylene protons located adjacent to an iodide (Figure 3.14).

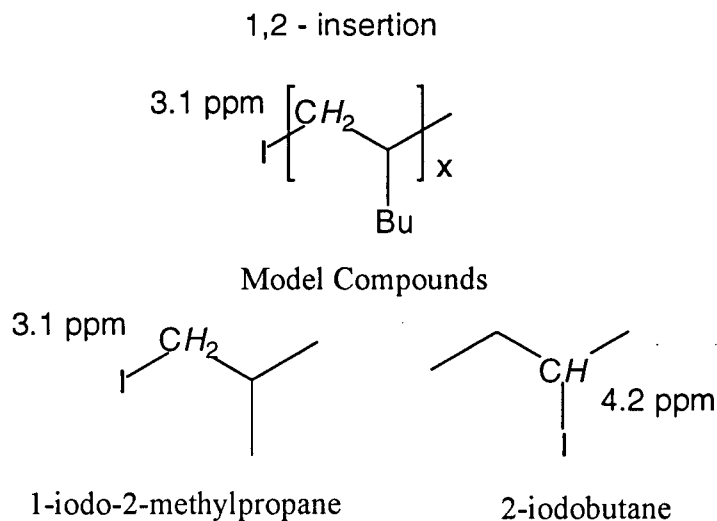
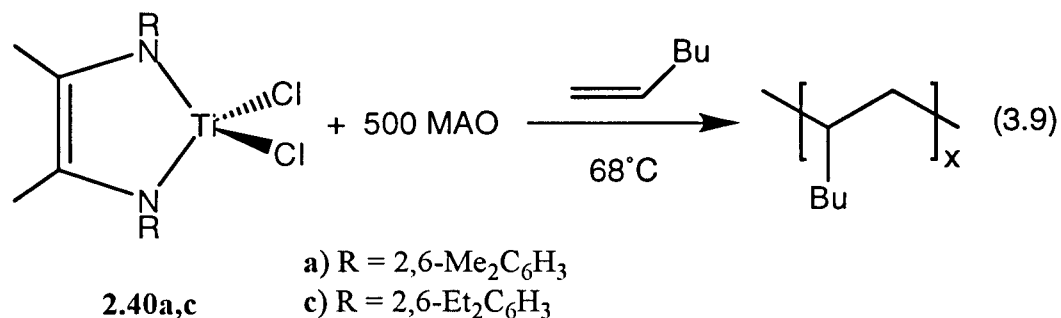


Figure 3.14: Possible products from quenching polymerization of 1-hexene with I_2

A similar study has been used to assign a secondary insertion mode to vanadium living polymerization systems.¹²³

Ene-Diamide complexes of titanium

The enediamide complexes **2.40a,c**, when activated with MAO, catalyze the polymerization of 1-hexene (eq. 3.9). The results of these polymerizations are



contained in Table 3.4. The molecular weight distributions are consistent with a single site homogeneous catalyst. The molecular weights of the poly(1-hexene) and the polydispersities for the two catalysts are quite similar. However, the molecular weights of the polymer are approximately ten times smaller than the molecular weights of the polymer obtained from the chelating bis(amido) system **2.10a,b**/MAO under similar conditions. Complexes **2.40a,c** are much less active catalyst precursors than complexes **2.10a,b**. Although complexes **2.10a,b** and complexes **2.40a,c** are very similar in nature, the latter complexes have an unsaturated link between the amide groups, which can undergo intramolecular coordination to the metal centre (3.9, Figure 3.15).

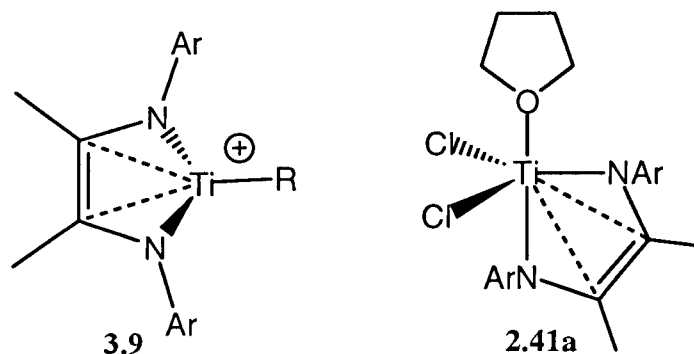


Figure 3.15: Proposed coordination of the double bond to the cationic alkyl

Table 3.4: Polymerization of 1-hexene with ene-diamide titanium complexes

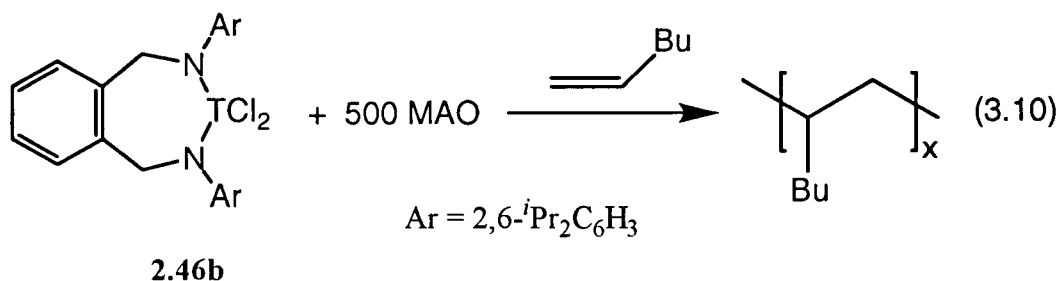
entry	catalyst system and conditions	yield (g)	time (min)	M_n^a	M_w^a	M_w/M_n	Activity ^b
1	2.40a/MAO, 68°C ^{c,e}	1.64	30	4000	6300	1.60	270
2	2.40c/MAO, 68°C ^{d,e}	3.90	30	3500	5500	1.57	730

^aBy GPC vs. polystyrene standards. ^bg poly(1-hexene)/mmol catalyst•h. ^c12.1 μmol of catalyst ^d10.7 μmol of catalyst ^e300 equiv of MAO

Intramolecular coordination of the double bond of the ligand is observed for the neutral complex **2.41a** (Chapter 2). The formation of the highly electrophilic titanium cation by reaction with MAO may render this interaction even stronger. The η^4 -coordination of the bis(amido) ligand may account for the lower activities and molecular weights observed with the **2.40a,c**/MAO systems. Interestingly, the activity of **2.40c**/MAO is greater than the activity of **2.40a**/MAO. A similar trend is observed for complexes **2.9a,b**, where the activity of **2.9b**/MAO is greater than that of **2.9a**/MAO. In general, for the complexes studied, the catalyst with the larger substitution on the aryl ring has the greater activity. This is probably a result of greater charge separation expected in the more hindered complex **2.40c**. Also, the coordination of the olefinic group of the ancillary ligand will probably be stronger with the smaller substituted ligand of complex **2.40a**.

Other Diamide Catalyst Precursors

The titanium dichloride **2.46b**, when activated with MAO, catalyzes the polymerization of 1-hexene (eq. 3.10). The results of the polymerizations are contained



in Table 3.5. The polydispersity of the polymer from the reaction indicates that a single species is active in solution. The number average molecular weight (M_n) of the polymer is approximately half of the M_n of the polymer obtained from the **2.10b**/MAO catalyst system (14000 vs. 31000). The **2.10b**/MAO system is also 30 times more active than the **2.46b**/MAO system (115,000 vs. 3300 g of poly(1-hexene)/mmol of cat. • h) under identical conditions.

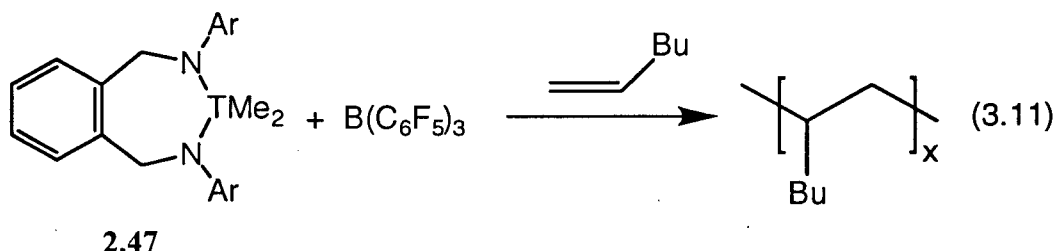
Table 3.5: Polymerization of 1-Hexene with potentially stereoselective catalysts

entry	catalyst system and conditions	yield (g)	time	M_w^a	M_n^a	M_w/M_n	activity ^b
1	2.46b/MAO, 68°C ^{c,h}	0.48	60 s	28900	14000	2.06	3300
2	2.47b/B(C ₆ F ₅) ₃ , 23°C ^{d,h}	0.08	10 min	12300	10400	1.19	30
3	2.50d/MAO, 68°C ^{e,f}	0.26	10 s	18900	9400	2.01	95500
4	2.51d/B(C ₆ F ₅) ₃ , 68°C ^{g,h}	0.11	30 s	16100	14600	1.10	1100

Catalyst was dissolved in solvent and added to 1-hexene (9 g) and 500 equivalents of MAO or 1 equivalent of B(C₆F₅)₃. ^aBy GPC vs. polystyrene standards. ^bg poly(1-hexene)/mmol catalyst•h. ^c8.7 μmol of catalyst. ^d18.8 μmol of catalyst. ^e9.8 μmol of catalyst. ^fsolvent = 1.0 g toluene. ^g11.3 μmol of catalyst. ^hsolvent = 1.0 g of pentane.

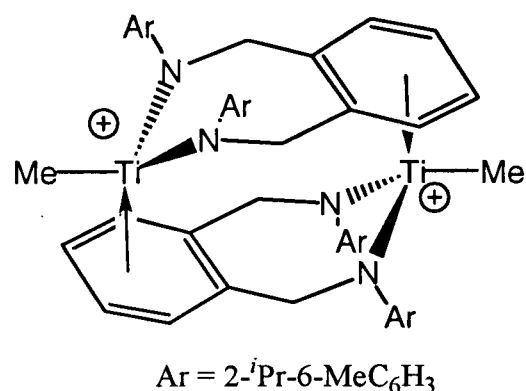
Carbon NMR spectroscopy revealed that the poly(1-hexene) obtained is atactic. The lack of tacticity in the polymer is in agreement with the observed C_{2v} symmetry in the 1H NMR spectrum of complex **2.46b** (Chapter 2). Interestingly, the 1H NMR spectrum of the polymer showed no olefinic resonances. This indicates that chain transfer to cocatalyst, rather than β -hydrogen elimination, is the primary mode of chain termination. Therefore, if the MAO was replaced by a cocatalyst to which chain transfer could not occur, a living polymerization system should result.

Activating the dimethyl derivative **2.47b** with $B(C_6F_5)_3$ instead of MAO resulted in the living polymerization of 1-hexene (eq. 3.11). The activity for the **2.47b**/ $B(C_6F_5)_3$



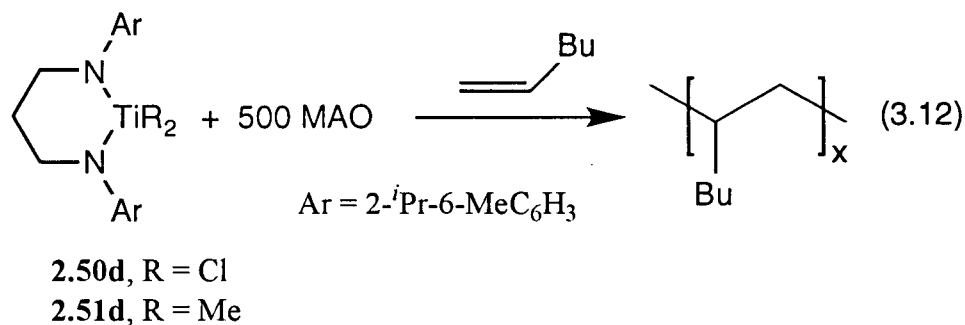
system is approximately the same as the **2.11b**/ $B(C_6F_5)_3$ system (30 versus 40 g poly(1-hexene)/mmol cat.·hr). Analysis of the polymer obtained by GPC indicated that, along with the poly(1-hexene), the catalyst also produced oligomer. The retention times for the oligomers corresponded exactly to known retention times for chains of four to seven hexene units (confirmed by GC-MS). The presence of both oligomers and high polymer suggest that more than one catalytically active species is present. This is also reflected in the fact that the molecular weights of the poly(1-hexene) are larger than for the **2.11b**/ $B(C_6F_5)_3$ system and yet the activity is about the same. Therefore, while some of the catalyst makes high molecular weight polymer, the remainder makes low molecular weight oligomer.

It is possible that some η^{π} -coordination of the aryl group of the ligand to the highly electrophilic titanium centre is occurring. This could result in the formation of a dimer where the aryl group of the ligand interacts with an adjacent titanium atom (**3.10**). The generation of a highly electrophilic metal centre coupled with the electron-rich aryl group could allow for this type of interaction resulting in a catalytically inactive species or one that yields only oligomer.



3.10

Complexes **2.50d** and **2.51d** are potentially stereospecific catalyst precursors. The rotamer *rac*-**2.50d** may produce isotactic poly(1-hexene) while *meso*-**2.50d** should lead to atactic polymer. Dichloride complex **2.50d**, when activated with MAO, yields a highly active 1-hexene polymerization catalyst (eq. 3.12). Under identical polymerization



conditions, complex **2.50d** is approximately 1/3 less active than complex **2.11b** (153000 vs. 95500 g of poly(1-hexene)/mmol of cat.·h). The number average molecular weight (M_n) of the polymer obtained is approximately one fifth of the M_n of the polymer obtained from the **2.11b**/MAO catalyst system (9400 vs. 47000). These results are probably attributable to the slight steric difference between the two ligands of complexes **2.50d** and **2.11b**. Carbon NMR

spectroscopy revealed that the polymer formed with this catalyst is atactic. NMR spectroscopy had previously revealed that complex **2.50d** is a 50:50 mixture of the *meso* and *rac* forms (chapter 2). Unlike complexes **2.46b** and **2.47b** which exhibit spectral resonances attributable to a time averaged C_{2v} -symmetric structure, the $^{13}\text{C}\{^1\text{H}\}$ NMR spectrum of **2.50d** displays resonances for a C_2 - and C_s -symmetric species. A comparison with known stereospecific catalysts may give some insight into why the polymer obtained was atactic.

The complex *meso*-**2.50d** exhibits C_s symmetry in its ^1H and $^{13}\text{C}\{^1\text{H}\}$ NMR spectra. Although *meso*-**2.50d** is C_s -symmetric, the mirror plane is perpendicular to the mirror plane in Ewen's C_s -symmetric fluorenyl-Cp complex (**1.4**) (Figure 3.16). Since the mirror plane lies in the TiCl_2 plane for complex *meso*-**2.50d**, this complex will be unable to discriminate between the two enantiotopic faces of a prochiral α -olefin. As a result, this complex should polymerize α -olefins in an atactic manner.

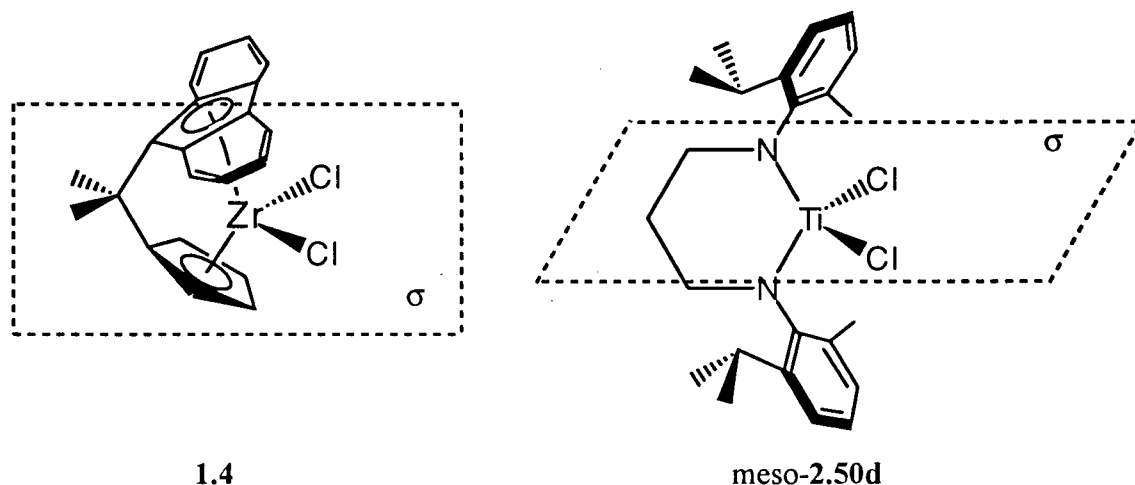
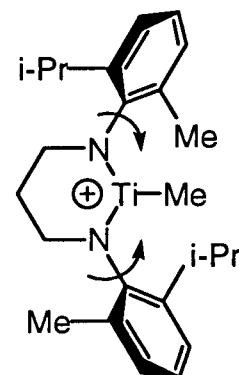


Figure 3.16: Comparison of the symmetry elements of a syndiospecific catalyst precursor and *meso*-**2.50d**

Complex *rac*-**2.50d** exhibits C_2 -symmetry in its ^1H and $^{13}\text{C}\{^1\text{H}\}$ NMR spectra. A comparison with Brintzinger's ethylenebis(tetrahydroindenyl)zirconium dichloride complex **1.3** indicates that the same symmetry elements are in place for this complex. Therefore, it is expected that complex *rac*-**2.50d** would enhance the isotactic fractions of poly(1-hexene)

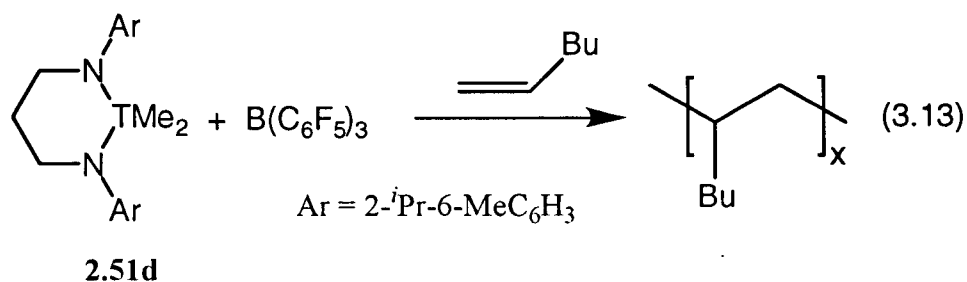
when activated with MAO. Since the polymer obtained was atactic, there must be another explanation for the stereochemistry of the catalyst not being imparted on the polymer.

It is impossible to know if complex **2.50d**, once activated with cocatalyst, is able to maintain its stereochemistry. It is possible that the active catalyst generated from the reaction of complex **2.50d** with MAO is unable to maintain the restricted rotation about the N–C_{ipso} bond (**3.11**). If the aryl groups can now rotate freely about this bond then the C₂-symmetric *rac* structure can isomerize to the *meso* structure and vice versa. If this rotation was relatively fast compared to the rate of polymerization, the overall stereochemistry of catalyst **2.50d**/MAO would be C_{2v} symmetric. This would lead to the formation of atactic poly(1-hexene).



3.11

The dimethyl complex **2.51d** is also a 50:50 mixture of the *rac* and *meso* isomers. This complex can be activated with one equivalent of B(C₆F₅)₃ generating a living catalyst system for the polymerization of 1-hexene (eq. 3.13). The polymer obtained from this system is atactic (by ¹³C{¹H} NMR spectroscopy). Comparison with the ¹³C{¹H} NMR spectrum of poly(1-hexene) generated from the **2.11b**/B(C₆F₅)₃



catalyst system revealed that the tacticity regions are superimposable. The activity of complex **2.51d** is slightly less than complex **2.11b** (1100 vs. 1800 g of poly(1-hexene)/mmol of cat.·h). The polydispersity of the polymer obtained from complex **2.51d** is slightly lower than for complex **2.11b** (1.10 vs. 1.15). The number average molecular weight (M_n) of the

polymer obtained is approximately the same as the M_n of the polymer obtained from the **2.11b**/ $B(C_6F_5)_3$ catalyst system (14,600 vs. 16,700). The lack of tacticity probably reflects a loss in stereochemistry of complex **2.51d** once it is activated with the cocatalyst.

Conclusions

Chelating diamide complexes of titanium serve as catalyst precursors for the polymerization of 1-hexene and other α -olefins.¹⁴⁵⁻¹⁴⁷ A variety of cocatalysts can be used to activate the complexes, however, these appear to be limited to highly electrophilic Lewis acids that do not bear halide groups. A pronounced difference in activity is noted between the borane-activated complexes and the MAO- and TB-activated systems. This marked variation in activity is assigned to the nature of the counter ion and its ability to coordinate to the metal centre. Chain transfer to aluminum has been identified as the sole chain termination step in the MAO-activated system. In contrast, the borane- and TB-activated diamide complexes are living catalysts as no chain termination is operative in these systems; however, these systems will engage in chain transfer if aluminum reagents are added. A primary insertion mode (1,2 insertion) has been assigned based on both the initiation of the polymer chain and its purposeful termination with iodine.

Experimental Details

General Details: All experiments were performed under an atmosphere of dry dinitrogen using standard Schlenk techniques or in an Innovative Technology Inc. glovebox. Pentane was first treated with a 5% solution of HNO_3 in H_2SO_4 to remove all olefins. Solvents were distilled from sodium/benzophenone ketyl or molten sodium (toluene) under argon, stored over sodium/potassium alloy and filtered through activated basic alumina just prior to use. 1-Hexene, 1-octene and 1-decene were obtained from Aldrich and distilled from sodium/benzophenone ketyl, stored over sodium/potassium alloy and filtered through activated basic alumina prior to use. CH_2Cl_2 was distilled from CaH_2 and passed through basic alumina prior to use. Proton (299.9 MHz) and $^{13}\text{C}\{^1\text{H}\}$ (75.46 MHz) NMR spectra were recorded in CDCl_3 , CD_2Cl_2 , C_6D_6 or BrC_6D_5 at approximately 23°C on a Varian XL-300 spectrometer. The proton chemical shifts were referenced to internal CHCl_3 ($\delta = 7.24$ ppm), CDHCl_2 ($\delta = 5.32$ ppm), $\text{C}_6\text{D}_5\text{H}$ ($\delta = 7.15$ ppm), and $\text{C}_6\text{D}_4\text{HBr}$ ($\delta = 7.15$ ppm), and the carbon resonances to CDCl_3 (77.0 ppm), CD_2Cl_2 ($\delta = 53.2$ ppm), C_6D_6 ($\delta = 128.0$ ppm) or $C_{ipso}\text{-C}_6\text{D}_5\text{Br}$ ($\delta = 122.5$ ppm). GPC analysis was carried out in THF with a Waters 600E solvent delivery unit (Waters Styragel HR 1, HR 3 and HR 4 columns) connected to a Waters 410 differential refractometer at 35°C relative to narrow polystyrene standards.

Table 3.1 – Entries 1–4, 7–10. The catalyst precursor (0.002 M, 0.5 mL, 1 μmol) and 250 equivalents of solid MAO (15 mg) (or MMAO, 17 mg) were premixed for 5 minutes. To a stirred solution of 1-hexene (5.0 g) and 250 equivalents of solid MAO (15 mg) (or MMAO, 17 mg) at 68°C was added this catalyst system. The mixture was stirred for the time indicated in Table 3.1 then quenched with 1.0 M HCl (5 mL). The organic phase was extracted with hexanes (3×100 mL), the solvent removed and the viscous polymer dried at 23°C for 16 h. The weight of the polymer was used in the calculation of activity and a small amount was used for GPC analysis. All the polymers showed identical $^{13}\text{C}\{^1\text{H}\}$ NMR spectra (see Figures 3.4 and 3.5).

Table 3.1 – Entries 5,6. The catalyst precursor (0.004 M, 0.25 mL, 1 μ mol) and 1 equiv of B(C₆F₅)₃ (0.004 M, 0.25 mL, 1 μ mol) were premixed for 5 minutes. To a stirring solution of 1-hexene (5.0 g) and 500 equivalents of solid MAO (29 mg) at 22°C was added this catalyst system. The mixture was stirred for 5.0 minutes then quenched with 1.0 M HCl (5 mL). The organic phase was extracted with hexanes (3 \times 100 mL), the solvent removed and the free flowing polymer dried at 23 °C for 16 h.

Table 3.1 – Entries 11,12. 2.11b (5.0 mg, 10.6 μ mol) and 500 equivalents of MAO (307 mg) in 5.0 mL of solvent (entry 11, toluene; entry 12, hexane) were added to a stirring solution of 1-hexene (5.0 mL). The solution was stirred at 68°C for 10 sec and then quenched by the addition of a 1N solution of HCl (5 mL). The polymer was extracted with hexanes and dried at 23 °C under vacuum overnight.

Table 3.2 – Entries 1–3. 2.11b (0.01 M, 0.67 mL, 6.7 μ mol) and B(C₆F₅)₃ (0.02 M, 0.35 mL, 6.7 μ mol) were added to a stirring solution of α -olefin (6 mL). The solution was stirred at room temperature for 10 min and then quenched by the addition of a 1N solution of HCl (2 mL). The polymer was extracted with hexanes and dried under vacuum overnight.

Table 3.2 – Entries 4–6. 2.11b (0.01 M, 0.67 mL, 6.7 μ mol) and B(C₆F₅)₃ (0.02 M, 0.35 mL, 6.7 μ mol) were added to a stirring solution of α -olefin (4 mL) and toluene (2 mL). The solution was stirred at room temperature for 30 min and then quenched by the addition of a 1N solution of HCl (2 mL). The polymer was extracted with hexanes and dried under vacuum overnight.

Table 3.2 – Entries 7–9. 2.11b (0.01 M, 0.67 mL, 6.7 μ mol) and B(C₆F₅)₃ (0.02 M, 0.35 mL, 6.7 μ mol) were added to a stirring solution of α -olefin (4 mL) and CH₂Cl₂ (2 mL). The solution was stirred at room temperature for 10 min and then quenched by the addition of a 1N solution of HCl (2 mL). The polymer was extracted with hexanes and dried under vacuum overnight.

Table 3.2 – Entries 10–12. 2.11a (0.01 M, 0.67 mL, 6.7 μ mol) and B(C₆F₅)₃ (0.02 M, 0.35 mL, 6.7 μ mol) were added to a stirring solution of α -olefin (6 mL). The solution

was stirred at room temperature for 30 min and then quenched by the addition of a 1N solution of HCl (2 mL). The polymer was extracted with hexanes and dried under vacuum overnight.

Table 3.3 – Entries 1–5. **2.11a** (5.0 mg, 10.6 μmol) was combined with the appropriate amount of cocatalyst and added to a stirring solution of 1-hexene (10.0 mL) at 68°C. Entry 4 had 100 equivalents of $\text{Al}(i\text{Bu})_3$ (255 mg) added to act as a chain transfer reagent while entry 5 had 100 equivalents of MAO (62 mg) added as the chain transfer reagent. The solution was stirred for either 30 or 10 sec and then quenched by the addition of a 1N solution of HCl (2 mL). The polymer was extracted with hexanes and dried under vacuum overnight.

Table 3.4 – Entry 1. **2.40a** (5 mg, 12.2 μmol) dissolved in pentane was added to 1-hexene (10 g) and 500 equiv of MAO (354 mg) heated to 68°C. After 30 min the reaction was quenched with 10 mL of 1 N HCl. The polymer was extracted with hexanes and dried overnight *in vacuo*.

Table 3.4 – Entry 2. **2.40c** (5 mg, 10.6 μmol) dissolved in pentane was added to 1-hexene (9 g) and 500 equiv of MAO (307 mg) heated to 68°C. After 30 min the reaction was quenched with 10 mL of 1 N HCl. The polymer was extracted with hexanes and dried overnight *in vacuo*.

Table 3.5 – Entry 1. **2.46b** (5.0 mg, 8.7 μmol) dissolved in pentane (1.0 g) was added to 1-hexene (9 g) and 500 equivalents of MAO (252 mg) heated to 68°C. After 60 s the reaction was quenched with 10 mL of 1 N HCl. The polymer was extracted with hexanes and dried overnight *in vacuo*.

Table 3.5 – Entry 2. **2.47b** (10 mg, 18.8 μmol) dissolved in pentane (1.0 g) was added to 1-hexene (9 g) and 1 equivalent of $\text{B}(\text{C}_6\text{F}_5)_3$ (10 mg) at 23 °C. After 10 min the reaction was quenched with 10 mL of 1 N HCl. The polymer was extracted with hexanes and dried overnight *in vacuo*.

Table 3.5 – Entry 3. 2.50 (5.0 mg, 9.8 μmol) dissolved in toluene (1.0 g) was added to 1-hexene (9 g) and 500 equivalents of MAO (284 mg) heated to 68°C. After 30 s the reaction was quenched with 10 mL of 1 N HCl. The polymer was extracted with hexanes and dried overnight *in vacuo*.

Table 3.5 – Entry 4. 2.51 (5.0 mg, 11.3 μmol) dissolved in pentane (1.0 g) was added to 1-hexene (9 g) and 1 equivalent of $\text{B}(\text{C}_6\text{F}_5)_3$ (6.0 mg) at 23 °C. After 10 min the reaction was quenched with 10 mL of 1 N HCl. The polymer was extracted with hexanes and dried overnight *in vacuo*.

Equivalents of MAO versus Time.

Data for Figures 3.8 and 3.9

equiv MAO	M_w	M_n	M_w/M_n	activity (g polymer/mmol cat.·hr)
400	11430	6240	1.83	21700
800	10450	5790	1.81	53500
1200	9100	5150	1.77	69900
1600	8100	4590	1.77	89000

M_n versus Time (0–30 min). 2.11a (0.011 g, 0.031 mmol) and $\text{B}(\text{C}_6\text{F}_5)_3$ (0.016 g, 0.031 mmol) were added to a stirring solution of 1-hexene (5 mL) and toluene (5 mL). Aliquots (1 mL) were removed from the reaction mixture every 5 min and quenched by the addition of a 1N solution of HCl (2 mL), extracted with hexanes, and dried under vacuum overnight.

Data for Figure 3.10 (0–30 min)

Time (min)	M_w	M_n	M_w/M_n
10	2590	2440	1.06
15	3990	3780	1.06
20	5410	5060	1.07
25	6910	6530	1.06
30	8690	8100	1.07

M_n versus Time (0–75 min). **2.11b** (0.005 g, 0.014 mmol) and $B(C_6F_5)_3$ (0.008 g, 0.015 mmol) were added to a stirring solution of 1-hexene (10 mL) and toluene (5 mL). Aliquots (1 mL) were removed from the reaction mixture every 15 min and quenched by the addition of a 1N solution of HCl (2 mL), extracted with hexanes, and dried under vacuum overnight.

Data for Figure 3.11 (0–75 min)

Time (min)	M_w	M_n	M_w/M_n
15	7420	8010	1.08
30	15410	16240	1.05
45	21050	22120	1.05
60	25710	27470	1.06
75	27840	29490	1.06

References

- (1) Natta, G.; Pino, P.; Corradini, P.; Danusso, F.; Mantica, E.; Moraglio, G. *J. Am. Chem. Soc.* **1955**, *77*, 1708.
- (2) Ziegler, K.; Gellert, H.-G. *Justus Liebigs Ann. Chem.* **1950**, *567*, 179.
- (3) Ziegler, K.; Gellert, H.-G. *Justus Liebigs Ann. Chem.* **1950**, *567*, 185.
- (4) Ziegler, K.; Gellert, H.-G. *Angew. Chem.* **1952**, *64*, 323.
- (5) Cossee, P. *Tet. Lett.* **1960**, *12*, 17.
- (6) Cossee, P. *J. Catal.* **1964**, *3*, 80.
- (7) Arlman, E. J. *J. Catal.* **1964**, *3*, 89.
- (8) Arlman, E. J.; Cossee, P. *J. Catal.* **1964**, *3*, 99.
- (9) Chatt, J.; Duncanson, L. A. *J. Chem. Soc.* **1953**, 2939.
- (10) Alderman, P. R. H.; Owston, P. G.; Row, J. M. *Acta Cryst.* **1960**, *13*, 149.
- (11) Chatt, J.; Shaw, B. L. *J. Chem. Soc.* **1959**, 705.
- (12) Breslow, D. S.; Newburg, N. R. *J. Am. Chem. Soc.* **1957**, *79*, 5072.
- (13) Natta, G.; Pino, P.; Mazzanti, P.; Giannini, U. *J. Am. Chem. Soc.* **1957**, *79*, 2975.
- (14) Breslow, D. S.; Newberg, N. R. *J. Am. Chem. Soc.* **1959**, *81*, 81.
- (15) Long, W. P. *J. Am. Chem. Soc.* **1959**, *81*, 5312.
- (16) Long, W. P.; Breslow, D. S. *J. Am. Chem. Soc.* **1960**, *82*, 1953.
- (17) Chien, J. C. W. *J. Am. Chem. Soc.* **1959**, *81*, 86.
- (18) Natta, G.; Mazzanti, G. *Tetrahedron* **1960**, *8*, 86.
- (19) Sinn, H.; Patat *Angew. Chem.* **1963**, *75*, 805.
- (20) Reichert, K. H.; Schubert, E. *Makromol. Chem.* **1969**, *123*, 58.
- (21) Reichert, K. H.; Berthold, J.; Dornow, V. *Makromol. Chem.* **1969**, *121*, 258.
- (22) Meyer, K.; Reichert, K. H. *Angew. Makromol. Chem.* **1970**, *12*, 175.
- (23) Reichert, K. H. *Angew. Makromol. Chem.* **1970**, *13*, 177.
- (24) Henrici-Olivé, G.; Olivé, S. *Angew. Chem., Int. Ed. Engl.* **1967**, *6*, 790.
- (25) Henrici-Olivé, G.; Olivé, S. *J. Organomet. Chem.* **1967**, *16*, 339.

- (26) Daychkovskii, F. S.; Shilova, A. K.; Shilov, A. E. *J. Polym. Sci. Part C* **1967**, *16*, 2333.
- (27) Jordan, R. F.; Bajgur, C. S.; Willett, R.; Scott, B. *J. Am. Chem. Soc.* **1986**, *108*, 7410.
- (28) Jordan, R. F.; Dasher, W. E.; Echols, S. F. *J. Am. Chem. Soc.* **1986**, *108*, 1718.
- (29) Jordan, R. F.; LaPointe, R. E.; Bajgur, C. S.; Echols, S. F.; Willett, R. *J. Am. Chem. Soc.* **1987**, *109*, 4111.
- (30) Jordan, R. F.; Bajgur, C. S.; Dasher, W. E.; Rheingold, A. L. *Organometallics* **1987**, *6*,
- (31) Jordan, R. F. *J. Chem. Edu.* **1988**, *65*, 285.
- (32) Jordan, R. F.; LaPointe, R. E.; Bradley, P. K.; Baenzinger, N. *Organometallics* **1989**, *8*, 2892.
- (33) Jordan, R. F.; Lapointe, R. E.; Baenziger, N.; Hinch, G. D. *Organometallics* **1990**, *9*, 1539.
- (34) Jordan, R. F.; Bradley, P. K.; LaPointe, R. E.; Taylor, D. F. *New J. Chem.* **1990**, *14*, 505.
- (35) Jordan, R. F.; Bradley, P. K.; Baenzinger, N. C.; LaPointe, R. E. *J. Am. Chem. Soc.* **1990**, *112*, 1289.
- (36) Jordan, R. F. *Adv. Organomet. Chem.* **1991**, *32*, 325.
- (37) Crowther, D. J.; Borkowsky, S. L.; Swenson, D.; Meyer, T. Y.; Jordan, R. F. *Organometallics* **1993**, *12*, 2897.
- (38) Bochmann, M.; Wilson, L. M. *J. Chem. Soc. Chem. Comm.* **1986**, 1610.
- (39) Bochmann, M.; Wilson, L. M.; Hursthouse, M. B.; Short, R. L. *Organometallics* **1987**, *6*, 2556.
- (40) Bochmann, M.; Wilson, L. M.; Hursthouse, M. B.; Motevalli, M. *Organometallics* **1988**, *7*, 1148.
- (41) Bochmann, M.; Jaggar, A. J.; Nivholls, J. C. *Angew. Chem., Int. Ed. Engl.* **1990**, *29*, 780.
- (42) Bochmann, M.; Jaggar, A. J. *J. Organomet. Chem.* **1992**, *424*, C5.
- (43) Bochmann, M.; Lancaster, S. J. *J. Organomet. Chem.* **1992**, *434*, C1.
- (44) Eshuis, J. J. W.; Tan, Y. Y.; Teuben, J. H.; Renkema, J. *J. Mol. Cat. Chemical* **1990**, *62*, 277.
- (45) Eshuis, J. J. W.; Tan, Y. Y.; Meetsma, A.; Teuben, J. H.; Renkema, J.; Evens, G. *Organometallics* **1990**, *11*, 362.
- (46) Taube, R.; Krukowka, L. *J. Organomet. Chem.* **1988**, *347*, C9.

- (47) Hlatky, G. G.; Eckman, R. R.; Turner, H. W. *Organometallics* **1992**, *11*, 1413.
- (48) Yang, X.; Stern, C. L.; Marks, T. J. *Organometallics* **1991**, *10*, 840.
- (49) Yang, X.; L, S. C.; Marks, T. J. *J. Am. Chem. Soc.* **1991**, *113*, 3623.
- (50) Yang, X.; L, S. C.; Marks, T. J. *Angew. Chem., Int. Ed. Engl.* **1992**, *31*, 1375.
- (51) Yang, X.; Stern, C. L.; Marks, T. J. *J. Am. Chem. Soc.* **1994**, *116*, 10015.
- (52) Kaminsky, W.; Kopf, J.; Sinn, H.; Vollmer, H.-J. *Angew. Chem., Int. Ed. Engl.* **1976**, *15*, 630.
- (53) Anderson, A.; Cordes, H.-G.; Herwig, J.; Kaminsky, W.; Merck, A.; Mottweiler, R.; Pein, J.; Sinn, H.; Vollmer, H.-J. *Angew. Chem., Int. Ed. Engl.* **1976**, *15*, 630.
- (54) Reichert, K. H.; Meyer, K. R. *Makromol. Chem.* **1973**, *169*, 163.
- (55) Long, W. P.; Breslow, D. S. *Justus Liebigs Ann. Chem.* **1975**, 463.
- (56) Sinn, H.; Kaminsky, W. *Adv. Organomet. Chem.* **1980**, *18*, 99.
- (57) Sishta, C.; Hathorn, R. M.; Marks, T. J. *J. Am. Chem. Soc.* **1992**, *114*, 1112.
- (58) Horton, A. D.; Frijns, J. H. G. *Angew. Chem., Int. Ed. Engl.* **1991**, *30*, 1152.
- (59) Hlatky, G. G.; Turner, H. W.; Eckman, R. R. *J. Am. Chem. Soc.* **1989**, *111*, 2728.
- (60) Hlatky, G. G.; Upton, D. J.; Turner, H. W. In (Exxon) US Pat. Appl. 459921: 1990.
- (61) Chien, J. C. W.; Tsai, W.-M.; Rausch, M. D. *J. Am. Chem. Soc.* **1991**, *113*, 8570.
- (62) Ewen, J. A.; Elder, M. J. In US Pat. Appl. 419017: 1989.
- (63) Zambelli, A.; Giongo, M. G.; Natta, G. *Makromol. Chem.* **1968**, *112*, 183.
- (64) Zambelli, A.; Gatti, G.; Sacchi, C.; Crain Jr., W. O.; Roberts, J. D. *Macromolecules* **1971**, *4*, 475.
- (65) Corradini, P.; Barone, V.; Fusco, R.; Guerra, G. *J. Catal.* **1982**, *77*, 32.
- (66) Zambelli, A.; Sacchi, M. C.; Locatelli, P.; Zannoni, G. *Macromolecules* **1982**, *15*, 211.
- (67) Zambelli, A.; Locatelli, P.; Sacchi, M. C.; Tritto, I. *Macromolecules* **1982**, *15*, 831.
- (68) Soga, K.; Shiono, T.; Takemura, S.; Kaminsky *Makromol. Chem., Rapid Comm* **1987**, *8*, 305.
- (69) Reiger, B.; Chien, J. C. W. *Polym. Bull.* **1987**, *21*, 159.
- (70) Toyota, A.; Tsutsui, T.; Kashiwa, N. *J. Mol. Cat.* **1989**, *56*, 483.

- (71) Grassi, A.; Zambelli, A.; Resconi, E.; Albizzati, E.; Mazzocchi, R. *Macromolecules* **1988**, *21*, 617.
- (72) Tsutsui, T.; Mizuno, A.; Kashiwa, N. *Makromol. Chem.* **1989**, *190*, 1177.
- (73) Asakura, T.; Nakayama, N.; Demura, M.; Asano, A. *Macromolecules* **1992**, *25*, 4876.
- (74) Spaleck, W.; Küber, F.; Winter, A.; Rohrmann, J.; Bachmann, B.; Antberg, M.; Dolle, V.; Paulus, E. F. *Organometallics* **1994**, *13*, 954.
- (75) Stehling, U.; Diebold, J.; Kirsten, R.; Röhl, W.; Brintzinger, H. H.; Jüngling, S.; Mülhaupt, R.; Langhauser, F. *Organometallics* **1994**, *13*, 964.
- (76) Kashiwa, N. *Polymer* **1980**, *12*, 603.
- (77) Kashiwa, N.; Yoshitake, J. *Makromol. Chem.* **1986**, *120*, 73.
- (78) Kaminsky, W.; Miri, M.; Sinn, H.; R, W. *Makromol. Chem. Rapid Commun.* **1983**, *4*, 417.
- (79) Flory, P. J. *Principles of Polymer Chemistry*; Cornell University Press: Ithaca, 1986.
- (80) Sinn, H.; Kaminsky, W.; Vollmer, H.-J.; Woldt, R. *Angew. Chem., Int. Ed. Engl.* **1980**, *19*, 396.
- (81) Herwig, J.; Kaminsky, W. *Polym. Bull.* **1983**, *9*, 464.
- (82) Kaminsky, W. *Naturwissenschaften* **1984**, *71*, 93.
- (83) Tsutsui, T.; Mizuno, H. *Polymer* **1989**, *30*, 428.
- (84) Kaminsky, W.; Ahlers, A.; Möller-Lindenhof, N. *Angew. Chem., Int. Ed. Engl.* **1989**, *28*, 1216.
- (85) Resconi, L.; Piemontesi, F.; Francisocono, G.; Abis, L.; Fiorani, T. *J. Am. Chem. Soc.* **1992**, *114*, 1025.
- (86) Jüngling, S.; Mülhaupt, R.; Stehling, U.; Brintzinger, H. H.; Fischer, D.; Langhauser, F. *J Polym. Sci.: Part A: Polym. Chem.* **1995**,
- (87) Resconi, L.; Fait, A.; Piemontesi, F.; Colonnaesi, M.; Rychlicki, H.; Zeigler, R. *Macromolecules* **1995**, *28*, 6667.
- (88) Resconi, L.; Piemontesi, F.; Camurati, I.; Rychlicki, H.; Colonnaesi, M.; Balboni, D. *Polym. Mater. Sci. Engin.* **1995**, *73*, 516.
- (89) Resconi, L.; Giannini, U.; Albizzati, E.; Piemontesi, F.; Fiorani, T. *ACS Polym. Prepr.* **1991**, *32*, 463.
- (90) Resconi, L.; Jones, R. L.; Rheingold, A. L.; Yap, G. P. A. *Organometallics* **1996**, *15*, 998.
- (91) Hajela, S.; Bercaw, J. E. *Organometallics* **1994**, *13*, 1147.

- (92) Guo, Z.; Swenson, D.; Jordan, R. *Organometallics* **1994**, *13*, 1424.
- (93) Kesti, M.; Waymouth, R. *J. Am. Chem. Soc.* **1992**, *114*, 3565.
- (94) Kaminsky, W.; Külper, K.; Niedoba, S. *Makromol. Chem., Macromol. Symp.* **1986**, *3*, 377.
- (95) Wanatabe, M.; Kuramoto, M.; Tani, N.; Idemitsu, K. In JP 01,207,248: 1989.
- (96) Chien, J.; Wang, B. J. *J. Polym. Sci. Chem. Edu.* **1990**, *28*, 15.
- (97) Resconi, L.; Bossi, S.; Abis, L. *Macromolecules* **1990**, *23*,
- (98) Jeske, G.; Schock, L. E.; Sweoston, P. N.; Schumann, H.; Marks, T. J. *J. Am. Chem. Soc.* **1985**, *107*, 8110.
- (99) Evans, W. J.; DeCoster, D. M.; Greaves, J. *Organometallics* **1996**, *15*, 3210.
- (100) Odian, G. G. *Principles of Polymerization*; Third ed.; John Wiley and Sons, Inc.: New York, 1991.
- (101) Szwarc, M. *Adv. Polym. Sci.* **1960**, *2*, 275.
- (102) Knoll, K.; Schrock, R. R. *J. Am. Chem. Soc.* **1989**, *111*, 7989.
- (103) Saunders, R. S.; Cohen, R. E.; Schrock, R. R. *Macromolecules* **1991**, *24*, 5599.
- (104) Feldman, J. R.; Schrock, R. R. *Prog. Inorg. Chem.* **1991**, *39*, 1.
- (105) Fox, H. H.; Schrock, R. R. *Organometallics* **1992**, *11*, 2763.
- (106) Faust, R.; Kennedy, J. P. *J. Polym. Sci. Chem. Edu.* **1987**, *25*, 1847.
- (107) Higashimura, T.; Sawamoto, M. *Makromol. Chem. Suppl.* **1985**, *12*, 153.
- (108) Kennedy, J. P. *Makromol. Chem., Macromol. Symp.* **1990**, *32*, 119.
- (109) Webster, O. W.; Hertler, W. R.; Sogah, D. Y.; Farnham, W. B.; Rajan-Babu, T. V. *J. Am. Chem. Soc.* **1983**, *105*, 5706.
- (110) Webster, O. W. *Science* **1991**, *251*, 887.
- (111) Collins, S.; Ward, D. G. *J. Am. Chem. Soc.* **1992**, *114*, 5460.
- (112) Bier, G. *Makromol. Chem.* **1964**, *70*, 44.
- (113) Doi, Y.; Ueki, S.; Keii, T. *Macromolecules* **1979**, *12*, 814.
- (114) Doi, Y.; Ueki, S.; Keii, T. *Makromol. Chem.* **1979**, *180*, 1359.
- (115) Schmidt, G. F.; Brookhart, M. *J. Am. Chem. Soc.* **1985**, *107*, 1443.
- (116) Brookhart, M.; DeSimone, J. M.; Grant, B. E.; Tanner, M. J. *Macromolecules* **1995**, *28*, 5378.

- (117) Killian, C. M.; Tempel, D. J.; Johnson, L. K.; Brookhart, M. *J. Am. Chem. Soc.* **1996**, *118*, 11664.
- (118) Mashima, K.; Fujikawa, S.; Tanaka, Y.; Urata, H.; Oshiki, T.; Tanaka, E.; Nakamura, A. *Organometallics* **1995**, *14*, 2633.
- (119) Baumann, R.; Davis, W. M.; Schrock, R. R. *J. Am. Chem. Soc.* **1997**, *119*, 3830.
- (120) Dawkins, J. V. In *Dictionary of Polymer Science* 1991; pp 231.
- (121) Moore, J. C. *J Polym. Sci.: Part A: Polym. Chem.* **1964**, *2*, 835.
- (122) Zambelli, A.; Gatti, G. *Macromolecules* **1978**, *11*, 485.
- (123) Doi, Y.; Nozawa, F.; Murata, M.; Suzuki, S.; Soga, K. *Makromol. Chem.* **1985**, *186*, 1825.
- (124) Canich, J. A.; Turner, H. W. In (Exxon) PCT Int. Appl. WO 92/12162: July 23, 1992.
- (125) Tinkler, S.; Deeth, R. J.; Duncalf, D. J.; McCamley, A. *J. Chem. Soc. Chem. Comm.* **1996**, 2623.
- (126) Longo, P.; Oliva, L.; Grassi, A.; Pellicchia, C. *Makromol. Chem.* **1989**, *190*, 2357.
- (127) Herfert, N.; Fink, G. *Makromol. Chem.* **1992**, *193*, 773.
- (128) Vizzini, J. C.; Chein, J. C. W.; Babu, G. N.; Newmark, R. A. *J. Polym. Sci. A, Polym. Chem.* **1994**, *32*, 2049.
- (129) Solari, E.; Floriani, C.; Chiesi-Villa, A.; Guastini, C. *J. Chem. Soc. Chem. Comm.* **1989**, 1747.
- (130) Gillis, D. J.; Tudoret, M. J.; Baird, M. C. *J. Am. Chem. Soc.* **1993**, *115*, 2543.
- (131) Lancaster, S. J.; Robinson, O. B.; Bochmann, M.; Coles, S. J.; Hursthouse, M. B. *Organometallics* **1995**, *14*, 2456.
- (132) Gillis, D. J.; Quyoum, R.; Tudoret, M.-J.; Wang, Q.; Jeremic, D.; Roszak, A. W.; Baird, M. C. *Organometallics* **1996**, *15*, 3600.
- (133) Babu, G. N.; Newmark, R. A.; Chien, J. C. W. *Macromolecules* **1994**, *27*, 3383.
- (134) Asakura, T.; Demura, M.; Nishiyama, Y. *Macromolecules* **1991**, *24*, 2334.
- (135) Caughlin, E.; Bercaw, J. E. *J. Am. Chem. Soc.* **1992**, *114*, 7606.
- (136) van der Linden, A.; Schaverien, C. J.; Meijboom, N.; Ganter, C.; Orpen, A. G. *J. Am. Chem. Soc.* **1995**, *117*, 3008.
- (137) Asanume, T.; Nishimori, Y.; Ito, M.; Uchikawa, N.; Shiomura, T. *Polym. Bull.* **1991**, *25*, 567.
- (138) Mason, M. R.; Sith, J. M.; Bott, S. G.; Barron, A. R. *J. Am. Chem. Soc.* **1993**, *115*, 4971.

- (139) Harlan, C. J.; Mason, M. R.; Barron, A. R. *Organometallics* **1994**, *13*, 2957.
- (140) Llinas, G. H.; Day, R. O.; Rausch, M. D.; Chien, J. C. W. *Organometallics* **1993**, *12*, 1283.
- (141) Massey, A. G.; Park, A. J. *J. Organomet. Chem.* **1964**, *2*, 245.
- (142) Canich, J. A. In (Exxon) European Patent Application EP-420-436-A1: April 4, 1991.
- (143) Andersen, R. A. *Inorg. Chem.* **1979**, *18*, 2928.
- (144) Bürger, H.; Wiegel, K.; Thewalt, U.; Schomburg, D. *J. Organomet. Chem.* **1975**, *87*, 301.
- (145) Scollard, J. D.; McConville, D. H.; Vittal, J. J. *Macromolecules* **1996**, *29*, 5241.
- (146) Scollard, J. D.; McConville, D. H. *J. Am. Chem. Soc.* **1996**, *118*, 10008.
- (147) Scollard, J. D.; McConville, D. H.; Payne, N. C.; Vittal, J. J. *J. Mol. Cat. Chemical* **1997**, Accepted for publication.

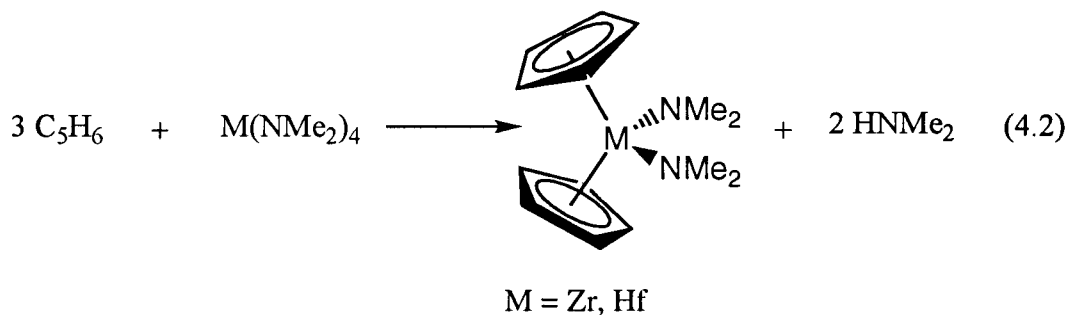
Chapter 4: Chelating Diamide Complexes of Zirconium

Introduction

An abundant number of amide complexes of the group 4 metals have been prepared by transmetallation reactions of MCl_4 compounds with anionic metal amides (Chapter 1). However, these procedures are inefficient and hampered by low yields and tedious purification steps. The transamination reaction, first described by Lappert¹ in 1968, is also a convenient route for the preparation of metal amides. Transamination reactions are usually used to generate heteroleptic amide complexes (eq. 4.1). The primary driving force for these reactions is the elimination of a volatile amine. In general, the more volatile amine is displaced from the metal centre.



The aminolysis reaction, a derivative of the transamination reaction, has been used recently to prepare metallocene derivatives of zirconium. Lappert found that the reaction of $Zr(NMe_2)_4$ with excess cyclopentadiene affords $Cp_2Zr(NMe_2)_2$ and two equivalents of Me_2NH (eq. 4.2).² Jordan has also used the aminolysis reaction to synthesize a series of *ansa*-zirconocenes from $Zr(NMe_2)_4$ and the corresponding bis(cyclopentadiene) (Figure 4.1).³⁻⁷



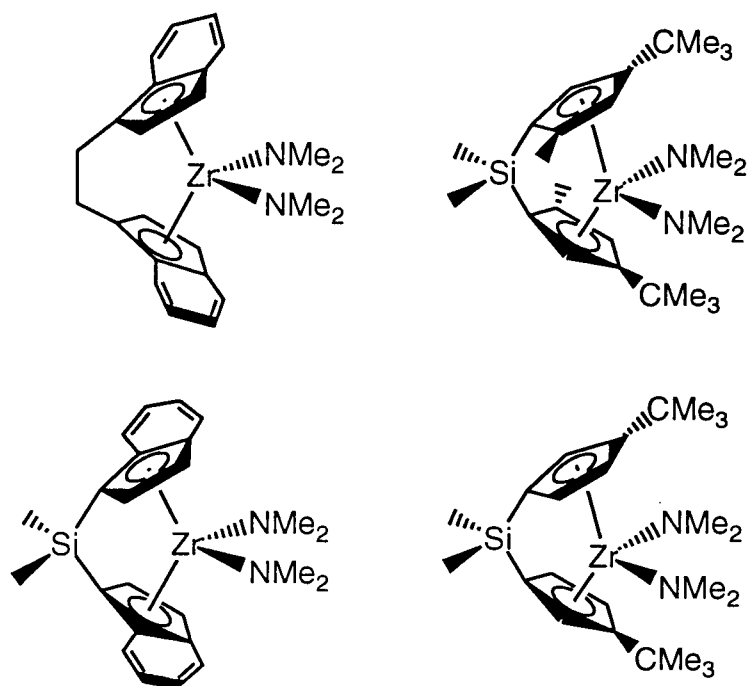
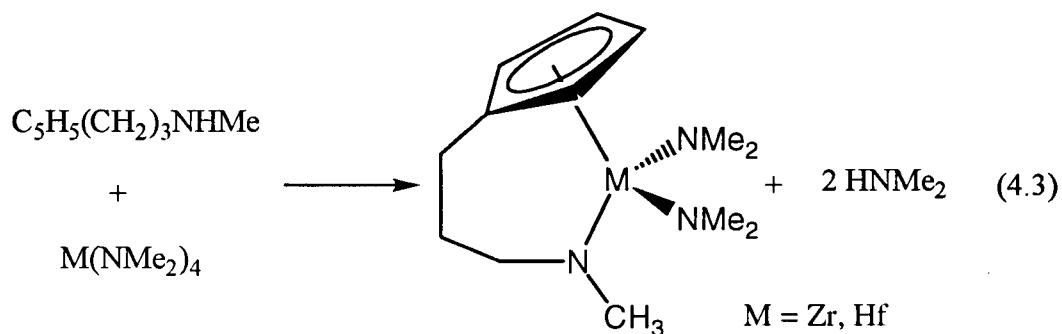


Figure 4.1: Zirconocene complexes formed by aminolysis of $\text{Zr}(\text{NMe}_2)_4$

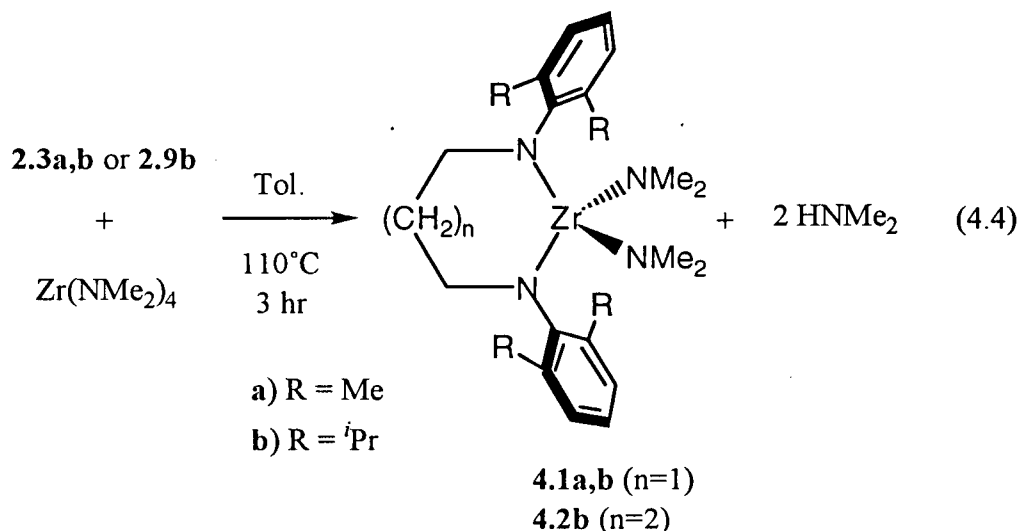
Recently, Teuben has utilized a combination aminolysis–transamination reaction between the cyclopentadiene–amine $\text{C}_5\text{H}_5(\text{CH}_2)_3\text{NHMe}$ and $\text{M}(\text{NMe}_2)_4$ ($\text{M} = \text{Zr}, \text{Hf}$) to afford the complexes $\{\eta^5\text{:}\eta^1\text{-C}_5\text{H}_4(\text{CH}_2)_3\text{NMe}\}\text{M}(\text{NMe}_2)_2$ in high yield (eq. 4.3).⁸



Given these results, it seemed reasonable that a diamine would undergo a transamination reaction with $\text{Zr}(\text{NMe}_2)_4$ to yield the heteroleptic tetraamide.

Results and Discussion

The addition of the diamines **2.3a,b** or **2.9b** to a toluene solution of $\text{Zr}(\text{NMe}_2)_4$ followed by refluxing 3 hours yields the heteroleptic tetraamidozirconium complexes **4.1a,b** or **4.2b** and two equivalents of dimethylamine, respectively (eq. 4.4). Pure complexes **4.1a,b** or **4.2b** were obtained by recrystallization from pentane at -30°C as white crystalline solids in 96–98 % yield.



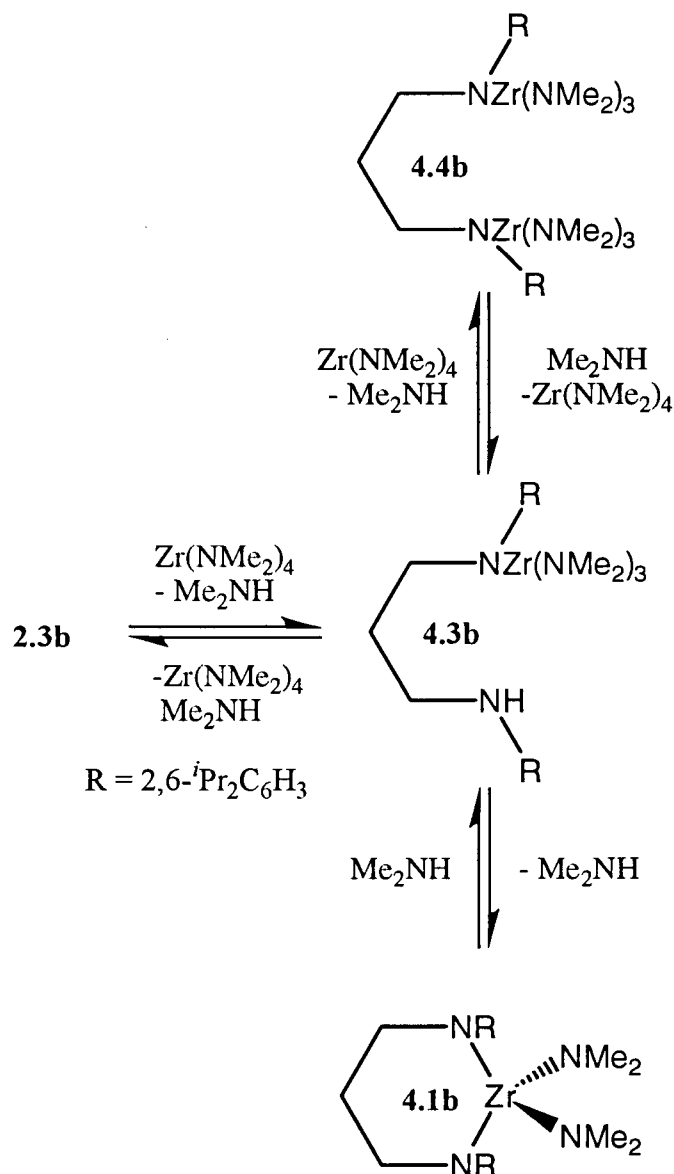
Proton NMR spectroscopy was used to monitor this reaction. If the reaction between compound **2.3b** and $\text{Zr}(\text{NMe}_2)_4$ is carried out in a sealed NMR tube, a mixture of products is formed even though the isolated yield of complex **4.1b** is high. The transamination reaction should be very close to thermoneutral, that is, ΔH° should be very close to zero since complex **4.1b** and $\text{Zr}(\text{NMe}_2)_4$ are both tetra-amides. However the entropy will increase ($\Delta S^\circ > 0$) in the reaction since two equivalents of dimethylamine are evolved. Therefore, for this reaction $\Delta G^\circ < 0$, which indicates it should proceed spontaneously. The driving force for this reaction, in an open system, is the irreversible removal of dimethylamine, a gas, from the reaction mixture.

In a closed system (sealed NMR tube), the dimethylamine is not removed from the reaction and remains dissolved in the solution and occupying the headspace of the NMR tube. Jordan has observed similar results with the reaction of $\text{Zr}(\text{NMe}_2)_4$ and 1,2-

ethylenebis(1-indene).⁴ He reports that a complex equilibrium is set up between monodentate, chelating and bridging species in a closed system. When the system is opened, the dimethylamine is removed, and only the chelating products are obtained.

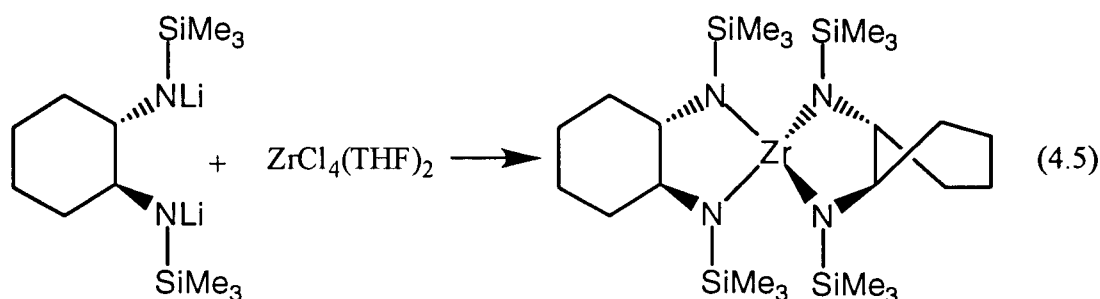
Attempts to isolate the intermediates of this reaction have been unsuccessful. It is likely, in a closed system, that an equilibrium exists between monodentate (**4.3b**), chelating (**4.1b**) and bridging (**4.4b**) complexes. In Scheme 4.1, monodentate complex **4.3b** is initially

Scheme 4.1: Proposed equilibrium in a sealed system between (BAIP)H₂ and Zr(NMe₂)₄



formed by the transamination of one dimethylamide by compound **2.3b**. Complex **4.3b** can then undergo reversible intermolecular aminolysis with a second equivalent of $\text{Zr}(\text{NMe}_2)_4$ to form the bridged species **4.4b**. Alternatively, reversible intramolecular aminolysis can occur giving the desired chelating diamide species **4.1b**. In a sealed NMR tube, the NCH_2 protons of complexes **4.3b** and **4.4b** should appear as first-order triplets in the ^1H NMR spectrum. Unfortunately the frequency where these protons occur in the NMR spectrum overlaps with the resonances of the isopropyl methine. Therefore it is difficult to distinguish a clean first-order triplet. There are seven isopropyl methyl resonances (appearing as doublets) which indicates the presence of at least three products. The complexes **4.1b**, **4.3b** and **4.4b** would give rise to seven doublets. An eighth doublet is also observed, which could be either dimethyl amine or the diamine **2.3b**. The rate of intramolecular aminolysis is generally greater than the rate of intermolecular reaction. Therefore, upon removal of the volatile dimethylamine, only complex **4.1b** is formed in high yield.

The steric bulk of the ligand precludes the formation of the bis(ligand) complex. Attempts to form the bis(ligand) complex by the addition of two equivalents of diamine **2.3b** to $\text{Zr}(\text{NMe}_2)_4$ were unsuccessful resulting in the formation of only complex **4.1b**. Bochmann has observed the formation of bis(ligand) complexes of zirconium with chelating diamide ligands bearing trimethylsilyl groups on nitrogen (eq. 4.5).⁹ These ligands have a much



smaller substitution at the nitrogen atom and the formation of the bis(ligand) complex could not be prevented irrespective of the ligand:Zr ratio.

Proton and $^{13}\text{C}\{^1\text{H}\}$ NMR spectra of complexes **4.1a,b** are consistent with C_{2v} -symmetry. Figure 4.2 contains the ^1H NMR spectrum of complex **4.1b**. Characteristic second-order patterns are observed for the methylene protons (NCH_2 and NCH_2CH_2) of the coordinated ligand in the ^1H NMR spectra of complexes **4.1a,b**. Additionally, the isopropyl methyl groups of the arene of complex **4.1b** are diastereotopic as a consequence of restricted rotation about the $\text{N}-\text{C}_{\text{ipso}}$ bond (Figure 4.3). The aryl group cannot pass through a molecular mirror plane which would lead to equivalent isopropylmethyl groups.

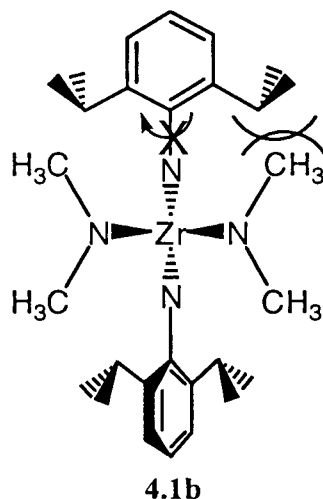


Figure 4.3: Restricted rotation of 2,6-diisopropylphenyl group (propyl backbone omitted for clarity)

Reaction between the butyl linked diamine **2.9b** and $\text{Zr}(\text{NMe}_2)_4$ results in the formation of the heteroleptic tetramido complex **4.2b** and two equivalents of dimethyl amine (eq. 4.4). The ^1H NMR spectrum of complex **4.2b** is similar to that of complex **4.1b**, except for the isopropylmethyl resonances in the ^1H NMR spectrum. A single doublet is observed for these resonances. However, in the $^{13}\text{C}\{^1\text{H}\}$ NMR spectrum there are two resonances attributable to the isopropylmethyl groups. Therefore, there is restricted rotation about the $\text{N}-\text{C}_{\text{ipso}}$ bonds on complex **4.2b**, and the isopropylmethyl resonances in the ^1H NMR spectrum are coincident.

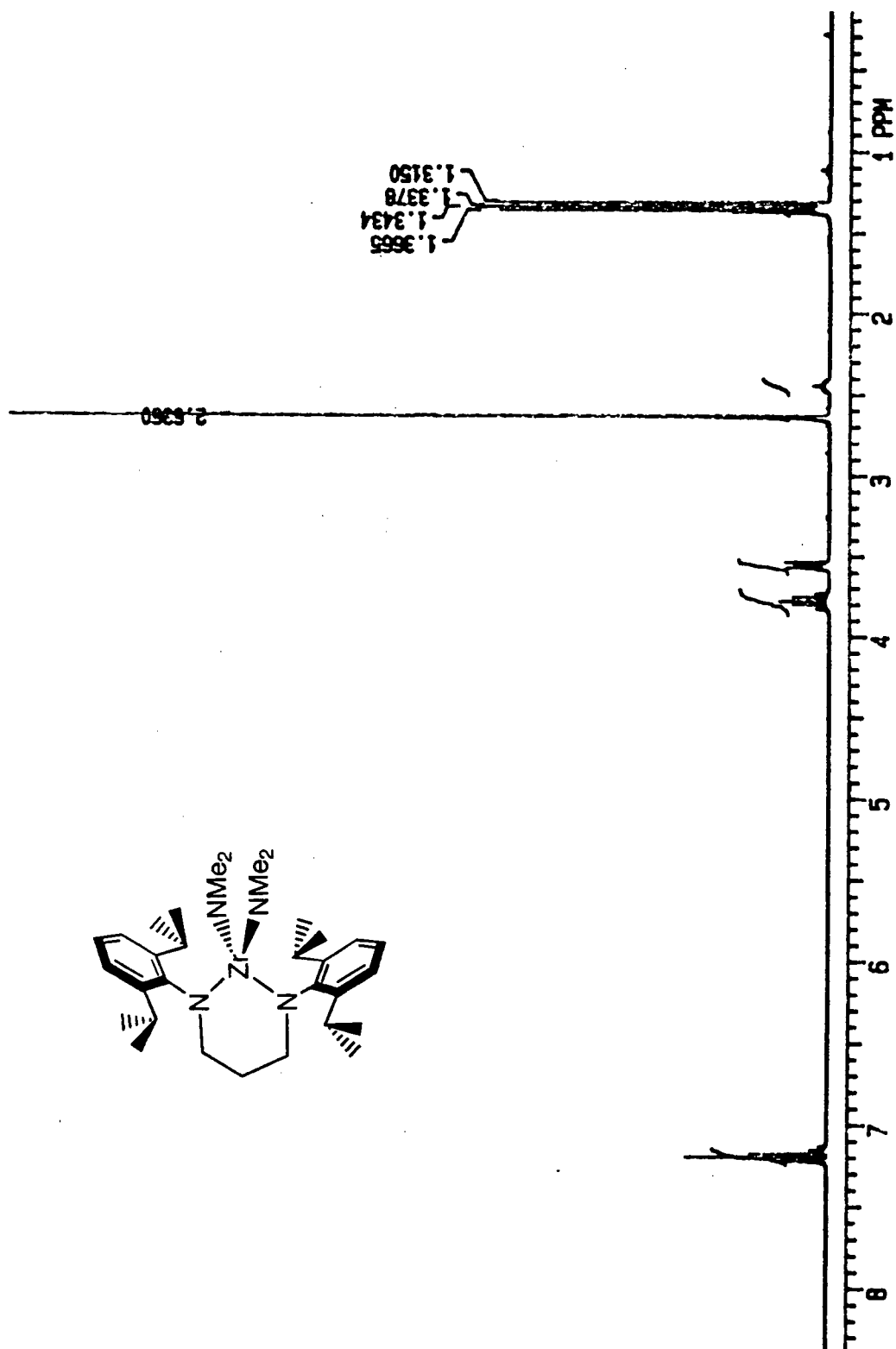


Figure 4.2: 300 MHz ^1H NMR spectrum of complex 4.1b in C_6D_6 at 25°C

The methodology that has been employed for the synthesis of complexes **4.1a,b** and **4.2b** does have a drawback. Although the chemistry of early transition metal amide complexes has been extensively investigated, compared with the halides of early transition metals, these compounds do not provide a direct route to alkyl complexes. Therefore a method to prepare the corresponding dihalide complex was sought.

The stoichiometric addition of acid provides a facile route to the corresponding dichloride complex. Complex **4.1b** reacts with two equivalents of $[\text{Me}_2\text{NH}_2]\text{Cl}$ to afford the octahedral dimethylamine adduct **4.5b** in nearly quantitative yield (Scheme 4.2). Complex **4.5b** is unstable toward loss of dimethylamine, possibly due to steric congestion about the zirconium centre. Proton and $^{13}\text{C}\{^1\text{H}\}$ NMR spectra are consistent with the formation of a single geometrical isomer. Although the structure of complex **4.5b** is speculative as to the location of the dimethylamine and chloride moieties, the C_{2v} symmetry indicated by the ^1H NMR spectrum necessitates a *cis,trans* arrangement (as opposed to *cis,cis*) of the chlorides and dimethylamines about zirconium (Figure 4.4). Unfortunately, on the basis of the available spectroscopic data, it was not possible to deduce which of the two possible *cis,trans* diastereomers was formed.

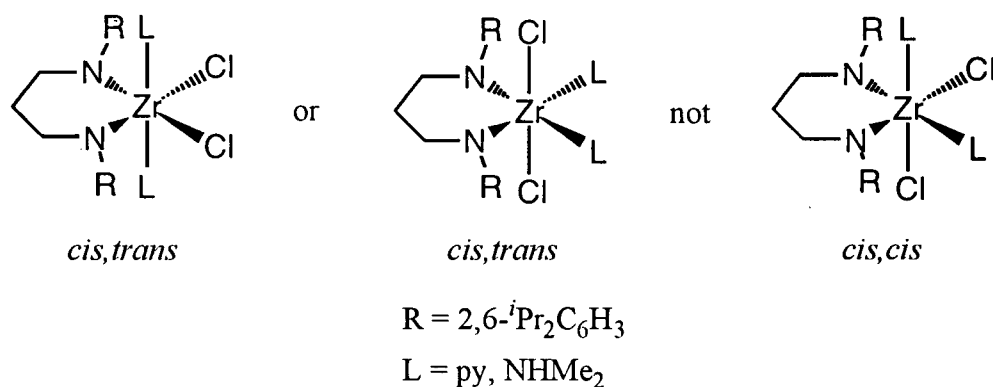
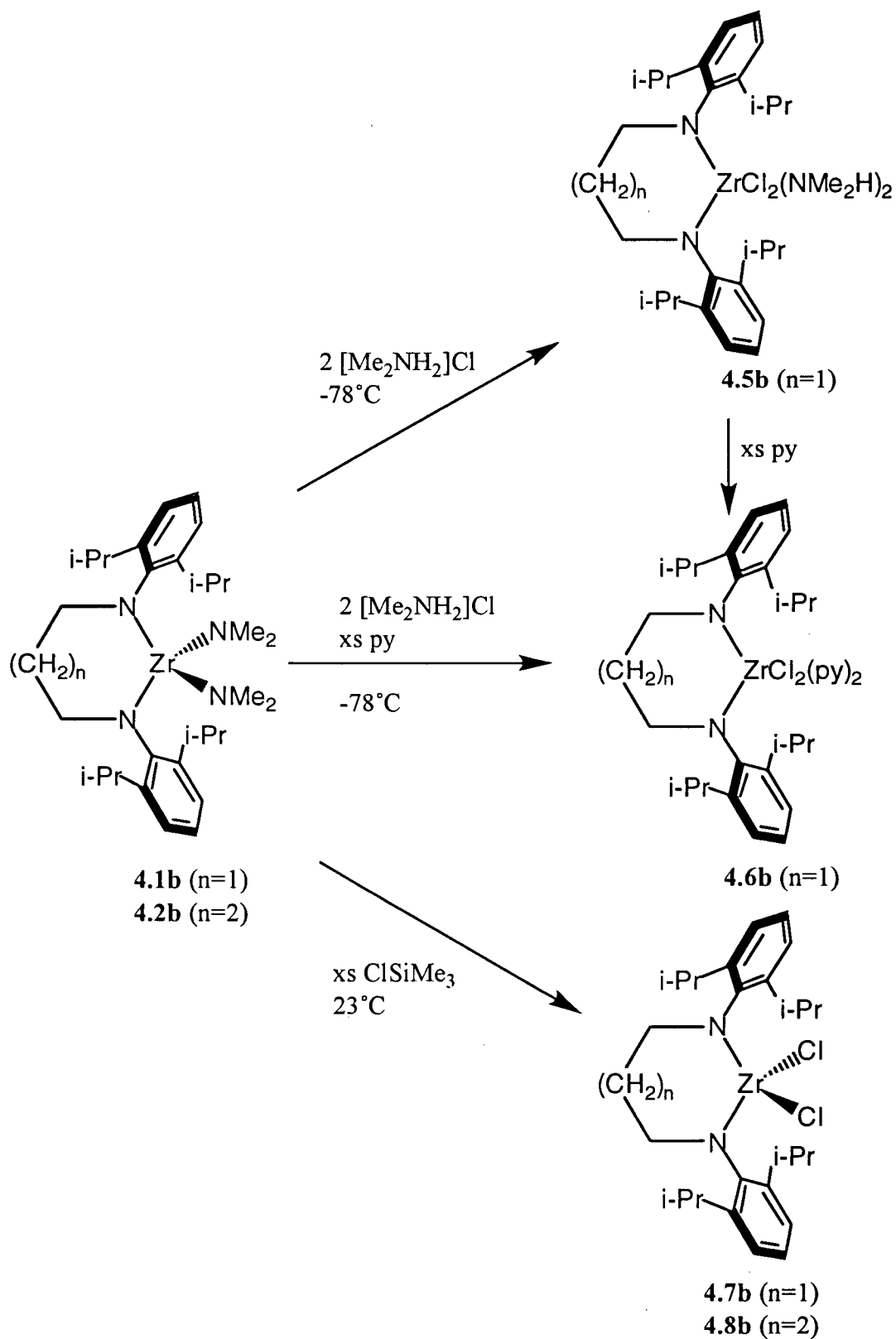
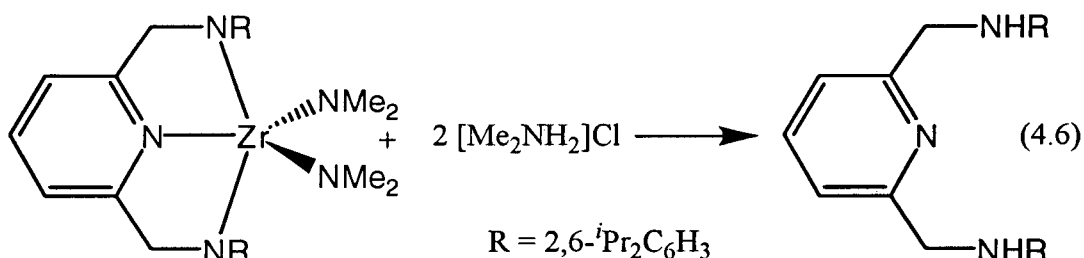


Figure 4.4: Possible diastereomers in complex **4.5b**

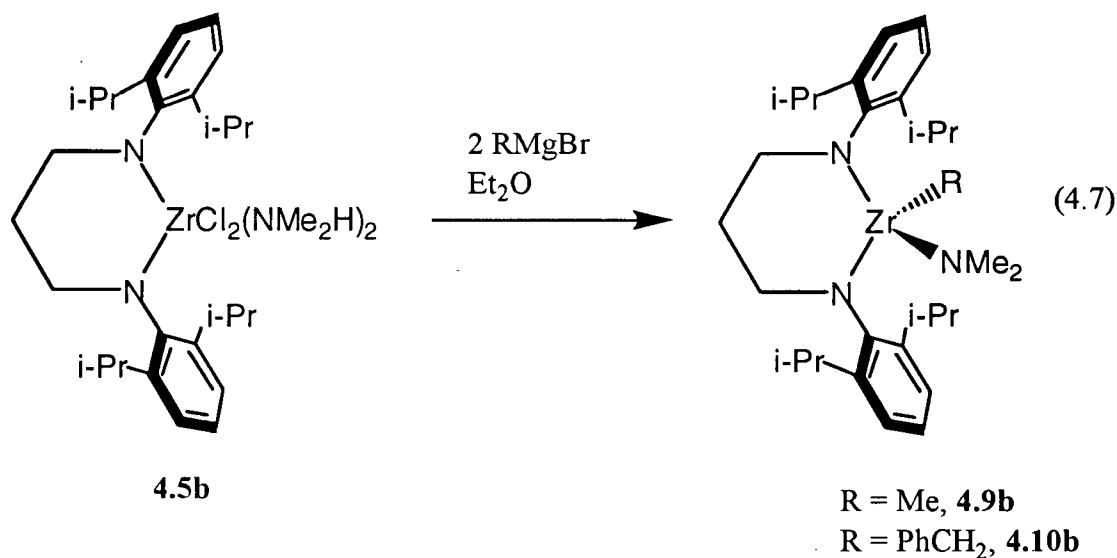
Scheme 4.2: Synthesis of dichlorides from complex **4.1b**



The chelating diamide ligand appears to be stable towards protonolysis in contrast to what has been observed for pyridine diamide derivatives of zirconium bearing ancillary dimethylamido ligands (eq. 4.6),¹⁰ and other chelating amide derivatives of zirconium.¹¹

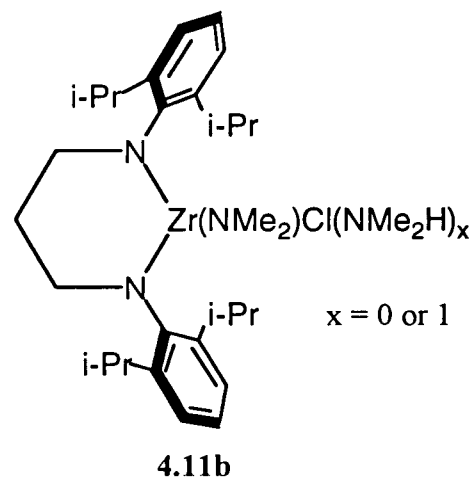


Attempts to form the dimethyl and dibenzyl derivatives of complex **4.5b** were thwarted by the presence of an acidic proton on the dimethylamime ligands. Addition of two equivalents of MeMgBr or PhCH₂MgBr to complex **4.5b** resulted in the formation of the alkyl dimethylamide complexes **4.9b** and **4.10b**, respectively (eq. 4.7). Since complex **4.5b** is



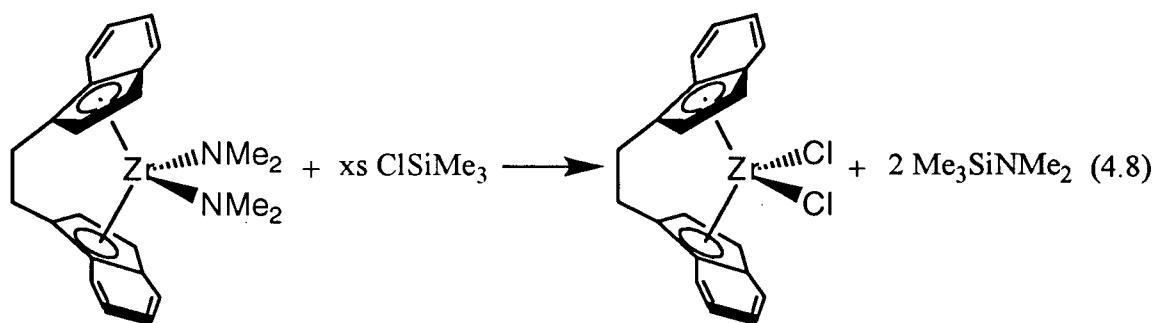
coordinatively saturated, it is likely that the first equivalent of Grignard abstracts a proton from the dimethylamine moiety to give the amido chloride complex **4.11b**. Complex **4.11b** can have a maximum coordination number of five, depending on whether or not the dimethylamine remains coordinated. The second equivalent of Grignard then undergoes a

metathesis reaction with complex **4.11b** resulting in the alkyl(dimethylamido)zirconium complexes **4.9b** and **4.10b**. The isopropylmethyl signals in the ^1H NMR spectra of complexes **4.9b** and **4.10b** appear as four separate doublets. Furthermore, four signals are observed for the NCH_2 and NCH_2CH_2 protons and two signals for the isopropylmethine protons. This is consistent with the C_s -symmetry expected for complexes **4.9b** and **4.10b**. With the aim of preparing zirconium dialkyl derivatives, an alternative base to dimethylamine was sought.



The octahedral bis(pyridine) adduct **4.6b** can be prepared by the addition of pyridine to complex **4.5b**, or by carrying out the protonolysis of complex **4.1b** in the presence of excess pyridine (Scheme 4.2). The ^1H NMR spectrum of complex **4.6b** confirms the presence of only two pyridine molecules and is spectroscopically similar to complex **4.5b**. A downfield shift of the ortho protons and an upfield shift for the meta and para protons of the coordinated pyridine is observed. Local C_{2v} -symmetry is indicated in the ^1H NMR spectrum of complex **4.6b**. Therefore a *cis,trans* arrangement of the chlorides and pyridines similar to complex **4.5b** must exist. Although complex **4.6b** is useful for the preparation of a number of bis(alkyl) derivatives, large alkyl groups (i.e., CH_2SiMe_3 , $\text{CH}_2\text{CMe}_2\text{Ph}$) give rise to products derived from proton abstraction from the coordinated pyridine (*vide infra*).

Jordan has previously reported that ClSiMe_3 reacts with the dimethylamido ligands in *rac*-[EBI] $\text{Zr}(\text{NMe}_2)_2$ to give the corresponding dichloride and two equivalents of $\text{Me}_3\text{SiNMe}_2$ (eq. 4.8).⁵ A similar reaction between complex **4.1b** and ClSiMe_3 should



result in the formation of the base-free dichloride complex. Due to the restricted rotation of the aryl group, it seemed reasonable to expect some kinetic protection of the nitrogens of the chelating diamide ligands (Figure 4.5). This protection should result in the selective removal of the dimethylamido groups.

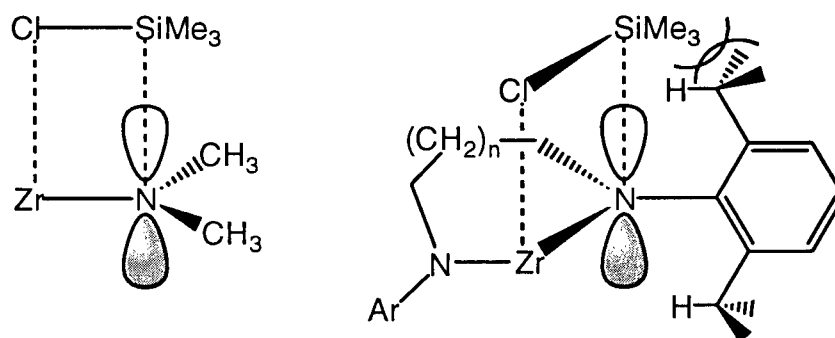


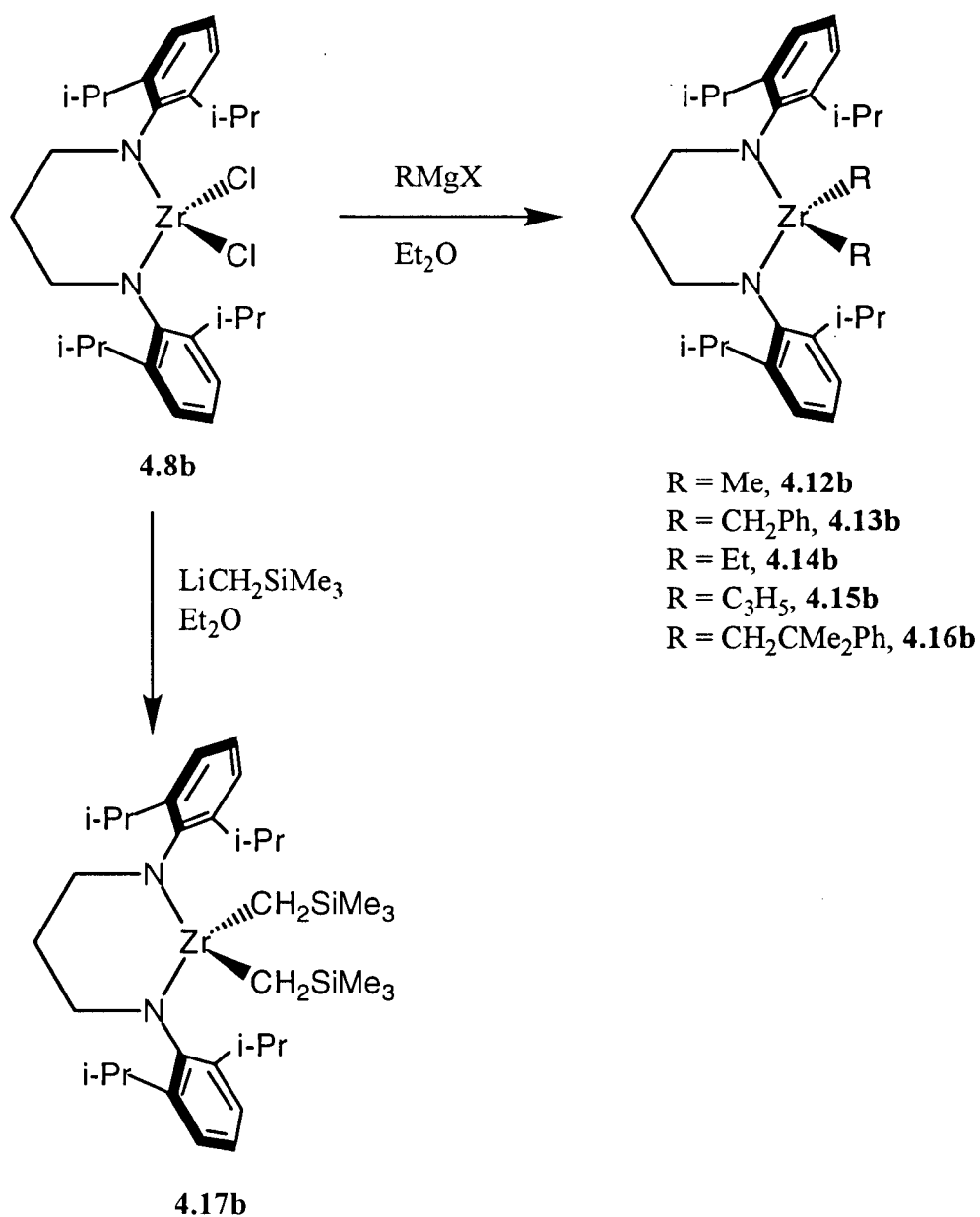
Figure 4.5: Comparison of the kinetic protection afforded the nitrogen atoms in complex **4.1b** and **4.2b**

Addition of excess ClSiMe_3 to complexes **4.1b** or **4.2b** affords the base-free dichloride complexes **4.7b** and **4.8b** in excellent yield (Scheme 4.2). The ^1H NMR spectra of complexes **4.7b** and **4.8b** are slightly broadened indicating the possibility of slow rotation of the aryl groups about the $\text{N}-\text{C}_{\text{ipso}}$ bond or a monomer-dimer equilibrium. Complex **4.7b** is highly electrophilic, irreversibly coordinating bases such as THF, pyridine, and PMe_3 . The spectral resonances of the base-stabilized complexes, in particular the isopropylmethyl signals, sharpen significantly indicating that the restricted $\text{N}-\text{C}_{\text{ipso}}$ bond rotation has been reestablished or that dimeric species are no longer present. With the aim of preparing

zirconium alkyl derivatives, the reaction of complexes **4.5b** and **4.6b** with various alkylating reagents has been investigated.

Addition of the appropriate Grignard, or alkyl lithium reagent to a diethyl ether suspension of complex **4.7b** resulted in the formation of the base-free bis alkyl complexes **4.12b – 4.17b** in yields ranging from 50 to 80% (Scheme 4.3).

Scheme 4.3: Alkylation of complex **4.7b**



The white crystalline dimethyl derivative **4.12b** was isolated from the reaction of complex **4.7b** with two equivalents of MeMgBr. The ^1H and $^{13}\text{C}\{^1\text{H}\}$ NMR spectra of complex **4.12b** display a Zr-CH₃ resonance at 0.42 ppm and a Zr-CH₃ signal at 39.9 ppm, respectively. These data are comparable to the closely related complex [(Me₃Si)₂N]₂ZrMe₂¹² (Zr-CH₃ δ = 0.94 ppm; Zr-CH₃ δ = 48.8 ppm) and others.¹³⁻¹⁵ Additionally, the ^1H NMR spectrum of complex **4.12b** is temperature dependent (Fig. 4.6).

Unlike all other four-coordinate dialkyl complexes bearing the diamido ligand (*vide infra*), the isopropyl methyl signals are broad and featureless at room temperature. Above 40 °C the resonances attributed to the diastereotopic isopropyl methyl groups sharpen to a single doublet, suggesting that the aryl groups pass through a molecular plane of symmetry via free rotation about the N-C_{ipso} bond. The low temperature limiting spectrum (-30 °C) shows two doublets for the isopropyl methyl groups. The temperature at which the two resonances coalesce is determined to be 30 °C. This corresponds to a barrier of rotation about the N-C_{ipso} bond of $\Delta G_{\text{Tc}}^\ddagger = 13.3(5) \text{ kcal mol}^{-1}$.¹⁶

Proton and $^{13}\text{C}\{^1\text{H}\}$ NMR spectroscopy was used to characterize the dibenzyl complex **4.13b**. The benzylic protons display a resonance at 1.95 ppm, however, more interestingly the ortho protons on the phenyl ring of the benzyl moiety appear as a high-field doublet at 6.65 ppm. The ^{13}C NMR spectrum displays a resonance at 64.2 ppm with a $^1J_{\text{C-H}} = 124$ Hz. Although the $^1J_{\text{C-H}}$ for the benzylic carbon is somewhat low, the data supports the presence of some η^2 -benzyl character in the bonding with zirconium.¹⁷⁻²² Perhaps the steric bulk of the diamido ligand prevents the close approach of the ipso carbon to zirconium, thus lowering the observed C-H coupling constant. The C_{2v} symmetry of complex **4.13b** is retained from 20°C to -80°C indicating that either both benzyl groups interact in an η^2 -fashion (less likely) or that they interconvert rapidly between η^2 and η^1 over the measured temperature range (Figure 4.7). However, in the absence of a crystal structure, the bonding involved between the benzyl groups and the metal remains difficult to determine.

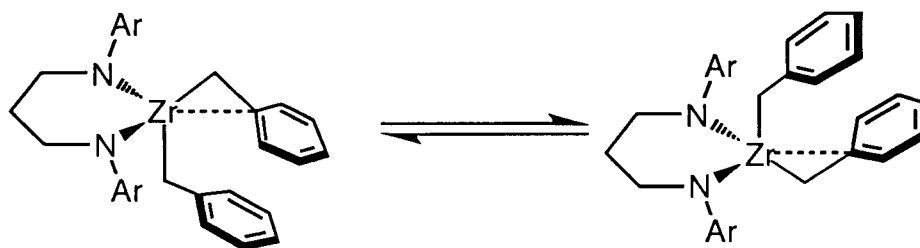


Figure 4.7: The interconversion between η^2 and η^1 benzyl groups

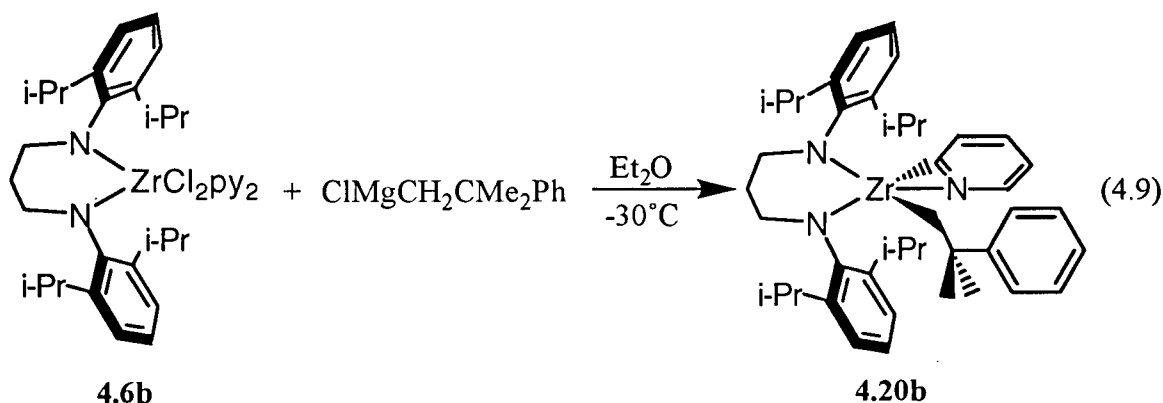
The ^1H NMR spectrum of the diethyl complex **4.14b** reveals diastereotopic isopropyl methyl resonances indicating the restricted rotation about the N-C_{ipso} bond has been restored. The increased size of the ethyl group versus the methyl group is enough to reestablish this feature. Complex **4.14b** does not undergo β -hydrogen elimination at room temperature in contrast to the titanium analogue (*chapter 2*). The ^1H NMR spectrum of complex **4.14b** is similar to the spectra of the other bis(alkyls), with the ethyl signals appearing as a quartet at 0.75 ppm and a triplet at 1.32 ppm.

The bis(allyl) complex **4.15b** could not be fully characterized as it decomposes slowly at room temperature. The ^1H NMR spectrum reveals C_{2v} symmetry and diastereotopic

isopropylmethyl resonances. The allyl resonances support η^3 bonding to the metal centre. The central allyl proton appears as a pentet at 5.61 ppm while the syn and anti protons appear as a doublet at 2.91 ppm. This is consistent with the fluxional nature of π -allyl complexes.

In an effort to explore the limit of bis(alkyl) substitution, larger alkylating reagents were employed. The bis(alkyl) complexes **4.16b** and **4.17b** are obtained as oils in high yield from compound **4.7b** and two equivalents of $\text{PhMe}_2\text{CCH}_2\text{MgCl}$ or $\text{LiCH}_2\text{SiMe}_3$, respectively. As expected, complexes **4.16b** and **4.17b** maintain C_{2v} symmetry in solution as evidenced by their ^1H NMR spectra. The ^1H and $^{13}\text{C}\{^1\text{H}\}$ NMR are spectroscopically similar to the other bis(alkyl) complexes **4.12b** – **4.14b**. The bis(neophyl) formulation of complex **4.14b** is unexpected given that the titanium analogue was not preparable (only the neophyl chloride was isolated). This is likely a result of the larger zirconium ion as compared to the titanium (the Zr–N bonds in complex **4.20b** (*vide infra*) are about 10 % longer than the Ti–N bonds in complex **2.10b** (Chapter 2)).

Starting from the bis(pyridine) dichloride complex **4.6b**, complexes **4.12b** – **4.15b** can be synthesized in the analogous manner. In contrast to the alkylation chemistry of the base-free dichloride **4.7b**, the reaction of complex **4.6b** with two equivalents of $\text{PhMe}_2\text{CCH}_2\text{MgCl}$ did not give the anticipated bis(neophyl) complex, but rather the η^2 -pyridyl complex **4.20b** (eq. 4.9). Spectroscopic data suggest that complex **4.20b** has C_s



symmetry (Figure 4.8) as evidenced by the four resonances observed for the methylene protons (NCH_2 and NCH_2CH_2) in the ^1H NMR spectrum (Figure 4.9). The isopropyl methyl

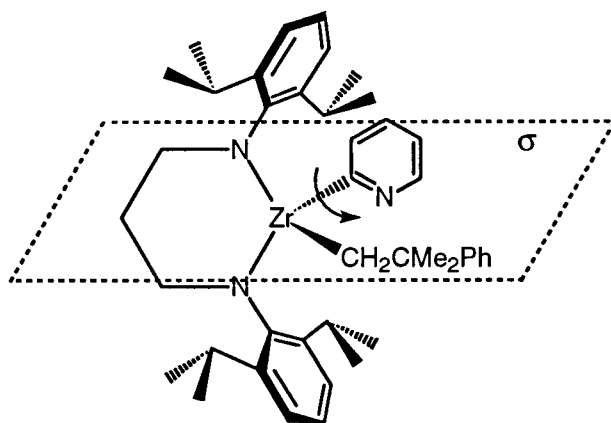


Figure 4.8: Mirror symmetry element associated with η^2 -pyridyl complex **4.20b**

resonances appear as four doublets in the ^1H NMR spectrum due to the restricted rotation about the N-C_{ipso} bond. The ^1H NMR spectrum exhibits resonances for the η^2 -pyridyl moiety that are comparable to other known complexes.²³⁻²⁵ It is interesting that a pyridyl complex is formed only with large alkylating reagents. Resonances attributable to an η^2 -pyridyl moiety were also observed in the crude ^1H NMR spectrum of the reaction between **4.6b** and two equivalents of $\text{LiCH}_2\text{SiMe}_3$. However, due to its high solubility, this complex proved difficult to isolate from the other byproducts.

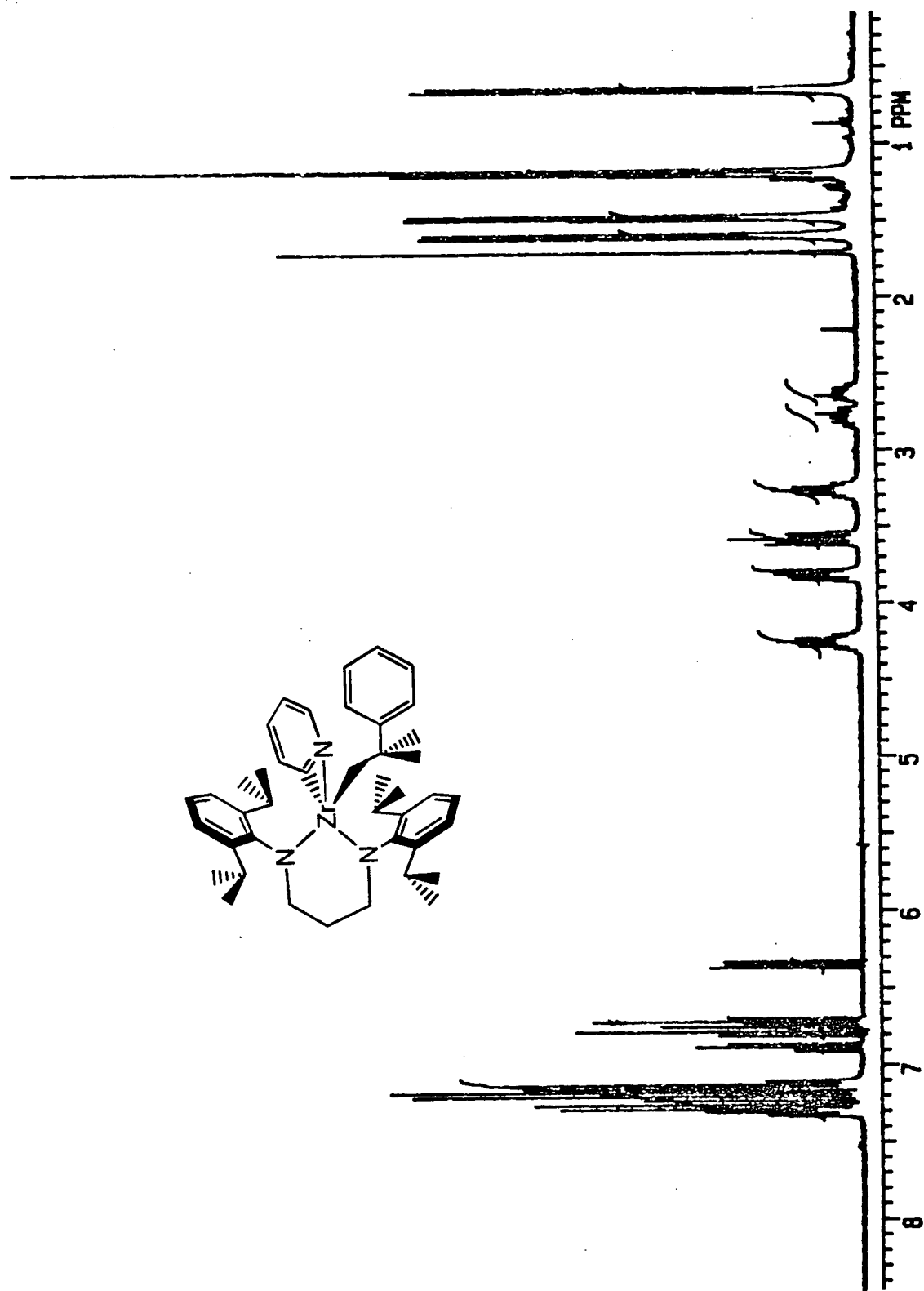


Figure 4.9: 300 MHz ^1H NMR spectrum of pyridyl complex 4.20b in C_6D_6 at 23°C

Colourless single crystals of complex **4.20b** suitable for an X-ray analysis were grown from a saturated pentane solution at -30°C . The molecular structure and core of complex **4.20b** are shown in Figure 4.10, while selected bond distances and angles are shown in Table 4.1. Overall the structure is best described as a edge-capped tetrahedron with the pyridyl nitrogen occupying the capping position. The Zr1–N3–C30 ring is structurally similar to the Zr–N–C ring in the cationic complex $[\text{Cp}_2\text{Zr}(\eta^2\text{-picolyl})(\text{PMe}_3)](\text{BPh}_4)$.²⁵ Each amide donor in complex **4.20b** is sp^2 -hybridized as evidenced by the sum of the angles about each nitrogen ($\text{N1} = 360.0^{\circ}$ and $\text{N2} = 359.8^{\circ}$). The molecular C_1 symmetry of complex **4.20b** coupled with the spectroscopically observed C_s symmetry in solution suggests that rapid rotation about the Zr1–C30 bond is occurring on the NMR time scale. The C_s symmetry of compound **4.20b** is maintained down to -80°C .

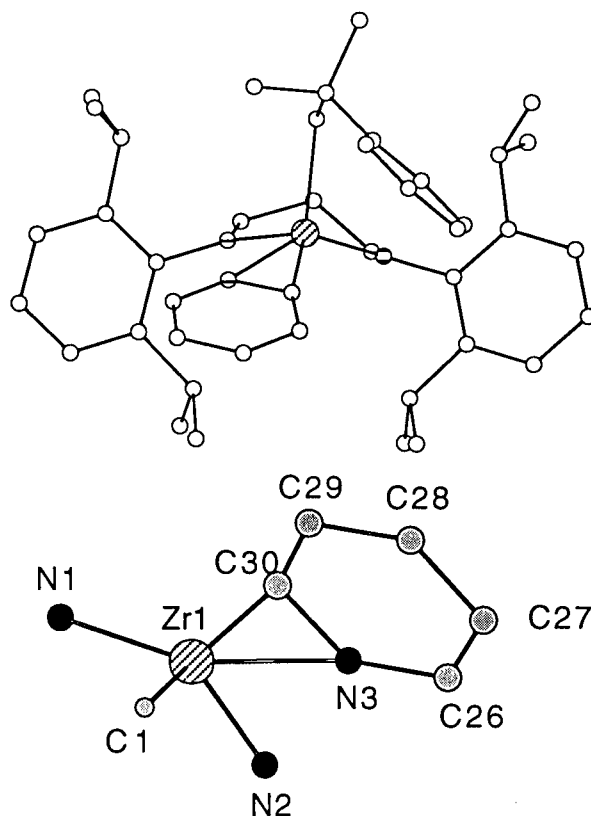
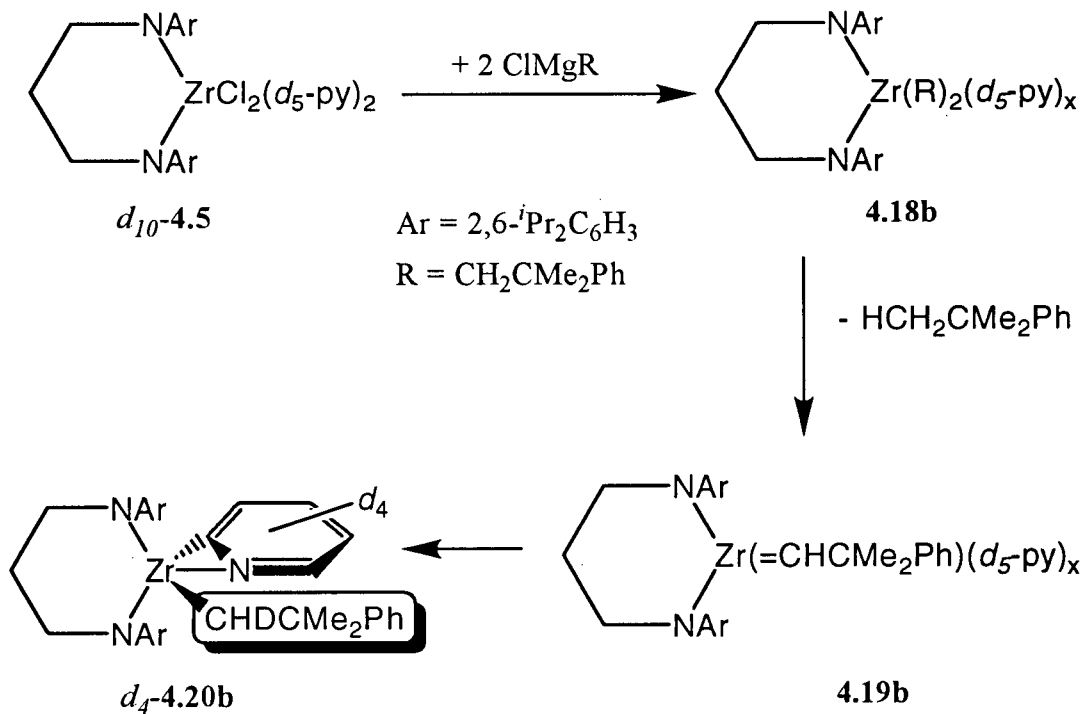


Figure 4.10: Chem 3D Plus representations of complex **4.20b** and the core of **4.20b**

Table 4.1: Selected bond distances (Å) and angles (°)			
Zr1-N1	2.050(9)	N1-Zr1-N2	95.4(4)
Zr1-N2	2.031(9)	C30-Zr1-C1	113.2(4)
Zr1-C1	2.268(12)	N1-Zr1-Cl	103.9(4)
Zr1-C30	2.219(12)	N1-Zr1-C30	120.8(4)
Zr1-N3	2.260(10)		

In order to study the mechanism of formation of the pyridyl complex, a series of experiments was carried out. There are at least two possibilities that can account for the formation of complex **4.20b**. Substituting d_5 -pyridine for pyridine in complex **4.6b** readily discriminates between two of the possible mechanisms. One such possibility is the formation of a bis(neophyl) complex followed by α -elimination to yield an intermediate zirconium alkylidene.²⁶ This intermediate could then activate the C-H bond of a pyridine molecule to give the pyridyl complex; this possible mechanism is shown in Scheme 4.4.

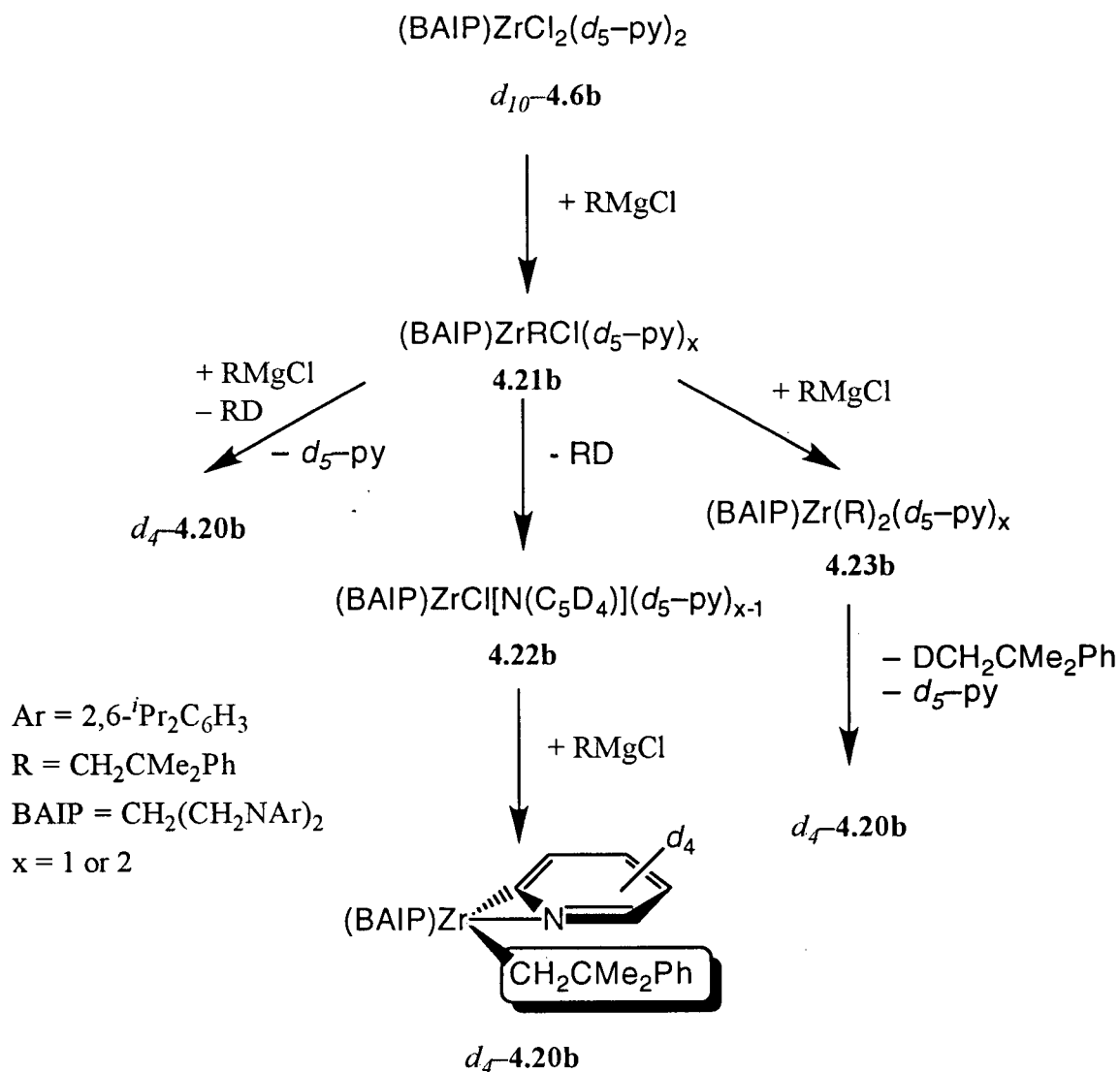
Scheme 4.4: Formation of complex d_4 -**4.20b** via an intermediate alkylidene complex



An alkylidene complex, although rare for group 4 metals,^{26,27} may arise due to steric crowding of the metal centre.^{28,29} Presumably, complex **4.18b** would have at least one pyridine coordinated since the bis(neophyl) complex **4.14b** is a stable compound. Transferring a deuterium from *d*₅-pyridine to the alkylidene would yield a *d*₁-neophyl group. The deuterium labeling experiment showed no deuterium incorporation into the remaining neophyl group (by ¹H and ²H NMR spectroscopy).

Alternatively, a neophyl group (either coordinated or as the Grignard) could abstract a proton from the coordinated pyridine in complex **4.6b** (Scheme 4.5).

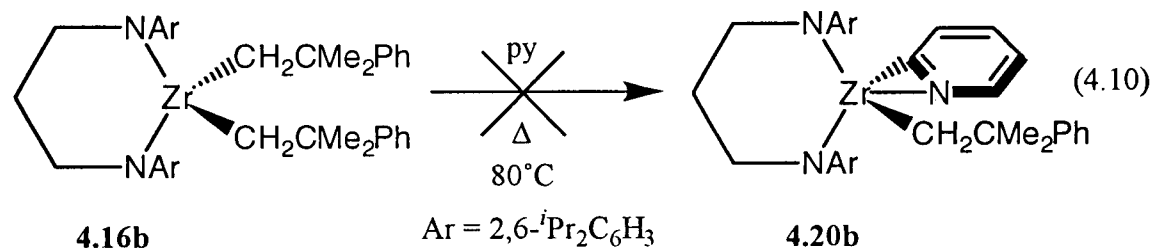
Scheme 4.5: Formation of complex *d*₄-**4.20b** via alkane elimination



The first equivalent of Grignard reacts with complex **4.6b** to give the mono(neophyl)chloride complex **4.21b**. Complex **4.21b** can undertake three different reaction pathways. In the first route, the second equivalent of Grignard acts as a base to abstract a proton from a coordinated pyridine to give the pyridyl complex **4.20b** directly. Similar arguments have been advanced to explain the preparation of $\text{Ta}(=\text{CH}^t\text{Bu})(\text{CH}_2^t\text{Bu})_3$ from $\text{TaCl}_2(\text{CH}_2^t\text{Bu})_3$ and neopentyl lithium.³⁰ Interestingly, Xue has reinvestigated this reaction and found that the elimination takes place via a transient penta(alkyl) derivative, $\text{Ta}(\text{CH}_2^t\text{Bu})_5$.³¹ Therefore, it is unlikely that neophyl Grignard abstracts the proton from coordinated *d*₅-pyridine.

The second route involves direct elimination of *tert*-butylbenzene from intermediate **4.21b** to give the pyridyl chloride complex **4.22b**. The driving force for the elimination of *tert*-butylbenzene would be the relief of steric congestion about the metal centre. Pyridyl complexes have been prepared previously by alkane elimination.²³⁻²⁵ It would appear that this route is a likely possibility.

For the third possibility, the second equivalent of Grignard can react with **4.21b** to give the bis(neophyl) complex **4.23b** which has either 1 or 2 coordinated pyridine ligands. Complex **4.23b** can then eliminate *tert*-butylbenzene to give the pyridyl complex **4.20b**. The third possibility can be excluded based on the following results. The bis(neophyl) complex **4.16b** was heated in neat *d*₅-pyridine to 80°C (eq. 4.10). Surprisingly, no reaction occurs

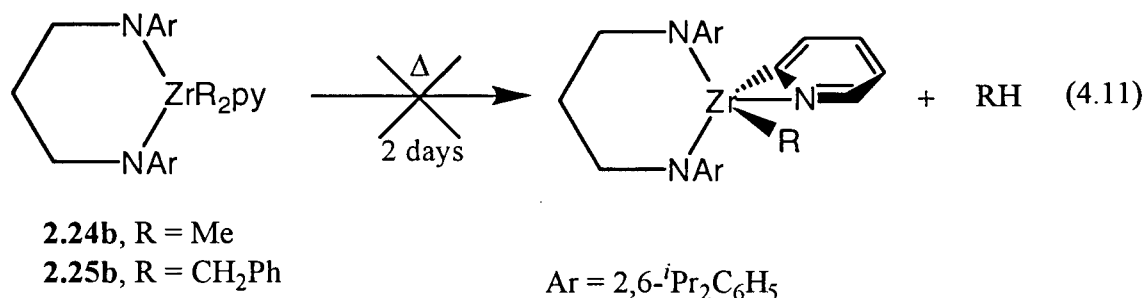


even after several days at 80°C suggesting that (1) pre-coordination of pyridine is required

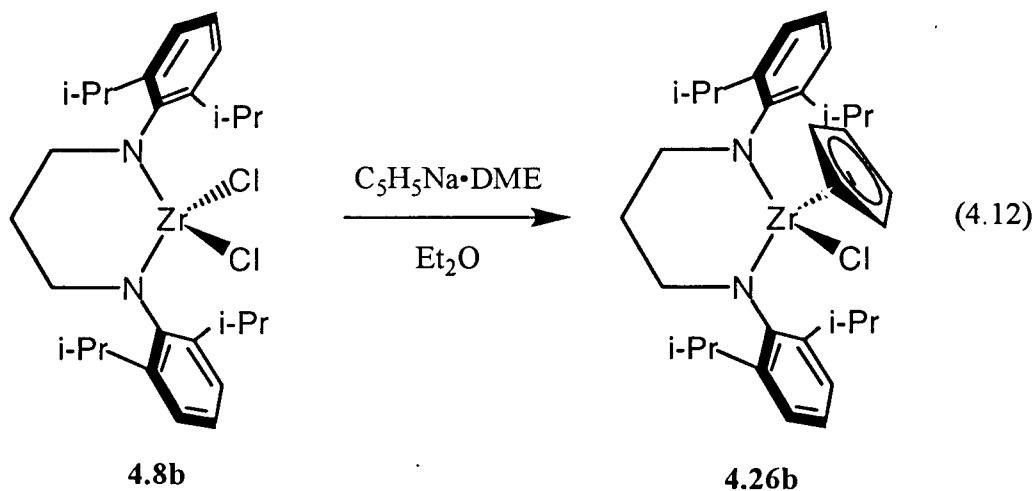
during the formation of complex **4.20b**, and (2) that it is unlikely that the reaction proceeds via a bis(neophyl) intermediate.

Based on these results and the labeling experiment, the following proposal is advanced. The transient monoalkyl derivative **4.21b** loses *tert*-butylbenzene slowly to yield the pyridine-stabilized pyridyl complex **4.22b** (Scheme 4.5). Alkylation of intermediate **4.22b** and loss of pyridine affords complex **4.20b**. Attempts to prepare the mono(neophyl) complex from **4.6b** and one equivalent of $\text{ClMgCH}_2\text{CMe}_2\text{Ph}$ have been unsuccessful leading to intractable material.

The bis(alkyl) monopyrindine complexes **2.24b** and **2.25b**, prepared from complexes **4.12b** and **4.13b** and excess pyridine, have been isolated. However, these species do not eliminate alkane at 80 °C (eq. 4.11). In fact, the pyridine adducts are stable for days at this temperature.

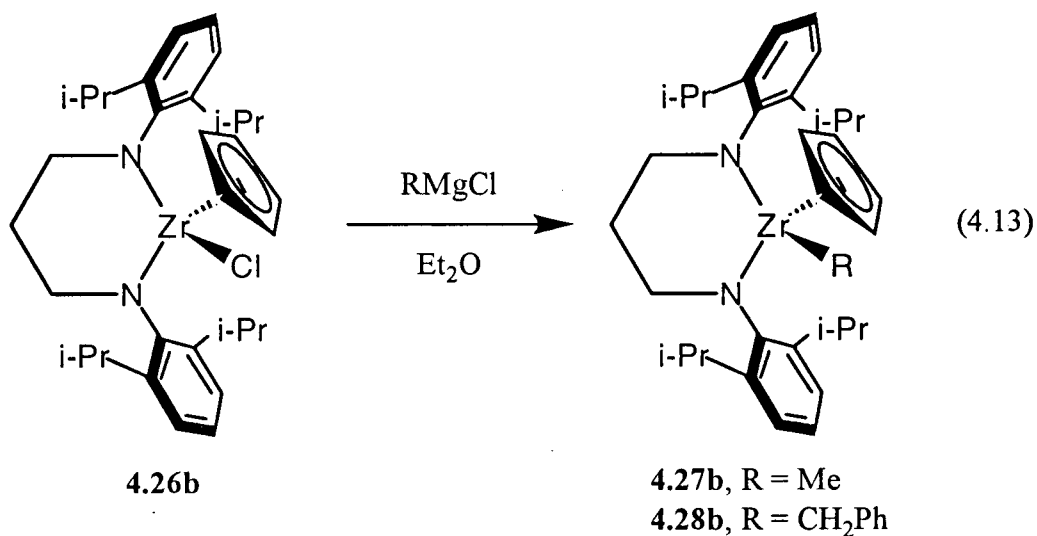


In order to further establish the steric parameters of complex **4.7b**, a mono(cyclopentadienyl) complex was synthesized. Complex **4.7b** reacts with one equivalent of NaCp(DME)^{32} to yield the 16-valence-electron mono(cyclopentadienyl) complex **4.26b** in 94% yield (eq. 4.12). Addition of an excess of NaCp(DME) does not result in the



formation of the bis(cyclopentadienyl) complex. The ^1H NMR spectrum of complex **4.26b** is consistent with a pseudo tetrahedral geometry and local C_s symmetry about zirconium, as indicated by the four isopropylmethyl signals and two isopropylmethine signals. The NCH_2 and NCH_2CH_2 protons also display second-order patterns similar to the C_s -symmetric complexes **4.9b** and **4.10b**.

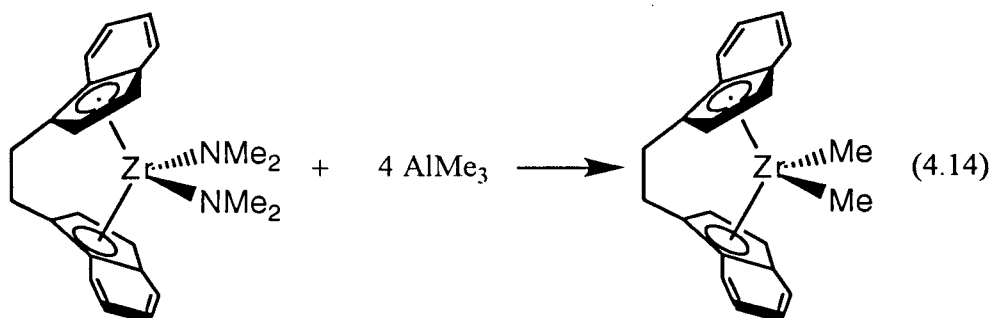
The remaining chloride in the Cp complex **4.26b** can be metathesized with alkylating reagents such as MeMgCl and PhCH_2MgCl to afford the Cp-alkyl derivatives **4.27b** and **4.28b** (eq. 4.13). The ^1H NMR spectrum confirms that local C_s symmetry is retained in these



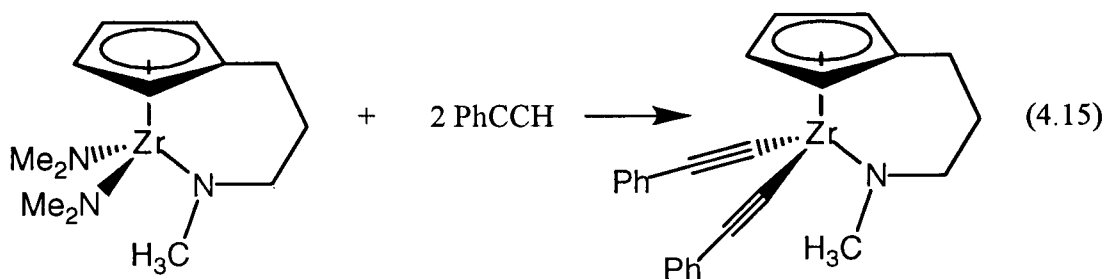
compounds with the methyl singlet occurring at 0.36 ppm and the benzylic singlet at 2.48

ppm. The cyclopentadienyl group has a deshielding effect on the benzylic protons as evidenced by an upfield shift from 1.95 ppm in the dibenzyl complex **2.13b** to 2.48 ppm in complex **2.28b**.

Although the reaction of metal–halide complexes with alkylating reagents is the most common method for the synthesis of metal–carbon bonds, there are other methods available for preparing metal–alkyl derivatives directly from amido complexes. For example, Jordan has prepared dimethylzirconocene complexes from bis(dimethylamido)zirconocene complexes and trimethylaluminum (eq. 4.14).⁵ The reaction of zirconium dimethylamido



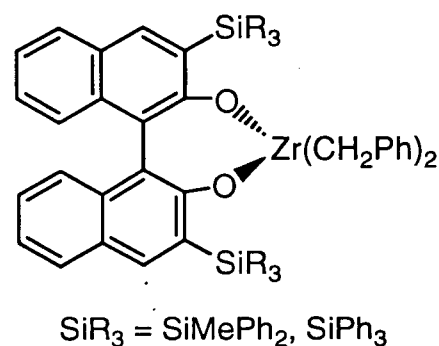
complex **4.1b** with $[\text{Me}_2\text{NH}_2]\text{Cl}$, a weak acid, was utilized to obtain the zirconium dichloride complexes **4.5b** and **4.6b**. The addition of a weakly acidic hydrocarbon to complex **4.1b** may result in the direct formation of a zirconium alkyl complex. Teuben has previously prepared acetylide complexes from zirconium dimethylamido complexes (eq. 4.15).⁸



The reactivity of acetylenes with late transition metals has been extensively investigated and $[2 + 2 + 2]$ cycloadditions are a common reaction pathway.³³ Although the reactivity of early transition metals with acetylenes has been explored, cyclic trimerizations

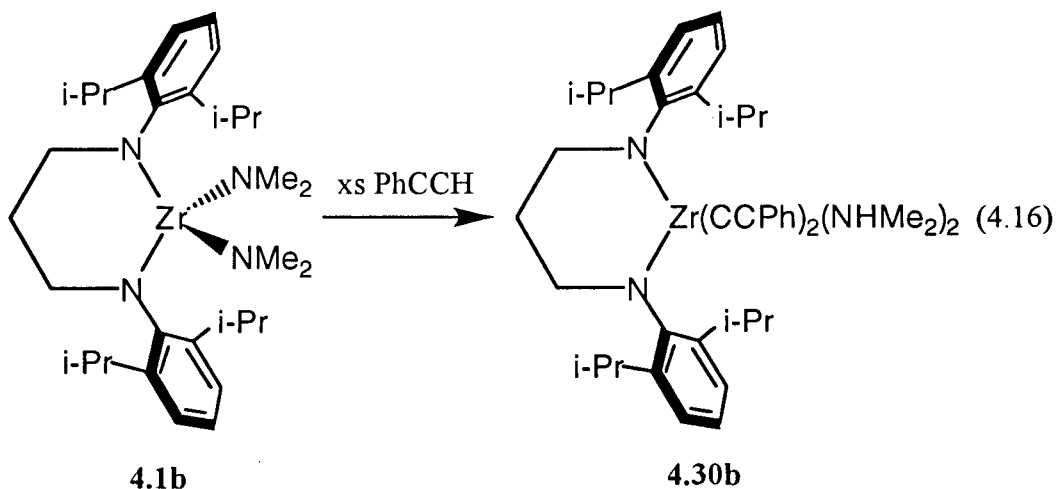
to substituted benzenes are rarely observed.³⁴⁻³⁸

Schaverien has recently reported the cyclotrimerization of alkynes by chelating binaphtholate complexes of zirconium (**4.29**).³⁹ The formation of a bis(acetylide) derivative of complex **4.1b** may lead to a route for the catalytic cyclotrimerization of alkynes.

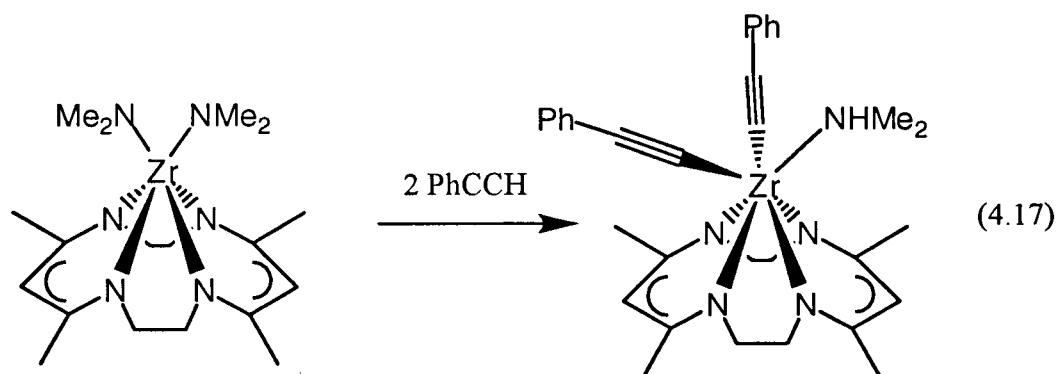


4.29

The addition of excess phenylacetylene to the bis(dimethylamido) complex **4.1b** results in protonation of both dimethylamido groups to form the bis(acetylide) bis(dimethylamine) adduct **4.30b** (eq. 4.16). The presence of two equivalents of coordinated dimethylamine was confirmed by ¹H NMR spectroscopy.

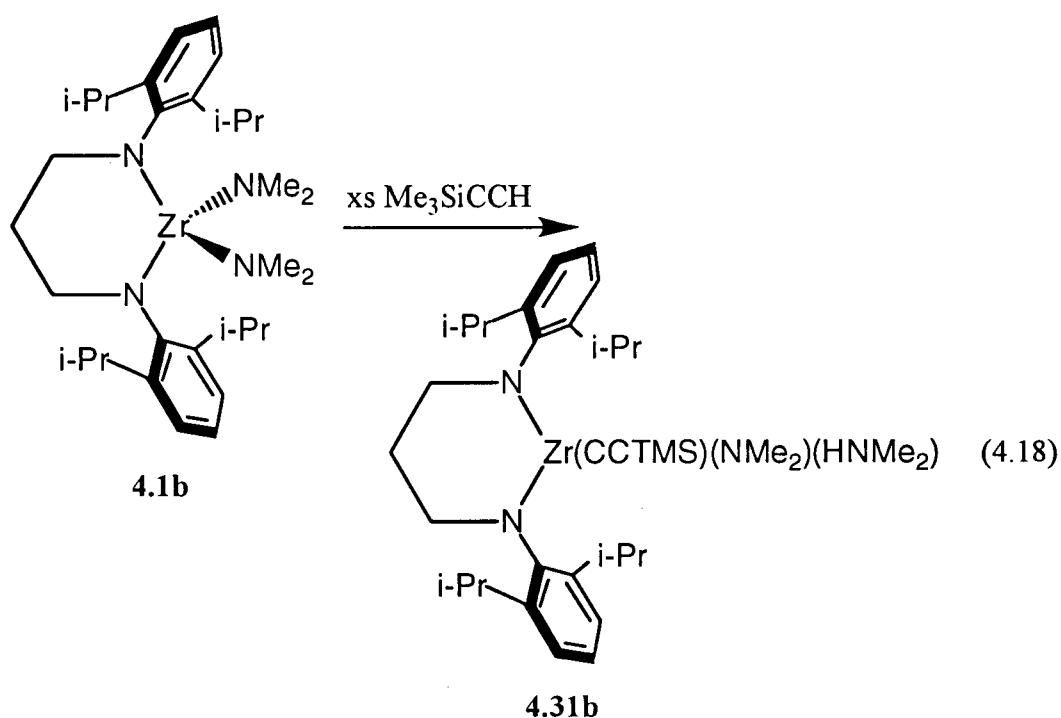


Jordan has reported the protonation of dimethylamido groups by phenylacetylene followed by coordination of dimethylamine (eq. 4.17).⁴⁰



The ^1H NMR spectrum of **4.30b** reveals a doublet at 2.07 ppm for the methyl groups of the dimethylamine moiety and the NH signal appears as a broad multiplet at 2.46 ppm. The $^{13}\text{C}\{^1\text{H}\}$ NMR spectrum of **4.30b** displays resonances at δ 148.7 and 106.9, which are assigned to the α and β alkynyl carbons, respectively. These values compare well to other acetylide complexes of early transition metals.^{8,40,41} The ^1H and $^{13}\text{C}\{^1\text{H}\}$ NMR data indicate that complex **4.30b** has C_{2v} -symmetry on the NMR time scale. This necessitates a *cis,trans* arrangement of the acetylides and dimethylamines about zirconium.

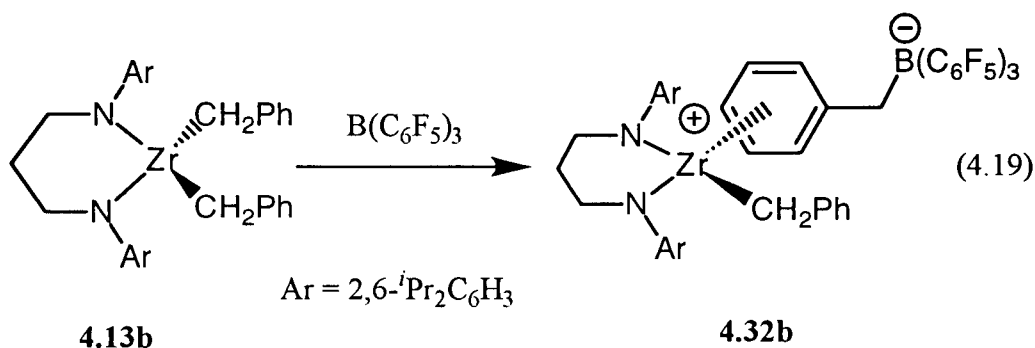
A similar reaction with complex **4.1b** occurs in the presence of excess trimethylsilylacetylene with different results (eq. 4.18).



The ^1H NMR spectrum clearly shows a single product with C_s -symmetry. On the basis of the ^1H NMR data, the product was assigned as the mono(acetylide) complex **4.31b**. The dimethylamido resonance occurs as a singlet at 2.37 ppm while the NH signal of dimethylamine occurs as a broad multiplet at 2.06 ppm and the methyl resonance as a doublet at 1.79 ppm. Trimethylsilylacetylene is larger than phenylacetylene which presumably results in the protonation of only a single dimethylamido group.

Polymerization Reactions

The activation of the dibenzyl complex **4.13b** with the Lewis acid $\text{B}(\text{C}_6\text{F}_5)_3$ was studied by ^1H NMR spectroscopy (eq. 4.19). Complex **4.13b** was chosen because the benzyl group in the putative cationic alkyl complex could assist in stabilizing the zirconium centre by η^2 coordination.^{22,42-44}

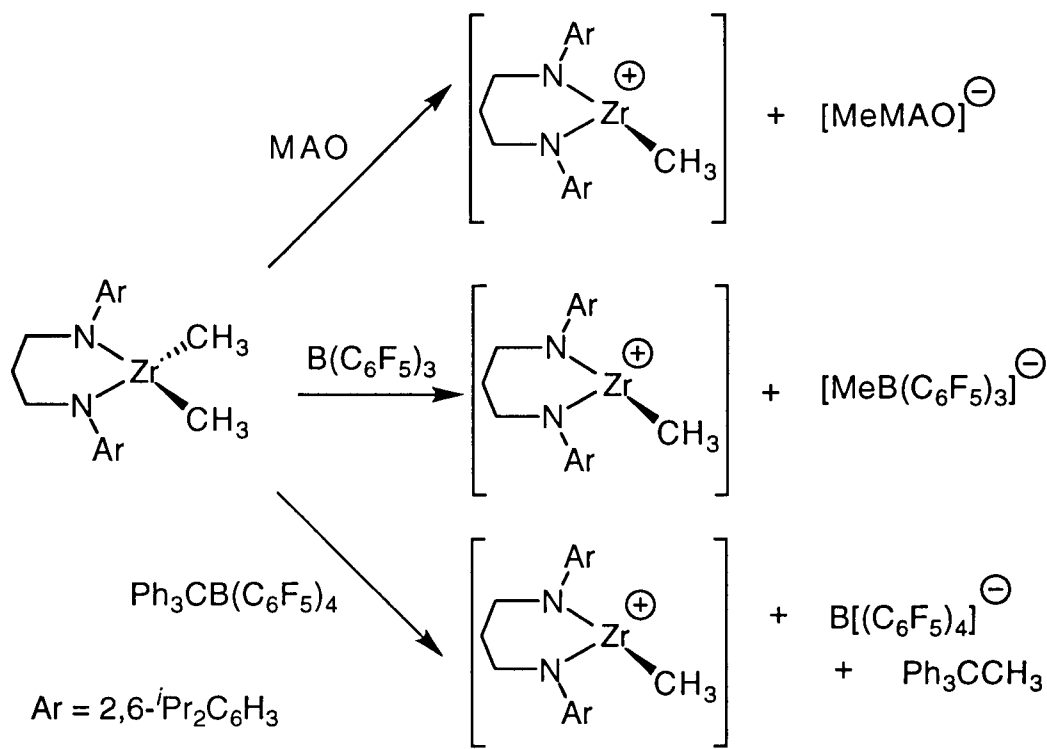


The ^1H NMR spectrum of the product revealed a single C_s -symmetric species was formed. The benzylic resonance of the $\text{Zr}-\text{CH}_2\text{Ph}$ group occurs as a singlet at 2.40 ppm. The C_s symmetry observed in the ^1H NMR spectrum indicates the presence of a fourth ligand, possibly from the $(\text{PhCH}_2)\text{B}(\text{C}_6\text{F}_5)_3$ anion. The ^1H NMR spectrum of complex **4.32b** shows a doublet-triplet-triplet pattern of resonances at 6.68, 6.42, and 5.58 ppm for the benzyl borate protons. Although NMR spectroscopy cannot unequivocally establish the coordination mode, these resonances are characteristic^{39,45,46} of an $\eta^6\text{-PhCH}_2$ group of a $\{(\eta^6\text{-PhCH}_2)\text{B}(\text{C}_6\text{F}_5)_3\}$ moiety. In related $\text{Zr}(\text{CH}_2\text{Ph})_3\{(\eta^6\text{-PhCH}_2)\text{B}(\text{C}_6\text{F}_5)_3\}$,⁴⁶ a doublet-triplet-triplet pattern of resonances at 6.39, 5.66, and 5.40 ppm was observed for the ortho,

meta, and para hydrogens, respectively, of the boron-bound benzyl group. Similar NMR patterns have been observed in $\{1,1'-(2,2',3,3'-\text{OC}_{10}\text{H}_5\text{SiPh}_3)\}_2\text{Zr}(\text{CH}_2\text{Ph})\{(\eta^6\text{-PhCH}_2)\text{B}(\text{C}_6\text{F}_5)_3\}$ ³⁹ and $\text{Zr}(\text{CH}_2\text{Ph})_3\{(\eta^6\text{-Ph})\text{BPh}_3\}$ ⁴³ in which η^n -coordination of a boron phenyl group was proposed. Therefore, based on the ^1H NMR data, the product from the reaction of complex **4.13b** with $\text{B}(\text{C}_6\text{F}_5)_3$ is the zwitterionic complex **4.32b**. Complex **4.32b** is inactive towards the polymerization of ethylene or 1-hexene at room temperature. Due to the strong interaction with the benzyl-borate group in complex **4.32b**, an olefin is unable to displace the anion which is necessary for the polymerization to occur.⁴⁷

The dimethyl complex **4.11b** was also studied as a catalyst precursor for the polymerization of olefins. Complex **4.12b** can be activated with the cocatalysts methylaluminoxane (MAO), $\text{B}(\text{C}_6\text{F}_5)_3$, and $\{\text{Ph}_3\text{C}\}[\text{B}(\text{C}_6\text{F}_5)_4]$ (TB). Scheme 4.6 shows the active species and counterion expected from the activation of complex **4.12b** with MAO, $\text{B}(\text{C}_6\text{F}_5)_3$ and TB, respectively.

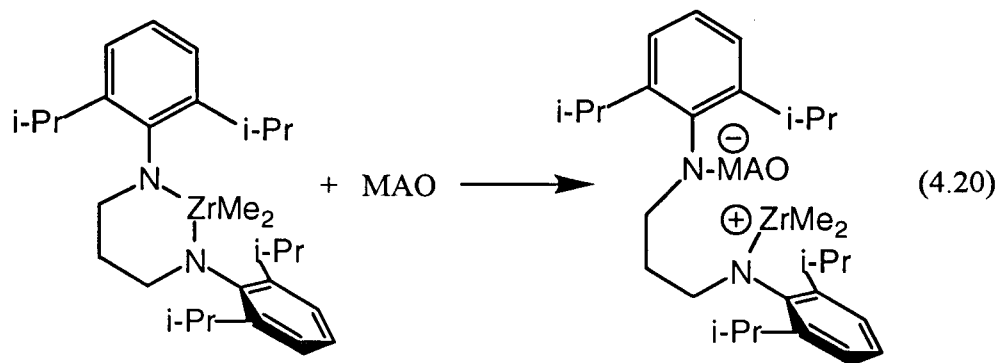
Scheme 4.6: The activation of complex **4.12b** with various co-catalysts



Theoretically, the metal species which carries out the polymerization is the same with each activator except with respect to their counter anion.

When activated with MAO, complex **4.12b** yields both high polymer (M_w , 26000; M_n , 15100; M_w/M_n , 1.72) and oligomers ($n = 2-7$, confirmed by GC-MS). Activities up to 150 g poly(1-hexene)/mmol catalyst•h were obtained in neat 1-hexene at 68°C. For comparison, the dimethyl titanium analogue **2.11b** yields only high polymer (Chapter 3, Table 3.1, entry 1) with an activity of 350,000 g poly(1-hexene)/mmol catalyst•h under the same reaction conditions.⁴⁸

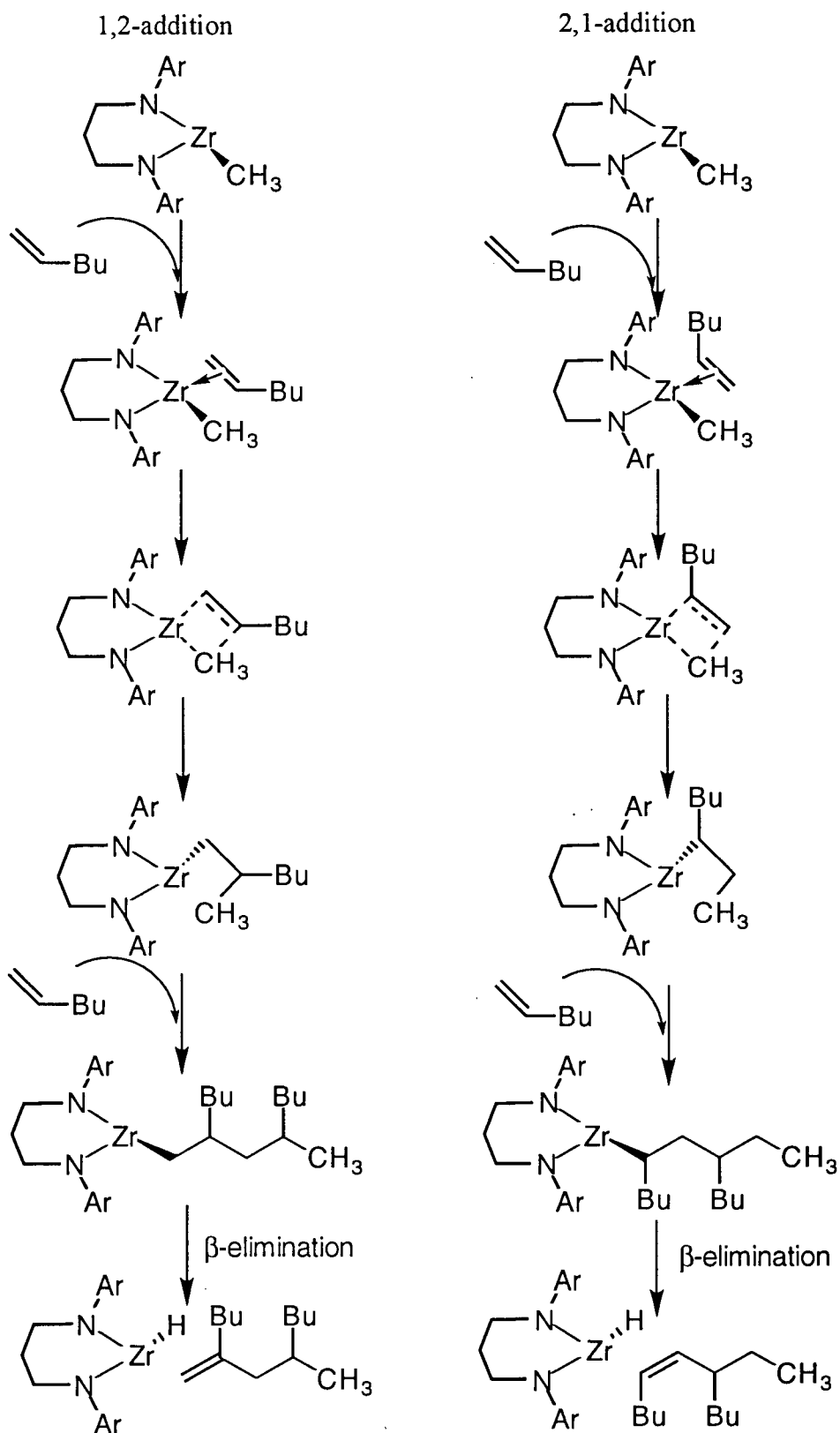
The room temperature ^1H NMR spectrum of **4.7b** suggests that the aryl groups on nitrogen are rotating slowly. Therefore the kinetic protection afforded the nitrogen atoms of the ancillary ligand may no longer exist. It is possible that MAO attacks the nitrogen atom of the ligand and changes the structure of the catalyst (eq. 4.20).



The resulting product may still be an active polymerization catalyst. In the absence of further data it is difficult to say whether this is the case or not.

Proton NMR spectroscopy was used to determine the mode of insertion of 1-hexene. Scheme 4.7 shows the insertion, via the Cossee-Arlman mechanism,⁴⁹ of two monomer units followed by a β -hydride elimination to yield a 2-mer.

Scheme 4.7: Possible modes of insertion of 1-hexene



The ^1H NMR spectrum of the polymer/oligomer sample from the **4.12b**/MAO system exhibits two doublets at 4.63 and 4.99 ppm. The coupling constant for these doublets is 2 Hz which is consistent with geminal coupling (Figure 4.11). Based on the NMR data it

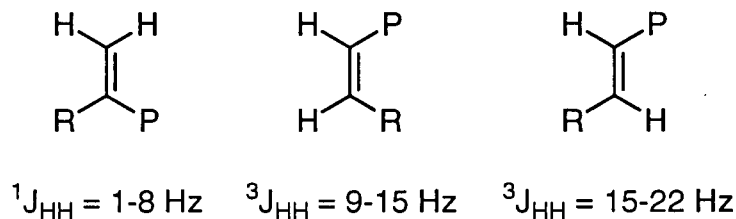


Figure 4.11: Expected coupling constants for geminal and vicinal coupling⁵⁰ appears that the monomer inserts in a primary (1,2) fashion prior to β -hydride elimination. This result is consistent with the titanium dimethyl complex **2.11b** which also inserts 1-hexene in a primary fashion (Chapter 3), however, these titanium systems do not engage in β -hydride elimination.⁵¹ It would appear that at least two active species are generated with MAO since both oligomers and high polymer are formed.

Although β -hydride elimination is not the only possible termination step, it is generally the most common way in which polymerizations of this type will terminate.⁵² Chain transfer to aluminum has also been observed for the analogous titanium system (Chapter 3).^{48,51,53-55} Recently, Teuben⁵⁶ and Resconi⁵⁷ found that a different chain termination mechanism, namely, β -methyl elimination, becomes an important termination route in propylene polymerizations. Although β -butyl elimination is highly unlikely, and unprecedented for 1-hexene, chain transfer to aluminum remains a viable alternative to β -H elimination. The ^1H NMR spectrum of poly/oligo(1-hexene) produced from the **4.12b**/MAO system is identical to the ^1H NMR spectrum of oligo(1-hexene) produced from the **4.12b**/TB system (*vide infra*).

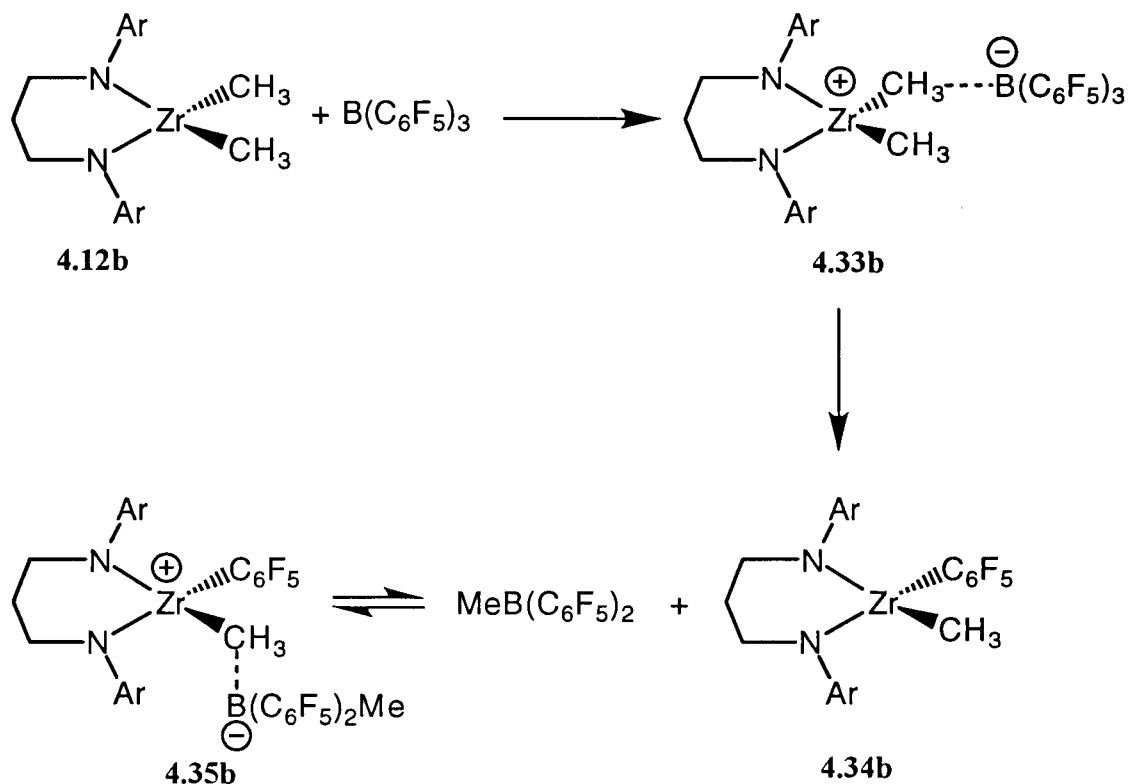
In contrast to the **4.12b**/MAO system, activation of the dimethyl complex **4.12b** with $\text{B}(\text{C}_6\text{F}_5)_3$ generates a system which is inactive for the polymerization of 1-hexene at 23°C. Multinuclear NMR spectroscopy was used to establish that several species are formed in the reaction between **4.12b** and $\text{B}(\text{C}_6\text{F}_5)_3$. Two distinct shielding environments have been

observed for boron-11. They are based on the local symmetry at the boron atom, with trigonal planar symmetry giving chemical shifts in the range δ 90 to δ -10 and tetrahedral symmetry giving shifts in the range δ 10 to δ -40.⁵⁸ The $^{11}\text{B}\{^1\text{H}\}$ NMR spectrum of equimolar amounts of compound **4.12b** and $\text{B}(\text{C}_6\text{F}_5)_3$ shows three boron containing species; one that is three-coordinate and two that are four-coordinate. In addition the ^{19}F NMR spectrum shows a total of nine resonances which is in agreement with the $^{11}\text{B}\{^1\text{H}\}$ NMR data. The ^1H NMR spectrum of **4.12b**/ $\text{B}(\text{C}_6\text{F}_5)_3$ shows at least three different species which could not be completely assigned. One of these species appears to be the starting dimethyl complex **4.12b**. Attempts to isolate these complexes have been unsuccessful.

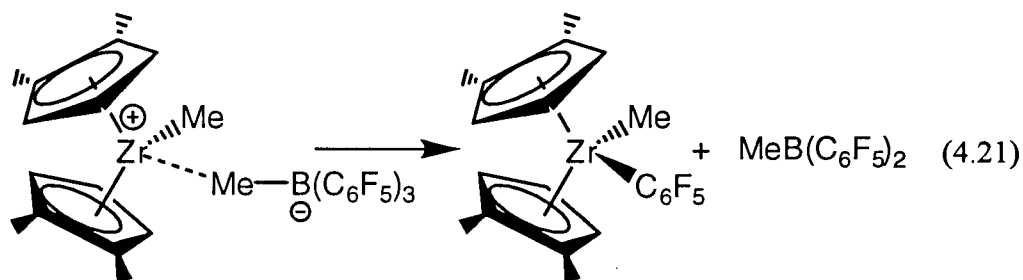
It is possible that the anion, $[\text{MeB}(\text{C}_6\text{F}_5)_3]^-$, is bound very tightly to the putative cationic alkyl.^{59,60} This is due to the highly electrophilic nature of the resulting product. Marks has evaluated the relative coordinative ability of the anions $\text{B}(\text{C}_6\text{F}_4\text{SiMe}_2^t\text{Bu})_4^-$, $\text{B}(\text{C}_6\text{F}_4\text{Si}(i\text{Pr})_3)_4^-$, $\text{B}(\text{C}_6\text{F}_5)_4^-$, and $\text{MeB}(\text{C}_6\text{F}_5)_3^-$.^{59,61,62} By studying the ion pair reorganization process in $(1,2\text{-Me}_2\text{Cp})_2\text{ZrMe}^+\text{X}^-$, Marks was able to determine the activation enthalpies and entropies from line shape analysis of the variable-temperature ^1H NMR spectra of these complexes. Marks showed that $\text{MeB}(\text{C}_6\text{F}_5)_3^-$ associates more tightly with the $(1,2\text{-Me}_2\text{Cp})_2\text{ZrMe}^+$ than do $\text{B}(\text{C}_6\text{F}_4\text{SiMe}_2^t\text{Bu})_4^-$, $\text{B}(\text{C}_6\text{F}_4\text{Si}(i\text{Pr})_3)_4^-$, and $\text{B}(\text{C}_6\text{F}_5)_4^-$. The lack of polymerization activity in the system **4.12b**/ $\text{B}(\text{C}_6\text{F}_5)_3$ may be in agreement with Marks results. This is in contrast to the reaction of **4.13b** with $\text{B}(\text{C}_6\text{F}_5)_3$, where a benzyl group is cleanly abstracted, however, the highly electrophilic zirconium centre is then stabilized by an $\{(\eta^6\text{-PhCH}_2)\text{B}(\text{C}_6\text{F}_5)_3\}$ counterion.

Based on the multinuclear NMR data and literature precedent the following proposal is advanced. Complex **4.12b** reacts with $\text{B}(\text{C}_6\text{F}_5)_3$ to form the borane adduct **4.33b** (Scheme 4.8). Complex **4.33b** could undergo a metathesis reaction where a pentafluorophenyl group is transferred from boron to zirconium to give complex **4.34b** and $\text{MeB}(\text{C}_6\text{F}_5)_2$.

Scheme 4.8: Proposed products from the reaction of complex **4.12b** with $\text{B}(\text{C}_6\text{F}_5)_3$



Marks has observed a similar reaction with a zirconocene derivative (eq. 4.21).⁵⁹ Furthermore, a similar reaction has been observed between the titanium analogue **2.11b** and



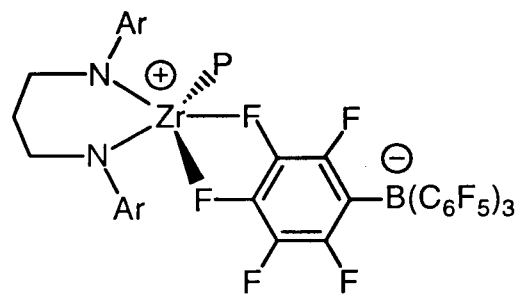
$\text{B}(\text{C}_6\text{F}_5)_3$ (Chapter 2).⁶³ The $\text{MeB}(\text{C}_6\text{F}_5)_2$ ⁵⁹ generated could then react with complex **4.34b** to generate the dimethylborate adduct **4.35b**. Complex **4.35b** may not be able to undergo further reaction. Complexes **4.34b** and **4.35b** would account for the two 4-coordinate boron

resonances in the $^{11}\text{B}\{^1\text{H}\}$ NMR spectrum, while the presence of $\text{MeB}(\text{C}_6\text{F}_5)_2$ would account for the 3-coordinate boron resonance. These proposed complexes are consistent with the multinuclear NMR data, however, it is still only speculation.

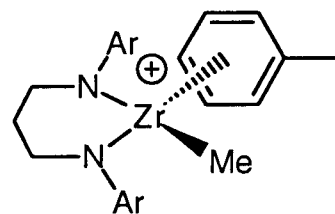
Borate stabilized cations of zirconium can be generated with a more reactive methide abstraction reagents; for example, equimolar amounts of complex **4.12b** and TB oligomerize ($n = 2-7$, confirmed by GC-MS) neat 1-hexene at 23°C with an activity of 130 g oligo(1-hexene)/mmol catalyst·h. The putative

zirconium cation is probably stabilized by the fluorine atoms of the $\text{B}(\text{C}_6\text{F}_5)_4^-$ anion (**4.36**)^{62,64}. The MAO-activated systems are slightly more active than the trityl borate-activated systems, as has been observed in the analogous titanium systems (Chapter 3, Table

3.3, entry 2 versus 3).⁵¹ In contrast to the MAO-activated system above, there is no evidence of high polymer formation in the trityl borate-activated complexes. For comparison, the catalyst system **2.11b**/TB is an active living polymerization catalyst at 68°C (Chapter 3, Table 3.3, entry 2).⁵¹ The zirconium MAO and trityl borate-activated systems above are dramatically effected by the presence of toluene.⁴⁸ For example, **4.12b**/MAO and **4.12b**/TB are inactive in a 10% toluene in 1-hexene mixture, likely a result of competitive binding of the arene to the electrophilic metal centre (**4.37**).



4.36



$\text{Ar} = 2,6\text{-}^i\text{Pr}_2\text{C}_6\text{H}_3$

4.37

Conclusions

In summary, a high yield route to chelating diamide complexes of zirconium has been demonstrated. The base-free dichloride complex **4.7b** serves as a starting point for the

synthesis of a variety of bis(alkyl) derivatives, while the pyridine-stabilized dichloride complex **4.6b** affords pyridyl complexes when the alkylating reagent is bulky. Moderately active olefin polymerization and oligomerization catalyst systems are obtained when the dimethyl complex **4.12b** is activated with MAO and $\{\text{Ph}_3\text{C}\}[\text{B}(\text{C}_6\text{F}_5)_4]$, respectively. Although the lack of polymerization activity in the borane system **2.12b**/ $\text{B}(\text{C}_6\text{F}_5)_3$ may reflect a strong binding of the cocatalyst to the electrophilic metal centre, spectroscopic data suggest that at least three different species are formed when these reagents are mixed resulting in an ill-defined system.

Experimental

General Details: All experiments were performed under an atmosphere of dry dinitrogen using standard Schlenk line techniques or in an Innovative Technology Inc. dry box. Solvents were distilled from sodium/benzophenone ketyl (dimethoxyethane, tetrahydrofuran, hexanes, diethylether), molten potassium (benzene), molten sodium (toluene) and CaH_2 (CH_2Cl_2) under argon and stored over activated 4Å molecular sieves. Chemicals were obtained from Aldrich Chemicals and Aesar (ZrCl_4). ZrCl_4 and 1,3-dibromopropane were used as received. N,N,N',N'-tetramethylethylenediamine (tmeda), 2,6-diisopropylaniline and chlorotrimethylsilane were distilled prior to use. $\text{Zr}(\text{NMe}_2)_4$ was synthesized following Bradley's method.⁶⁵ Proton (299.9 MHz), carbon (75.46 MHz), boron (96.2 MHz), and fluorine (282.2 MHz) NMR spectra were recorded in C_6D_6 at approximately 22°C on Varian Gemini-300 and Varian XL-300 spectrometers. The chemical shifts were referenced to internal $\text{C}_6\text{D}_5\text{H}$ ($\delta = 7.15$ ppm) or $\text{C}_6\text{D}_5\text{CD}_2\text{H}$ ($\delta = 2.09$ ppm) and the carbon resonances to C_6D_6 ($\delta = 128.0$ ppm) or $C_{ipso}\text{-C}_6\text{D}_5\text{CD}_3$ ($\delta = 137.5$ ppm). Fluorine and boron chemical shifts were referenced externally to CFCl_3 ($\delta = 0.0$ ppm) and $\text{BF}_3\cdot\text{Et}_2\text{O}$ ($\delta = 0.0$ ppm) respectively. Mass spectra were performed on a Finnigan MAT model 8230 spectrometer coupled to a Varian 3400 Gas Chromatograph. GPC analyses (in THF) versus polystyrene standards were performed using a Waters GPC equipped with Waters Styragel columns (HR 1, HR 3, HR 4). Elemental analyses were performed by Oneida Research Services Inc., Whitesboro, NY and by Mr. Peter Borda at the University of British Columbia.

(BAMP) $\text{Zr}(\text{NMe}_2)_2$, (4.1a). Compound 2.3a (2.00 g, 7.08 mmol) and $\text{Zr}(\text{NMe}_2)_4$ (1.89 g, 7.08 mmol) were dissolved in toluene and heated to 110 °C for 3 h. The solvent was removed in *vacuo* and the resulting solid extracted with pentane (3×100 mL) and filtered through Celite. The volume of the filtrate was reduced to 50 mL and cooled to -30°C for 12 h. A white crystalline solid was isolated by filtration and dried under vacuum (3.19 g, 6.94

mmol, 98%). ^1H NMR δ 7.11 (m, 4H, Ar), 6.95 (m, 2H, Ar), 3.45 (m, 4H, NCH_2), 2.67 (s, 12H, NMe_2), 2.42 (m, 2H, NCH_2CH_2), 2.42 (s, 12H, ArMe_2). $^{13}\text{C}\{^1\text{H}\}$ NMR δ 148.3, 135.8, 129.0, 124.8, 55.7, 41.7, 32.8, 18.6.

(BAIP)Zr(NMe₂)₂, (4.1b). Compound **2.3b** (2.95 g, 7.48 mmol) and $\text{Zr}(\text{NMe}_2)_4$ (2.00 g, 7.48 mmol) were dissolved in toluene and heated to 110 °C for 3 h. The solvent was removed in *vacuo* and the resulting solid extracted with pentane (3 × 100 mL) and filtered through Celite. The volume of the filtrate was reduced to 50 mL and cooled to -30°C for 12 h. A white crystalline solid was isolated by filtration and dried under vacuum (4.21 g, 7.34 mmol, 98%). ^1H NMR δ 7.20 (m, 6H, Ar), 3.78 (sept, 4H, CHMe_2), 3.55 (m, 4H, NCH_2), 2.64 (s, 12H, NMe_2), 2.44 (m, 2H, NCH_2CH_2), 1.34 (d, 12H, CHMe_2), 1.32 (d, 12H, CHMe_2). $^{13}\text{C}\{^1\text{H}\}$ NMR δ 146.4, 145.8, 125.2, 124.1, 59.1, 41.8, 32.3, 28.3, 26.2, 25.0. Anal. Calcd for $\text{C}_{31}\text{H}_{52}\text{N}_4\text{Zr}$: C, 65.09; H, 9.16; N, 9.79. Found: C, 64.75; H, 9.19; N, 9.65.

(BAIB)Zr(NMe₂)₂, (4.2b). Diamine **2.9b** (3.50 g, 8.56 mmol) and $\text{Zr}(\text{NMe}_2)_4$ (2.29 g, 8.56 mmol) were dissolved in toluene (50 mL) and heated to reflux for 3 hours. The solvent was removed in *vacuo* and the resulting oil dissolved in hexanes and filtered through celite. The solvent was reduced and the produce recrystallized at -30°C (4.80 g, 8.20 mmol, 96 %). ^1H NMR δ 7.12 (m, 6H, Ar), 3.78 (sept, 4H, CHMe_2), 3.35 (m, 4H, NCH_2), 2.50 (s, 12H, NMe_2), 2.13 (m, 4H, NCH_2CH_2), 1.30 (d, 24H, CHMe_2). $^{13}\text{C}\{^1\text{H}\}$ NMR δ 147.3, 146.0, 126.0, 124.3, 59.5, 42.5, 29.4, 28.2, 26.6, 24.8.

(BAIP)ZrCl₂(NHMe₂)₂, (4.5b). Compound **4.1b** (1.92 g, 3.37 mmol) was dissolved in CH_2Cl_2 (25 mL) and cooled to -78°C. $[\text{Me}_2\text{NH}_2]\text{Cl}$ (0.550 g, 6.74 mmol) was added slowly as a solid. The resulting solution was allowed to warm to RT and stirred overnight. The solvent was removed in *vacuo* and the resulting yellow solid dissolved in toluene and filtered through Celite. The solution volume was reduced until a slurry formed. Hexane (60 mL) was added and the solution was filtered to yield a yellow crystalline solid (2.16 g, 3.35 mmol, 99%). ^1H NMR δ 7.13 (m, 6H, Ar), 3.97 (sept, 4H, CHMe_2), 3.67 (m, 4H, NCH_2),

2.58 (m, 2H, NCH_2CH_2), 2.17 (s, 2H, NH), 1.86 (s, 12H, NMe_2), 1.45 (d, 12H, CHMe_2), 1.29 (d, 12H, CHMe_2). This compound loses NHMe_2 .

(BAIP)ZrCl₂(py)₂, (4.6b). Compound **4.1b** (4.80 g, 8.39 mmol) was dissolved in a mixture of CH_2Cl_2 (50 mL) and pyridine (2 mL) and cooled to -78°C . $[\text{Me}_2\text{NH}_2]\text{Cl}$ (1.37 g, 16.8 mmol) was added slowly as a solid. The resulting solution was allowed to warm to RT and stirred overnight. The solvent was removed in *vacuo* and the resulting yellow solid dissolved in toluene and filtered through Celite. The solution volume was reduced until a slurry formed. Hexanes (60 mL) was added and the solution was filtered to yield a yellow crystalline solid (4.60 g, 6.45 mmol, 77%). ^1H NMR δ 8.86 (dd, 4H, py), 7.11 (m, 6H, Ar), 6.52 (tt, 2H, py), 6.27 (tt, 4H, py), 4.29 (sept, 4H, CHMe_2), 4.05 (m, 4H, NCH_2), 2.43 (m, 2H, NCH_2CH_2), 1.30 (d, 12H, CHMe_2), 1.15 (d, 12H, CHMe_2). $^{13}\text{C}\{^1\text{H}\}$ NMR δ 151.7, 145.8, 137.6, 128.5, 125.7, 124.0, 123.2, 61.3, 33.0, 28.2, 27.8, 23.3. Carbon analyses for this compound were routinely low. Anal. Calcd for $\text{C}_{37}\text{H}_{48}\text{Cl}_2\text{N}_4\text{Zr}$: C, 62.33; H, 7.07; N, 7.86. Found: C, 60.65; H, 7.22; N, 7.35.

(BAIP)ZrCl₂, (4.7b). Compound **4.1b** (0.50 g, 0.87 mmol) was dissolved in hexanes. Excess chlorotrimethylsilane (1.0 g, 9.26 mmol) was added dropwise at room temperature and the solution stirred overnight. After 12h complex **4.7b** precipitated from the solution and was collected by filtration and washed with cold hexanes. Analytically pure **4.7b**•1/2pentane was obtained as a yellow microcrystalline solid (0.43 g, 0.78 mmol, 90%) from the recrystallization of **4.7b** at -30°C from a mixture toluene/pentane. ^1H NMR: δ 7.07 (m, 6H, Ar), 3.59 (sept, 4H, CHMe_2), 3.51 (t, 4H, NCH_2), 2.39 (m, 2H, NCH_2CH_2), 1.35 (d, 12H, CHMe_2), 1.23 (d, 12H, CHMe_2). $^{13}\text{C}\{^1\text{H}\}$ NMR δ 146.9, 145.6, 129.8, 126.9, 62.1, 31.9, 30.9, 28.4, 27.4. Anal. Calcd for $\text{C}_{27}\text{H}_{40}\text{Cl}_2\text{N}_2\text{Zr}\cdot\text{C}_5\text{H}_{12}$: C, 59.97; H, 7.85; N, 4.74. Found: C, 59.84; H, 7.69; N, 4.21 (the pentane of crystallization was confirmed by ^1H NMR spectroscopy).

(BAIB)ZrCl₂, (4.8b). Complex **4.2b** (2.00 g, 3.41 mmol) was dissolved in hexanes (50 mL) and 10 equivalents of ClSiMe_3 (3.71 g, 34.1 mmol) was added dropwise. Complex

4.8b precipitated from the solution and was collected by filtration, washed with hexanes and dried in vacuo (1.92 g, 3.38 mmol, 99 %). ^1H NMR δ 7.10 (m, 6H, Ar), 3.75 (sept, 4H, CHMe_2), 3.45 (m, 4H, NCH_2), 2.08 (m, 4H, NCH_2CH_2), 1.47 (d, 12H, CHMe_2), 1.22 (d, 12H, CHMe_2). $^{13}\text{C}\{^1\text{H}\}$ NMR δ 146.4, 140.3, 128.3, 125.0, 59.4, 28.8, 27.8, 26.4, 24.6.

(BAIP)ZrMe(NMe₂), (**4.9b**). Complex **4.1b** (0.50 g, 0.78 mmol) was dissolved in Et₂O (25 mL). MeMgBr (2.4 M, 0.33 mL, 0.79 mmol) was added dropwise and the resulting solution was stirred overnight at 23 °C. The solvent was removed in *vacuo* and the resulting yellow solid dissolved in hexanes and filtered through Celite. The solution was removed *in vacuo* and the product analyzed by ^1H NMR spectroscopy. ^1H NMR δ 7.15 (m, 6H, Ar), 3.82 (sept, 2H, CHMe_2), 3.69 (m, 2H, NCH_2), 3.59 (sept, 2H, CHMe_2), 3.32 (m, 2H, NCH_2), 2.75 (m, 1H, NCH_2CH_2), 2.36 (s, 6H, NCH_3), 2.14 (m, 1H, NCH_2CH_2), 1.35 (d, 6H, CHMe_2), 1.33 (d, 6H, CHMe_2), 1.29 (d, 6H, CHMe_2), 1.28 (d, 6H, CHMe_2), 0.35 (s, 3H, ZrCH_3).

(BAIP)Zr(CH₂Ph)(NMe₂), (**4.10b**). Complex **4.1b** (0.50 g, 0.78 mmol) was dissolved in Et₂O (25 mL). PhCH₂MgBr (1.4 M, 0.56 mL, 0.79 mmol) was added dropwise and the resulting solution was stirred overnight at 23 °C. The solvent was removed in *vacuo* and the resulting yellow solid dissolved in hexanes and filtered through Celite. The solution was removed *in vacuo* and the product analyzed by ^1H NMR spectroscopy. ^1H NMR δ 7.15 (m, 9H, Ar), 6.83 (m, 2H, Bz), 3.76 (sept, 2H, CHMe_2), 3.60 (m, 2H, NCH_2), 3.54 (sept, 2H, CHMe_2), 3.42 (m, 2H, NCH_2), 2.95 (m, 1H, NCH_2CH_2), 2.48 (s, 2H, CH_2Ph), 2.18 (s, 6H, NCH_3), 2.05 (m, 1H, NCH_2CH_2), 1.36 (d, 6H, CHMe_2), 1.31 (d, 6H, CHMe_2), 1.30 (d, 6H, CHMe_2), 1.25 (d, 6H, CHMe_2).

(BAIP)ZrMe₂, (**4.12b**). MeMgBr (2.4 M, 1.17 mL, 2.8 mmol) was added dropwise to a stirring suspension of complex **4.7b** (1.00 g, 1.40 mmol) in Et₂O (50 mL) at -20°C. The solution was warmed to 23°C and stirred overnight. Dimethoxyethane (2 mL) was added and the solvent removed in *vacuo*. The resulting solid was extracted with toluene and filtered through Celite. The toluene was removed in *vacuo* and the product recrystallized from

pentane at -30°C (0.42 g, 0.82 mmol, 58%). ^1H NMR δ 7.17 (m, 6H, Ar), 3.75 (sept, 4H, CHMe_2), 3.47 (m, 2H, NCH_2), 2.25 (m, 2H, NCH_2CH_2), 1.36 (m, 12H, CHMe_2), 1.34 (m, 12H, CHMe_2), 0.42 (s, 6H, ZrMe_2). $^{13}\text{C}\{^1\text{H}\}$ NMR δ 145.6, 143.2, 126.8, 124.5, 59.4, 39.9 (ZrMe), 29.9, 28.6, 25.8. Anal. Calcd for $\text{C}_{29}\text{H}_{46}\text{N}_2\text{Zr}$: C, 67.78; H, 9.02; N, 5.45. Found: C, 68.04; H, 9.27; N, 5.40.

(BAIP) $\text{Zr}(\text{CH}_2\text{Ph})_2$, (4.13b). PhCH_2MgCl (1.40 M, 2.00 mL, 2.80 mmol) was added dropwise to a stirring suspension of 4.7b (1.00 g, 1.40 mmol) in Et_2O (50 mL) at -20°C . The solution was warmed to RT and stirred overnight. The solvent was removed in *vacuo* and the solid extracted with toluene and filtered through Celite. The solution was concentrated and cooled to -30°C to yield yellow crystalline 4.13b (0.40 g, 0.60 mmol, 43%). ^1H NMR δ 7.19 (m, 6H, Ar), 7.01 (tt, 4H, *o*-Ph), 6.82 (tt, 2H, *p*-Ph), 6.65 (dd, 4H, *m*-Ph), 3.78 (sept, 4H, CHMe_2), 3.49 (m, 2H, NCH_2), 2.31 (m, 2H, NCH_2CH_2), 1.95 (s, 4H, CH_2Ph), 1.32 (d, 12H, CHMe_2), 1.27 (d, 12H, CHMe_2). $^{13}\text{C}\{^1\text{H}\}$ NMR δ 145.9, 145.1, 145.0, 130.1, 126.6, 126.5, 124.7, 122.7, 64.2 (CH_2Ph , $^1J_{\text{CH}} = 124$ Hz), 58.8, 29.1, 28.4, 26.6, 25.1. Anal. Calcd for $\text{C}_{41}\text{H}_{54}\text{N}_2\text{Zr}$: C, 73.93; H, 8.17; N, 4.21. Found: C, 73.54; H, 8.33; N, 4.27.

(BAIP) ZrEt_2 , (4.14b). EtMgBr (3.6 M, 0.61 mL, 2.2 mmol) was added dropwise to a stirring suspension of 4.7b (0.78 g, 1.1 mmol) in Et_2O (20 mL) at -20°C . The solution was allowed to warm to RT and stirred overnight. The solvent was removed in *vacuo* and the resulting solid extracted with pentane and filtered through Celite. The pentane was removed in *vacuo* to leave complex 4.14b (0.37 g, 0.68 mmol, 62%). ^1H NMR δ 7.17 (m, 6H, Ar), 3.77 (sept, 4H, CHMe_2), 3.51 (m, 2H, NCH_2), 2.32 (m, 2H, NCH_2CH_2), 1.37 (d, 12H, CHMe_2), 1.32 (d, 12H, CHMe_2), 1.32 (t, 6H, CH_2CH_3), 0.75 (q, 4H, ZrCH_2).

(BAIP) $\text{Zr}(\eta^3\text{-C}_3\text{H}_5)_2$, (4.15b). Compound 4.7b (1.0 g, 1.4 mmol) was suspended in diethyl ether (50 mL) and cooled to -20°C . $\text{C}_3\text{H}_5\text{MgCl}$ (2.0M, 1.4 mL, 2.8 mmol) was added dropwise. The solution was allowed to warm to 23°C and stirred overnight. The solvent was removed in *vacuo* and the resulting solid dissolved in toluene and filtered

through celite. The toluene was removed in *vacuo* to leave a orange-brown solid which decomposed slowly over a couple of days (0.35 g, 0.62 mmol, 44%). ^1H NMR: δ 7.10 (m, 6H, Ar), 5.61 (pent, 2H, CH_2CHCH_2), 3.76 (sept, 4H, CHMe_2), 3.62 (m, 4H, NCH_2), 2.91 (d, 8H, CH_2CHCH_2), 2.61 (m, 2H, NCH_2CH_2), 1.30 (d, 12H, CHMe_2), 1.28 (d, 12H, CHMe_2).

(BAIP)Zr($\text{CH}_2\text{CMe}_2\text{Ph}$)₂, (4.16b). Compound 4.7b (1.00 g, 1.40 mmol) was suspended in THF (50 mL) and cooled to -20°C . ($\text{PhMe}_2\text{CCH}_2$)₂Mg (0.190 M, 14.7 mL, 2.80 mmol, prepared from $\text{PhMe}_2\text{CCH}_2\text{MgCl}$ and 1,4-dioxane) was added dropwise. The solution was allowed to warm to RT and stirred overnight. The solvent was removed in *vacuo* and the resulting solid dissolved in hexanes and filtered through celite. The hexanes was removed in *vacuo* yielding compound 4.16b as a yellow oil (0.90 g, 1.2 mmol, 86%). ^1H NMR: δ 7.22 (m, 10H, Ar), 7.05 (m, 6H, Ar), 3.89 (sept, 4H, CHMe_2), 3.47 (m, 4H, NCH_2), 2.18 (m, 2H, NCH_2CH_2), 1.42 (d, 12H, CHMe_2), 1.31 (d, 12H, CHMe_2), 1.31 (s, 12H, CMe_2Ph), 1.18 (s, 4H, $\text{CH}_2\text{CMe}_2\text{Ph}$). $^{13}\text{C}\{^1\text{H}\}$ NMR δ 153.7, 146.5, 145.0, 128.5, 126.4, 125.3, 125.3, 124.8, 87.6, 58.5, 42.0, 33.9, 28.2, 26.9, 25.1.

(BAIP)Zr(CH_2SiMe_3)₂, (4.17b). Compound 4.7b (1.00 g, 1.40 mmol) was suspended in Et_2O (50 mL). $\text{LiCH}_2\text{SiMe}_3$ (0.264 g, 2.80 mmol) was then added as a solid. The solution was allowed to warm to RT and stirred overnight. The solvent was removed in *vacuo* and the resulting solid dissolved in hexanes and filtered through celite. The hexanes was removed in *vacuo* yielding compound 4.17b as a light yellow oil (0.860 g, 1.30 mmol, 93%). ^1H NMR: δ 7.19 (m, 6H, Ar), 3.85 (sept, 4H, CHMe_2), 3.50 (m, 4H, NCH_2), 2.43 (m, 2H, NCH_2CH_2), 1.44 (d, 12H, CHMe_2), 1.35 (d, 12H, CHMe_2), 0.51 (s, 4H, CH_2SiMe_3), 0.08 (s, 18H, SiMe_3). $^{13}\text{C}\{^1\text{H}\}$ NMR δ 145.0, 144.7, 126.6, 124.7, 58.9, 58.2, 29.1, 28.2, 26.3, 25.6, 2.7.

(BAIP)Zr($\eta^2\text{-N,C-NC}_5\text{H}_4$)($\text{CH}_2\text{CMe}_2\text{Ph}$), (4.20b). $\text{PhMe}_2\text{CCH}_2\text{MgCl}$ (0.89 M, 3.15 mL, 2.80 mmol) was added dropwise to a stirring THF (50 mL) suspension of 4.6b (1.00 g, 1.40 mmol) at -20°C . The solution was allowed to warm to RT and stirred

overnight. The solvent was removed in *vacuo* and the resulting solid extracted with toluene and filtered through Celite. The toluene was removed in *vacuo* and the product recrystallized from pentane at -30°C (0.40 g, 0.58 mmol, 43%). ^1H NMR δ 7.33–7.10 (m, 10H, Ar, Ph, py), 6.88 (m, 1H, Ph), 6.78 (tt, 1H, py), 6.72 (m, 2H, Ph), 6.35 (ddd, 1H, py), 4.26 (sept, 2H, CHMe_2), 3.82 (m, 2H, NCH_2), 3.58 (m, 2H, NCH_2), 3.26 (sept, 2H, CHMe_2), 2.76 (m, 1H, NCH_2CH_2), 2.64 (m, 1H, NCH_2CH_2), 1.70 (s, 2H, $\text{CH}_2\text{CMe}_2\text{Ph}$), 1.59 (d, 6H, CHMe_2), 1.47 (d, 6H, CHMe_2), 1.18 (d, 6H, CHMe_2), 1.17 (s, 6H, CMe_2Ph), 0.64 (d, 6H, CHMe_2). $^{13}\text{C}\{^1\text{H}\}$ NMR δ 153.9, 149.7, 145.5, 144.6, 144.5, 134.8, 129.3, 128.1, 125.3, 125.1, 125.1, 124.7, 124.0, 123.8, 68.0, 59.6, 41.0, 35.5, 31.7, 28.3, 28.1, 27.0, 26.6, 25.2, 24.1. Anal. Calcd for $\text{C}_{42}\text{H}_{57}\text{N}_3\text{Zr}$: C, 72.57; H, 8.26; N, 6.04. Found: C, 72.85; H, 8.61; N, 5.95.

(BAIP)ZrMe₂(py), (4.24b). Complex 4.24b was isolated by recrystallization of complex 4.12b from a mixture of hexanes and pyridine. ^1H NMR δ 8.02 (m, 2H, *o*-py), 7.15 (m, 6H, Ar), 6.62 (tt, 1H, *p*-py), 6.32 (m, 2H, *m*-py), 4.05 (sept, 4H, CHMe_2), 3.66 (m, 2H, NCH_2), 2.59 (m, 2H, NCH_2CH_2), 1.39 (m, 12H, CHMe_2), 1.28 (m, 12H, CHMe_2), 0.35 (s, 6H, ZrMe_2).

(BAIP)Zr(CH₂Ph)₂(py), (4.25b). Complex 4.25b was isolated by recrystallization of complex 4.13b from a mixture of toluene and pyridine. ^1H NMR δ 7.98 (dd, 2H, *o*-py), 7.17 (m, 6H, Ar), 7.01 (tt, 4H, *o*-Ph), 6.82 (tt, 2H, *p*-Ph), 6.80 (tt, 1H, *p*-py), 6.54 (dd, 4H, *p*-Ph), 6.32 (m, 2H, *m*-py), 3.90 (sept, 4H, CHMe_2), 3.64 (m, 2H, NCH_2), 2.44 (m, 2H, NCH_2CH_2), 2.30 (s, 4H, CH_2Ph), 1.31 (d, 12H, CHMe_2), 1.29 (d, 12H, CHMe_2).

(BAIP)ZrCpCl, (4.26b). NaCp(DME) (0.250 g, 1.40 mmol) was added as a solid to a stirring toluene (50 mL) solution of 4.8b (1.00 g, 1.40 mmol). The solution was stirred overnight at RT and then filtered through Celite. The volume of toluene was reduced to 10 mL and hexane (50 mL) added. Cooling to -30°C afforded white crystals of 4.26b (0.770 g, 1.32 mmol, 94%). ^1H NMR δ 7.12 (m, 6H, Ar), 5.93 (s, 5H, C_5H_5), 3.91 (m, 1H, NCH_2CH_2), 3.61 (sept, 2H, CHMe_2), 3.60 (sept, 2H, CHMe_2), 3.60 (m, 2H, NCH_2), 3.35 (m, 2H, NCH_2), 2.01 (m, 1H, NCH_2CH_2), 1.40 (d, 6H, CHMe_2), 1.32 (d, 6H, CHMe_2), 1.27 (d,

6H, CHMe₂), 1.23 (d, 6H, CHMe₂). ¹³C{¹H} NMR δ 151.1, 145.1, 142.3, 125.9, 124.6, 124.2, 114.7, 57.9, 28.0, 27.9, 27.2, 25.9, 25.6, 25.1, 25.0. Anal. Calcd for C₃₂H₄₅ClN₂Zr: C, 65.77; H, 7.76; N, 4.79. Found: C, 66.24; H, 7.86; N, 4.72.

(BAIP)ZrCpMe, (4.27b). Compound 4.26b (1.00 g, 1.40 mmol) was suspended in Et₂O (50 mL) at 23°C. MeMgCl (3.0 M, 0.47 ml 1.40 mmol) was added all at once. The solution was stirred overnight at RT and the solvent removed *in vacuo*. The resulting oil was taken up in hexane (50 mL) and filtered. Compound 4.27b formed as white crystals (0.637 g, 1.12 mmol, 80%) upon cooling to -30°C. ¹H NMR: δ 7.11 (m, 6H, Ar), 5.79 (s, 5H, C₅H₅), 3.67 (sept, 2H, CHMe₂), 3.54 (m, 2H, NCH₂), 3.47 (sept, 2H, CHMe₂), 3.46 (m, 1H, NCH₂CH₂), 3.29 (m, 2H, NCH₂), 2.07 (m, 1H, NCH₂CH₂), 1.42 (d, 6H, CHMe₂), 1.31 (d, 6H, CHMe₂), 1.23 (d, 6H, CHMe₂), 1.20 (d, 6H, CHMe₂), 0.36 (s, 3H, ZrMe). ¹³C{¹H} NMR δ 151.0, 144.7, 142.9, 128.3, 125.4, 124.2, 112.8, 58.1, 28.0, 27.6, 27.3, 27.2, 25.4, 25.0, 20.8, 19.9.

(BAIP)ZrCp(CH₂Ph), (4.28b). Compound 4.26b (1.0 g, 1.4 mmol) was suspended in Et₂O (50 mL). PhCH₂MgCl (.69M, 2.03 ml, 1.4 mmol) was then added all at once. The solution was stirred overnight at RT and the solvent removed *in vacuo*. The resulting oil was dissolved in hexane (50 mL), filtered through celite, reduced in volume and cooled to -30°C. Compound 4.28b formed as white crystals (0.677 g, 1.05 mmol, 75%). ¹H NMR: δ 7.29 (m, 2H, Ph), 7.13 (m, 7H, Ar, Ph), 7.01 (m, 2H, Ph), 5.77 (s, 5H, C₅H₅), 3.55 (sept, 2H, CHMe₂), 3.51 (sept, 2H, CHMe₂), 3.51 (m, 2H, NCH₂), 3.38 (m, 1H, NCH₂CH₂), 3.28 (m, 2H, NCH₂), 2.48 (s, 2H, ZrCH₂Ph), 2.07 (m, 1H, NCH₂CH₂), 1.40 (d, 6H, CHMe₂), 1.29 (d, 6H, CHMe₂), 1.28 (d, 6H, CHMe₂), 1.25 (d, 6H, CHMe₂). ¹³C{¹H} NMR δ 153.0, 151.6, 144.5, 142.6, 128.6, 125.9, 125.6, 124.4, 124.4, 120.8, 113.8, 69.6, 57.4, 51.1, 28.0, 27.7, 27.1, 25.9, 25.4, 24.8.

(BAIP)Zr(HNMe₂)₂(CCPh)₂, (4.30b). Compound 4.1b (100 mg, 0.175 mmol) was dissolved in hexanes (10 mL) and phenyl acetylene (36 mg, 0.35 mmol) was added dropwise.

The solution was stirred for 2 hours and the solvent removed in vacuo. The yield was quantitative according to the ^1H NMR. ^1H NMR: δ 7.39 (m, 4H, *o*-Ph), 7.18 (m, 6H, Ar), 7.05 (m, 2H, *p*-Ph), 6.91 (m, 4H, *m*-Ph), 4.30 (sept, 4H, CHMe_2), 3.75 (t, 4H, NCH_2), 2.80 (m, 2H, $\text{CH}_2\text{CH}_2\text{CH}_2$), 2.46 (s, 2H, HNMe_2), 2.09 (d, 12H, HNMe_2), 1.53 (d, 12H, CHMe_2), 1.36 (d, 12H, CHMe_2). $^{13}\text{C}\{^1\text{H}\}$ NMR δ 148.7, 145.4, 145.1, 131.8, 128.8, 128.4, 127.0, 125.9, 124.5, 106.9, 60.0, 39.9, 31.9, 28.2, 27.1, 25.0.

(BAIP)Zr(NMe₂)(CCSiMe₃)(HNMe₂), (4.31b). Compound **4.1b** (100 mg, 0.175 mmol) was dissolved in hexanes (10 mL) and trimethylsilylacetylene (34 mg, 0.35 mmol) was added dropwise. The solution was stirred for 2 hours and the solvent removed in vacuo. The yield was quantitative according to the ^1H NMR. ^1H NMR: δ 7.18 (m, 6H, Ar), 4.33 (sept, 2H, CHMe_2), 3.85 (sept, 2H, CHMe_2), 3.71 (m, 2H, NCH_2), 3.53 (m, 2H, NCH_2), 3.53 (m, 3H, $\text{CH}_2\text{CH}_2\text{CH}_2$), 2.37 (s, 6H, NMe_2), 2.15 (m, 3H, $\text{CH}_2\text{CH}_2\text{CH}_2$), 2.11 (s, 1H, HNMe_2), 1.78 (d, 6H, HNMe_2), 1.47 (d, 6H, CHMe_2), 1.39 (d, 6H, CHMe_2), 1.36 (d, 6H, CHMe_2), 1.34 (d, 6H, CHMe_2), 0.31 (s, 9H, SiMe_3). $^{13}\text{C}\{^1\text{H}\}$ NMR δ 150.1, 145.0, 144.6, 125.2, 124.6, 123.5, 115.4, 67.8, 59.5, 39.2, 39.0, 32.9, 28.6, 27.7, 27.2, 27.0, 25.0, 24.3, 1.1.

[(BAIP)Zr(CH₂Ph)]⁺[η^6 -PhCH₂B(C₆F₅)₃]⁻, (4.32b) Compound **4.13b** (10 mg, 0.015 mmol) and B(C₆F₅)₃ (7.7 mg, 0.015 mmol) were dissolved in C₆D₆ (2 mL). ^1H NMR: δ 7.10 (m, 11H, Ar), 6.68 (d, 2H, Bz-B), 6.42 (t, 2H, Bz-B), 5.58 (t, 1H, Bz-B), 3.18 (m, 4H, NCH_2), 3.14 (sept, 2H, CHMe_2), 2.88 (sept, 2H, CHMe_2), 2.78 (m, 2H, PhCH_2B), 2.40 (s, 2H, PhCH_2Zr), 2.01 (m, 1H, $\text{CH}_2\text{CH}_2\text{CH}_2$), 1.58 (m, 1H, $\text{CH}_2\text{CH}_2\text{CH}_2$), 1.27 (d, 6H, CHMe_2), 1.14 (d, 6H, CHMe_2), 1.01 (d, 6H, CHMe_2), 0.95 (d, 6H, CHMe_2).

Polymerization Details.

Complex **4.12b** (5.0 mg, 9.7 μmol) was combined with 500 equivalents of MAO or 1 equivalent of $\{\text{Ph}_3\text{C}\}[\text{B}(\text{C}_6\text{F}_5)_4]$ in pentane (1 mL) and added to 5.0 g of 1-hexene at 23°C or 68°C. The polymerizations were quenched after 30 min (23°C) or 10 min (68°C) by the addition of a 1N solution of HCl (2 mL). The polymer/oligomer was extracted with THF and dried under vacuum overnight. The samples were dissolved in THF for GPC analysis.

References

- (1) Chandra, G.; Lappert, M. F. *J. Chem. Soc. (A)* 1968, 1940.
- (2) Lappert, M. F.; Power, P. P.; Sanger, A. R.; Srivastava, R. C. *Metal and Metaloid Amides*; Ellis Horwood: Chichester, West Sussex, U.K., 1980; .
- (3) Christopher, J. N.; Diamond, G. M.; Jordan, R. F. *Organometallics* 1996, **15**, 4038.
- (4) Diamond, G. M.; Rodewald, S.; Jordan, R. F. *Organometallics* 1995, **14**, 5.
- (5) Diamond, G. M.; Jordan, R. F.; Peterson, J. L. *J. Am. Chem. Soc.* 1996, **118**, 8024.
- (6) Diamond, G. M.; Jordon, R. F.; Peterson, J. L. *Organometallics* 1996, **15**, 4045.
- (7) Diamond, G. M.; Jordon, R. F.; Peterson, J. L. *Organometallics* 1996, **15**, 4030.
- (8) Hughes, A. K.; Meetsma, A.; Teuben, J. H. *Organometallics* 1993, **12**, 1936.
- (9) Male, N. A. H.; Thornton-Pett, M.; Bochmann, M. *J. Chem. Soc., Dalton Trans.* 1997, 2487.
- (10) Guérin, F.; McConville, D. H.; Vittal, J. J. *IS* 1996, 5586.
- (11) Mu, Y.; Piers, W. E.; MacGillivray, L. R.; Zaworotko, M. K. *Polyhedron* 1995, **14**, 1.
- (12) Andersen, R. A. *Inorganic Chemistry* 1979, **18**, 2928.
- (13) Jordan, R. F.; Bajgur, C. S.; Willett, R.; Scott, B. *J. Am. Chem. Soc.* 1986, **108**, 7410.
- (14) Andersen, R. A. *Inorganic Chemistry* 1979, **18**, 1788.
- (15) Cummins, C. C.; Baxter, S. M.; Wolczanski, P. T. *Journal of the American Chemical Society* 1988, **110**, 8731.
- (16) Kost, D.; Carlson, E. H.; Raban, M. *J. Chem. Soc., Chem. Commun.* 1971, 656.
- (17) Lubben, T. V.; Wolczanski, P. T.; Van Duyne, G. D. *Organometallics* 1984, **3**, 977.
- (18) Latesky, S. L.; McMullen, A. K.; Niccolai, G. P.; Rothwell, I. P.; Huffman, J. C. *Organometallics* 1985, **4**, 902.
- (19) Wolczanski, P. T.; Bercaw, J. E. *Organometallics* 1982, **1**, 793.
- (20) Fryzuk, M. D.; Mao, S. S. H.; Duval, P. B.; Rettig, S. J. *Polyhedron* 1995, **14**, 11.
- (21) Crowther, D. J.; Jordan, R. F.; Baenziger, N.; Verma, A. *Organometallics* 1990, **9**, 2574.

- (22) Jordan, R. F.; Lapointe, R. E.; Baenziger, N.; Hinch, G. D. *Organometallics* 1990, **9**, 1539.
- (23) Thompson, M. E.; Baxter, S. M.; Bulls, A. R.; Burger, B. J.; Nolan, M. C.; Santarsiero, B. D.; Schaefer, W. P.; Bercaw, J. E. *J. Am. Chem. Soc.* 1987, **109**, 203.
- (24) den Haan, K. H.; Wielstra, Y.; Teuben, J. H. *Organometallics* 1987, **6**, 2053.
- (25) Jordan, R. F.; Taylor, D. F.; Baenziger, N. C. *Organometallics* 1990, **9**, 1546.
- (26) Fryzuk, M. D.; Mao, S. S. H.; Zaworotko, M. J.; MacGillivray, L. R. *J. Am. Chem. Soc.* 1993, **115**, 5336.
- (27) Schwartz, J.; Gell, K. *J. Organomet. Chem.* 1980, **184**, C1.
- (28) Davidson, P. J.; Lappert, M. F.; Pearce, R. *Chem. Rev.* 1976, **76**, 219.
- (29) Schrock, R. R.; Parshall, G. W. *Chem. Rev.* 1976, **76**, 243.
- (30) Schrock, R. R. *J. Am. Chem. Soc.* 1974, **96**, 6796.
- (31) Li, L.; Diminnie, J. B.; Liu, X.; Pollitte, J. L.; Xue, Z. *Organometallics* 1996, **15**, 3520.
- (32) Smart, J. C.; Curtis, C. J. *Inorganic Chemistry* 1977, **16**, 1788.
- (33) Volhardt, K. P. C. *Angew. Chem., Int. Ed. Engl.* 1984, **23**, 539.
- (34) Smith, D. P.; Strickler, J. R.; Gray, S. D.; Bruck, M. A.; Holmes, R. S.; Wigley, D. E. *Organometallics* 1992, **11**, 1275.
- (35) Strickler, J. R.; Bruck, M. A.; Wigley, D. E. *J. Am. Chem. Soc.* 1990, **112**, 2814.
- (36) Heeres, H. J.; Heeres, A.; Teuben, J. H. *Organometallics* 1990, **9**, 1508.
- (37) Johnson, E. S.; Balaich, G. J.; Rothwell, I. P. *J. Am. Chem. Soc.* 1997, **119**, 7685.
- (38) Johnson, E. S.; Balaich, G. J.; Fanwick, P. E.; Rothwell, I. P. *J. Am. Chem. Soc.* 1997, **119**, 11086.
- (39) van der Linden, A.; Schaverien, C. J.; Meijboom, N.; Ganter, C.; Orpen, A. G. *J. Am. Chem. Soc.* 1995, **117**, 3008.
- (40) Black, D. G.; Swenson, D. C.; Jordan, R. F.; Rogers, R. D. *Organometallics* 1995, **14**, 3539.
- (41) Erker, G.; Frömberg, W.; Benn, R.; Mynott, R.; Angermund, K.; Krüger, C. *Organometallics* 1989, **8**, 911.

- (42) Jordan, R. F.; LaPointe, R. E.; Bajgur, C. S.; Echols, S. F.; Willett, R. *Journal of the American Chemical Society* 1987, **109**, 4111.
- (43) Bochmann, M.; Lancaster, S. J. *Organometallics* 1993, **12**, 633.
- (44) Jordan, R. F. *J. Chem. Educ.* 1988, **65**, 285.
- (45) Pellecchia, C.; Immirzi, A.; Grassi, A.; Zambelli, A. *Organometallics* 1993, **12**, 4473.
- (46) Pellecchia, C.; Grassi, A.; Immirzi, A. *J. Am. Chem. Soc.* 1993, **115**, 1160.
- (47) Daychkovskii, F. S.; Shilova, A. K.; Shilov, A. E. *J. Polym. Sci. Part C* 1967, **16**, 2333.
- (48) Scollard, J. D.; McConville, D. H.; Vittal, J. J. *Macromolecules* 1996, **29**, 5241.
- (49) Cossee, P. *J. Catal.* 1964, **3**, 80.
- (50) Lambert, J. B.; Shurvell, H. F.; Lightner, D. A.; Cooks, R. G. *Introduction to Organic Spectroscopy*; MacMillan Publishing Company: New York, 1987; .
- (51) Scollard, J. D.; McConville, D. H.; Payne, N. C.; Vittal, J. J. *jmolcat* 1997, Accepted for publication.
- (52) Kaminsky, W.; Ahlers, A.; Möller-Lindenhof, N. *Angew. Chem., Int. Ed. Engl.* 1989, **28**, 1216.
- (53) Chien, J.; Wang, B. J. *Journal of Polymer Science: Chemical Education* 1990, **28**, 15.
- (54) Resconi, L.; Bossi, S.; Abis, L. *Macromolecules* 1990, **23**,
- (55) Scollard, J. D.; McConville, D. H. *J. Am. Chem. Soc.* 1996, **118**, 10008.
- (56) Eshuis, J. J. W.; Tan, Y. Y.; Teuben, J. H.; Renkema, J. *jmolcat* 1990, **62**, 277.
- (57) Resconi, L.; Giannini, U.; Albizzati, E.; Piemontesi, F.; Fiorani, T. *ACS Polym. Prepr.* 1991, **32**, 463.
- (58) Kidd, R. G. In *NMR of Newly Accessible Nuclei*; P. Laszlo, Ed.; Academic Press: New York, 1983; Vol. 2.
- (59) Yang, X.; Stern, C. L.; Marks, T. J. *J. Am. Chem. Soc.* 1994, **116**, 10015.
- (60) Baumann, R.; Davis, W. M.; Schrock, R. R. *J. Am. Chem. Soc.* 1997, **119**, 3830.
- (61) Deck, P. A.; Marks, T. J.; Petersen, J. L. *J. Am. Chem. Soc.* 1995, **117**, 6128.
- (62) Jia, L.; Yang, X.; Stern, C. L.; Marks, T. J. *Organometallics* 1997, **16**, 842.
- (63) Scollard, J. D.; McConville, D. H.; Rettig, S. J. *Organometallics* 1997, **16**, 1810.

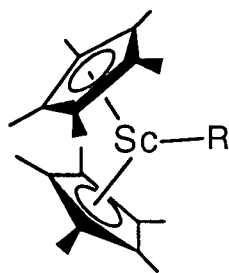
- (64) Jia, L.; Yang, X.; Ishihara, A.; Marks, T. J. *Organometallics* 1995, **14**, 3135.
- (65) Bradley, D. C.; Thomas, I. M. *Chemical Society London. Proceedings* 1959, 225.

Chapter 5: Chelating Diamide Complexes of Scandium

Introduction

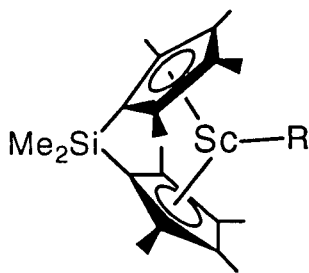
Compared with the other transition metals, the organometallic chemistry of scandium is still largely unexplored. Much of the impetus for studying the organometallic chemistry of scandium was derived from the need to understand the mechanistic details of the activation of H_2 and C–H bonds by group 4 metallocenes.¹⁻³ Use of large cyclopentadienyl ligands such as C_5Me_5 , to favour monomeric complexes, is necessary due to the propensity for these highly electron-deficient species to form less reactive dimers or oligomers.

Since the neutral group 3 metallocene hydrides and alkyls are isoelectronic with the cationic group 4 analogues, it was anticipated that they would function as single component catalysts for the polymerization of olefins. Indeed, permethylscandocene alkyls (**5.1**) do serve as well-defined single component catalysts for ethylene polymerization.⁴ However, polymerization of higher order olefins is considerably more difficult and σ -bond metathesis, rather than olefin insertion, occurs with α -olefins.¹

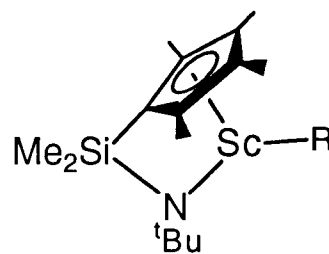


5.1

R = H, Alkyl



5.2



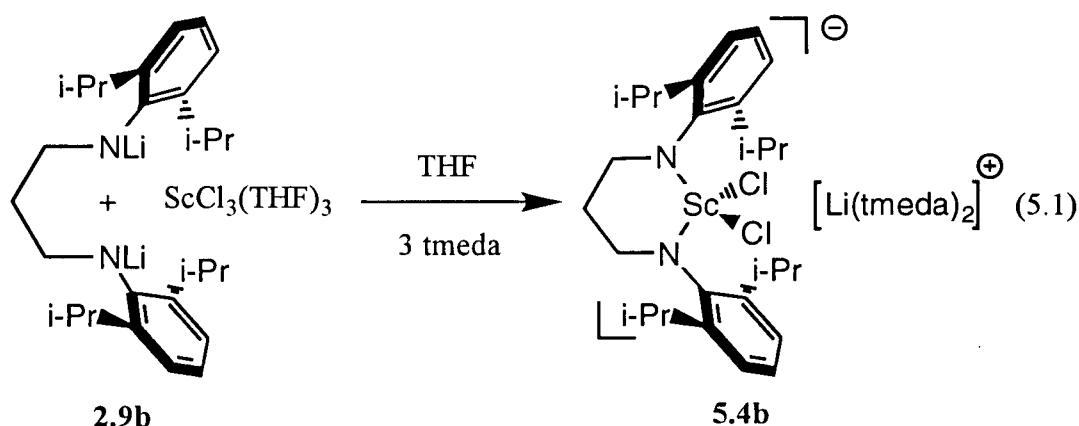
5.3

More open *ansa*-metallocenes (**5.2**) have been prepared resulting in the dimerization of α -olefins.¹ Substitution of one of the cyclopentadienyl ligands by an amido ligand renders the linked systems more reactive. Thus complex **5.3** is capable of producing low molecular weight polymers of propylene and higher order α -olefins.¹

With the success of chelating diamide complexes **2.10a,b** and **2.11a,b** as catalyst precursors for the polymerization of α -olefins, and given the analogy drawn between the chelating diamide and metallocene complexes, an investigation of the corresponding Sc(III) complexes stabilized by the chelating diamido ligands was initiated.

Results and Discussion

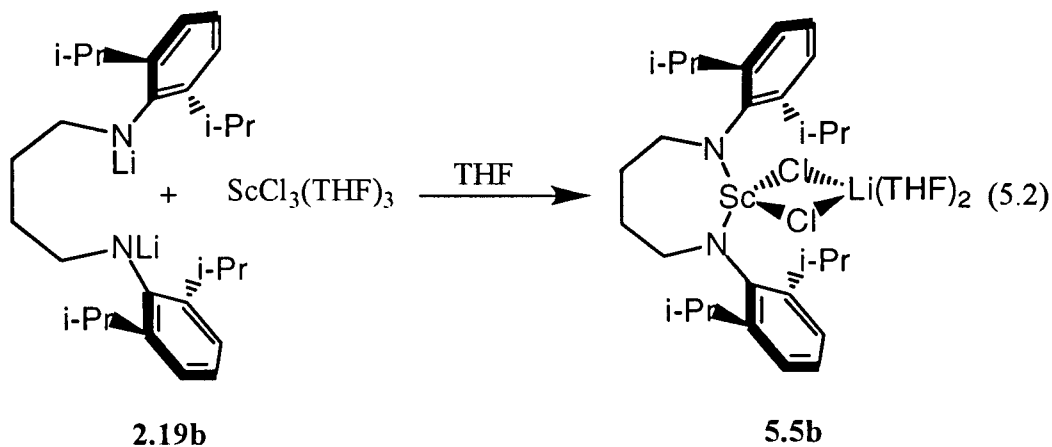
The reaction of the dilithium salt of the ligand (**2.9b**) with $\text{ScCl}_3(\text{THF})_3$ ¹ results in the formation of the bis(amide) as the discrete 'ate' complex **5.4b** (eq. 5.1). A small excess of



N,N,N',N'-tetramethylethylenediamine (tmeda) was needed to obtain analytically pure **5.4b**. The ¹H NMR spectrum reveals that complex **5.4b** has C_{2v}-symmetry in solution. Interestingly, there is only one doublet resonance for the isopropyl methyl groups in the ¹H NMR spectrum. However, there are two carbon resonances for the isopropylmethyl carbons in the ¹³C{¹H} NMR spectrum. This is indicative of diastereotopic isopropylmethyl groups. Therefore the isopropylmethyl doublets in the ¹H NMR spectrum are coincident. This is consistent with restricted rotation about the N-C_{ipso} bond. The ¹H NMR spectrum of the zirconium analogue (**4.7b**) also exhibits slightly broad isopropylmethyl resonances which is likely a result of slow rotation of the aryl groups about the N-C_{ipso} bond. The average Sc-N bond length is approximately 2.11 Å.⁵⁻⁸ The average Zr-N bond length for complex **4.20b** is 2.04 Å (Chapter 4). Therefore the scandium atom is very close in size to the zirconium atom.

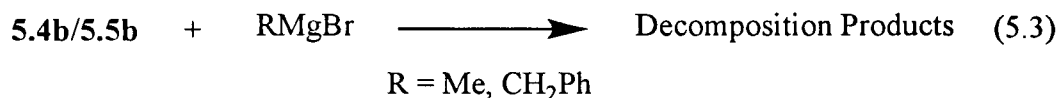
Also, the ionic radius of Sc^{3+} (0.88\AA) is slightly larger than the ionic radius of Zr^{4+} (0.86\AA).⁹ Since the zirconium and scandium atoms are about the same size, it seems reasonable for these complexes to exhibit similar features in their respective NMR spectra. The remainder of resonances in the ^1H NMR spectrum of complex **5.4b** remain sharp. The NCH_2 and NCH_2CH_2 proton resonances are consistent with chelation as evidenced by the second-order patterns associated with magnetically inequivalent protons. The presence of two equivalents of tmeda was confirmed by integration of the proton resonances of tmeda with respect to the proton resonances of the ligand. The presence of lithium chloride was confirmed by elemental analysis.

A similar reaction between the lithium salt of the butyl linked ligand and $\text{ScCl}_3(\text{THF})_3$ is observed (eq. 5.2). The presence of tmeda had a detrimental effect on the



synthesis of complex **5.5b**. The ^1H NMR spectrum reveals that complex **5.5b** has C_{2v} -symmetry in solution. The resonances in the ^1H NMR spectrum are all broad indicating that an exchange process is occurring. The ^1H NMR spectrum of the zirconium analogue is almost identical, with all the protons exhibiting broad ill-defined resonances. Again this is probably a result of partial rotation of the aryl groups on nitrogen. Two carbon resonances are observed for the isopropylmethyl carbons in the $^{13}\text{C}\{^1\text{H}\}$ NMR spectrum. Therefore, the isopropylmethyl groups are diastereotopic, and restricted rotation about the N-C_{ipso} bond is occurring. The presence of two equivalents of THF was confirmed by NMR spectroscopy.

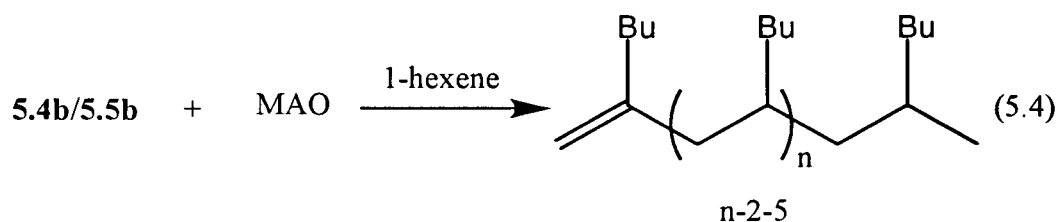
The formation of alkyl complexes of scandium using **5.4b** and **5.5b** did not proceed smoothly. Addition of alkyl Grignards, such as MeMgBr and PhCH₂MgBr, did not result in the formation of characterizable complexes (eq. 5.3). Fryzuk has reported similar problems



in forming dialkyl complexes of scandium with Grignard reagents.⁷ With the chloride complexes in hand, the activation of complexes **5.4b** and **5.5b** in the presence of 1-hexene was studied.

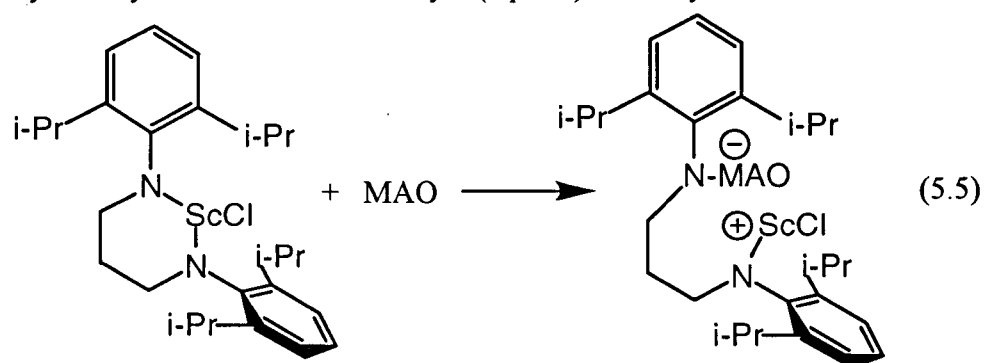
Oligomerization of 1-hexene

The dichloride complexes **5.4b** and **5.5b** can be activated with MAO in the presence of 1-hexene to form oligo(1-hexene) (eq. 5.4). In lieu of having an authentic scandium alkyl



complex, the addition of MAO to the chloride complexes **5.4b** and **5.5b** will result in the formation of the methyl complexes. MAO is also useful as a scavenger for water and as a chain transfer reagent. No high polymer was formed with these systems. Only low molecular weight oligomers of 4 to 7 monomer units were formed (confirmed by GPC analysis). These systems differ slightly from the analogous zirconium/MAO system which produced both high polymer and oligomer (Chapter 4). The catalyst systems **5.4b**/MAO and **5.5b**/MAO behave in much the same manner as the ansa-scandocene complexes **5.2**.¹ It is possible that the ligand is not suitably large enough to properly stabilize the scandium alkyl complexes. Furthermore, like in the zirconium system, if free rotation of the aryl group is

possible, MAO could attack the nitrogen atom of the ligand creating yet another complex which may or may not be an active catalyst (eq. 5.5). Clearly the removal of MAO from the



catalyst system and the generation of an authentic scandium alkyl complex is needed before these questions can be answered.

Conclusions

The use of bulky chelating diamido ligands makes possible the isolation of scandium 'ate' complexes. Attempts to synthesize alkyl complexes from the 'ate' complexes with Grignard reagents resulted in the formation of intractable materials. The activation of these scandium 'ate' complexes with MAO in the presence of 1-hexene leads to the oligomerization of the monomer. These complexes exhibit similar reactivity as the zirconium analogues. It is proposed that MAO may play a role in the decomposition of these catalyst systems.

Experimental

General Details: All experiments were performed under an atmosphere of dry dinitrogen using standard Schlenk line techniques or in an Innovative Technology Inc. dry box. Solvents were distilled from sodium/benzophenone ketyl (tetrahydrofuran, hexanes, diethylether), molten potassium (benzene), molten sodium (toluene) and CaH_2 (CH_2Cl_2) under argon and stored over activated 4Å molecular sieves. Chemicals were obtained from Aldrich Chemicals. N,N,N',N'-tetramethylethylenediamine (tmeda) was distilled prior to use. $\text{ScCl}_3(\text{THF})_3$ was synthesized according to literature procedure.¹ Proton (299.9 MHz) and carbon (75.46 MHz) NMR spectra were recorded in C_6D_6 at approximately 22°C on Varian Gemini-300 and Varian XL-300 spectrometers. The chemical shifts were referenced to internal $\text{C}_6\text{D}_5\text{H}$ ($\delta = 7.15$ ppm) and the carbon resonances to C_6D_6 ($\delta = 128.0$ ppm). GPC analyses (in THF) versus polystyrene standards were performed using a Waters GPC equipped with Waters Styragel columns (HR 1, HR 3, HR 4). Elemental analyses were performed by Mr. Peter Borda at the University of British Columbia.

[(BAIP) ScCl_2][Li(tmeda) $_2$], 5.4b. MeLi (1.48 M, 3.58 mL, 5.22 mmol) was added dropwise to a stirring solution of diamine **2.3b** (1.00 g, 2.60 mmol) in Et_2O (25 mL) at -30 °C. The solution was warmed to 23 °C where it was kept for 30 minutes. Tmeda (0.925 g, 7.80 mmol) was added dropwise and the resulting slurry added to a suspension of $\text{ScCl}_3(\text{THF})_3$ (0.996 g, 2.60 mmol) in THF (25mL) at -30 °C. The solution was stirred overnight at 23 °C. The solvent was removed *in vacuo* and the resulting paste dissolved in toluene and filtered through celite. The toluene was reduced in volume and hexanes was added until the solution was slightly turbid. The solution was cooled to -30 °C at which point pure complex **5.4b** crystallized (0.86 g, 1.15 mmol, 44 %). ^1H NMR δ 7.04 (m, 6H, Ar), 3.83 (sept, 4H, CHMe_2), 3.41 (t, 4H, NCH_2), 2.68 (m, 2H, NCH_2CH_2), 2.37 (s, 8H, NCH_2 , tmeda), 2.19 (s, 24H, NMe_2) 1.24 (d, 24H, CHMe_2). $^{13}\text{C}\{^1\text{H}\}$ NMR δ 149.8, 146.5,

123.6, 123.6, 60.4, 57.4, 46.1, 34.8, 27.9, 26.3, 25.3. Anal. Calcd. for $C_{39}H_{72}Cl_2LiN_6Sc$: C, 62.64; H, 9.70; N, 11.24. Found: C, 62.46; H, 9.68; N, 10.93.

[(BAIB)ScCl₂][Li(THF)₂], 5.5b. MeLi (1.48 M, 3.38 mL, 5.00 mmol) was added dropwise to a stirring solution of diamine **2.6b** (1.00 g, 2.45 mmol) in Et₂O (25 mL) at -30 °C. The solution was warmed to 23 °C where it was kept for 30 minutes. The resulting slurry was added to a suspension of ScCl₃(THF)₃ (0.901 g, 2.45 mmol) in THF (25 mL) at -30 °C. The solution was stirred overnight at 23 °C. The solvent was removed *in vacuo* and the resulting paste dissolved in toluene and filtered through celite. The toluene was reduced in volume and hexanes was added until the solution was slightly turbid. The solution was cooled to -30 °C at which point pure complex **5.5b** crystallized (0.923 g, 1.37 mmol, 56 %). ¹H NMR δ 7.10 (m, 6H, Ar), 4.08 (sept, 4H, CHMe₂), 3.58 (m, 4H, NCH₂), 3.13 (m, 8H, OCH₂), 2.44 (m, 4H, NCH₂CH₂), 1.57 (d, 12H, CHMe₂), 1.39 (d, 12H, CHMe₂), 1.17 (m, 8H, OCH₂CH₂). ¹³C { ¹H } NMR δ 148.3, 146.8, 124.6, 123.8, 68.6, 57.9, 30.2, 28.4, 27.1, 25.3, 24.6.

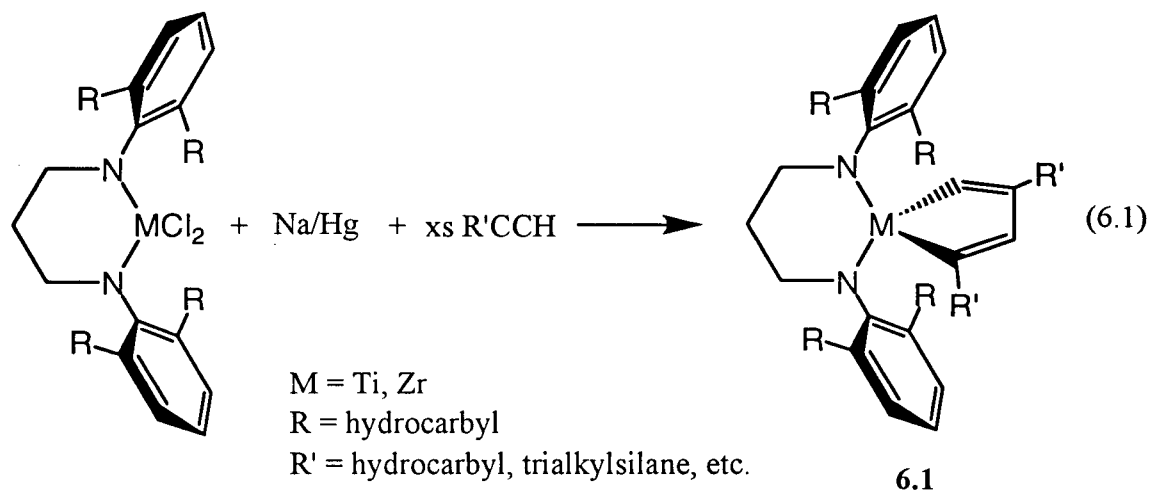
References

- (1) Piers, W. E.; Shapiro, P. J.; Bunel, E. E.; Bercaw, J. E. *Synlett* **1990**, 74.
- (2) McAlister, D. R.; Erwin, D. K.; Bercaw, J. E. *J. Am. Chem. Soc.* **1978**, *100*, 5966.
- (3) Bercaw, J. E. *Adv. Chem.* **1978**, *167*, 136.
- (4) Thompson, M. E.; Bercaw, J. E. *Pure Appl. Chem.* **1984**, *56*, 1.
- (5) Devore, D. D.; Timmers, F. J.; Hasha, D. L.; Rosen, R. K.; Marks, T. J.; Deck, P. A.; Stern, C. L. *Organometallics* **1995**, *14*, 3132.
- (6) Carpenetti, D. W.; Kloppenburg, L.; Kupec, J. T.; Peterson, J. L. *Organometallics* **1996**, *15*, 1572.
- (7) Fryzuk, M. D.; Giesbrecht, G.; Rettig, S. J. *Organometallics* **1996**, *15*, 3329.
- (8) Shapiro, P. J.; Bunel, E.; Schaefer, W. P.; Bercaw, J. E. *Organometallics* **1990**, *9*, 867.
- (9) Huheey, J. E. *Inorganic Chemistry: Principles of Structure and Reactivity*; Third ed.; Harper & Row Inc.: New York, 1983.

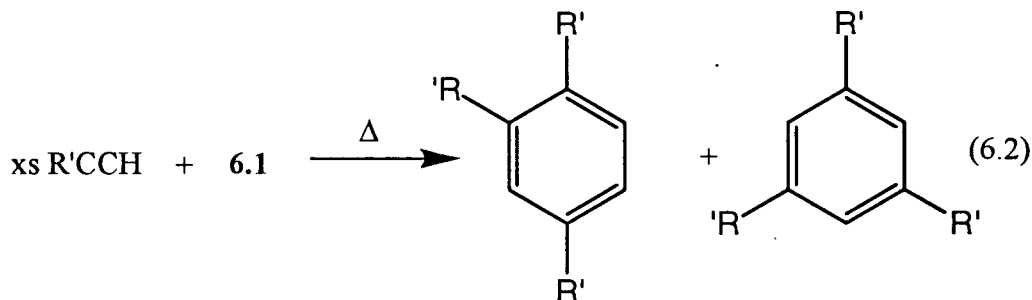
Chapter 6: Future Considerations

Cyclotrimerization of Alkynes

The catalytic [2 + 2 + 2] cyclotrimerization of alkynes has been observed with early transition metal organometallic catalysts. These catalysts have typically been based on group 4 aryloxides¹⁻⁴ or binaphtholate⁵ catalysts. Metallacyclopentadiene complexes are key intermediates in the catalytic cyclotrimerization of alkynes.⁶ A metallacyclopentadiene complex could conceivably be synthesized by reducing the bis(amido)dichloride derivatives in the presence of excess terminal acetylene (eq. 6.1).



The metallacyclopentadiene **6.1** may catalyze the cyclotrimerization of terminal acetylenes to 1,3,5- and 1,2,4-trisubstituted benzenes (eq. 6.2).



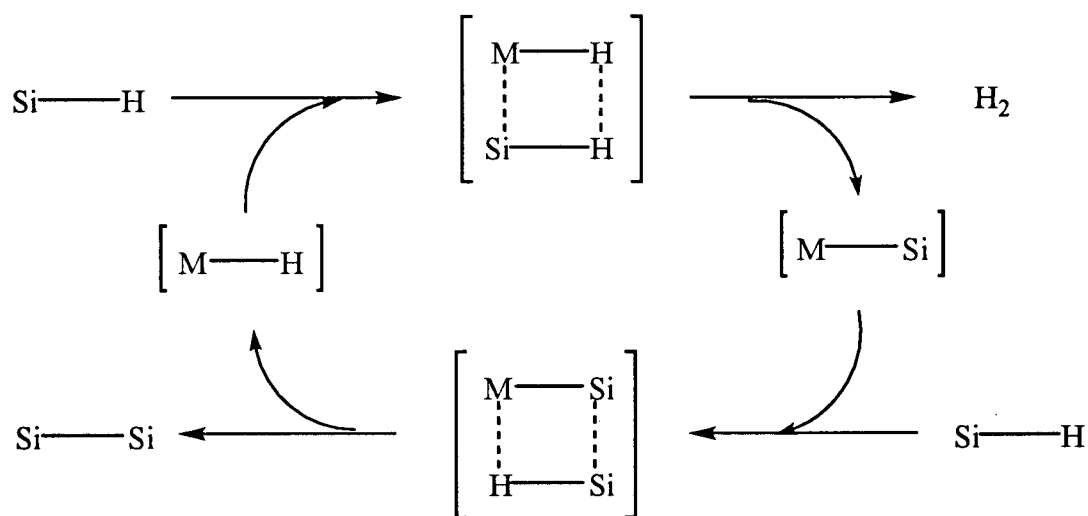
There are a number of interesting features which can be studied with this chemistry. For instance, will the product distribution of the substituted benzenes be ligand-dependent?

Can internal alkynes be cyclized to form C_6R_6 compounds? How will the size of the alkyne and/or size of the ligand in eq. 6.1 affect the substitution of the metallacyclopentadiene?

Dehydropolymerization of Silanes

Synthetic routes to polysilanes are of scientific and technological interest as these polymers show great potential in the field of advanced materials for electronics and integrated optics.^{7,8} While most industrial interest in polysilanes has focused on their use as ceramic precursors for the manufacture of silicon carbide-based materials, other potential applications have been identified. For example, photochemical depolymerizations have been investigated with respect to photoresist technology in the manufacture of computer chips.^{9,10} Also, σ -conjugation in the polysilane chains gives rise to conducting, photoconducting, and thermochromic behaviour. Further applications as third-order nonlinear optical devices and electrophotographic materials have also been considered.^{9,10}

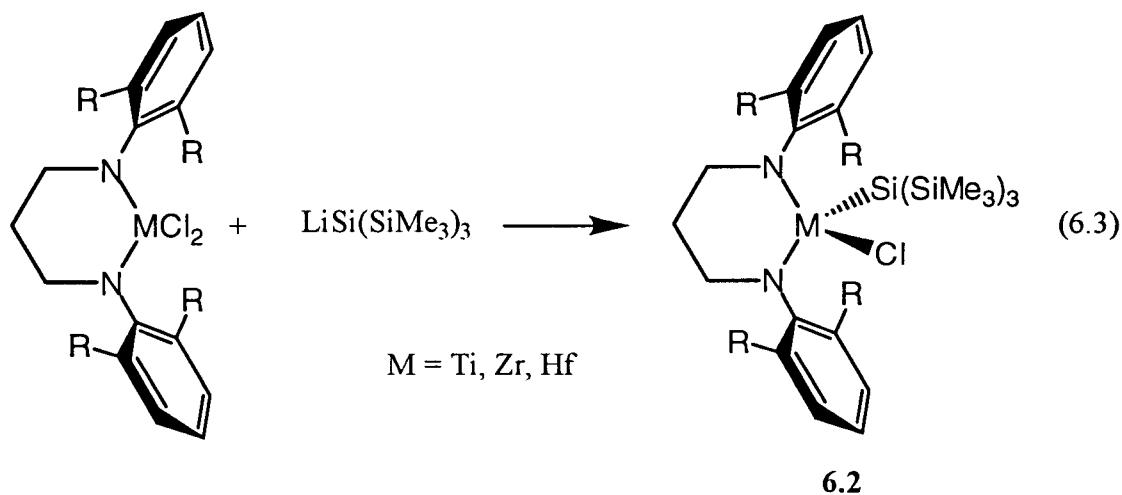
The mechanism of the dehydrocoupling reaction is still under consideration. The most widely accepted one is a constant oxidation state σ -bond metathesis with a transition state similar to that postulated for Ziegler-Natta olefin polymerization (Scheme 6.1).¹¹⁻¹³ It is believed that the active catalysts are coordinatively unsaturated metal hydride derivatives



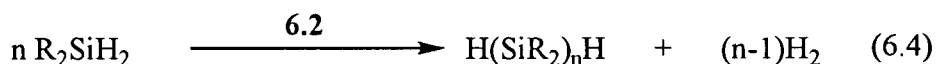
Scheme 6.1: The proposed mechanism of the dehydrocoupling of silanes

which form during an induction period for the polymerization.^{14,15} The mechanism involves two σ -bond metathesis steps which pass through four-centred transition states. The reactions may also be described as concerted $2\sigma + 2\sigma$ cycloadditions, similar to the $2\sigma + 2\pi$ process that is responsible for the coordination polymerization of α -olefins. It might be expected, therefore, that metal fragments which provide good olefin polymerization catalysts might also be active in dehydropolymerizations.

Metallocene complexes active for the dehydropolymerization of silanes have been synthesized.^{14,15} Given the relationship between metallocene complexes and the chelating bis(amide) complexes discussed, it seems reasonable to pursue dehydropolymerization catalysts bearing chelating bis(amide) ancillary ligands. These catalysts could be based on the existing ligand systems. Reaction between a dichloride derivative with tris(trimethylsilyl)silyllithium should generate the monosilyl derivative **6.2** (eq. 6.3). Due to



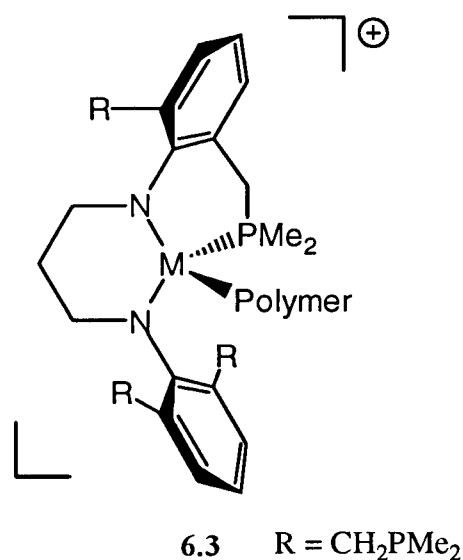
the rather large silyl ligand, it is highly unlikely that two tris(trimethylsilyl)silyl groups could be attached to the metal. Furthermore, the synthesis of a metal hydride is avoided with this reagent. Complex **6.2** may be an active catalyst for the dehydrocoupling of silanes (eq. 6.4).



Synthesis of Block Co-polymers

Given the fact that complexes **2.11a,b** give rise to a living coordination polymerization system when activated with $\text{B}(\text{C}_6\text{F}_5)_3$ and $\{\text{Ph}_3\text{C}\}[\text{B}(\text{C}_6\text{F}_5)_4]$ (Chapter 3), the next logical step is to attempt to form diblock and triblock co-polymers. One problem identified with these catalyst systems was a decomposition route which arose in the absence of monomer. This problem will have to be overcome before block co-polymers can be synthesized with narrow molecular weight distributions. One way in which this problem may be resolved is to introduce a side chain, with donor functionality, on the aryl groups on nitrogen.

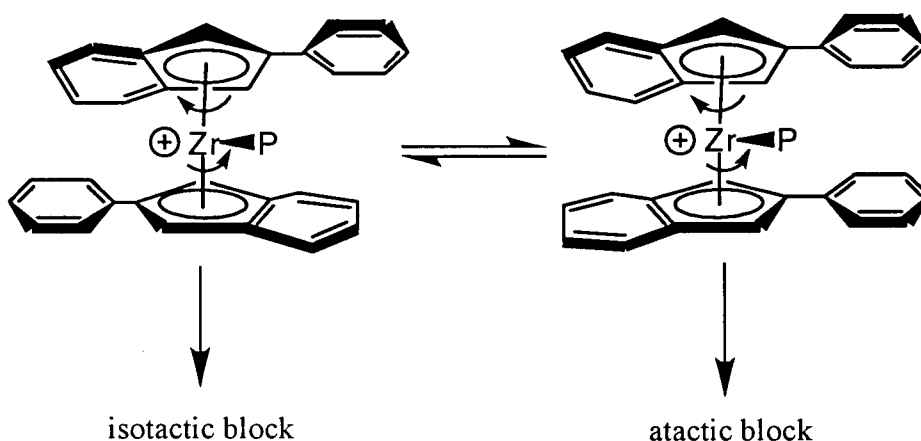
Complex **6.3** could possess the features necessary to stabilize the active catalyst. The dimethylphosphino group on the ligand may be able to stabilize the metal centre in the absence of monomer. Hopefully complex **6.3** will still be an active living coordination polymerization catalyst. Block co-polymers could be synthesized by adding monomer to complex **6.3**, waiting for it to be consumed entirely, and then adding the second monomer. If complex **6.3** does not decompose or deactivate in the absence of monomer, block co-polymers with high molecular weights and remarkably narrow molecular weight distributions could be synthesized. This could lead to the development of new materials with as yet undiscovered properties.



Potentially Stereoselective Catalysts

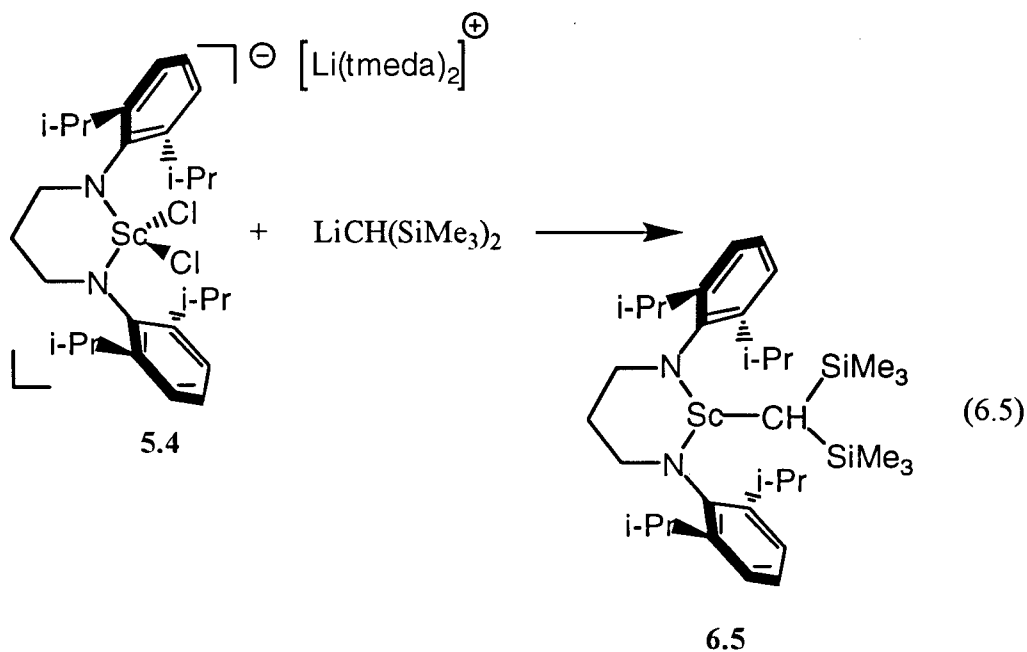
There has been some interest in the oscillating metallocene catalysts derived by Waymouth and co-workers.¹⁶ The catalyst, $(2\text{-phenylindenyl})_2\text{ZrCl}_2/\text{MAO}$, appears to isomerize by restricted rotation of its indenyl ligands, between chiral and achiral coordination

geometries during chain growth. This catalyst yields atactic–isotactic stereoblock polypropylene with elastomeric properties (Scheme 6.2).¹⁷

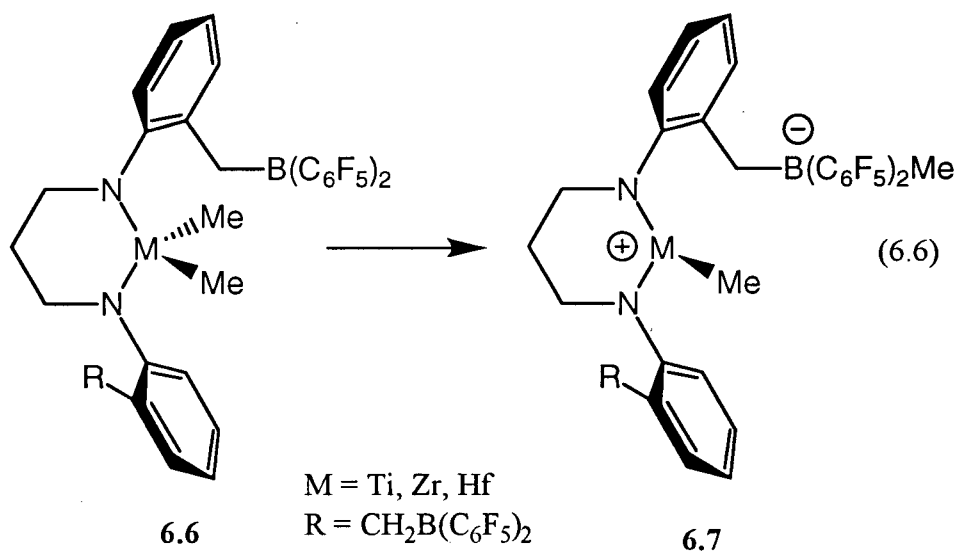


Scheme 6.2: Oscillating metallocene catalysts

Due to the restricted rotation about the N-C_{ipso} bond, present in many of the complexes studied in previous chapters, a potentially oscillating catalyst may be developed. By combining an *ortho*-substituted aryl group at nitrogen in the chelating diamido ligand, more electrophilic analogues (6.4) to the oscillating metallocene catalysts could be achieved (Scheme 6.3). Unlike the unsymmetrically 2,6-dialkyl aryl substituted complexes of chapter 2, which could not interconvert between the two rotamers, these *ortho*-aryl substituted complexes should be able to interconvert between chiral (*rac*-6.4) and achiral (*meso*-6.4) coordination geometries. The *ortho*-substituent on the aryl group will probably have to be extremely large to affect the enantiofacial selectivity of the incoming α -olefin. Polymerization studies of the unsymmetrically 2,6-dialkyl aryl substituted complexes revealed no enantiofacial selectivity for a methyl/isopropyl aryl substitution at nitrogen. Possibly an *ortho*-phenyl substituted aryl group or an *ortho*-adamantyl substituted aryl group would affect the incoming monomer. Controlling the rate of interconversion between the two rotamers will also be important. If the rotamers interconvert faster than the rate of polymerization, only atactic polymer will be produced. The ligand may have to be adjusted to slow the isomerization between the *rac*- and *meso*-rotamers.



A single component, self-activating, group 4 olefin polymerization catalyst could be synthesized by incorporating¹⁹ a strong Lewis acid into the aryl group on nitrogen. Complex **6.6** could be activated by intramolecular abstraction of a methyl group with the diaryl borane on the ancillary ligand to form the zwitterionic complex **6.7** (eq. 6.6). Complex **6.7**, if stable, could be a single component group 4 olefin polymerization catalyst.



References

- (1) Smith, D. P.; Strickler, J. R.; Gray, S. D.; Bruck, M. A.; Holmes, R. S.; Wigley, D. E. *Organometallics* **1992**, *11*, 1275.
- (2) Johnson, E. S.; Balaich, G. J.; Rothwell, I. P. *J. Am. Chem. Soc.* **1997**, *119*, 7685.
- (3) Johnson, E. S.; Balaich, G. J.; Fanwick, P. E.; Rothwell, I. P. *J. Am. Chem. Soc.* **1997**, *119*, 11086.
- (4) Heeres, H. J.; Heeres, A.; Teuben, J. H. *Organometallics* **1990**, *9*, 1508.
- (5) van der Linden, A.; Schaverien, C. J.; Meijboom, N.; Ganter, C.; Orpen, A. G. *J. Am. Chem. Soc.* **1995**, *117*, 3008.
- (6) Collman, J. P.; Hegedus, L. S.; Norton, J. R.; Finke, R. G. *Principles and Applications of Organotransition Metal Chemistry*; 2nd ed.; University Science Books: Mill Valley, CA, 1987, pp 509.
- (7) *Inorganic and Organometallic Polymers*; Zeldin, M.; Wynne, K. J.; Allcock, H. R., Ed.; ACS Symposium Series 360. American Chemical Society: Washington, DC, 1988.
- (8) Mark, J. E.; Allcock, H. R.; West, R. C. *Inorganic Polymers*; Prentice Hall: Englewood Cliffs, NJ, 1992.
- (9) Miller, R. D.; Michl, J. *Chem. Rev.* **1989**, *89*, 1359.
- (10) West, R. *J. Organomet. Chem.* **1986**, *300*, 327.
- (11) Woo, H.-G.; Tilley, T. D. *J. Am. Chem. Soc.* **1989**, *111*, 8043.
- (12) Woo, H.-G.; Tilley, T. D. *J. Am. Chem. Soc.* **1992**, *114*, 7047.
- (13) Tilley, T. D. *Acc. Chem. Res.* **1993**, *26*, 22.
- (14) Imori, T.; Tilley, T. D. *Polyhedron* **1994**, *13*, 2231.
- (15) Dioumaev, V. K.; Harrod, J. F. *J. Organomet. Chem.* **1996**, *521*, 133.
- (16) Coates, G. W.; Waymouth, R. M. *Science* **1995**, *267*, 217.
- (17) Brintzinger, H. H.; Fischer, D.; Mülhaupt, R.; Rieger, B.; Waymouth, R. M. *Angew. Chem., Int. Ed. Engl.* **1995**, *34*, 1143.
- (18) Burger, B. J.; Cotter, W. D.; Coughlin, E. B.; Chacon, S. T.; Hajela, S.; Herzog, T. A.; Köhn, R.; Mitchell, J.; Piers, W. E.; Shapiro, P. J.; Bercaw, J. E. In *Ziegler*

Catalysts: Recent Scientific Innovations and Technological Improvements; G. Fink, R. Mülhaupt and H. H. Brintzinger, Ed.; Springer-Verlag: Berlin, 1995.

- (19) Duchateau, R.; Lancaster, S. J.; Thorntonpett, M.; Bochmann, M. *Organometallics* **1997**, *16*, 4995.

Appendix A: X-ray Crystallography

X-ray Crystallography of Complex 2.10b

A suitable crystal of complex **2.10b** was grown from saturated toluene and hexanes at -30°C. Crystal data may be found in Table A1. Data were collected on a Siemens P4 diffractometer with the XSCANS software package.¹ The cell constants were obtained by centring 42 reflections ($11.3 \leq 2\theta \leq 49.9^\circ$). The Laue symmetry 2/m was determined by merging symmetry equivalent positions. The data were collected in the range of $\theta = 1.90$ - 22.5° ($-1 \leq h \leq 10$, $-1 \leq k \leq 15$, $-22 \leq l \leq 22$) in the ω scan mode at variable scan speeds (2-20 deg/min.). Four standard reflections monitored at the end of every 297 reflections collected showed no decay of the crystal. The data processing, solution and refinement were done using *SHELXTL-PC* programs.² The final refinements were performed using *SHELXL-93* software programs.³ An empirical absorption correction was applied to the data using the ψ scans data. Anisotropic thermal parameters were refined for all non-hydrogen atoms in the neutral molecule except for two phenyl ring carbon atoms. Large thermal motions were observed for C(2), C(26), and C(27) carbon atoms. The carbon atom C(2) has positional disorder with an occupancy factor of 0.8/0.2 (derived from electron density ratios). The isotropic temperature factor for atom C(2A) was refined. Two different orientations (0.5/0.5) were found for the methyl carbon atoms C(26) and C(27). Individual isotropic thermal parameters were refined for these carbon atoms in the least-squares cycles. All the C-C bond and C-C-C bond angles in the isopropyl groups were restrained using the option SADI. No attempt was made to locate the hydrogen atoms, however, they were placed in calculated positions. In the final difference Fourier synthesis the electron density fluctuates in the range 0.44(7) to -0.27(7) e Å⁻³.

Table A1. Crystal Data and Experimental Details for complex **2.10b**

Empirical formula	C ₂₇ H ₄₀ Cl ₂ N ₂ Ti ₁
Formula weight	511.41
Temperature	25 °C
Wavelength	0.71073 Å
Crystal system	Monoclinic
Space group	P2 ₁ /n
Unit cell dimensions	a = 9.771(1) Å b = 14.189(1) Å c = 21.081(2) Å β = 96.27(1) °
Volume	2905.2(5) Å ³
Z	4
Density, calcd	1.169 g.cm ⁻³
Absorption coefficient	0.494 mm ⁻¹
F(000)	1088
Reflections Collected	4724
Independent reflections	3754 [R(int) = 0.0371]
Refinement method	Full-matrix least-squares on F ²
Data/restraints/parameters	3754/73/217
Goodness-of-fit (GooF) on F ²	1.081
Final R indices [I>2sigma(I)]	R1 = 0.0701, wR2 = 0.1495
R indices (all data)	R1 = 0.1454, wR2 = 0.1800

$$R1 = \sum (||F_o| - |F_c||) / \sum |F_o|;$$

$$wR2 = \left[\sum w(F_o^2 - F_c^2)^2 / \sum wF_o^4 \right]^{1/2}$$

$$GooF = \left[\sum w(F_o^2 - F_c^2)^2 / (n - p) \right]^{1/2}$$

where n is the number of reflections and p is the number of parameters refined.

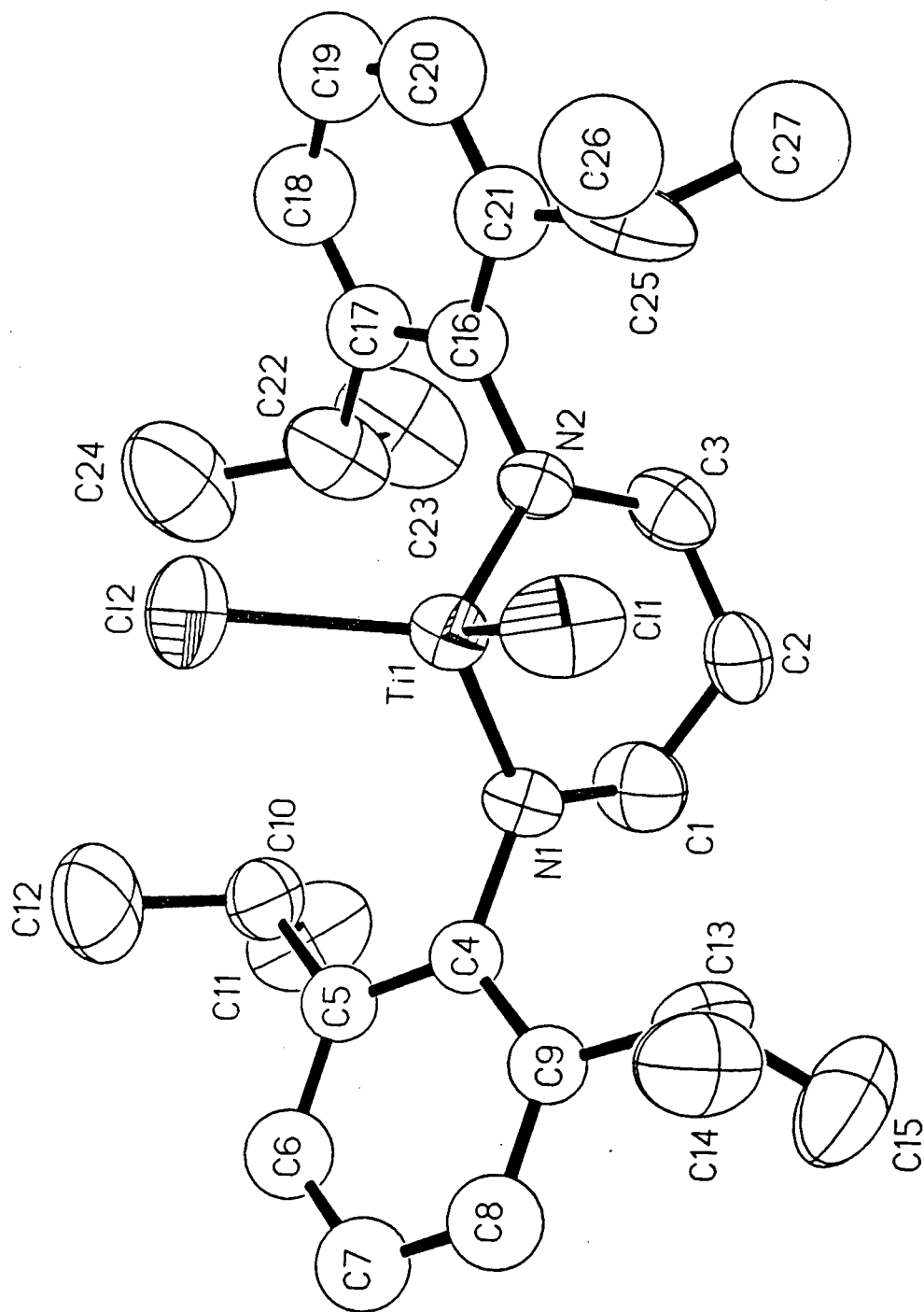


Figure A1: Molecular Structure of Complex 2.10b

Table A2: Atomic coordinates ($\times 10^4$) and equivalent isotropic displacement parameters ($\text{\AA}^2 \times 10^3$) of complex **2.10b**. $U(\text{eq})$ is defined as one third of the trace of the orthogonalized U_{ij} tensor.

Atom	x	y	z
Ti (1)	-0.115	-0.075	1.025
Cl (2)	0.093	-1.244	2.945
Cl (3)	-0.469	2.070	1.566
N (4)	-1.397	-0.894	-0.039
C (5)	-1.034	-1.762	-1.160
C (6)	0.301	-2.370	-1.013
C (7)	1.481	-1.460	-0.984
C (8)	-2.812	-0.761	0.189
C (9)	-3.522	0.313	-0.336
C (10)	-4.891	0.409	-0.128
C (11)	-5.555	-0.572	0.604
C (12)	-4.845	-1.645	1.128
C (13)	-3.473	-1.740	0.920
C (14)	-2.845	1.372	-1.229
C (15)	-3.180	1.148	-2.697
C (16)	-3.216	2.791	-0.799
C (17)	-2.760	-2.963	1.512
C (18)	-2.986	-3.093	3.031
C (19)	-3.175	-4.235	0.805
C (20)	2.474	0.555	-0.046
C (21)	2.491	1.624	-0.933
C (22)	3.562	2.513	-0.931
C (23)	4.615	2.330	-0.042
C (24)	4.596	1.260	0.845
C (25)	3.527	0.372	0.843
C (26)	1.365	1.848	-1.948
C (27)	1.851	1.580	-3.386
C (28)	0.767	3.255	-1.865
C (29)	3.554	-0.820	1.791
C (30)	3.776	-0.694	3.205
C (31)	4.575	-1.944	1.197
N (32)	1.362	-0.342	-0.039

Table A3. Bond Lengths (Å) of Complex 2.10b

Ti(1)-Cl(2)	2.257	C(14)-C(15)	1.523
Ti(1)-Cl(3)	2.240	C(14)-C(16)	1.529
Ti(1)-N(4)	1.856	C(17)-C(18)	1.541
Ti(1)-N(32)	1.840	C(17)-C(19)	1.513
N(4)-C(5)	1.464	C(20)-C(21)	1.389
N(4)-C(8)	1.439	C(20)-C(25)	1.390
C(5)-C(6)	1.475	C(20)-N(32)	1.429
C(6)-C(7)	1.490	C(21)-C(22)	1.392
C(7)-N(32)	1.470	C(21)-C(26)	1.533
C(8)-C(9)	1.390	C(22)-C(23)	1.390
C(8)-C(13)	1.389	C(23)-C(24)	1.391
C(9)-C(10)	1.389	C(24)-C(25)	1.389
C(9)-C(14)	1.542	C(25)-C(29)	1.523
C(10)-C(11)	1.392	C(26)-C(27)	1.541
C(11)-C(12)	1.389	C(26)-C(28)	1.531
C(12)-C(13)	1.390	C(29)-C(30)	1.436
C(13)-C(17)	1.534	C(29)-C(31)	1.630

Table A4. Bond Angles (°) of complex **2.10b**

Cl(2)-Ti(1)-Cl(3)	107.748	C(15)-C(14)-C(16)	110.740
Cl(2)-Ti(1)-N(4)	108.835	C(13)-C(17)-C(18)	112.283
Cl(2)-Ti(1)-N(32)	110.051	C(13)-C(17)-C(19)	111.259
Cl(3)-Ti(1)-N(4)	116.840	C(18)-C(17)-C(19)	110.474
Cl(3)-Ti(1)-N(32)	113.894	C(21)-C(20)-C(25)	120.022
N(4)-Ti(1)-N(32)	99.177	C(21)-C(20)-N(32)	119.720
Ti(1)-N(4)-C(5)	121.932	C(25)-C(20)-N(32)	120.255
Ti(1)-N(4)-C(8)	123.217	C(20)-C(21)-C(22)	120.007
C(5)-N(4)-C(8)	114.829	C(20)-C(21)-C(26)	121.773
N(4)-C(5)-C(6)	113.154	C(22)-C(21)-C(26)	118.213
C(5)-C(6)-C(7)	117.840	C(21)-C(22)-C(23)	119.977
C(6)-C(7)-N(32)	114.401	C(22)-C(23)-C(24)	119.946
N(4)-C(8)-C(9)	120.885	C(23)-C(24)-C(25)	120.054
N(4)-C(8)-C(13)	119.108	C(20)-C(25)-C(24)	120.001
C(9)-C(8)-C(13)	119.993	C(20)-C(25)-C(29)	120.968
C(8)-C(9)-C(10)	120.031	C(24)-C(25)-C(29)	118.998
C(8)-C(9)-C(14)	121.685	C(21)-C(26)-C(27)	111.145
C(10)-C(9)-C(14)	118.174	C(21)-C(26)-C(28)	112.645
C(9)-C(10)-C(11)	120.010	C(27)-C(26)-C(28)	109.495
C(10)-C(11)-C(12)	119.930	C(25)-C(29)-C(30)	123.147
C(11)-C(12)-C(13)	120.031	C(25)-C(29)-C(31)	108.916
C(8)-C(13)-C(12)	120.014	C(30)-C(29)-C(31)	108.813
C(8)-C(13)-C(17)	122.911	Ti(1)-N(32)-C(7)	123.191
C(12)-C(13)-C(17)	117.071	Ti(1)-N(32)-C(20)	122.490
C(9)-C(14)-C(15)	111.170	C(7)-N(32)-C(20)	114.287
C(9)-C(14)-C(16)	111.619		

Table A5. Calculated Hydrogen Atom Positional ($\times 10^4$) and Thermal ($\times 10^3$) Parameters for complex **2.10b**

Atom	x	y	z	Ueq
H(1A)	445(8)	6258(5)	1548(4)	83
H(1B)	970(8)	5514(5)	1082(4)	83
H(2A)	2795(8)	6039(8)	1722(4)	73
H(2B)	2563(8)	4980(8)	1882(4)	73
H(2A1)	1161(40)	6764(22)	2054(12)	74
H(2A2)	2471(40)	6408(22)	1770(12)	74
H(3A)	3147(7)	5717(5)	2810(3)	76
H(3B)	2071(7)	6521(5)	2642(3)	76
H(6)	-4317(4)	5040(4)	623(3)	79
H(7)	-3789(6)	3859(5)	-72(2)	83
H(8)	-1628(7)	3163(4)	49(3)	81
H(10)	-2127(7)	5915(5)	1950(3)	70
H(11A)	-1908(20)	6921(23)	1101(27)	159
H(11B)	-3055(67)	7318(8)	1493(12)	159
H(11C)	-3464(49)	6788(18)	848(17)	159
H(12A)	-4205(24)	5154(25)	2075(27)	156
H(12B)	-4938(11)	5705(47)	1489(5)	156
H(12C)	-4400(33)	6249(25)	2114(26)	156
H(13)	1092(7)	3675(5)	1251(3)	67
H(14A)	1349(9)	2103(6)	1010(25)	123
H(14B)	18(50)	2113(6)	522(9)	123
H(14C)	-101(45)	2211(5)	1255(17)	123
H(15A)	2193(31)	3387(37)	337(17)	157
H(15B)	1478(60)	4378(9)	304(19)	157
H(15C)	790(32)	3531(42)	-88(4)	157
H(18)	-110(7)	7090(4)	4518(4)	111
H(19)	1217(9)	6245(6)	5303(2)	120
H(20)	2556(7)	4995(5)	5022(3)	108
H(22)	-399(8)	6629(6)	2850(4)	104
H(23A)	-471(40)	8315(17)	2946(31)	190
H(23B)	1027(40)	7906(8)	3050(36)	190
H(23C)	282(77)	8213(22)	3639(7)	190
H(24A)	-2496(14)	7193(52)	3006(12)	187
H(24B)	-2043(15)	7440(41)	3723(26)	187
H(24C)	-2255(24)	6385(14)	3513(35)	187
H(25)	2702(8)	4183(6)	3438(4)	109
H(26A)	3472(121)	2941(24)	3947(41)	149
H(26B)	2011(23)	3145(43)	4158(62)	149
H(26C)	3337(132)	3398(20)	4614(20)	149
H(27A)	4573(23)	5258(48)	3731(57)	158

Atom	x	y	z	Ueq
H(27B)	5101(31)	4214(47)	3753(57)	158
H(27C)	4889(48)	4741(91)	4388(11)	158
H(26D)	2575(96)	2787(10)	4067(50)	152
H(26E)	1221(27)	3377(52)	4075(52)	152
H(26F)	2340(115)	3394(51)	4667(11)	152
H(27D)	4398(20)	4533(93)	4621(25)	162
H(27E)	4907(36)	4723(81)	3953(42)	162
H(27F)	4757(48)	3685(24)	4192(60)	162

X-ray Crystallography of Complex 2.11a

Very air-sensitive, rectangular, yellow crystals of complex **2.11a** were grown from a pentane solution. A suitable crystal with the dimensions 0.24 x 0.23 x 0.20 mm was mounted inside a Lindemann capillary tube, flame sealed and used for the experiments. The X-ray diffraction experiments were carried out on a Enraf-Nonius CAD4F diffractometer controlled by the Enraf-Nonius CAD4 software package⁴ using graphite monochromated Mo K α radiation at 23°C. The cell constants were obtained by centering 24 reflections ($21.9^\circ \leq 2\theta \leq 24.3^\circ$). The Laue symmetry mmm was confirmed by inspection of reflection intensities. The data were collected in the θ range $1.0 - 25.0^\circ$ ($-1 \leq h \leq 9$, $-1 \leq k \leq 18$, $-1 \leq l \leq 20$) in $\theta - 2\theta$ scan mode at variable scan speeds (2-20 deg/min). Moving background measurements were made at 25% extensions of the scan range. Four standard reflections were monitored at the end of every 297 reflection collected. The data processing was carried out using the Enraf-Nonius structure determination package,⁵ solution and initial refinements were done using *SHELXTL-PC*² programs. The final cycles of refinement were performed using *SHELXL-93*³ software programs. An empirical absorption correction was applied to the data using the ψ scans data. Anisotropic thermal parameters were refined for all of the non-hydrogen atoms in the molecule except for the phenyl ring carbon atoms and the carbon and nitrogen atoms of the metallocycle ring. Individual isotropic thermal parameters were refined for these atoms in the least-squares cycles. The methyl hydrogen atoms were fitted in their idealized positions, while the methylene and phenyl hydrogen atoms were placed in their calculated positions. In a final least-squares refinement cycles on F^2 , the model converged at $R1 = 0.0759$, $wR1 = 0.1458$ and $Goof = 0.947$ for 1360 observations with $F_o \geq 4\sigma(F_o)$ and 133 parameters, and $R2 = 0.1438$ and $wR2 = 0.1693$ for all 2597 data. In the final difference Fourier synthesis the electron density fluctuates in the range 0.27(6) to -0.30(6) e \AA^{-3} . The experimental details and crystal data, the positional and thermal parameters, bond distances and angles have been included below.

Table A6. Crystal Data and Experimental Details for complex **2.11a**

Empirical formula	C ₂₇ H ₃₀ N ₂ Ti
Formula weight	358.37
Temperature	23 °C
Wavelength	0.71073 Å
Crystal system	Orthorhombic
Space group	P2 ₁ 2 ₁ 2 ₁
Unit cell dimensions	a = 8.0955(10) Å b = 15.288(4) Å c = 16.909(3) Å
Volume	2092.8(7) Å ³
Z	4
Density, calcd	1.137 g.cm ⁻³
Absorption coefficient	0.413 mm ⁻¹
F(000) electrons	768
Reflections Collected	2785
Independent reflections	2597 [R(int) = 0.024]
Refinement method	Full-matrix least-squares on F ²
Data/restraints/parameters	2597 / 0 / 133
Goodness-of-fit (GooF) on F ²	0.947
Final R indices [I>2sigma(I)]	R1 = 0.0759, wR2 = 0.1458
R indices (all data)	R1 = 0.1438, wR2 = 0.1693

$$R1 = \sum (||F_o| - |F_c||) / \sum |F_o|;$$

$$wR2 = \left[\sum w(F_o^2 - F_c^2)^2 / \sum wF_o^4 \right]^{1/2}$$

$$GooF = \left[\sum w(F_o^2 - F_c^2)^2 / (n - p) \right]^{1/2}$$

where n is the number of reflections and p is the number of parameters refined.

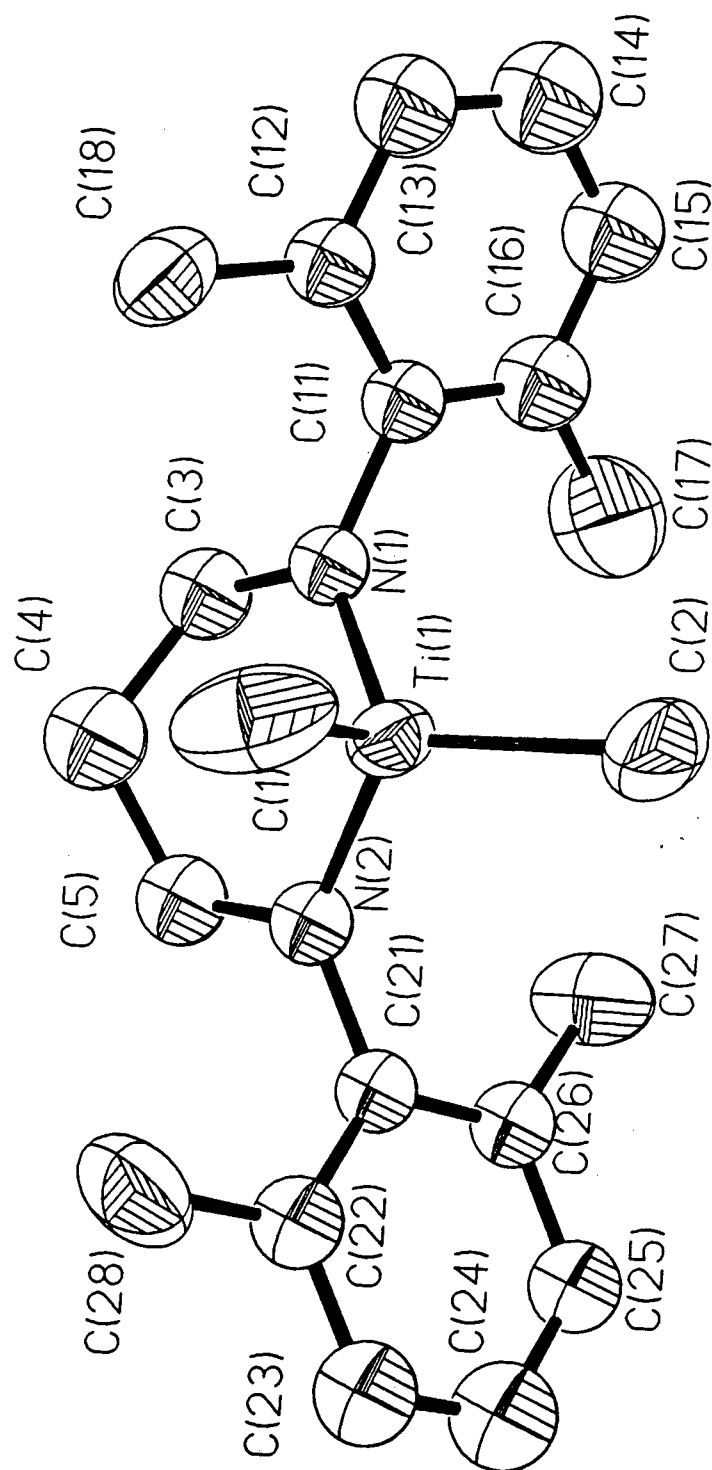


Figure A2: Molecular Structure of Complex 2.11a

Table A7. Atomic coordinates ($\times 10^4$) and equivalent isotropic displacement parameters ($\text{\AA}^2 \times 10^3$) for complex **2.11a**. $U(\text{eq})$ is defined as one third of the trace of the orthogonalized U_{ij} tensor.

atom	x	y	z	Ueq
Ti (1)	-1342 (2)	-4258 (1)	-7806 (1)	47 (1)
C (12)	1214 (12)	-4637 (5)	-9683 (4)	52 (2)
C (13)	1177 (13)	-4756 (6)	-10491 (5)	68 (3)
C (14)	321 (12)	-4175 (7)	-10946 (6)	84 (3)
C (15)	-517 (12)	-3490 (6)	-10636 (5)	74 (3)
C (16)	-511 (12)	-3374 (6)	-9821 (5)	66 (3)
C (11)	334 (10)	-3958 (5)	-9348 (4)	47 (2)
C (22)	-2438 (11)	-3789 (5)	-5652 (5)	55 (2)
C (23)	-3680 (13)	-3548 (6)	-5102 (5)	68 (2)
C (24)	-4732 (12)	-2899 (6)	-5274 (6)	78 (3)
C (25)	-4631 (11)	-2445 (6)	-5962 (5)	59 (2)
C (26)	-3396 (10)	-2631 (5)	-6523 (4)	51 (2)
C (21)	-2316 (9)	-3323 (5)	-6355 (4)	45 (2)
C (1)	-904 (14)	-5567 (6)	-7491 (5)	98 (4)
C (2)	-3726 (11)	-4301 (7)	-8258 (5)	94 (3)
N (1)	300 (8)	-3860 (4)	-8484 (3)	44 (2)
C (3)	1711 (11)	-3348 (6)	-8175 (5)	61 (3)
C (4)	1932 (11)	-3504 (6)	-7278 (5)	76 (3)
C (5)	543 (10)	-3129 (5)	-6764 (5)	60 (2)
N (2)	-1059 (8)	-3549 (4)	-6918 (3)	47 (2)
C (27)	-3338 (12)	-2122 (5)	-7270 (5)	82 (3)
C (18)	2136 (10)	-5283 (5)	-9184 (5)	67 (3)
C (28)	-1291 (13)	-4531 (6)	-5462 (5)	89 (3)
C (17)	-1342 (15)	-2582 (7)	-9483 (6)	112 (4)

Table A8. Bond Distances (Å) for complex **2.11a**

Ti (1)-N(1)	1.858 (6)	Ti (1)-N(2)	1.867 (6)
Ti (1)-C (2)	2.077 (9)	Ti (1)-C (1)	2.100 (9)
C (12)-C (13)	1.378 (10)	C (12)-C (11)	1.380 (10)
C (12)-C (18)	1.498 (10)	C (13)-C (14)	1.364 (11)
C (14)-C (15)	1.354 (12)	C (15)-C (16)	1.388 (11)
C (16)-C (11)	1.380 (11)	C (16)-C (17)	1.499 (12)
C (11)-N(1)	1.470 (9)	C (22)-C (21)	1.390 (10)
C (22)-C (23)	1.418 (11)	C (22)-C (28)	1.501 (11)
C (23)-C (24)	1.340 (11)	C (24)-C (25)	1.357 (11)
C (25)-C (26)	1.407 (10)	C (26)-C (21)	1.401 (10)
C (26)-C (27)	1.485 (10)	C (21)-N(2)	1.436 (9)
N(1)-C (3)	1.480 (9)	C (3)-C (4)	1.546 (10)
C (4)-C (5)	1.532 (10)	C (5)-N(2)	1.470 (9)

Table A9. Bond Angles(°) for complex **2.11a**

N(1)-Ti (1)-N(2)	102.6 (3)	N(1)-Ti (1)-C (2)	116.7 (3)
N(2)-Ti (1)-C (2)	115.4 (3)	N(1)-Ti (1)-C (1)	110.3 (3)
N(2)-Ti (1)-C (1)	109.2 (3)	C (2)-Ti (1)-C (1)	102.7 (4)
C (13)-C (12)-C (11)	119.6 (9)	C (13)-C (12)-C (18)	118.9 (9)
C (11)-C (12)-C (18)	121.4 (7)	C (14)-C (13)-C (12)	119.0 (10)
C (15)-C (14)-C (13)	122.6 (9)	C (14)-C (15)-C (16)	118.8 (10)
C (11)-C (16)-C (15)	119.6 (9)	C (11)-C (16)-C (17)	121.6 (8)
C (15)-C (16)-C (17)	118.7 (10)	C (16)-C (11)-C (12)	120.3 (7)
C (16)-C (11)-N(1)	120.1 (7)	C (12)-C (11)-N(1)	119.6 (7)
C (21)-C (22)-C (23)	118.6 (8)	C (21)-C (22)-C (28)	121.8 (8)
C (23)-C (22)-C (28)	119.6 (8)	C (24)-C (23)-C (22)	120.0 (9)
C (23)-C (24)-C (25)	121.8 (10)	C (24)-C (25)-C (26)	121.2 (9)
C (25)-C (26)-C (21)	117.3 (7)	C (25)-C (26)-C (27)	119.3 (8)
C (21)-C (26)-C (27)	123.3 (7)	C (22)-C (21)-C (26)	121.1 (8)
C (22)-C (21)-N(2)	119.6 (7)	C (26)-C (21)-N(2)	119.3 (7)
C (11)-N(1)-C (3)	112.9 (6)	C (11)-N(1)-Ti (1)	126.4 (5)
C (3)-N(1)-Ti (1)	120.6 (5)	N(1)-C (3)-C (4)	110.7 (7)
C (5)-C (4)-C (3)	114.5 (8)	N(2)-C (5)-C (4)	112.5 (6)
C (21)-N(2)-C (5)	113.8 (6)	C (21)-N(2)-Ti (1)	125.9 (5)
C (5)-N(2)-Ti (1)	120.3 (5)		

Table A10. Calculated Hydrogen Atom Positional ($\times 10^4$) and Thermal ($\times 10^3$) Parameters for complex **2.11a**

Atom	x	y	z	U(eq)
H(13A)	1769(13)	-5236(6)	-10722(5)	126(7)
H(14A)	315(12)	-4256(7)	-11509(6)	126(7)
H(15A)	-1115(12)	-3091(6)	-10967(5)	126(7)
H(23A)	-3760(13)	-3867(6)	-4614(5)	126(7)
H(24A)	-5581(12)	-2756(6)	-4899(6)	126(7)
H(25A)	-5400(11)	-1983(6)	-6074(5)	126(7)
H(1A)	-1821(14)	-5784(6)	-7189(5)	126(7)
H(1B)	85(14)	-5602(6)	-7180(5)	126(7)
H(1C)	-777(14)	-5913(6)	-7961(5)	126(7)
H(2A)	-4446(11)	-3961(7)	-7928(5)	126(7)
H(2B)	-4103(11)	-4896(7)	-8270(5)	126(7)
H(2C)	-3732(11)	-4066(7)	-8784(5)	126(7)
H(3A)	2696(11)	-3516(6)	-8453(5)	126(7)
H(3B)	1529(11)	-2735(6)	-8263(5)	126(7)
H(4A)	1947(11)	-4125(6)	-7192(5)	126(7)
H(4B)	2980(11)	-3276(6)	-7112(5)	126(7)
H(5A)	828(10)	-3192(5)	-6216(5)	126(7)
H(5B)	450(10)	-2515(5)	-6878(5)	126(7)
H(27A)	-4130(12)	-2354(5)	-7636(5)	126(7)
H(27B)	-2252(12)	-2160(5)	-7495(5)	126(7)
H(27C)	-3595(12)	-1520(5)	-7162(5)	126(7)
H(18A)	1454(10)	-5461(5)	-8748(5)	126(7)
H(18B)	3127(10)	-5017(5)	-8986(5)	126(7)
H(18C)	2416(10)	-5785(5)	-9497(5)	126(7)
H(28A)	-1776(13)	-5072(6)	-5634(5)	126(7)
H(28B)	-1107(13)	-4553(6)	-4901(5)	126(7)
H(28C)	-258(13)	-4444(6)	-5729(5)	126(7)
H(17A)	-1733(15)	-2217(7)	-9905(6)	126(7)
H(17B)	-568(15)	-2261(7)	-9166(6)	126(7)
H(17C)	-2258(15)	-2761(7)	-9160(6)	126(7)

X-ray Crystallography of Complex 2.41a

An air-sensitive, block-like, dark-red crystals of complex **2.41a** were grown from a solution of hexanes. A crystal with the dimension 0.32 x 0.21 x 0.19 mm was mounted inside a Lindemann capillary tube, flame sealed and used for the data collection. The X-ray diffraction experiments were carried out on a Siemens P4 diffractometer with XSCANS software package¹ using graphite monochromated Mo K α radiation at 25°C. The cell constants were obtained by centering 22 reflections ($22.2 \leq 2\theta \leq 23.0^\circ$). The Laue symmetry 2/m was determined by merging symmetry equivalent reflections. A total of 4516 data were collected in the θ range 2.0 - 23.0° ($-1 \leq h \leq 10$, $-1 \leq k \leq 12$, $-27 \leq l \leq 27$) in ω scan mode at variable scan speeds (2-20 deg/min). Background measurements were made at the ends of the scan range. Four standard reflections were monitored at the end of every 297 reflection collection. The data processing, solution and refinements were done using *SHELXTL*^{2,3} programs. The faces of the data crystal was indexed and the distances between them were measured (8 faces and the face indices are {001}, {011}, (101) and (-10-1)). A Gaussian absorption was applied to the data. The maximum and minimum transmission factors were 0.913 and 0.902 respectively. The methylene carbon atom C(6) was found to have occupy two positions and the occupancies were refined close to 0.7 and 0.3. The Ti, Cl, N, O and the non-phenyl carbon atoms except C(6) were refined anisotropically. Individual isotropic thermal parameters were refined for the phenyl carbon atoms and the disordered C(6). The two phenyl rings were treated as regular hexagons. No attempt was made to locate the hydrogen atoms. However most of the hydrogen atoms were placed in the calculated positions. In the final least-squares refinement cycles on F^2 , the model converged at $R1 = 0.0729$, $wR2 = 0.1484$ and $Goof = 1.002$ for 1857 observations with $F_o \geq 4\sigma(F_o)$ and 192 parameters, and $R1 = 0.1500$ and $wR2 = 0.1783$ for all 3412 data. In the final difference Fourier synthesis the electron density fluctuates in the range 0.65 to -0.31 e Å⁻³. The maximum shift/esd and maximum shift in the final cycles were 0.006 and 0.00 respectively. The experimental

details and crystal data, the positional and thermal parameters, bond distances and angles, anisotropic thermal parameters, hydrogen atom coordinates and selected torsion angles have been included in the supporting materials.

Table A11. Crystal Data and Experimental Details for complex **2.41a**

Empirical formula	C ₂₄ H ₃₂ Cl ₂ N ₂ OTi
Formula weight	483.32
Temperature	25°C
Wavelength	0.71073 Å
Crystal system	Monoclinic
Space group	P2 ₁ /n
Unit cell dimensions	a = 9.131(1)Å b = 10.927(2)Å c = 24.621(4)Å β = 90.56(1)°
Volume	2456.4(7) Å ³
Z	4
Density, calcd.	1.307 g.cm ⁻³
Absorption coefficient	0.584 mm ⁻¹
F(000)	1016
Reflections Collected	4516
Independent reflections	3412 [R(int) = 0.0484]
Refinement method	Full-matrix least-squares on F ²
Data/restraints/parameters	1857/13/192
Goodness-of-fit (GooF) on F ²	1.002
Final R indices [I>2sigma(I)]	R1 = 0.0729, wR2 = 0.1484
R indices (all data)	R1 = 0.1500, wR2 = 0.1783

$$R1 = \sum (||F_o| - |F_c||) / \sum |F_o|;$$

$$wR2 = \left[\sum w(F_o^2 - F_c^2)^2 / \sum wF_o^4 \right]^{1/2}$$

$$GooF = \left[\sum w(F_o^2 - F_c^2)^2 / (n - p) \right]^{1/2}$$

where n is the number of reflections and p is the number of parameters refined.

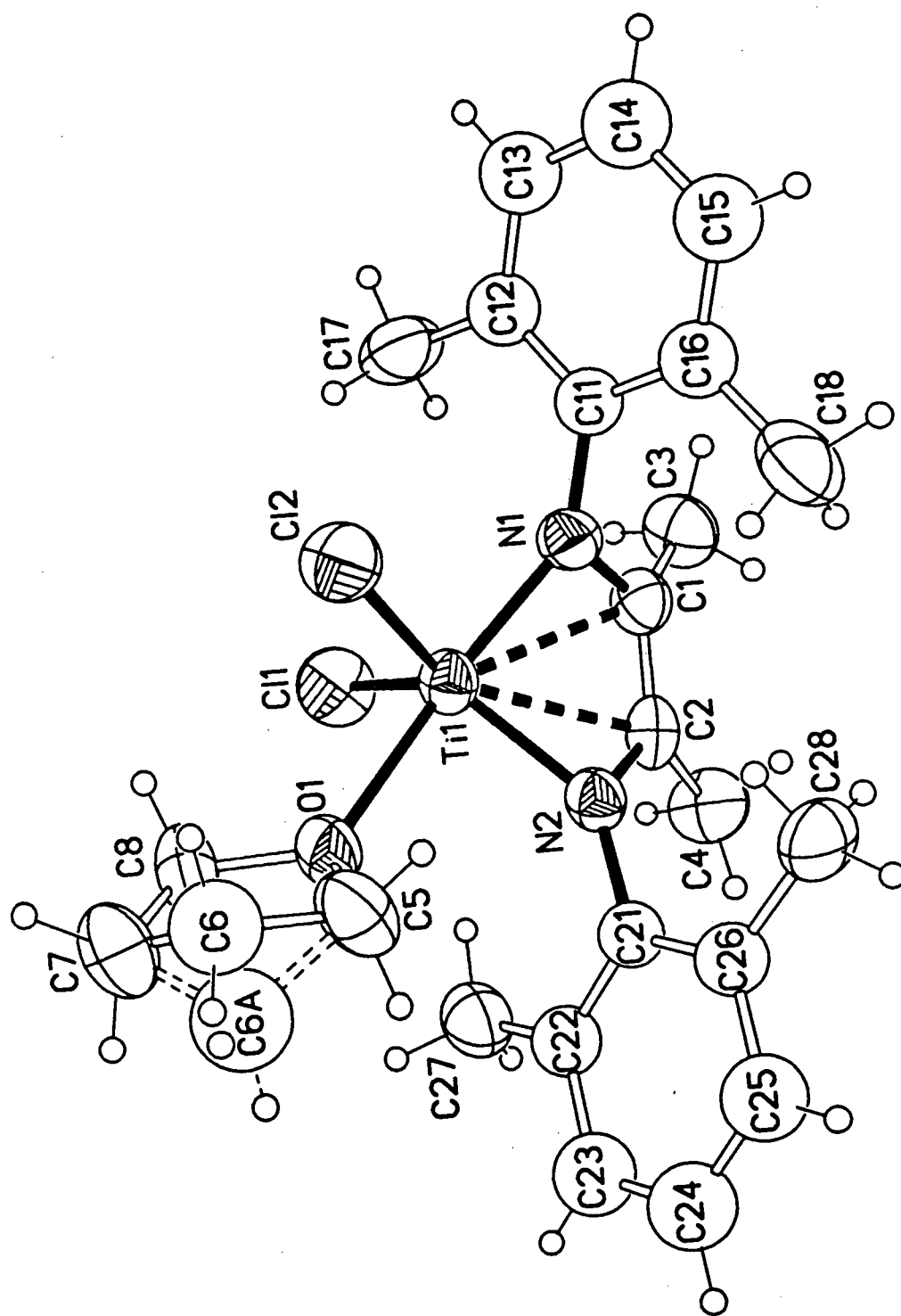


Figure A3: Molecular Structure of Complex 2.41a

Table A12. Atomic coordinates ($\times 10^4$) and equivalent isotropic displacement parameters ($\text{\AA}^2 \times 10^3$) for complex **2.41a**. $U(\text{eq})$ is defined as one third of the trace of the orthogonalized U_{ij} tensor.

atom	x	y	z	Ueq
Ti (1)	526.5 (14)	6402.0 (11)	8427.1 (5)	41.3 (4)
Cl (1)	1287 (3)	6806 (2)	7564 (1)	67.4 (6)
Cl (2)	-1948 (2)	5957 (2)	8481 (1)	66.8 (6)
N (1)	130 (6)	7926 (5)	8772 (2)	46 (2)
N (2)	2080 (6)	6161 (5)	8944 (2)	41 (1)
C (1)	1585 (8)	8271 (7)	8802 (3)	45 (2)
C (2)	2589 (8)	7349 (7)	8884 (2)	43 (2)
C (3)	2018 (9)	9557 (7)	8663 (3)	61 (2)
C (4)	4222 (7)	7581 (7)	8850 (3)	62 (2)
O (1)	648 (5)	4418 (4)	8266 (2)	51 (1)
C (5)	296 (10)	3568 (7)	8697 (3)	69 (2)
C (6) a	-729 (14)	2680 (12)	8458 (4)	78 (4)
C (6A) a	328 (39)	2368 (18)	8432 (7)	95 (11)
C (7)	-262 (11)	2597 (7)	7879 (4)	96 (3)
C (8)	295 (9)	3856 (7)	7753 (3)	68 (2)
C (11)	-1037 (5)	8743 (4)	8895 (2)	47 (2)
C (12)	-1824 (6)	9320 (5)	8482 (1)	58 (2)
C (13)	-2992 (5)	10081 (5)	8609 (2)	70 (2)
C (14)	-3372 (5)	10265 (5)	9148 (2)	76 (3)
C (15)	-2585 (6)	9688 (5)	9561 (2)	73 (3)
C (16)	-1418 (5)	8927 (5)	9434 (2)	58 (2)
C (17)	-1432 (9)	9152 (8)	7901 (3)	75 (3)
C (18)	-595 (10)	8304 (8)	9884 (3)	78 (3)
C (21)	2958 (5)	5209 (4)	9170 (2)	44 (2)
C (22)	3850 (6)	4473 (5)	8853 (1)	52 (2)
C (23)	4570 (5)	3478 (4)	9084 (2)	72 (2)
C (24)	4396 (6)	3218 (4)	9633 (2)	76 (3)
C (25)	3504 (6)	3953 (5)	9950 (1)	70 (2)
C (26)	2784 (5)	4949 (4)	9718 (2)	52 (2)
C (27)	4144 (8)	4738 (7)	8272 (3)	66 (2)
C (28)	1900 (9)	5768 (8)	10073 (3)	66 (2)

Occupancies of C(6) and C(6A) are 0.7 and 0.3 respectively.

Table A13. Bond Distances (Å) for complex **2.41a**

Ti (1) -N (1)	1.906 (6)	Ti (1) -N (2)	1.914 (5)
Ti (1) -O (1)	2.207 (5)	Ti (1) -Cl (1)	2.284 (2)
Ti (1) -Cl (2)	2.316 (2)	Ti (1) -C (2)	2.417 (7)
Ti (1) -C (1)	2.437 (7)	N (1) -C (1)	1.382 (8)
N (1) -C (11)	1.424 (6)	N (2) -C (2)	1.387 (8)
N (2) -C (21)	1.424 (6)	C (1) -C (2)	1.376 (9)
C (1) -C (3)	1.500 (10)	C (2) -C (4)	1.516 (9)
O (1) -C (8)	1.438 (7)	O (1) -C (5)	1.450 (8)
C (5) -C (6A)	1.47 (2)	C (5) -C (6)	1.468 (12)
C (6) -C (7)	1.494 (12)	C (6A) -C (7)	1.48 (2)
C (7) -C (8)	1.500 (10)	C (12) -C (17)	1.490 (8)
C (16) -C (18)	1.495 (8)	C (22) -C (27)	1.488 (8)
C (26) -C (28)	1.494 (8)		

Table A14. Bond Angles (°) for complex **2.41a**

N(1)-Ti(1)-N(2)	88.1(2)	N(1)-Ti(1)-O(1)	161.6(2)
N(2)-Ti(1)-O(1)	86.9(2)	N(1)-Ti(1)-Cl(1)	107.8(2)
N(2)-Ti(1)-Cl(1)	114.5(2)	O(1)-Ti(1)-Cl(1)	90.35(14)
N(1)-Ti(1)-Cl(2)	88.2(2)	N(2)-Ti(1)-Cl(2)	130.5(2)
O(1)-Ti(1)-Cl(2)	81.66(14)	Cl(1)-Ti(1)-Cl(2)	113.54(10)
N(1)-Ti(1)-C(2)	64.5(2)	N(2)-Ti(1)-C(2)	35.0(2)
O(1)-Ti(1)-C(2)	117.7(2)	Cl(1)-Ti(1)-C(2)	96.2(2)
Cl(2)-Ti(1)-C(2)	145.0(2)	N(1)-Ti(1)-C(1)	34.4(2)
N(2)-Ti(1)-C(1)	64.8(2)	O(1)-Ti(1)-C(1)	150.6(2)
Cl(1)-Ti(1)-C(1)	93.9(2)	Cl(2)-Ti(1)-C(1)	122.5(2)
C(2)-Ti(1)-C(1)	32.9(2)	C(1)-N(1)-C(11)	122.6(5)
C(1)-N(1)-Ti(1)	94.3(4)	C(11)-N(1)-Ti(1)	142.0(4)
C(2)-N(2)-C(21)	122.5(5)	C(2)-N(2)-Ti(1)	92.8(4)
C(21)-N(2)-Ti(1)	140.5(4)	C(2)-C(1)-N(1)	116.6(6)
C(2)-C(1)-C(3)	122.8(7)	N(1)-C(1)-C(3)	119.9(7)
C(2)-C(1)-Ti(1)	72.8(4)	N(1)-C(1)-Ti(1)	51.2(3)
C(3)-C(1)-Ti(1)	143.4(5)	C(1)-C(2)-N(2)	118.5(6)
C(1)-C(2)-C(4)	121.6(7)	N(2)-C(2)-C(4)	119.6(7)
C(1)-C(2)-Ti(1)	74.3(4)	N(2)-C(2)-Ti(1)	52.3(3)
C(4)-C(2)-Ti(1)	144.0(5)	C(8)-O(1)-C(5)	108.7(5)
C(8)-O(1)-Ti(1)	124.5(4)	C(5)-O(1)-Ti(1)	119.0(4)
O(1)-C(5)-C(6A)	104.0(10)	O(1)-C(5)-C(6)	105.9(6)
C(5)-C(6)-C(7)	103.7(8)	C(5)-C(6A)-C(7)	104.4(13)
C(6A)-C(7)-C(8)	103.0(10)	C(6)-C(7)-C(8)	104.1(7)
O(1)-C(8)-C(7)	106.5(6)	C(12)-C(11)-N(1)	120.7(4)
C(16)-C(11)-N(1)	119.2(4)	C(11)-C(12)-C(17)	121.3(4)
C(13)-C(12)-C(17)	118.7(4)	C(15)-C(16)-C(18)	119.1(4)
C(11)-C(16)-C(18)	120.9(4)	C(22)-C(21)-N(2)	122.3(4)
C(26)-C(21)-N(2)	117.4(4)	C(23)-C(22)-C(27)	117.2(4)
C(21)-C(22)-C(27)	122.7(4)	C(25)-C(26)-C(28)	119.1(4)
C(21)-C(26)-C(28)	120.8(4)		

Table A15. Calculated Hydrogen Atom Positional ($\times 10^4$) and Thermal $\times 10^3$) Parameters for complex **2.41a**

Atom	x	y	z	Ueq
H(3A)	1265(25)	10111(8)	8777(17)	92
H(3B)	2144(52)	9626(13)	8278(4)	92
H(3C)	2921(28)	9757(16)	8846(16)	92
H(4A)	4505(12)	7615(45)	8476(3)	93
H(4B)	4742(8)	6930(24)	9029(18)	93
H(4C)	4454(11)	8345(23)	9024(18)	93
H(5A)	-154(10)	3994(7)	8998(3)	83
H(5B)	1174(10)	3160(7)	8829(3)	83
H(6A)	-1731(14)	2966(12)	8483(4)	94
H(6B)	-647(14)	1892(12)	8637(4)	94
H(6A1)	-277(39)	1785(18)	8624(7)	114
H(6A2)	1321(39)	2054(18)	8417(7)	114
H(7A)	-1083(11)	2385(7)	7644(4)	116
H(7B)	503(11)	1991(7)	7836(4)	116
H(8A)	1159(9)	3809(7)	7527(3)	82
H(8B)	-448(9)	4327(7)	7562(3)	82
H(13)	-3518(8)	10467(7)	8333(2)	84
H(14)	-4154(7)	10774(6)	9233(3)	91
H(15)	-2840(8)	9811(7)	9921(2)	87
H(17A)	-1695(59)	8340(20)	7787(7)	113
H(17B)	-397(14)	9267(53)	7859(5)	113
H(17C)	-1952(50)	9740(36)	7683(4)	113
H(18A)	429(13)	8489(42)	9856(14)	117
H(18B)	-736(50)	7435(9)	9857(14)	117
H(18C)	-951(44)	8588(40)	10227(3)	117
H(23)	5167(7)	2986(6)	8872(3)	86
H(24)	4878(8)	2551(5)	9787(3)	91
H(25)	3388(8)	3779(7)	10316(2)	83
H(27A)	3874(55)	4042(20)	8055(4)	99
H(27B)	5168(13)	4907(48)	8227(5)	99
H(27C)	3580(45)	5436(31)	8158(7)	99
H(28A)	902(13)	5776(36)	9947(13)	99
H(28B)	2291(33)	6583(13)	10060(16)	99
H(28C)	1939(46)	5473(27)	10440(5)	99

X-ray Crystallography of Complex 2.54b•CH₂Cl₂

A yellow needle crystal of complex 2.54b•CH₂Cl₂ having approximate dimensions of 0.08 x 0.25 x 0.60 mm was mounted in a glass capillary. All measurements were made on a Rigaku AFC6S diffractometer with graphite monochromated Cu-K α radiation. The cell constants were obtained by centring 25 reflections in the range $31.5 \leq 2\theta \leq 45.6^\circ$. The data were collected at a temperature of $21 \pm 1^\circ\text{C}$ using the ω - 2θ scan technique to a maximum 2θ value of 155° . A total of 10798 reflections were collected, 10503 were unique ($R_{\text{int}} = 0.037$); equivalent reflections were merged. The intensities of three standard reflections, measured every 200 reflections, decayed linearly by 1.8%. A linear correction factor was applied to the data to account for this phenomenon.

The data were processed, corrected for Lorentz and polarization effects, decay, and absorption (empirical: based on azimuthal scans). The structure was solved by direct methods⁶ and expanded using Fourier techniques.⁷ The CH₂Cl₂ solvate is severely disordered. The six largest peaks in the solvent region were refined as Cl and the next four as C. The occupancy factors and isotropic thermal parameters were refined for all ten solvent peaks. All other non-hydrogen atoms were refined anisotropically. Hydrogen atoms (except those associated with the disordered solvent) were fixed in calculated positions with C-H = 0.98 Å. In the final least-squares refinement cycle on F^2 , the model converged at $R1 = 0.041$, $wR1 = 0.034$ and $\text{Goof} = 1.64$ for 3442 observed reflections ($I \geq 3\sigma(I)$) and 637 parameters. In the final difference fourier synthesis the electron density fluctuates in the range 0.20 and -0.19 e Å⁻³. All calculations were performed using the teXsan crystallographic software package of Molecular Structure Corporation.⁸

Table A16. Crystallographic data for 2.54•CH₂Cl₂.^a

Empirical Formula	C ₄₆ H ₄₂ BF ₁₅ N ₂ Ti•CH ₂ Cl ₂
Formula Weight	1051.47
Crystal size (mm)	0.08 × 0.25 × 0.60
Crystal system	monoclinic
Space group	<i>P</i> 2 ₁ / <i>n</i> (No. 14)
<i>a</i> , Å	20.292(2)
<i>b</i> , Å	11.253(2)
<i>c</i> , Å	23.459(2)
β°	114.967(7)
<i>V</i> (Å ³)	4856(1)
<i>Z</i>	4
<i>T</i> (°C)	21
<i>D</i> _c (g/cm ³)	1.438
<i>F</i> (000)	2144
μ(Cu <i>K</i> α) (cm ⁻¹)	33.36
Transmission factors	0.70-1.00
Scan type	ω-2θ
Scan range (deg in ω)	0.89 + 0.20 tan θ
Scan speed (deg/min.)	16 (up to 8 rescans)
Data collected	+ <i>h</i> , + <i>k</i> , ± <i>l</i>
2θ _{max} (deg)	155
Crystal decay (%)	1.8
Total no. of reflns	10 798
Unique reflections	10 503
<i>R</i> _{merge}	0.037
No. with <i>I</i> ≥ 3σ(<i>I</i>)	3442
No. of variables	637
<i>R</i>	0.041
<i>R</i> _w	0.034
gof	1.64
Max Δ/σ	0.002
Residual density (e/Å ³)	-0.19, 0.20

^a Rigaku AFC6S diffractometer, takeoff angle 6.0°, aperture 6.0 × 6.0 mm at a distance of 285 mm from the crystal, stationary background counts at each end of the scan (scan/background time ratio 2:1), Cu *K*α radiation (λ = 1.54178 Å), graphite monochromator, σ²(*F*²) = [*S*²(*C* + 4*B*)]/*Lp*² (*S* = scan speed, *C* = scan count, *B* = normalized background count), function minimized Σ*w*(|*F*_o| - |*F*_c|)² where *w* = 4/*F*_o²σ²(*F*_o²), *R* = Σ||*F*_o| - |*F*_c||/Σ|*F*_o|, *R*_w = (Σ*w*(|*F*_o| - |*F*_c|)²/Σ*w**F*_o²)^{1/2}, and gof = [Σ*w*(|*F*_o| - |*F*_c|)²/(*m* - *n*)]^{1/2}. Values given for *R*, *R*_w, and gof are based on those reflections with *I* ≥ 3σ(*I*).

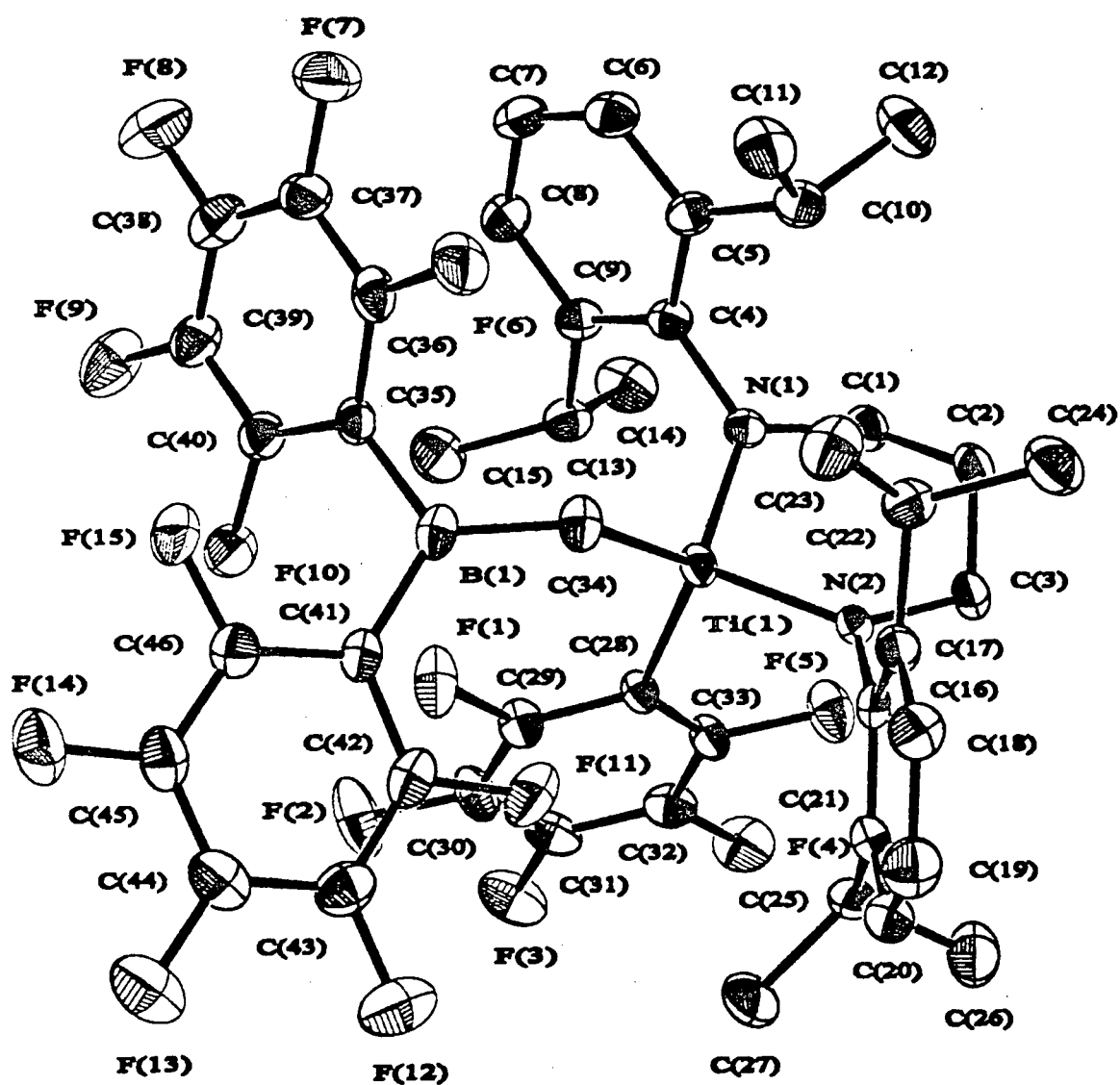


Figure A4. Molecular Structure of complex 2.54b·CH₂Cl₂

Table A17. Atomic coordinates, B_{eq} and Occupancy Factors for complex **2.54b**•CH₂Cl₂

atom	x	y	z	B_{eq}	occ
Ti (1)	0.51149 (5)	0.39763 (7)	0.32626 (4)	3.70 (2)	
Cl (1)	0.508 (2)	0.298 (1)	0.0157 (5)	15.7 (6)	0.33 (2)
Cl (2)	0.582 (1)	0.310 (1)	0.0352 (6)	17.1 (6)	0.41 (2)
Cl (3)	0.4436 (7)	0.378 (1)	0.0498 (5)	13.1 (5)	0.48 (2)
Cl (4)	0.4117 (9)	0.405 (1)	0.0664 (7)	10.2 (6)	0.20 (1)
Cl (5)	0.454 (1)	0.317 (2)	0.0276 (9)	12.4 (8)	0.21 (2)
Cl (6)	0.516 (2)	0.400 (1)	0.0693 (7)	17.3 (8)	0.25 (1)
F (1)	0.5218 (2)	0.1142 (2)	0.3152 (1)	7.29 (10)	
F (2)	0.4895 (2)	-0.0758 (3)	0.3665 (2)	9.7 (1)	
F (3)	0.4263 (2)	-0.0493 (2)	0.4463 (1)	8.2 (1)	
F (4)	0.3971 (2)	0.1707 (3)	0.4755 (1)	7.57 (10)	
F (5)	0.4300 (2)	0.3606 (2)	0.4258 (1)	6.90 (10)	
F (6)	0.6909 (2)	0.4150 (3)	0.2512 (2)	8.2 (1)	
F (7)	0.8310 (2)	0.3629 (3)	0.3133 (2)	9.6 (1)	
F (8)	0.8726 (2)	0.1487 (3)	0.3694 (2)	10.1 (1)	
F (9)	0.7716 (2)	-0.0160 (3)	0.3587 (2)	9.4 (1)	
F (10)	0.6312 (2)	0.0307 (2)	0.2936 (1)	6.72 (9)	
F (11)	0.4164 (2)	0.2183 (3)	0.2045 (2)	8.1 (1)	
F (12)	0.3336 (2)	0.0555 (3)	0.1239 (2)	9.9 (1)	
F (13)	0.3880 (2)	-0.0835 (3)	0.0603 (2)	9.7 (1)	
F (14)	0.5261 (2)	-0.0514 (3)	0.0748 (1)	9.3 (1)	
F (15)	0.6110 (2)	0.1072 (3)	0.1564 (1)	7.12 (9)	
N (1)	0.5835 (2)	0.4659 (3)	0.3965 (2)	3.67 (10)	
N (2)	0.4385 (2)	0.5096 (3)	0.3068 (2)	3.48 (10)	
C (1)	0.5626 (3)	0.5429 (4)	0.4378 (2)	4.7 (1)	
C (2)	0.5062 (3)	0.6357 (4)	0.4022 (2)	5.0 (1)	
C (3)	0.4340 (3)	0.5934 (4)	0.3543 (2)	4.7 (1)	
C (4)	0.6607 (3)	0.4504 (4)	0.4150 (2)	3.9 (1)	
C (5)	0.6998 (3)	0.5365 (5)	0.3980 (2)	4.3 (1)	
C (6)	0.7722 (3)	0.5140 (5)	0.4137 (3)	5.5 (2)	
C (7)	0.8062 (3)	0.4135 (6)	0.4453 (3)	5.7 (2)	
C (8)	0.7688 (3)	0.3316 (5)	0.4637 (2)	5.3 (2)	
C (9)	0.6954 (3)	0.3483 (4)	0.4490 (2)	4.3 (1)	
C (10)	0.6660 (3)	0.6525 (5)	0.3668 (2)	5.3 (2)	
C (11)	0.6838 (3)	0.6865 (5)	0.3118 (3)	7.4 (2)	
C (12)	0.6890 (3)	0.7532 (5)	0.4156 (3)	8.2 (2)	
C (13)	0.6576 (2)	0.2621 (4)	0.4754 (2)	4.9 (1)	
C (14)	0.6787 (3)	0.2874 (5)	0.5446 (3)	7.3 (2)	
C (15)	0.6731 (3)	0.1327 (5)	0.4658 (3)	7.2 (2)	
C (16)	0.3812 (3)	0.5236 (4)	0.2438 (2)	3.8 (1)	

atom	x	y	z	B _{eq}	occ
C(17)	0.3922(3)	0.6013(4)	0.2019(3)	4.6(1)	
C(18)	0.3370(3)	0.6129(5)	0.1422(3)	6.0(2)	
C(19)	0.2728(3)	0.5512(6)	0.1239(3)	6.9(2)	
C(20)	0.2629(3)	0.4774(5)	0.1658(3)	6.0(2)	
C(21)	0.3157(3)	0.4613(4)	0.2268(3)	4.8(2)	
C(22)	0.4604(3)	0.6749(5)	0.2193(2)	5.3(2)	
C(23)	0.4918(3)	0.6722(5)	0.1709(3)	7.5(2)	
C(24)	0.4448(3)	0.8037(5)	0.2311(3)	7.4(2)	
C(25)	0.3010(2)	0.3819(4)	0.2720(2)	5.1(1)	
C(26)	0.2483(3)	0.4399(5)	0.2940(3)	8.0(2)	
C(27)	0.2731(3)	0.2600(5)	0.2450(3)	8.2(2)	
C(28)	0.4757(2)	0.2479(4)	0.3658(2)	3.8(1)	
C(29)	0.4890(3)	0.1335(4)	0.3544(2)	4.7(1)	
C(30)	0.4729(3)	0.0333(5)	0.3797(3)	5.4(2)	
C(31)	0.4417(3)	0.0468(5)	0.4196(3)	5.3(2)	
C(32)	0.4273(3)	0.1573(5)	0.4352(2)	5.1(2)	
C(33)	0.4449(3)	0.2519(4)	0.4079(2)	4.5(1)	
C(34)	0.5415(2)	0.3743(4)	0.2511(2)	4.9(1)	
C(35)	0.6526(3)	0.2276(4)	0.2714(2)	4.3(1)	
C(36)	0.7082(4)	0.3069(5)	0.2790(3)	5.3(2)	
C(37)	0.7810(4)	0.2812(6)	0.3099(3)	6.1(2)	
C(38)	0.8015(4)	0.1732(7)	0.3374(3)	6.7(2)	
C(39)	0.7508(4)	0.0908(6)	0.3325(3)	6.0(2)	
C(40)	0.6784(3)	0.1182(5)	0.2993(3)	5.0(2)	
C(41)	0.5189(3)	0.1685(4)	0.1863(2)	4.5(1)	
C(42)	0.4465(4)	0.1525(5)	0.1736(3)	5.7(2)	
C(43)	0.4024(4)	0.0701(6)	0.1322(3)	6.4(2)	
C(44)	0.4292(4)	0.0006(6)	0.0994(3)	6.6(2)	
C(45)	0.4997(4)	0.0146(6)	0.1084(3)	6.3(2)	
C(46)	0.5422(3)	0.0965(5)	0.1505(3)	5.3(2)	
C(47)	0.395(2)	0.458(4)	0.020(2)	15(1)	0.35(3)
C(48)	0.612(2)	0.386(4)	0.004(2)	19(1)	0.30(2)
C(49)	0.547(2)	0.266(3)	0.021(1)	7(1)	0.40(7)
C(50)	0.570(1)	0.366(2)	0.0755(9)	12.1(8)	0.65(4)
B(1)	0.5702(3)	0.2608(5)	0.2363(3)	4.5(2)	

Table A18. Bond Lengths(Å) for complex **2.54b**•CH₂Cl₂.

atom	atom	distance	atom	atom	distance
Ti(1)	N(1)	1.846(4)	Ti(1)	N(2)	1.849(3)
Ti(1)	C(28)	2.191(4)	Ti(1)	C(34)	2.111(4)
F(1)	C(29)	1.360(5)	F(2)	C(30)	1.343(5)
F(3)	C(31)	1.352(5)	F(4)	C(32)	1.337(5)
F(5)	C(33)	1.369(5)	F(6)	C(36)	1.354(5)
F(7)	C(37)	1.346(6)	F(8)	C(38)	1.344(6)
F(9)	C(39)	1.335(6)	F(10)	C(40)	1.341(5)
F(11)	C(42)	1.350(5)	F(12)	C(43)	1.336(6)
F(13)	C(44)	1.339(6)	F(14)	C(45)	1.347(6)
F(15)	C(46)	1.349(5)	N(1)	C(1)	1.491(5)
N(1)	C(4)	1.447(5)	N(2)	C(3)	1.492(5)
N(2)	C(16)	1.452(5)	C(1)	C(2)	1.515(6)
C(2)	C(3)	1.498(6)	C(4)	C(5)	1.413(5)
C(4)	C(9)	1.406(6)	C(5)	C(6)	1.379(6)
C(5)	C(10)	1.512(6)	C(6)	C(7)	1.368(6)
C(7)	C(8)	1.376(6)	C(8)	C(9)	1.391(6)
C(9)	C(13)	1.523(6)	C(10)	C(11)	1.529(6)
C(10)	C(12)	1.537(6)	C(13)	C(14)	1.520(6)
C(13)	C(15)	1.527(6)	C(16)	C(17)	1.403(6)
C(16)	C(21)	1.403(6)	C(17)	C(18)	1.382(6)
C(17)	C(22)	1.512(6)	C(18)	C(19)	1.375(7)
C(19)	C(20)	1.365(7)	C(20)	C(21)	1.390(7)
C(21)	C(25)	1.508(6)	C(22)	C(23)	1.520(6)
C(22)	C(24)	1.534(6)	C(25)	C(26)	1.519(6)
C(25)	C(27)	1.517(6)	C(28)	C(29)	1.365(5)
C(28)	C(33)	1.373(6)	C(29)	C(30)	1.377(6)
C(30)	C(31)	1.340(6)	C(31)	C(32)	1.362(6)
C(32)	C(33)	1.366(6)	C(34)	B(1)	1.503(6)
C(35)	C(36)	1.390(6)	C(35)	C(40)	1.388(6)
C(35)	B(1)	1.567(7)	C(36)	C(37)	1.375(7)
C(37)	C(38)	1.356(7)	C(38)	C(39)	1.353(7)
C(39)	C(40)	1.376(7)	C(41)	C(42)	1.381(6)
C(41)	C(46)	1.386(6)	C(41)	B(1)	1.584(7)
C(42)	C(43)	1.369(7)	C(43)	C(44)	1.359(7)
C(44)	C(45)	1.365(7)	C(45)	C(46)	1.361(7)

Table A19. Bond Angles(°) for complex **2.54b**•CH₂Cl₂.

atom	atom	atom	angle	atom	atom	atom	angle
N(1)	Ti(1)	N(2)	100.8(2)	N(1)	Ti(1)	C(28)	102.8(2)
N(1)	Ti(1)	C(34)	113.5(2)	N(2)	Ti(1)	C(28)	104.8(2)
N(2)	Ti(1)	C(34)	111.2(2)	C(28)	Ti(1)	C(34)	121.5(2)
Ti(1)	N(1)	C(1)	119.1(3)	Ti(1)	N(1)	C(4)	124.5(3)
C(1)	N(1)	C(4)	116.3(4)	Ti(1)	N(2)	C(3)	122.8(3)
Ti(1)	N(2)	C(16)	122.7(3)	C(3)	N(2)	C(16)	114.6(3)
N(1)	C(1)	C(2)	113.5(4)	C(1)	C(2)	C(3)	117.8(4)
N(2)	C(3)	C(2)	114.3(4)	N(1)	C(4)	C(5)	119.9(4)
N(1)	C(4)	C(9)	119.3(4)	C(5)	C(4)	C(9)	120.8(4)
C(4)	C(5)	C(6)	117.5(5)	C(4)	C(5)	C(10)	122.3(4)
C(6)	C(5)	C(10)	120.1(5)	C(5)	C(6)	C(7)	122.2(5)
C(6)	C(7)	C(8)	120.3(5)	C(7)	C(8)	C(9)	120.5(5)
C(4)	C(9)	C(8)	118.6(4)	C(4)	C(9)	C(13)	122.2(4)
C(8)	C(9)	C(13)	118.9(5)	C(5)	C(10)	C(11)	113.9(4)
C(5)	C(10)	C(12)	110.1(4)	C(11)	C(10)	C(12)	109.8(4)
C(9)	C(13)	C(14)	110.6(4)	C(9)	C(13)	C(15)	112.1(4)
C(14)	C(13)	C(15)	110.8(4)	N(2)	C(16)	C(17)	118.9(5)
N(2)	C(16)	C(21)	119.5(5)	C(17)	C(16)	C(21)	121.6(5)
C(16)	C(17)	C(18)	117.8(5)	C(16)	C(17)	C(22)	123.4(5)
C(18)	C(17)	C(22)	118.7(5)	C(17)	C(18)	C(19)	121.7(5)
C(18)	C(19)	C(20)	119.4(6)	C(19)	C(20)	C(21)	122.4(6)
C(16)	C(21)	C(20)	117.0(5)	C(16)	C(21)	C(25)	122.7(5)
C(20)	C(21)	C(25)	120.3(5)	C(17)	C(22)	C(23)	114.3(5)
C(17)	C(22)	C(24)	109.4(4)	C(23)	C(22)	C(24)	109.7(4)
C(21)	C(25)	C(26)	111.2(4)	C(21)	C(25)	C(27)	113.1(5)
C(26)	C(25)	C(27)	109.7(4)	Ti(1)	C(28)	C(29)	120.9(3)
Ti(1)	C(28)	C(33)	127.7(4)	C(29)	C(28)	C(33)	111.1(4)
F(1)	C(29)	C(28)	118.5(4)	F(1)	C(29)	C(30)	115.8(5)
C(28)	C(29)	C(30)	125.7(5)	F(2)	C(30)	C(29)	121.3(5)
F(2)	C(30)	C(31)	120.2(5)	C(29)	C(30)	C(31)	118.4(5)
F(3)	C(31)	C(30)	120.1(6)	F(3)	C(31)	C(32)	119.2(5)
C(30)	C(31)	C(32)	120.6(5)	F(4)	C(32)	C(31)	120.6(5)
F(4)	C(32)	C(33)	122.2(5)	C(31)	C(32)	C(33)	117.2(5)
F(5)	C(33)	C(28)	118.6(4)	F(5)	C(33)	C(32)	114.6(5)
C(28)	C(33)	C(32)	126.8(5)	Ti(1)	C(34)	B(1)	125.1(3)
C(36)	C(35)	C(40)	112.6(5)	C(36)	C(35)	B(1)	122.9(5)
C(40)	C(35)	B(1)	124.5(5)	F(6)	C(36)	C(35)	118.9(6)
F(6)	C(36)	C(37)	116.5(6)	C(35)	C(36)	C(37)	124.5(6)
F(7)	C(37)	C(36)	120.2(7)	F(7)	C(37)	C(38)	120.8(7)
C(36)	C(37)	C(38)	119.0(6)	F(8)	C(38)	C(37)	119.4(7)
F(8)	C(38)	C(39)	120.4(7)	C(37)	C(38)	C(39)	120.3(7)

atom	atom	atom	angle	atom	atom	atom	angle
F(9)	C(39)	C(38)	119.8(6)	F(9)	C(39)	C(40)	121.1(6)
C(38)	C(39)	C(40)	119.1(6)	F(10)	C(40)	C(35)	119.6(5)
F(10)	C(40)	C(39)	116.0(5)	C(35)	C(40)	C(39)	124.4(6)
C(42)	C(41)	C(46)	113.4(5)	C(42)	C(41)	B(1)	123.4(5)
C(46)	C(41)	B(1)	123.1(5)	F(11)	C(42)	C(41)	119.7(6)
F(11)	C(42)	C(43)	116.4(6)	C(41)	C(42)	C(43)	123.9(6)
F(12)	C(43)	C(42)	121.1(7)	F(12)	C(43)	C(44)	119.3(7)
C(42)	C(43)	C(44)	119.6(6)	F(13)	C(44)	C(43)	120.7(7)
F(13)	C(44)	C(45)	119.9(7)	C(43)	C(44)	C(45)	119.4(7)
F(14)	C(45)	C(44)	119.8(7)	F(14)	C(45)	C(46)	120.8(6)
C(44)	C(45)	C(46)	119.4(6)	F(15)	C(46)	C(41)	119.3(6)
F(15)	C(46)	C(45)	116.5(6)	C(41)	C(46)	C(45)	124.2(6)
C(34)	B(1)	C(35)	120.9(5)	C(34)	B(1)	C(41)	122.0(5)
C(35)	B(1)	C(41)	117.1(4)				

Table A20. Calculated hydrogen atom coordinates and B_{iso} for complex $2.54b \cdot CH_2Cl_2$.

atom	x	y	z	B_{iso}
H(1)	0.5430	0.4923	0.4610	5.7
H(2)	0.6063	0.5836	0.4676	5.7
H(3)	0.4970	0.6828	0.4333	6.0
H(4)	0.5272	0.6868	0.3803	6.0
H(5)	0.4057	0.6628	0.3320	5.6
H(6)	0.4088	0.5529	0.3764	5.6
H(7)	0.8002	0.5720	0.4018	6.6
H(8)	0.8575	0.3999	0.4548	6.8
H(9)	0.7939	0.2609	0.4872	6.4
H(10)	0.6131	0.6439	0.3504	6.4
H(11)	0.7362	0.7005	0.3272	8.9
H(12)	0.6693	0.6218	0.2809	8.9
H(13)	0.6574	0.7590	0.2919	8.9
H(14)	0.7420	0.7611	0.4345	9.8
H(15)	0.6668	0.8279	0.3949	9.8
H(16)	0.6727	0.7348	0.4484	9.8
H(17)	0.6051	0.2748	0.4527	5.9
H(18)	0.6532	0.2321	0.5606	8.8
H(19)	0.7313	0.2772	0.5683	8.8
H(20)	0.6652	0.3692	0.5494	8.8
H(21)	0.6451	0.0803	0.4807	8.7
H(22)	0.6590	0.1181	0.4210	8.7
H(23)	0.7251	0.1165	0.4894	8.7
H(24)	0.3437	0.6664	0.1121	7.2
H(25)	0.2345	0.5602	0.0812	8.3
H(26)	0.2168	0.4343	0.1525	7.1
H(27)	0.4973	0.6434	0.2588	6.3
H(28)	0.5024	0.5899	0.1640	9.0
H(29)	0.4565	0.7060	0.1312	9.0
H(30)	0.5367	0.7190	0.1862	9.0
H(31)	0.4901	0.8496	0.2468	8.9
H(32)	0.4098	0.8388	0.1917	8.9
H(33)	0.4246	0.8051	0.2624	8.9
H(34)	0.3472	0.3706	0.3090	6.2
H(35)	0.2668	0.5183	0.3118	9.6
H(36)	0.2007	0.4488	0.2583	9.6
H(37)	0.2433	0.3900	0.3262	9.6
H(38)	0.2255	0.2680	0.2092	9.9
H(39)	0.3074	0.2227	0.2310	9.9

X-ray Crystallography of Complex 4.20b

Very air-sensitive, colorless platy crystals of complex **4.20b** were grown from pentane. A suitable crystal was mounted inside a Lindemann capillary tube, flame sealed and used for the experiments. The X-ray diffraction experiments were carried out on a Siemens P4 diffractometer with XSCANS software package¹ using graphite monochromated Mo K α radiation at 25°C. The cell constants were obtained by centering 20 reflections ($21.0 \leq 2\theta \leq 24.6^\circ$). The Laue symmetry $\bar{1}$ was determined by merging symmetry equivalent reflections. The data were collected in the θ range $2.0 - 23^\circ$ ($-1 \leq h \leq 11$, $-13 \leq k \leq 13$, $-17 \leq l \leq 18$) in θ - 2θ scan mode at variable scan speeds (2-20 deg/min). Background measurements were made at the ends of the scan range. Four standard reflections were monitored at the end of every 297 reflection collection. The data processing, solution and initial refinements were done using *SHELXTL-PC*² programs. The final refinements were performed using *SHELXL-93*³ software programs. An empirical absorption correction was applied to the data using the routine 'XEMP' using the ψ scans data ($\mu = 0.312 \text{ mm}^{-1}$). Anisotropic thermal parameters were refined for all the non-hydrogen atoms in the neutral molecule except for two phenyl ring carbon atoms. No attempt was made to locate the hydrogen atoms. However all the hydrogen atoms were placed in the calculated positions. All the C-C and the C-C-C angles in the isopropyl groups were restrained to be equal using the option SADI. In the final least-squares refinement cycles on F^2 , the model converged at $R1 = 0.0951$, $wR2 = 0.2287$ and $Goof = 1.014$ for 2999 observations with $F_o \geq 4\sigma(F_o)$ and 289 parameters, and $R1 = 0.1733$ and $wR2 = 0.2918$ for all 5405 data. In the final difference Fourier synthesis the electron density fluctuates in the range 1.03 to $-0.635 \text{ e } \text{\AA}^{-3}$. The top three peaks in the difference Fourier map were near Zr atom at distances of 0.99 to 1.03 \AA . The mean and the maximum shift/esd in the final cycles were -0.001 and 0.000 . The experimental details and crystal data, the positional and thermal parameters, bond distances and angles have been included below.

Table A21. Crystal Data and Experimental Details for complex **4.20b**.

Empirical formula	C ₄₂ H ₅₇ N ₃ Zr ₁
Formula weight	695.13
Temperature	25°C
Wavelength	0.71073 Å
Crystal system	Triclinic
Space group	P $\bar{1}$
Unit cell dimensions	a = 10.146(2) Å b = 12.336(2) Å c = 16.723(2) Å α = 81.00(2) ° β = 74.99(2) ° γ = 76.24(2) °
Volume	1953.6(6) Å ³
Z	2
Density, calcd.	1.182 g.cm ⁻³
Absorption coefficient	0.312 mm ⁻¹
F(000)	740
Reflections Collected	6209
Independent reflections	5405 [R(int) = 0.0558]
Refinement method	Full-matrix least-squares on F ²
Data/restraints/parameters	5405/40/289
Goodness-of-fit (GooF) on F ²	1.014
Final R indices [I>2sigma(I)]	R1 = 0.0951, wR2 = 0.2287
R indices (all data)	R1 = 0.1733, wR2 = 0.2918

$$R1 = \sum (||F_o| - |F_c||) / \sum |F_o|;$$

$$wR2 = \left[\sum w(F_o^2 - F_c^2)^2 / \sum wF_o^4 \right]^{1/2}$$

$$GooF = \left[\sum w(F_o^2 - F_c^2)^2 / (n - p) \right]^{1/2}$$

where n is the number of reflections and p is the number of parameters refined.

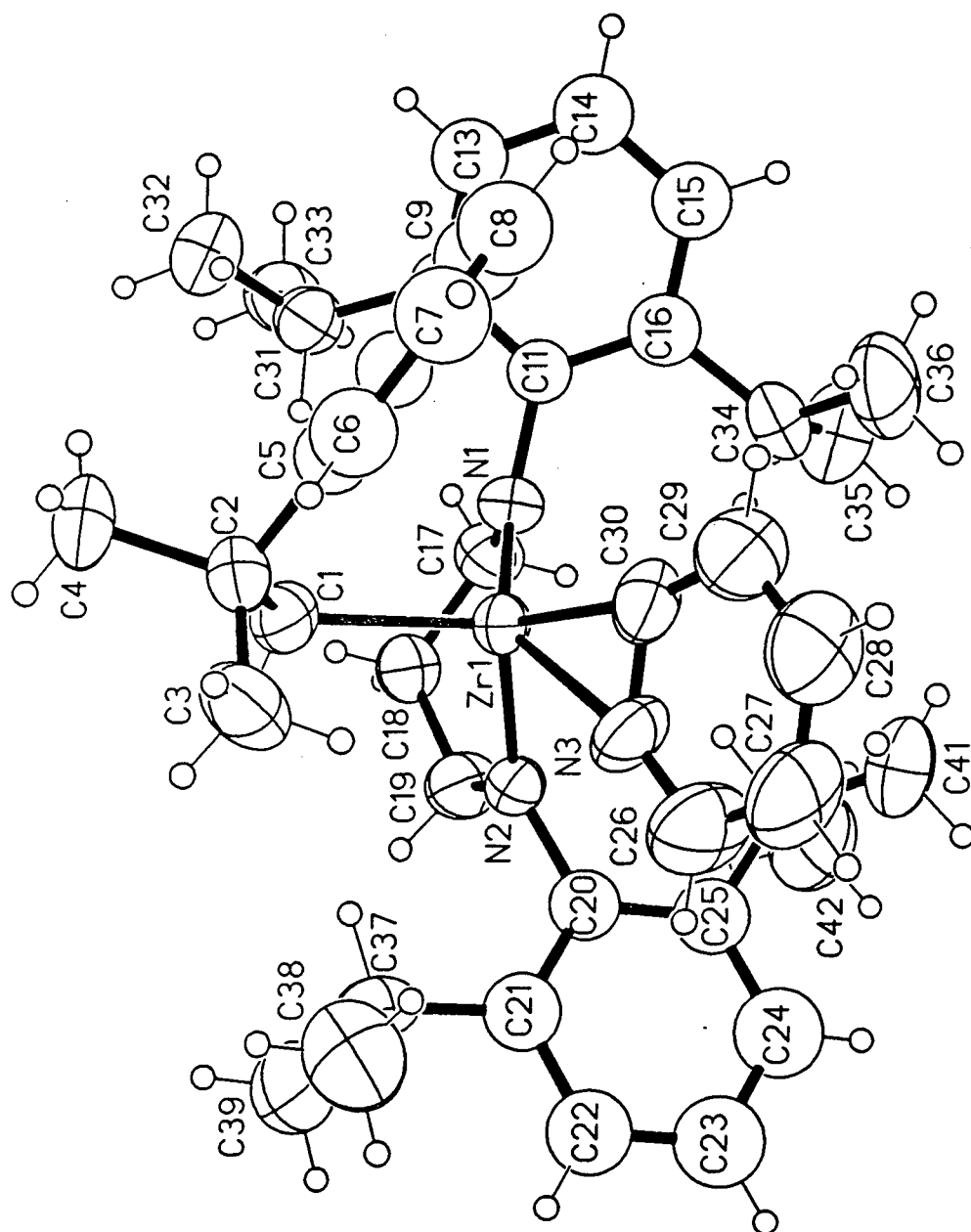


Figure A5: Molecular Structure of Complex 4.20b

Table A22. Atomic coordinates ($\times 10^4$) and equivalent isotropic displacement parameters ($\text{\AA}^2 \times 10^3$) for complex **4.20b**. $U(\text{eq})$ is defined as one third of the trace of the orthogonalized U_{ij} tensor.

atom	x	y	z	Ueq
Zr(1)	1177.1(12)	2164.2(10)	2687.5(7)	46.4(4)
N(1)	3145(9)	1512(7)	2870(6)	53(2)
N(2)	871(9)	3560(7)	3270(5)	48(2)
C(1)	-162(13)	1075(10)	3604(7)	55(3)
C(2)	-1025(12)	457(10)	3274(7)	57(3)
C(3)	-2365(13)	1279(13)	3198(9)	80(4)
C(4)	-1414(15)	-558(11)	3895(9)	78(4)
C(5)	-226(7)	8(7)	2433(4)	55(3)
C(6)	-936(6)	-151(7)	1867(5)	68(3)
C(7)	-196(8)	-571(8)	1118(5)	79(4)
C(8)	1253(8)	-832(7)	935(4)	80(4)
C(9)	1963(6)	-674(7)	1502(5)	74(4)
C(10)	1223(7)	-253(7)	2251(4)	58(3)
C(11)	4182(7)	642(5)	2430(4)	47(3)
C(12)	4425(7)	-452(6)	2806(3)	52(3)
C(13)	5339(8)	-1298(4)	2358(5)	68(3)
C(14)	6008(7)	-1050(6)	1535(5)	72(4)
C(15)	5765(8)	44(7)	1160(4)	70(4)
C(16)	4852(8)	889(5)	1607(4)	59(3)
C(17)	3630(12)	1940(11)	3498(7)	61(3)
C(18)	2410(12)	2423(10)	4191(6)	56(3)
C(19)	1508(14)	3522(10)	3977(8)	65(3)
C(20)	171(7)	4698(5)	3045(5)	55(3)
C(21)	-1246(7)	5053(6)	3378(5)	65(3)
C(22)	-1911(6)	6148(7)	3180(6)	77(4)
C(23)	-1158(9)	6889(5)	2649(6)	90(5)
C(24)	260(9)	6533(7)	2317(5)	89(4)
C(25)	924(6)	5438(7)	2514(5)	65(3)
N(3)	-31(12)	3276(8)	1797(6)	66(3)
C(26)	-853(17)	4077(13)	1418(10)	93(5)
C(27)	-934(18)	4056(14)	629(10)	95(5)
C(28)	-124(18)	3139(15)	215(10)	94(5)
C(29)	742(18)	2347(13)	603(9)	87(5)
C(30)	778(14)	2417(10)	1421(7)	61(3)
C(31)	3769(12)	-804(10)	3722(7)	62(3)
C(32)	3070(14)	-1801(11)	3835(9)	81(4)
C(33)	4827(14)	-1051(11)	4260(8)	78(4)
C(34)	4738(13)	2084(10)	1181(7)	67(3)
C(35)	5920(16)	2605(13)	1220(10)	95(5)

atom	x	y	z	Ueq
C(36)	4606(17)	2170(14)	286(8)	98(5)
C(37)	-2122(13)	4291(10)	3974(8)	74(4)
C(38)	-3406(17)	4244(16)	3690(11)	112(6)
C(39)	-2541(19)	4637(14)	4853(9)	105(6)
C(40)	2512(13)	5103(10)	2135(8)	72(4)
C(41)	2754(18)	5177(13)	1184(8)	99(5)
C(42)	3348(18)	5774(14)	2391(11)	112(6)

Table A23. Bond Distances(Å) for complex **4.20b**.

Zr(1)-N(2)	2.031(9)	Zr(1)-N(1)	2.050(9)
Zr(1)-C(30)	2.219(12)	Zr(1)-N(3)	2.260(10)
Zr(1)-C(1)	2.268(12)	N(1)-C(11)	1.453(10)
N(1)-C(17)	1.479(14)	N(2)-C(20)	1.455(10)
N(2)-C(19)	1.475(14)	C(1)-C(2)	1.53(2)
C(2)-C(3)	1.51(2)	C(2)-C(5)	1.542(13)
C(2)-C(4)	1.55(2)	C(12)-C(31)	1.543(11)
C(16)-C(34)	1.525(12)	C(17)-C(18)	1.53(2)
C(18)-C(19)	1.49(2)	C(21)-C(37)	1.521(13)
C(25)-C(40)	1.551(13)	N(3)-C(26)	1.33(2)
N(3)-C(30)	1.31(2)	C(26)-C(27)	1.35(2)
C(27)-C(28)	1.39(2)	C(28)-C(29)	1.36(2)
C(29)-C(30)	1.40(2)	C(31)-C(33)	1.521(13)
C(31)-C(32)	1.524(14)	C(34)-C(35)	1.509(14)
C(34)-C(36)	1.522(14)	C(37)-C(38)	1.51(2)
C(37)-C(39)	1.52(2)	C(40)-C(42)	1.49(2)
C(40)-C(41)	1.537(14)		

Table A24. Bond Angles(°) for complex 4.20b.

N(2)-Zr(1)-N(1)	95.4(4)	N(2)-Zr(1)-C(30)	117.0(4)
N(1)-Zr(1)-C(30)	120.8(4)	N(2)-Zr(1)-N(3)	86.2(4)
N(1)-Zr(1)-N(3)	143.7(4)	C(30)-Zr(1)-N(3)	34.0(4)
N(2)-Zr(1)-C(1)	104.0(4)	N(1)-Zr(1)-C(1)	103.9(4)
C(30)-Zr(1)-C(1)	113.2(4)	N(3)-Zr(1)-C(1)	110.9(4)
C(11)-N(1)-C(17)	113.6(8)	C(11)-N(1)-Zr(1)	126.5(7)
C(17)-N(1)-Zr(1)	119.9(7)	C(20)-N(2)-C(19)	110.9(8)
C(20)-N(2)-Zr(1)	128.5(6)	C(19)-N(2)-Zr(1)	120.4(7)
C(2)-C(1)-Zr(1)	118.8(7)	C(3)-C(2)-C(1)	106.9(10)
C(3)-C(2)-C(5)	111.5(10)	C(1)-C(2)-C(5)	111.7(9)
C(3)-C(2)-C(4)	107.8(10)	C(1)-C(2)-C(4)	111.2(10)
C(5)-C(2)-C(4)	107.7(10)	C(6)-C(5)-C(2)	120.9(6)
C(10)-C(5)-C(2)	119.1(6)	C(12)-C(11)-N(1)	120.3(6)
C(16)-C(11)-N(1)	119.5(6)	C(13)-C(12)-C(31)	116.1(6)
C(11)-C(12)-C(31)	123.9(6)	C(15)-C(16)-C(34)	117.0(7)
C(11)-C(16)-C(34)	122.7(7)	N(1)-C(17)-C(18)	111.7(9)
C(19)-C(18)-C(17)	117.3(10)	N(2)-C(19)-C(18)	115.4(9)
C(21)-C(20)-N(2)	119.9(6)	C(25)-C(20)-N(2)	120.1(6)
C(22)-C(21)-C(37)	117.5(7)	C(20)-C(21)-C(37)	122.5(7)
C(24)-C(25)-C(40)	117.4(7)	C(20)-C(25)-C(40)	122.6(7)
C(26)-N(3)-C(30)	121.9(12)	C(26)-N(3)-Zr(1)	166.8(10)
C(30)-N(3)-Zr(1)	71.3(7)	C(27)-C(26)-N(3)	122.6(16)
C(26)-C(27)-C(28)	117.4(15)	C(29)-C(28)-C(27)	119.2(14)
C(30)-C(29)-C(28)	120.6(14)	C(29)-C(30)-N(3)	118.3(13)
C(29)-C(30)-Zr(1)	167.0(11)	N(3)-C(30)-Zr(1)	74.7(7)
C(33)-C(31)-C(32)	109.5(10)	C(33)-C(31)-C(12)	111.7(9)
C(32)-C(31)-C(12)	113.7(10)	C(35)-C(34)-C(36)	110.3(11)
C(35)-C(34)-C(16)	112.6(10)	C(36)-C(34)-C(16)	112.9(10)
C(38)-C(37)-C(39)	109.9(11)	C(38)-C(37)-C(21)	112.3(12)
C(39)-C(37)-C(21)	111.6(11)	C(42)-C(40)-C(41)	111.9(12)
C(42)-C(40)-C(25)	113.4(11)	C(41)-C(40)-C(25)	108.8(11)

Table A25. Calculated Hydrogen Atom Positions ($\times 10^4$) and Thermal ($\times 10^3$) Parameters for complex 4.20b.

Atom	x	y	z	Ueq
H(1A)	445(13)	517(10)	3896(7)	66
H(1B)	-801(13)	1546(10)	4013(7)	66
H(3A)	-2938(13)	922(13)	2993(9)	119
H(3B)	-2154(13)	1917(13)	2818(9)	119
H(3C)	-2855(13)	1520(13)	3734(9)	119
H(4A)	-578(15)	-1094(11)	3954(9)	117
H(4B)	-1995(15)	-904(11)	3688(9)	117
H(4C)	-1907(15)	-302(11)	4426(9)	117
H(6)	-1905(6)	24(11)	1989(7)	81
H(7)	-671(11)	-677(11)	739(6)	94
H(8)	1748(11)	-1113(11)	434(5)	96
H(9)	2933(6)	-848(11)	1379(7)	88
H(10)	1698(9)	-147(10)	2630(6)	69
H(13)	5501(12)	-2029(5)	2610(6)	81
H(14)	6619(10)	-1616(7)	1236(6)	87
H(15)	6213(11)	209(9)	609(4)	84
H(17A)	4144(12)	2520(11)	3228(7)	73
H(17B)	4259(12)	1336(11)	3740(7)	73
H(18A)	1821(12)	1876(10)	4389(6)	67
H(18B)	2786(12)	2504(10)	4650(6)	67
H(19A)	767(14)	3712(10)	4463(8)	78
H(19B)	2063(14)	4093(10)	3851(8)	78
H(22)	-2859(6)	6386(10)	3402(8)	93
H(23)	-1602(12)	7621(6)	2517(9)	108
H(24)	764(12)	7029(9)	1962(8)	107
H(26)	-1395(17)	4677(13)	1707(10)	112
H(27)	-1507(18)	4630(14)	371(10)	114
H(28)	-177(18)	3072(15)	-322(10)	113
H(29)	1317(18)	1751(13)	321(9)	105
H(31)	3044(12)	-166(10)	3931(7)	74
H(32A)	2402(14)	-1645(11)	3496(9)	122
H(32B)	2605(14)	-1929(11)	4409(9)	122
H(32C)	3763(14)	-2456(11)	3672(9)	122
H(33A)	5267(14)	-422(11)	4188(8)	116
H(33B)	5520(14)	-1706(11)	4097(8)	116
H(33C)	4361(14)	-1179(11)	4834(8)	116
H(34)	3877(13)	2534(10)	1488(7)	81
H(35A)	5992(16)	2546(13)	1787(10)	143
H(35B)	5743(16)	3381(13)	1006(10)	143
H(35C)	6777(16)	2220(13)	891(10)	143

Atom	x	y	z	Ueq
H(36A)	3850(17)	1837(14)	270(8)	147
H(36B)	5458(17)	1783(14)	-46(8)	147
H(36C)	4426(17)	2945(14)	69(8)	147
H(37)	-1546(13)	3531(10)	3990(8)	89
H(38A)	-3134(17)	4025(16)	3134(11)	168
H(38B)	-4015(17)	4971(16)	3697(11)	168
H(38C)	-3884(17)	3708(16)	4057(11)	168
H(39A)	-1722(19)	4663(14)	5030(9)	157
H(39B)	-3019(19)	4102(14)	5222(9)	157
H(39C)	-3148(19)	5365(14)	4862(9)	157
H(40)	2824(13)	4316(10)	2334(8)	87
H(41A)	2201(18)	4735(13)	1043(8)	149
H(41B)	3723(18)	4898(13)	947(8)	149
H(41C)	2489(18)	5945(13)	968(8)	149
H(42A)	3172(18)	5707(14)	2987(11)	168
H(42B)	3090(18)	6547(14)	2186(11)	168
H(42C)	4322(18)	5500(14)	2164(11)	168

References:

- (1) Siemens Inc. (1990). "XSCANS", Siemens Analytical X-Ray Instruments Inc., Madison.
- (2) Sheldrick, G. M. (1990). "SHELXTL-PC", V4.1, Siemens Analytical X-Ray Instruments Inc., Madison, WI, U.S.A.
- (3) Sheldrick, G. M. (1993). "SHELXL-93", Institute fuer Anorg. Chemie, Goettingen, Germany.
- (4) Enraf-Nonius (1984). "Enraf-Nonius Data Collection Package", 5.0, Delft, The Netherlands.
- (5) Enraf-Nonius (1983). "Enraf-Nonius Structure Determination Package", 3.0, Delft, The Netherlands.
- (6) Altomare, A.; Cascarano, M.; Giacovazzo, C.; Guagliardi, A. *J. Appl. Cryst.* **1993**, *26*, 343.
- (7) Beurskens, P. T.; Admiraal, G.; Beurskens, G.; Bosman, W. P.; de Gelder, R.; Isreal, R.; Smits, J. M. M. (1994). "DIRDIF94", Technical Report of the Crystallography Laboratory, University of Nijmegen,, The Netherlands.
- (8) Molecular Structure Corporation (1985-1992). "teXsan", Crystal Structure Analysis Package,, Molecular Structure Corporation.

Summary of Experience:

- Postdoctoral Scholar, California Institute of Technology, Pasadena, CA (1998-present)
- Ph.D. Inorganic Chemistry, University of British Columbia, CANADA, (1998).
- M.Sc. Organic Chemistry, University of Western Ontario, CANADA, (1993).
- Wide breadth of expertise in chemical, biochemical, spectroscopic and computational techniques.

Objectives:

- To secure a permanent position where my experience and technical background in chemistry, as well as my problem solving ability, can be utilized for mutual benefit.

Education:

Ph.D., University of British Columbia, CANADA, **Inorganic Chemistry, 1998.**
Thesis: *Chelating Diamide Complexes of Titanium, Zirconium and Scandium: New Polymerization Catalysts based on Non-Cp Ligand Environments*
Supervisor: Prof. David H. McConville

M.Sc., University of Western Ontario, CANADA, **Organic Chemistry, 1993.**
Thesis: *Studies Towards Polymer Bound Radiopharmaceutical Kits*
Supervisor: Prof. Duncan H. Hunter

B.Sc., University of Western Ontario, CANADA, **Chemistry, 1991.**
Thesis: *Studies Towards the Synthesis of a Potential Bis-Diene Precursor of an [8]Cyclacene*
Supervisor: Prof. Robert M. Cory

Research Accomplishments:

Postdoctoral Scholar in the lab of Professor John E. Bercaw, Arnold and Mabel Beckman Laboratories of Chemical Synthesis, California Institute of Technology, Feb. 1998 - present.

Graduate Student in the lab of Professor David H. McConville, Department of Chemistry, University of Western Ontario and University of British Columbia, May 1994 - 1998.

- Studying the chemistry and properties of early transition metal chelating diamides
- Discovered the first living polymerization of α -olefins at room temperature.

Research Assistant in the lab of Professor David H. McConville, Department of Chemistry, University of Western Ontario, Oct. 1993 - April 1994

- Responsible for setting up a new research laboratory

Graduate Student in the lab of Professor Duncan H. Hunter, Department of Chemistry, University of Western Ontario, May 1991 - Sept. 1993.

- Was a member of the Radiopharmaceutical Development Group at the University of Western Ontario. In this position I performed as both a synthetic organic chemist and a biochemist by first developing new pharmaceuticals and then proceeding with radiolabelling and studying of its distribution in various laboratory animals.
- Worked on a novel radiolabelling system based on polymer-bound pharmaceuticals.

Publications:

7. Scollard, J.D., McConville, D.H., Rettig, S.J. *Chelating Diamide Complexes of Titanium: New Catalyst Precursors for the Highly Active and Living Polymerization of α -Olefins*. J. of Molec. Cat., Accepted for Publication.
6. Scollard, J.D., McConville D.H., Vittal J.J. *Bulky Chelating Diamide Complexes of Zirconium: Synthesis, Structure and Reactivity of d^0 Alkyl Derivatives*. Organometallics. **16**, 4415-4420 (1997).
5. Scollard, J.D., McConville, D.H., Rettig, S.J. *Living Polymerization of α -Olefins: Catalyst Precursor Deactivation via the Unexpected Cleavage of a B-C₆F₅ Bond*. Organometallics **16**, 1810-1812 (1997).
4. Scollard J.D., McConville D.H. *Living Polymerization of α -Olefins by Chelating Diamide Complexes of Titanium*. J. Am. Chem. Soc. **118**, 10008-10009 (1996).
3. Scollard J.D., McConville D.H., Payne N.C., Vittal J.J. *Polymerization of α -Olefins by Chelating Diamide Complexes of Titanium*. Macromolecules. **29**, 5241-5243 (1996).
2. Scollard J.D., McConville D.H., Vittal J.J. *Sterically Demanding Diamide Ligands: Synthesis and Structure of d^0 Group 4 Alkyl Derivatives*. Organometallics. **14**, 5478-5480 (1995).
1. Scollard, J.D. *Studies Towards Polymer Bound Radiopharmaceutical Kit's*. M.Sc. Thesis, University of Western Ontario (1993).

Conference Proceedings:

3. *Chelating Diamide Complexes of Ti. and Zr: Living Polymerization of α -Olefins*. John D. Scollard, David H. McConville. 80th Canadian Society for Chemistry Conference, Windsor, Ontario, Canada, June 1997.
2. *Bisamides of Zirconium: Unexpected C-H activation of a Pyridine Molecule..* John D. Scollard, David H. McConville. 1997 Alberta/British Columbia Inorganic Chemistry Colloquium, University College of the Cariboo, Kamloops, British Columbia, May 1997.
1. *Sterically Demanding Diamide Ligands: Synthesis and Structure of d^0 Group 4 Alkyl Derivatives*. John D. Scollard, David H. McConville and Jagadese J. Vittal. 25th Inorganic Discussion Weekend, University of Western , Ontario, Ontario, Canada, November 1995.

Specific Research Skills:

Experienced in the following chemical techniques:

- Schlenk technique
- Drybox manipulations
- High Pressure Polymerizations

Experienced in the following biochemical techniques:

- Quality control through nuclear assays.
- Maintenance of a radioactive laboratory, including wipe tests, and disposal of biohazardous and nuclear waste.

Experienced in the following spectroscopic techniques:

- GPC, TGA, DSC, HPLC, HPIC, GC, AA
- NMR, X-ray Crystallography
- UV-Vis and FT-IR Spectroscopy
- X-ray Photoelectron Spectroscopy (XPS)
- Single Photon Emission Computed Tomography (SPECT)

Experienced in the following computational techniques:

- Visulation, molecular mechanics and dynamics using CAChe™ software
- UNIX, DOS, Macintosh and Windows operating system environments
- HTML Programming and web-site management

Additional Work Experience:

Computer Technologist at The Sudbury Memorial Hospital, Sudbury, Ontario, May 1990 - Sept. 1990.

- Programmed a database for the perfusion department. Extensive consultation and collaboration with the chief perfusionist and the director of cardiopulmonary was necessary to achieve this task.

Computer Technologist at The Sudbury Memorial Hospital, Sudbury, Ontario, May 1989 - Sept. 1989.

- Was in charge of computerizing the Cardiopulmonary department of the Hospital. This entailed helping install the computers, meeting with the Doctors and staff to design the computer forms, creating the forms and then training the staff on the operation of the computer system.

Computer Technologist at The Sudbury Memorial Hospital, Sudbury, Ontario, May 1988 - Sept. 1988.

- Was responsible for the computerization of the Heart Catheterization Lab of the Cardiopulmonary department. I had to organize meetings with the cardiologists and nurses to develop the computer forms and then train the nurses on the operation of the computer system.